Supplement of Geosci. Model Dev., 13, 5875–5896, 2020
https://doi.org/10.5194/gmd-13-5875-2020-supplement

Geoscientific Model Development
Open Access

Supplement of

Implementation of the RCIP scheme and its performance for 1-D age computations in ice-sheet models

Fuyuki Saito et al.

Correspondence to: Fuyuki Saito (saitofuyuki@jamstec.go.jp)

S1 Comprehensive experiment sheets

In addition to the experiments presented in the main paper, several experimental configuration combinations of parameters are examined. In this Supplement, some representative results of them are provided. All of the experiments shown are examined under non-steady surface mass balance configurations. Each page contains two figures: the upper one is the result obtained using a square-wave type surface mass balance input, while the lower is one with the same configuration except for applying a cosine-wave type input. One figure contains five sub-figures. (a) profiles of the computed age, (b,d) The computed age differences relative to the result of the RCIP+corr case, and (c,e) the annual layer thickness. The upper sub-figures (a-c) show the profiles in terms of depths, while the lower sub-figures (d-e) show them in terms of the computed ages. The surface mass balance input used in each experiment is shown in the lower left figure for only first 200 or 100 kyr. The prescribed time evolution of ice-thickness is also shown in the lower left figure for the non-steady thickness experiments. The grey and black lines in (a,c,e) correspond to 'benchmark' profiles which are computed using constant surface/basal mass balance and thickness.

Figures S1 to S6 are the results of a most standard experiments: constant $H = 3000\,\mathrm{m}$, $a_{\mathsf{H}}, a_{\mathsf{L}} = 3, 1.5\,\mathrm{cm\,yr^{-1}}$, $P_{\mathsf{T}} = 100\,\mathrm{kyr}$, $P_{\mathsf{H}} : P_{\mathsf{L}} = 1 : 1$, and the uniform discretization of 129 levels (see Eq.57 in the main text about definition of a_{H}, a_{L}, P_{T}, P_{H} and P_{L}). Basal mass balances are set as constant $M_{\mathrm{b}} = 0\,\mathrm{mm\,yr^{-1}}$ (S1,S2), $M_{\mathrm{b}} = 0.3\,\mathrm{mm\,yr^{-1}}$ (S3,S4), and $M_{\mathrm{b}} = 3\,\mathrm{mm\,yr^{-1}}$ (S5,S6). All of the results are the snapshots at $t = 1\,\mathrm{Myr}$.

Figures S7 to S12 are the same combination as presented above except for $a_{\mathsf{L}} = 0.75\,\mathrm{cm\,yr^{-1}}$. Figures S13 to S18 are the same except for $a_{\mathsf{L}} = 0\,\mathrm{cm\,yr^{-1}}$. Figures S19 to S22 are the same except for $a_{\mathsf{L}} = -15\,\mathrm{cm\,yr^{-1}}$.

Two types of sensitivity experiments regarding to the shape of prescribed time-evolution of surface mass balance inputs are performed: one type obtained using a different $P_{\mathsf{H}} : P_{\mathsf{L}}$, and the other using a different P_{T}. Figures S23 to S26 are the results obtained using a longer P_{H}, as $P_{\mathsf{H}} : P_{\mathsf{L}} = 7 : 1$, and Figures S27 to S30 are the results using a shorter P_{H}, as $P_{\mathsf{H}} : P_{\mathsf{L}} = 1 : 7$. Figures S31 to S38 are the results obtained using $P_{\mathsf{T}} = 50\,\mathrm{kyr}$, Figures S39 to S46 using $P_{\mathsf{T}} = 20\,\mathrm{kyr}$, and Figures S47 to S54 using $P_{\mathsf{T}} = 10\,\mathrm{kyr}$.

Two types of sensitivity experiments regarding to the shape of prescribed time evolution of ice-thickness are performed: one type with $\tau_H = 10\,\mathrm{kyr}$ (Figs.S55 to S58), and the other with $\tau_H = 3\,\mathrm{kyr}$ (Figs.S59 to S62). (see Eq.61 in the main text about definition of τ_H).

The series of experiments obtained using constant $H = 3000\,\mathrm{m}$ and $M_{\mathrm{b}} = 0\,\mathrm{mm\,yr^{-1}}$ are repeated by higher resolution configurations. Figures.S63 to S70 are the results of $P_{\mathsf{T}} = 100\,\mathrm{kyr}$; Figures.S71 to S94 are results obtained using a uniform discretization of 513 levels. Figures.S95 to S126 are the same results but using a smooth non-uniform discretization of 513 levels. Figures.S127 to S158 are the same results but using a non-smooth non-uniform discretization of 477 levels. The snapshots at $t = 2\,\mathrm{Myr}$ are plotted for those experiment with higher resolutions. Designs of these higher resolution discretization are shown in Fig. 14 in the main text.

Furthermore, the series of experiments obtained using constant $H = 3000\,\mathrm{m}$ and $M_{\mathrm{b}} = 0\,\mathrm{mm\,yr^{-1}}$ are repeated by lower resolution configurations. Figures.S159 to S166 are the results of $P_{\mathsf{T}} = 100\,\mathrm{kyr}$, obtained using a uniform discretization of 33 levels.

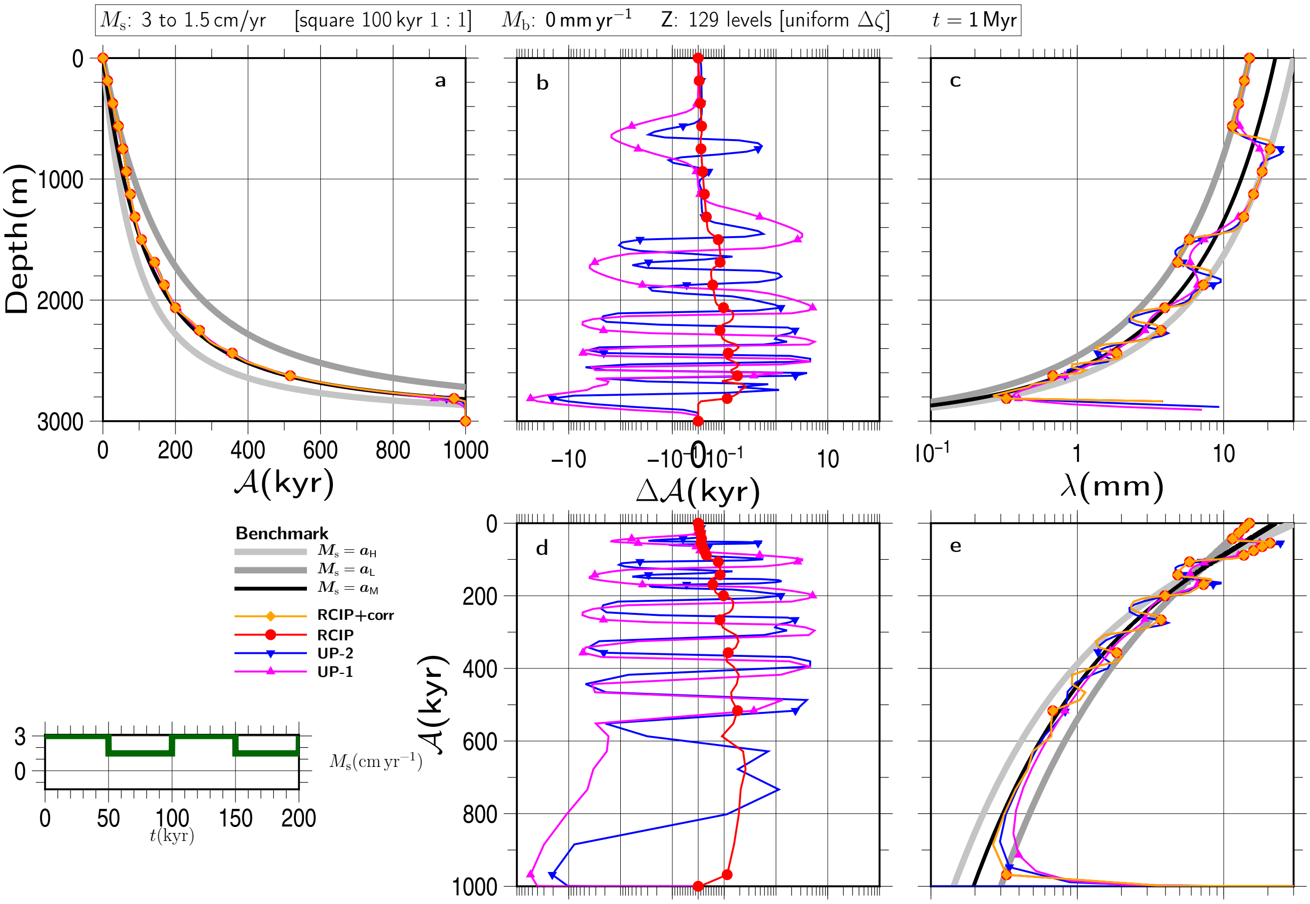

Figure S1

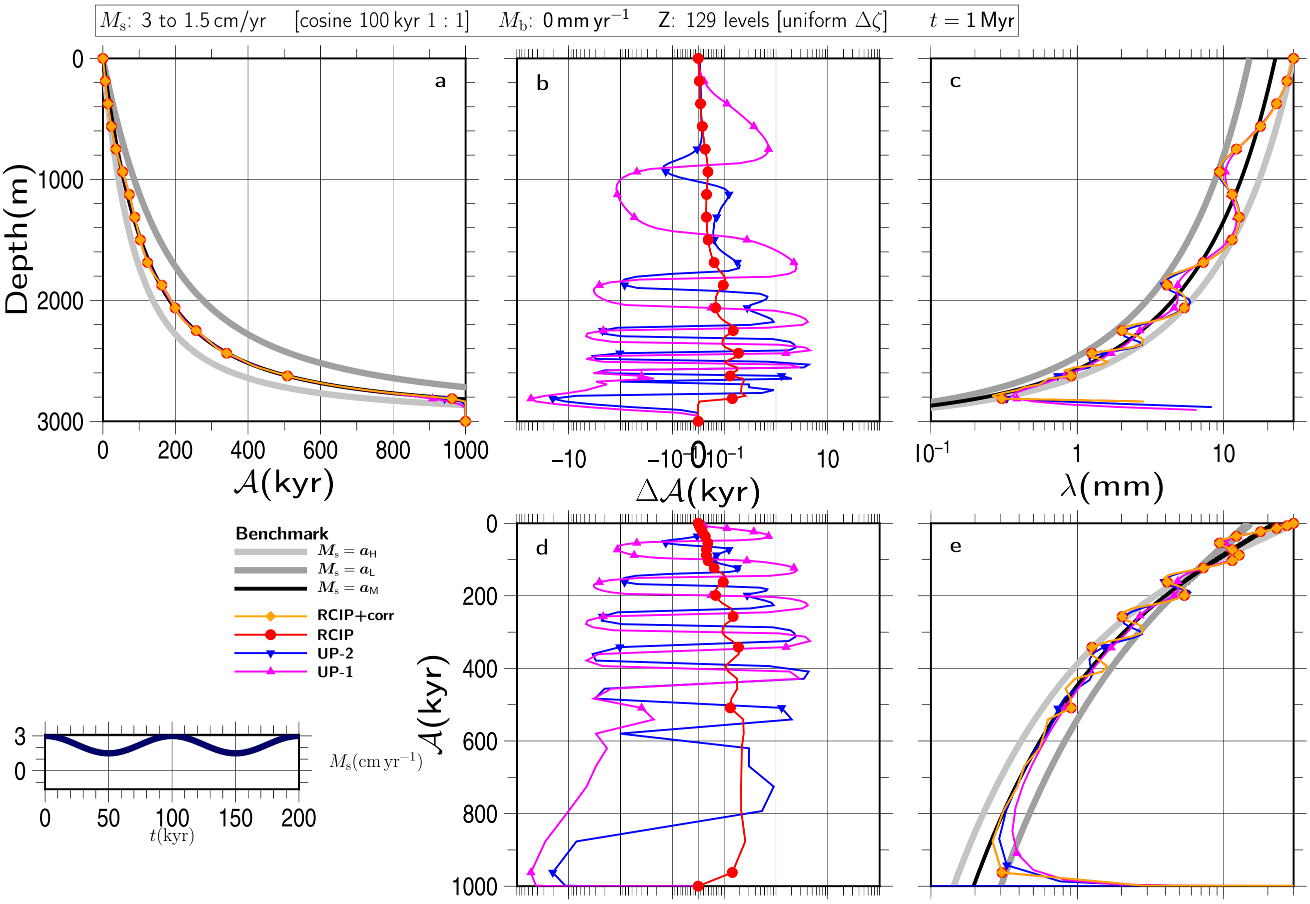

Figure S2

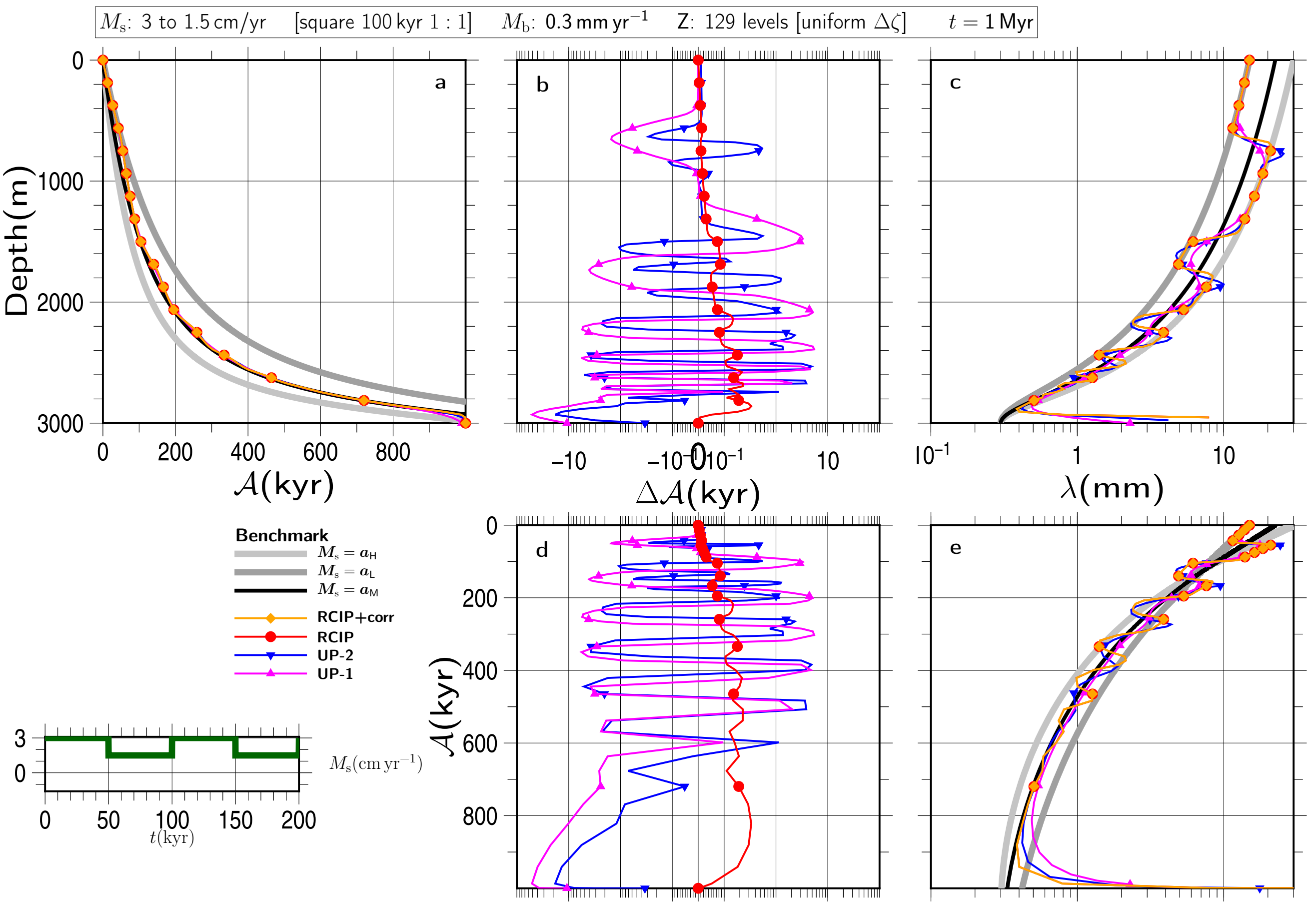

Figure S3

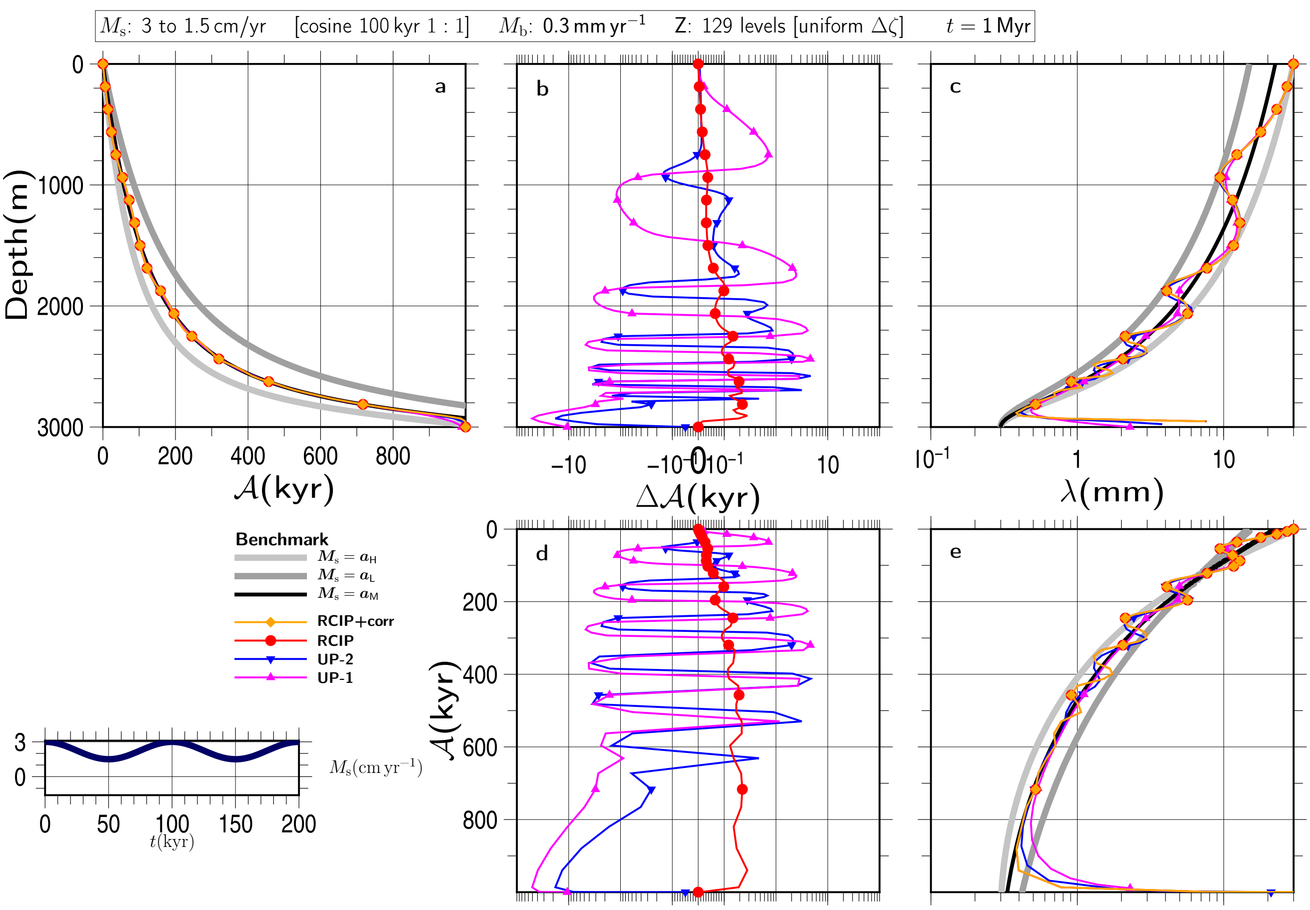

Figure S4

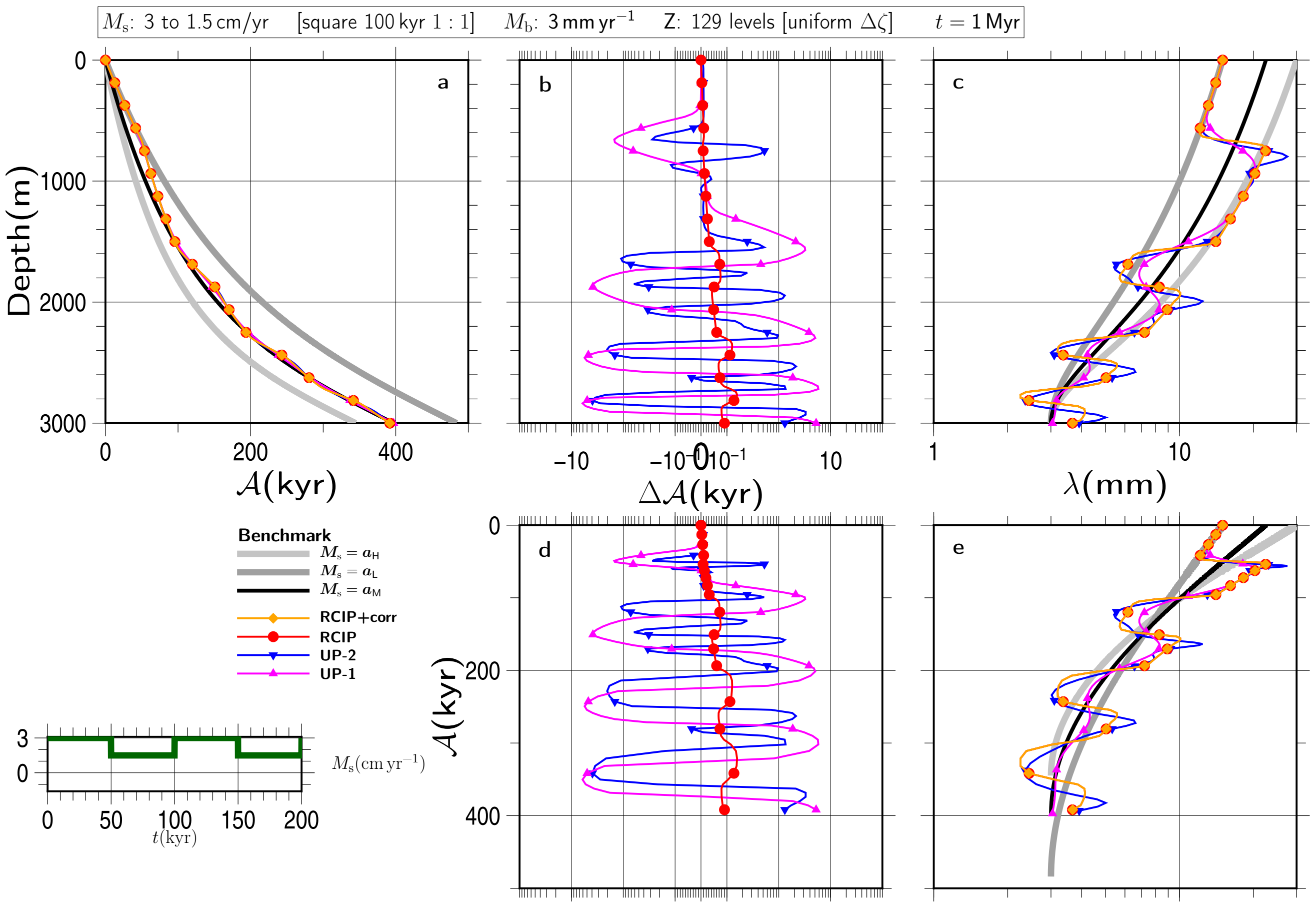

Figure S5

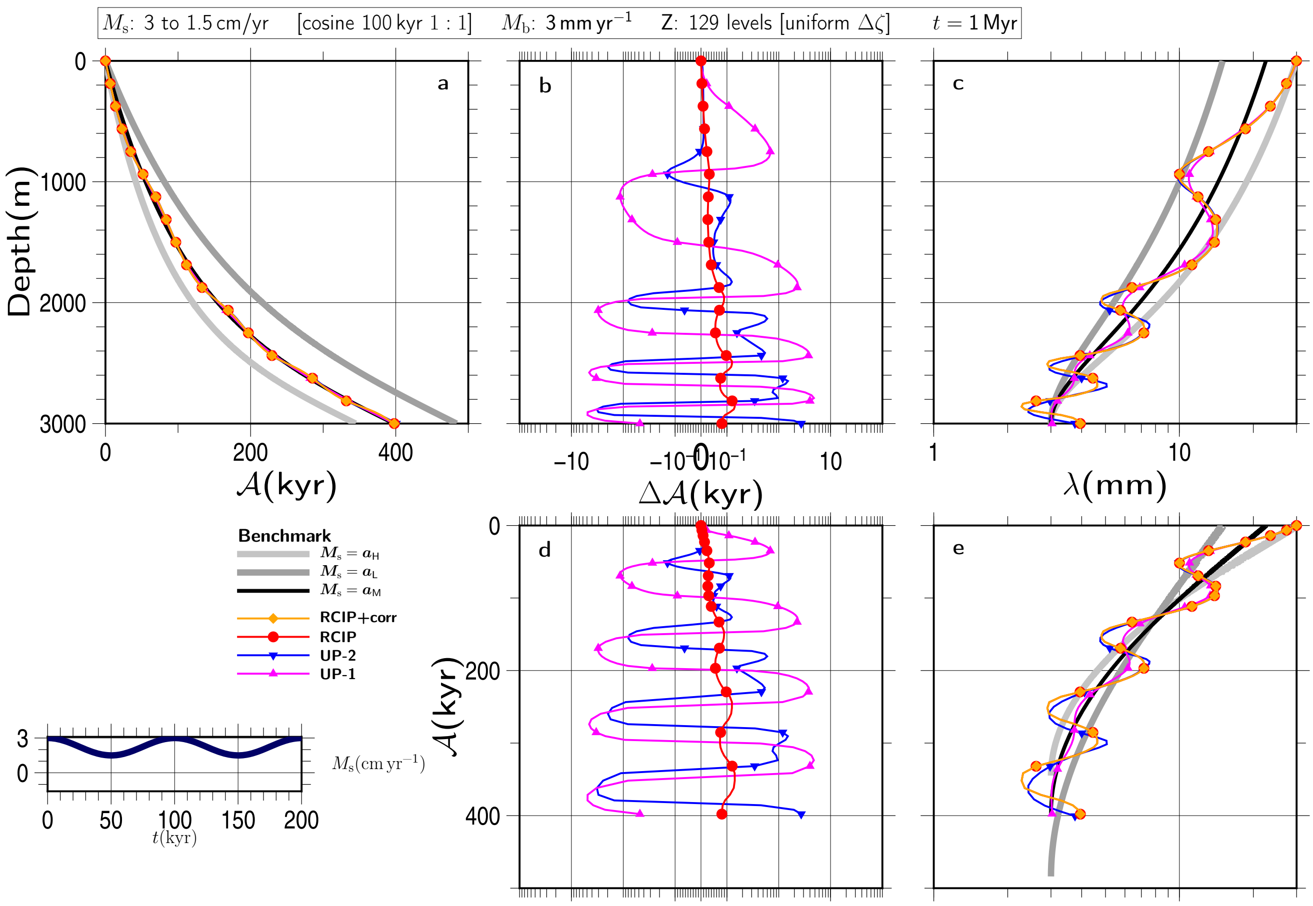

Figure S6

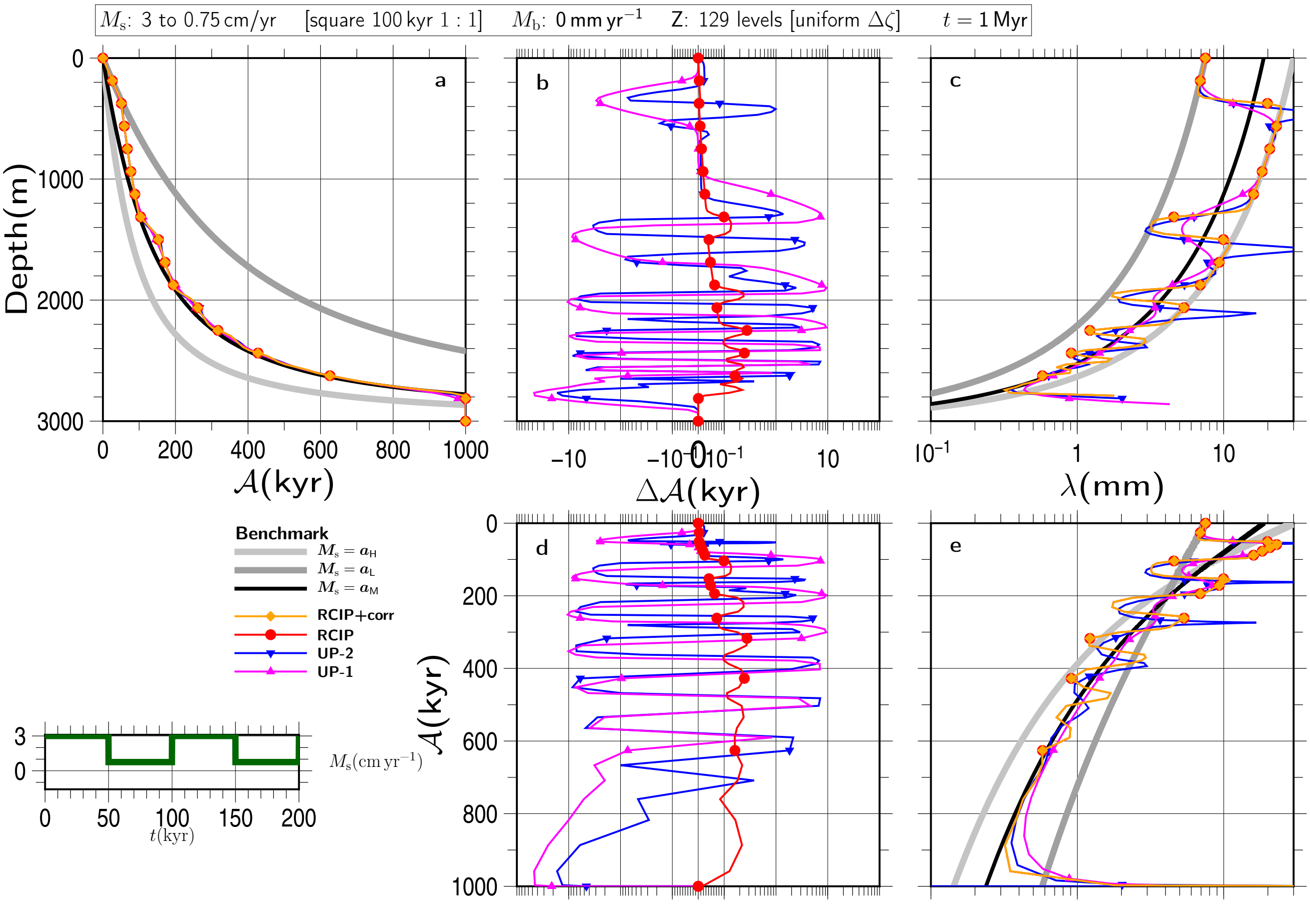

Figure S7

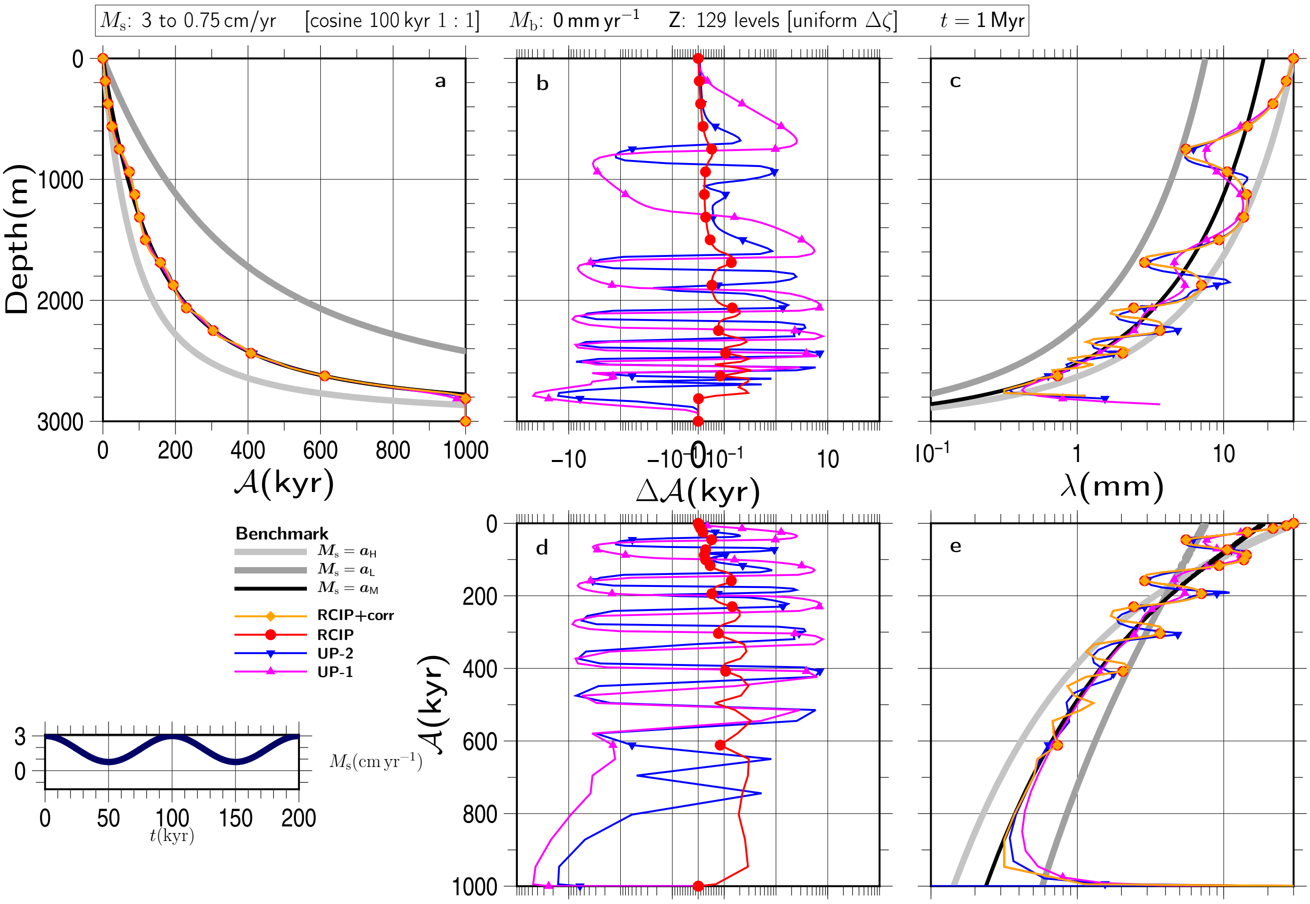

Figure S8

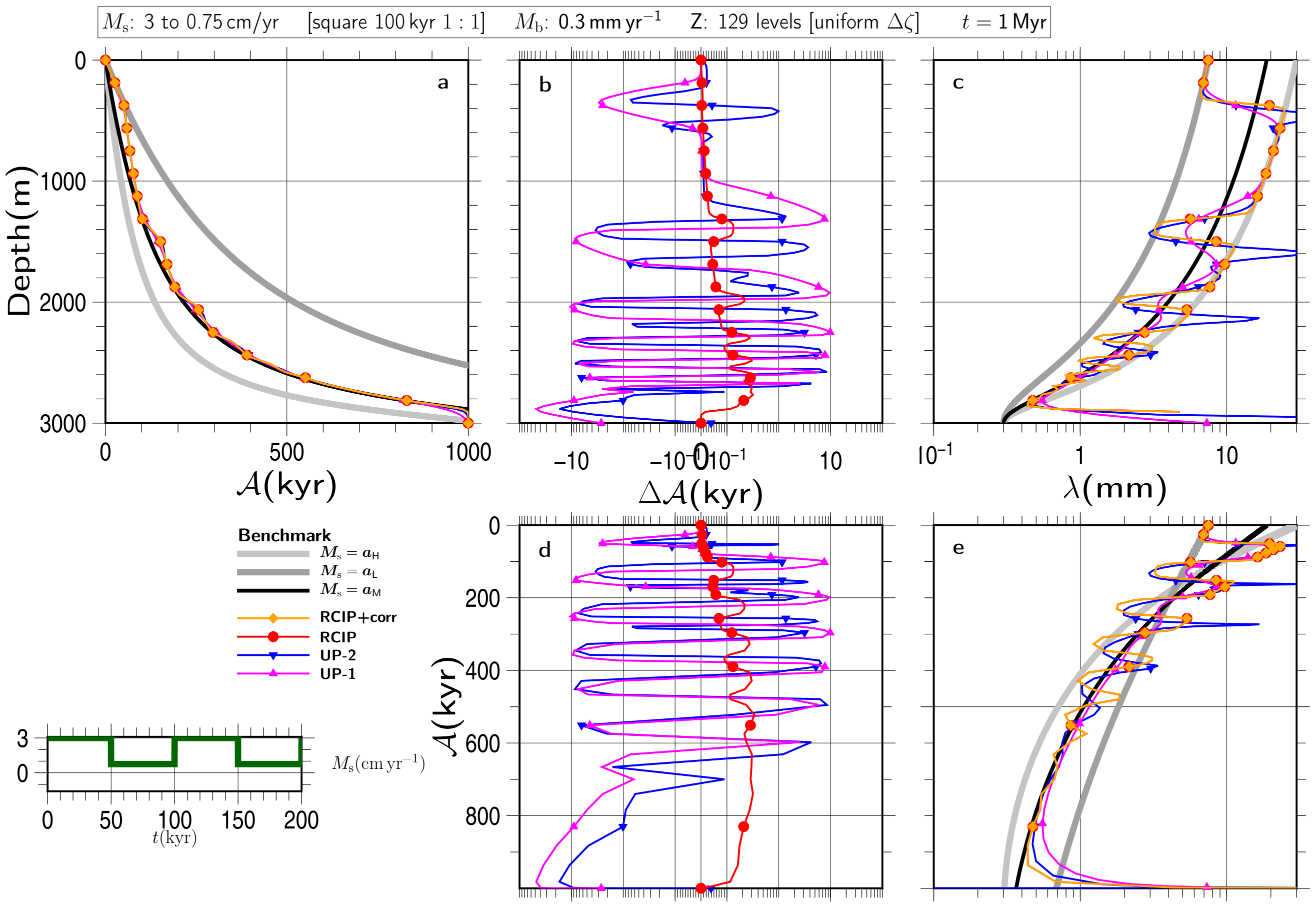

Figure S9

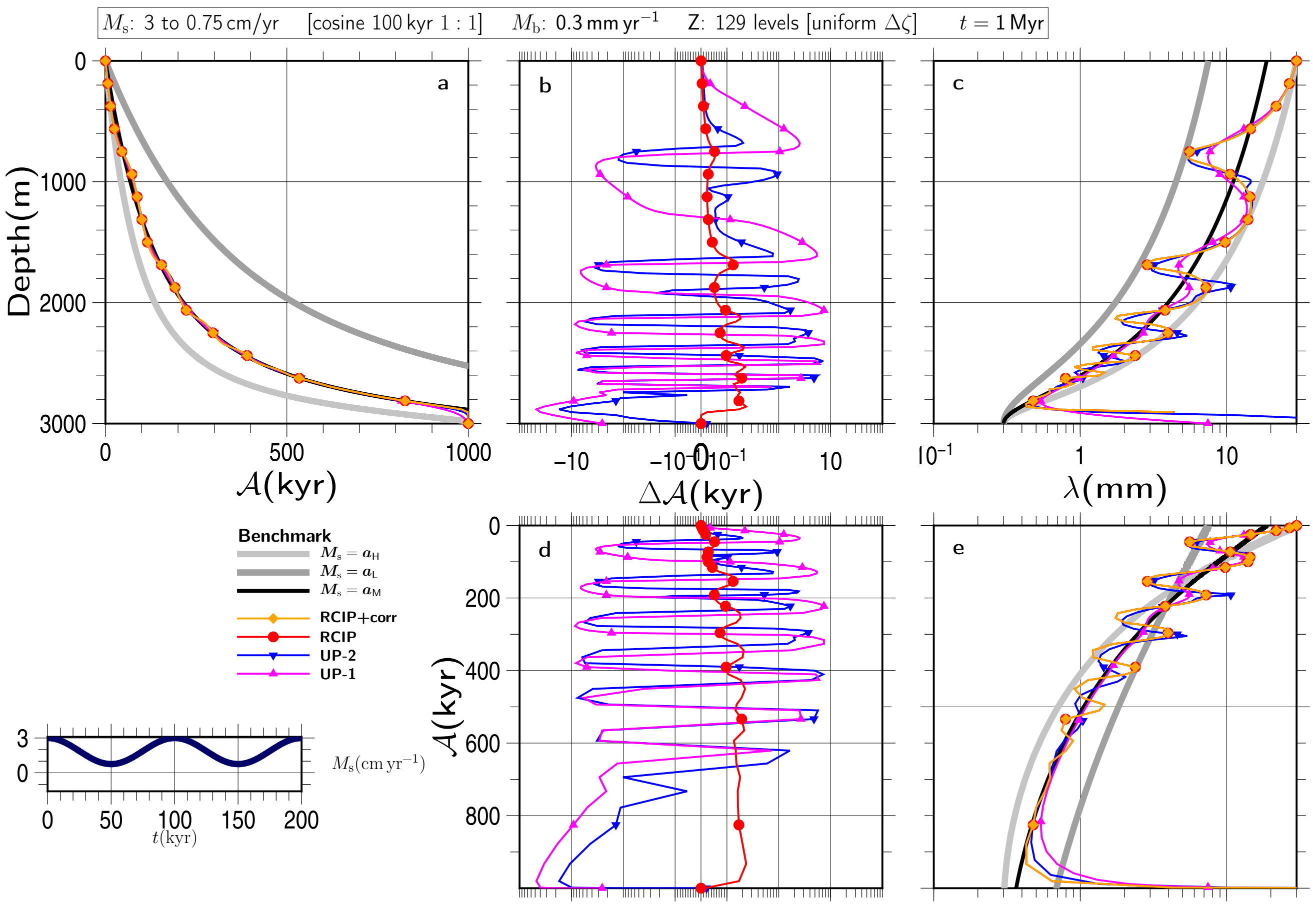

Figure S10

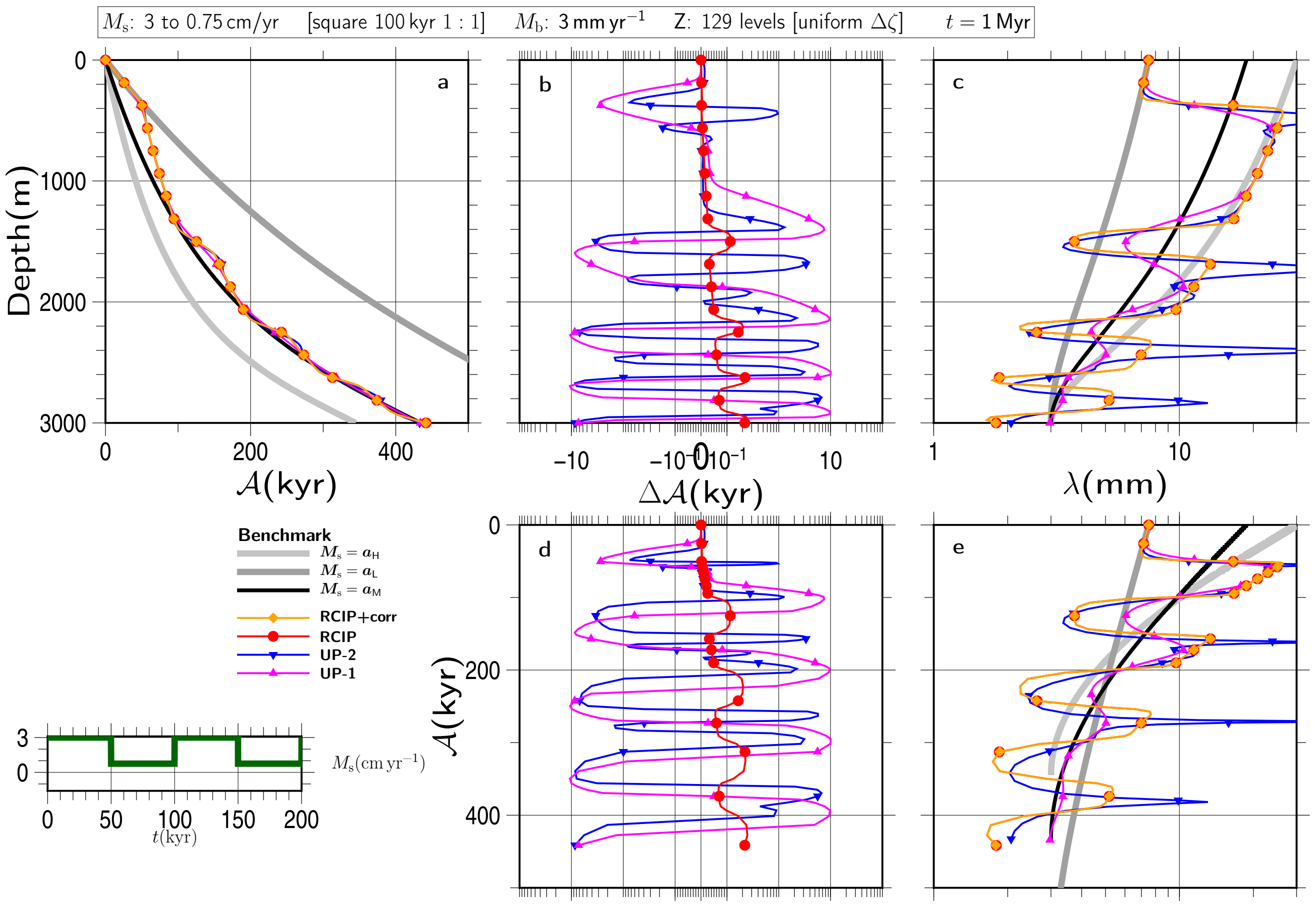

Figure S11

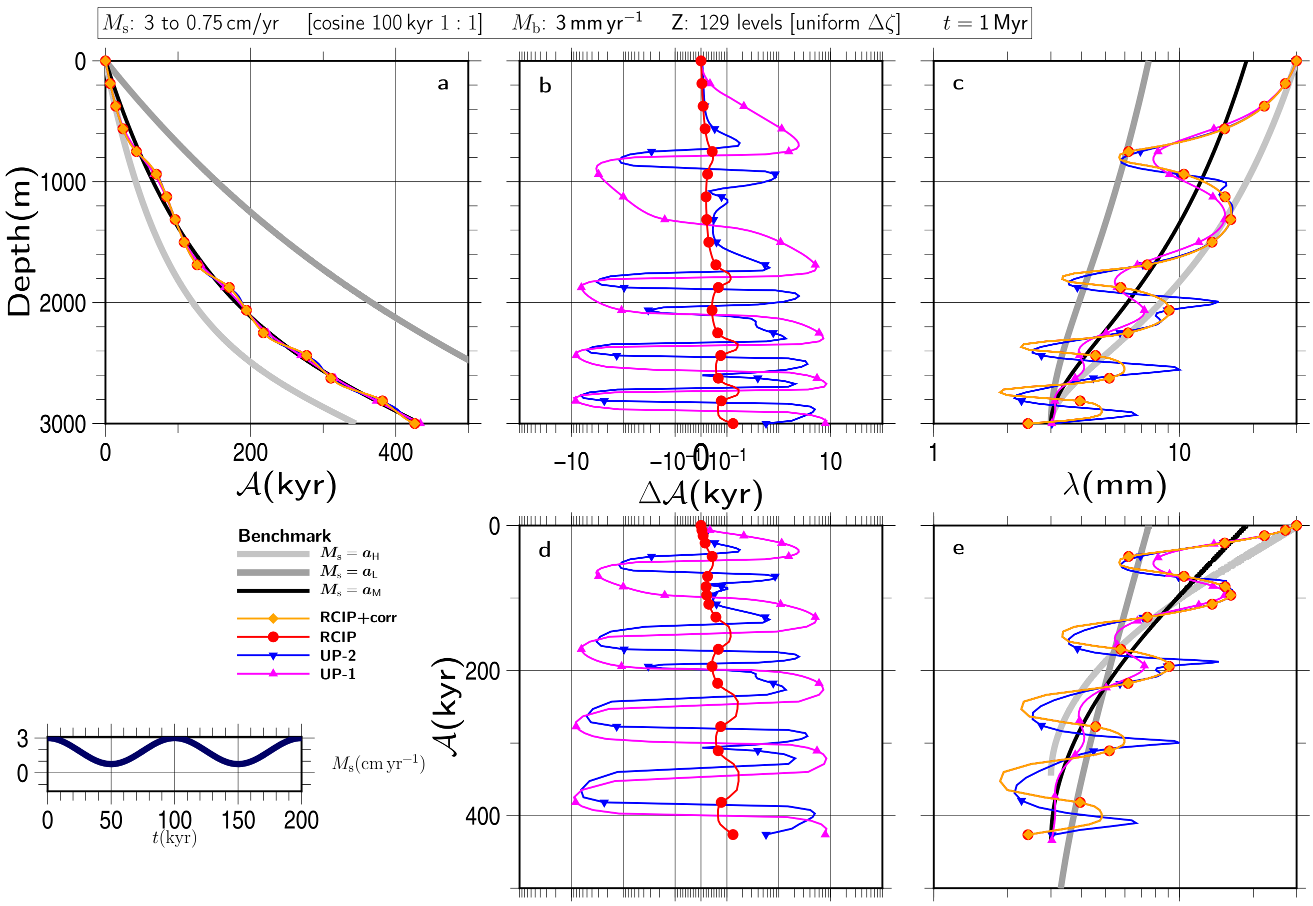

Figure S12

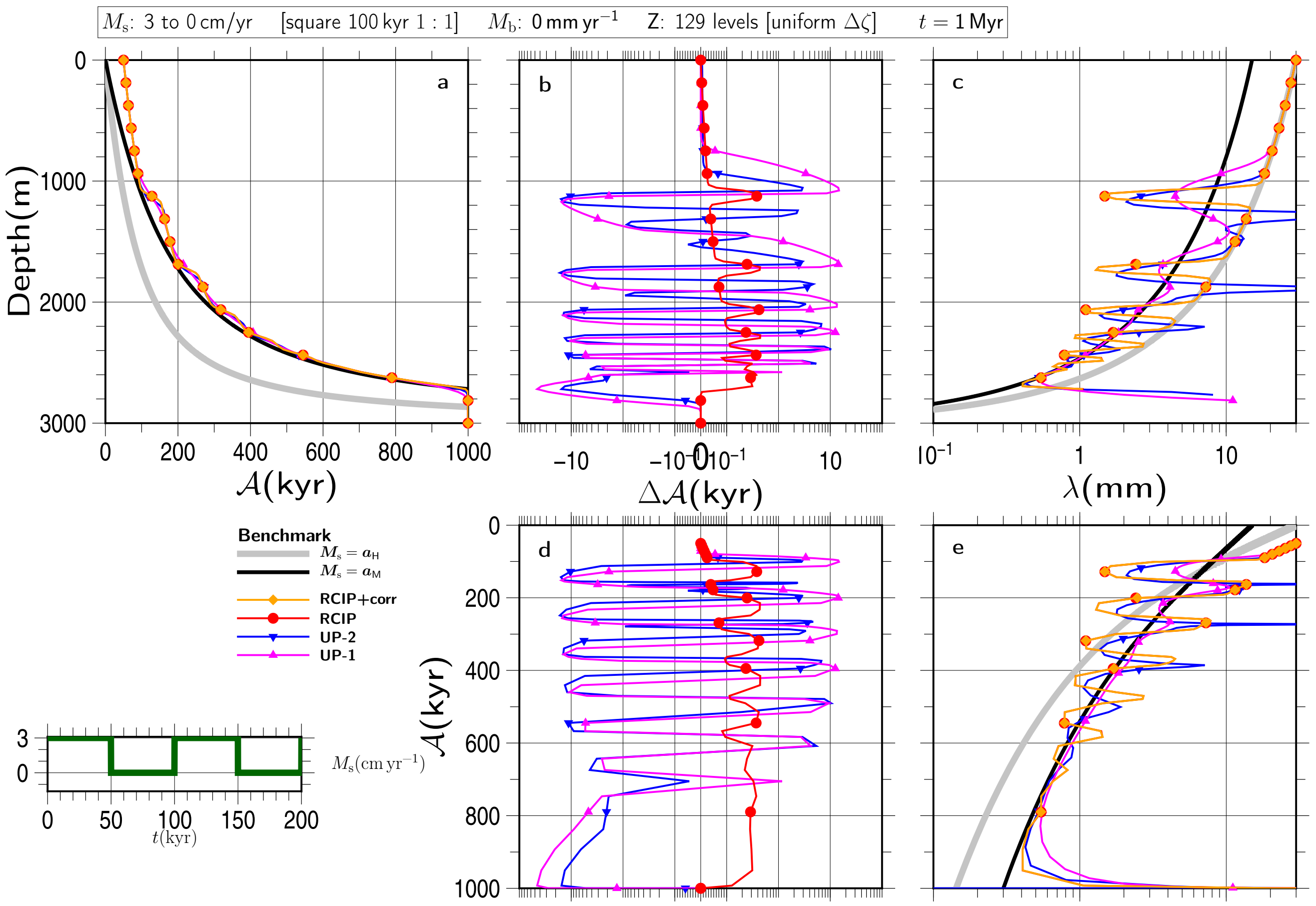

Figure S13

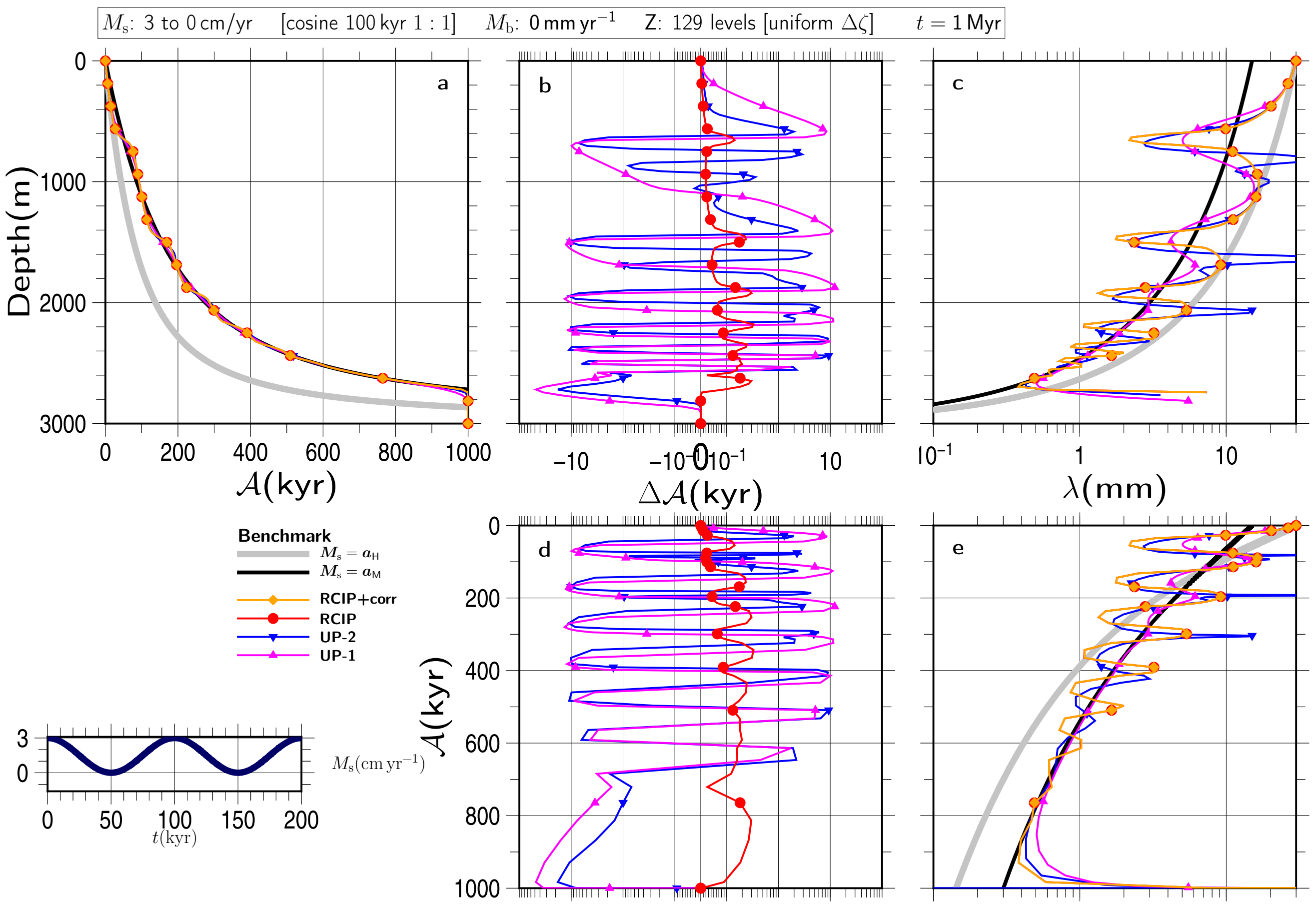

Figure S14

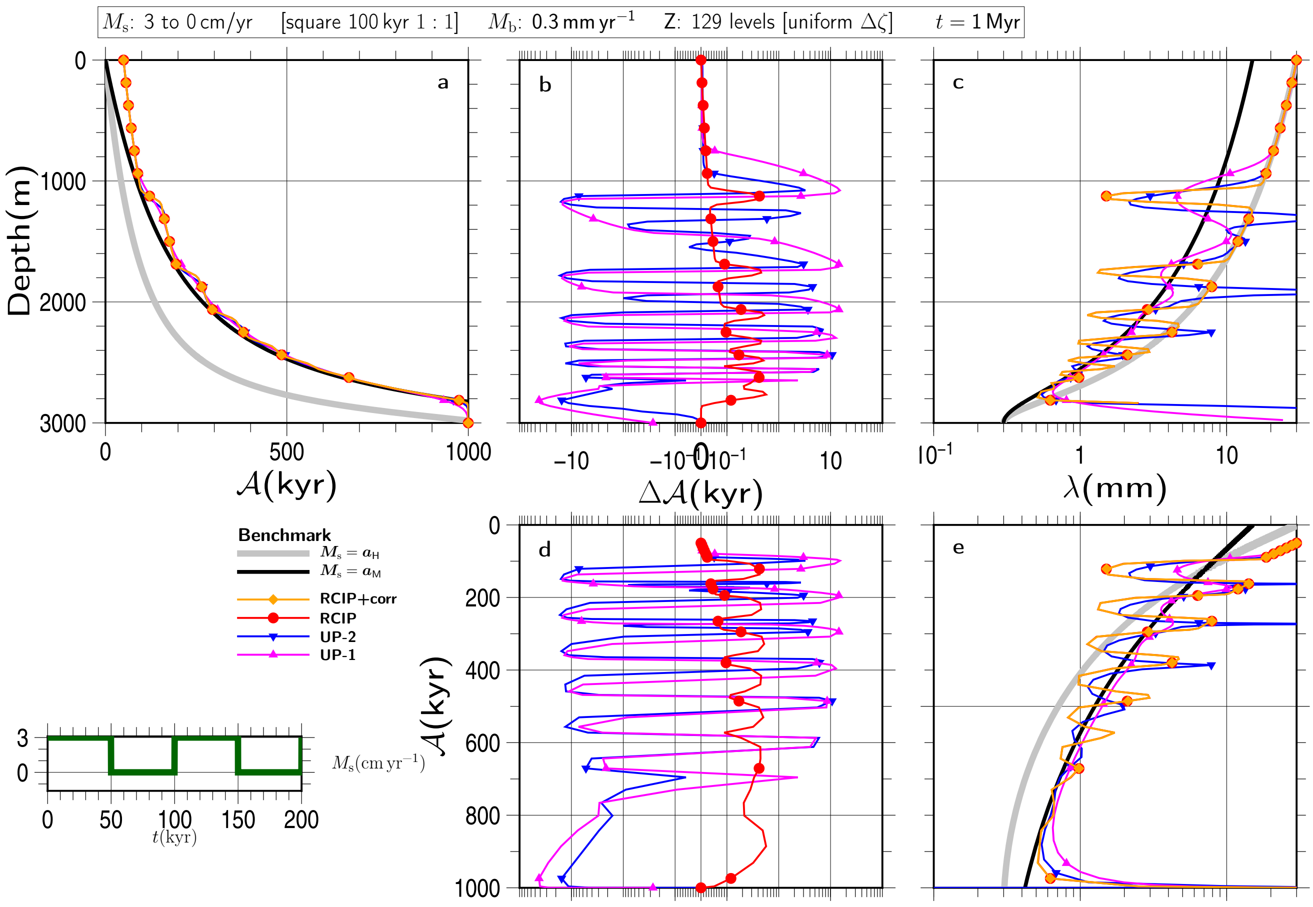

Figure S15

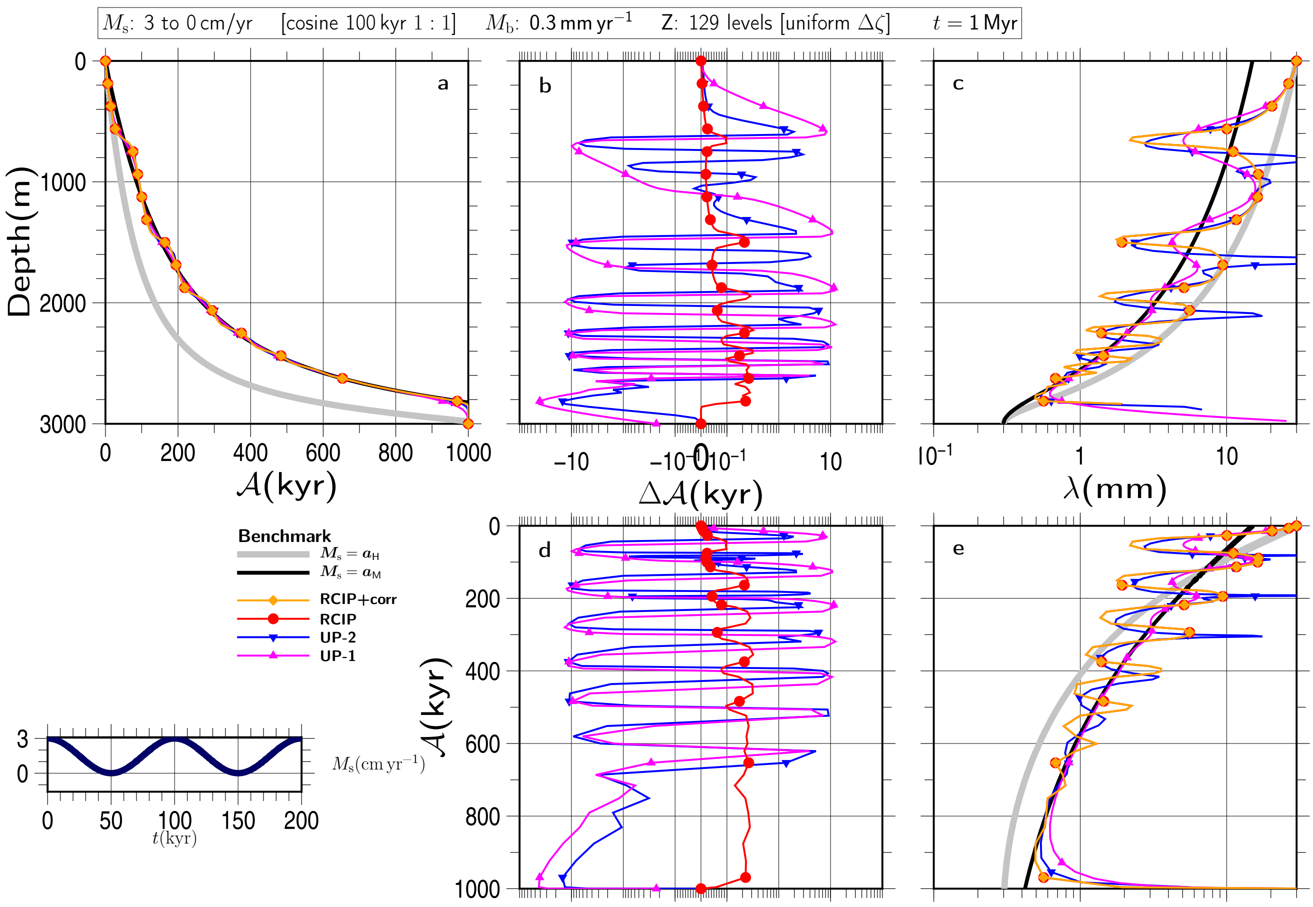

Figure S16

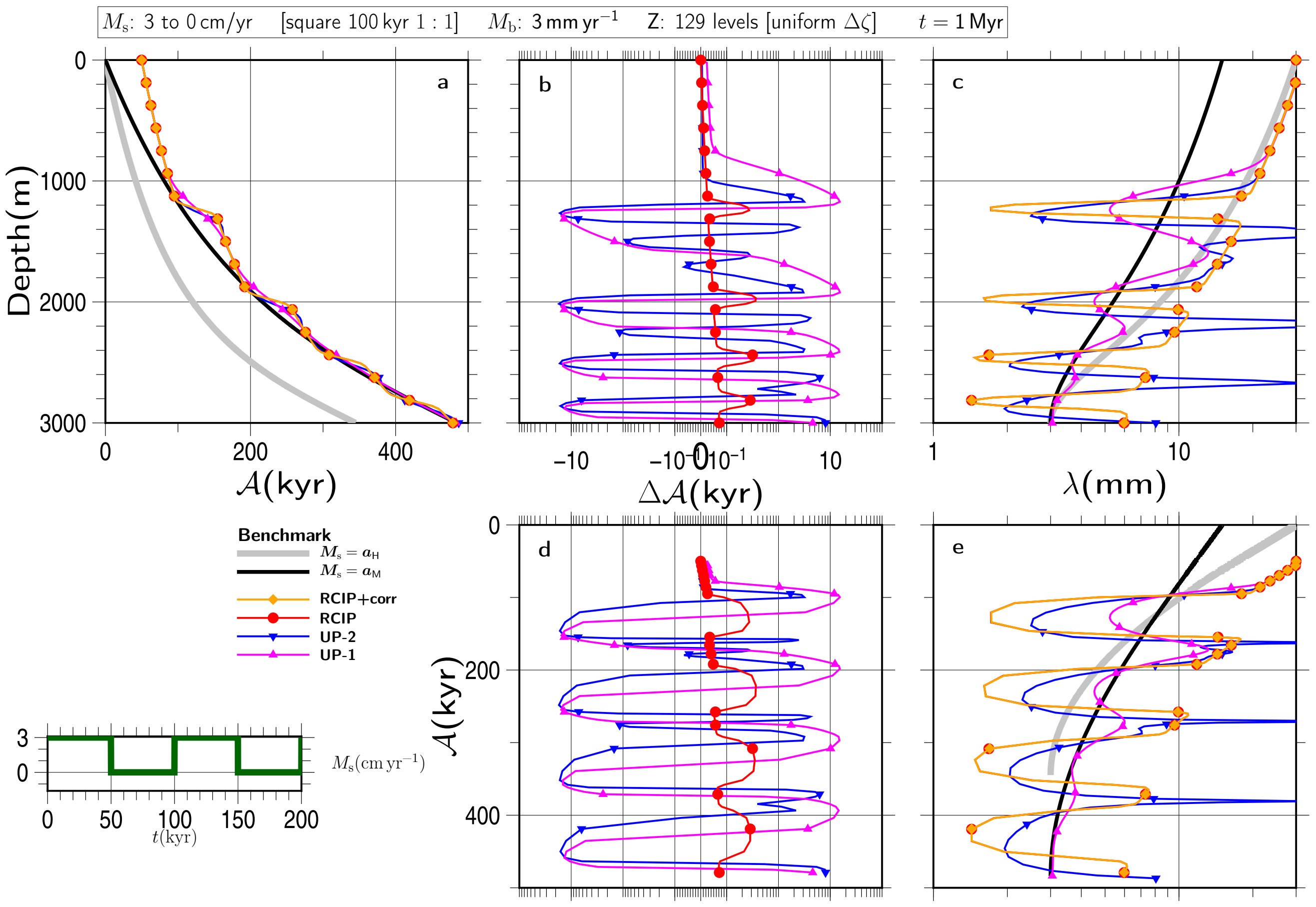

Figure S17

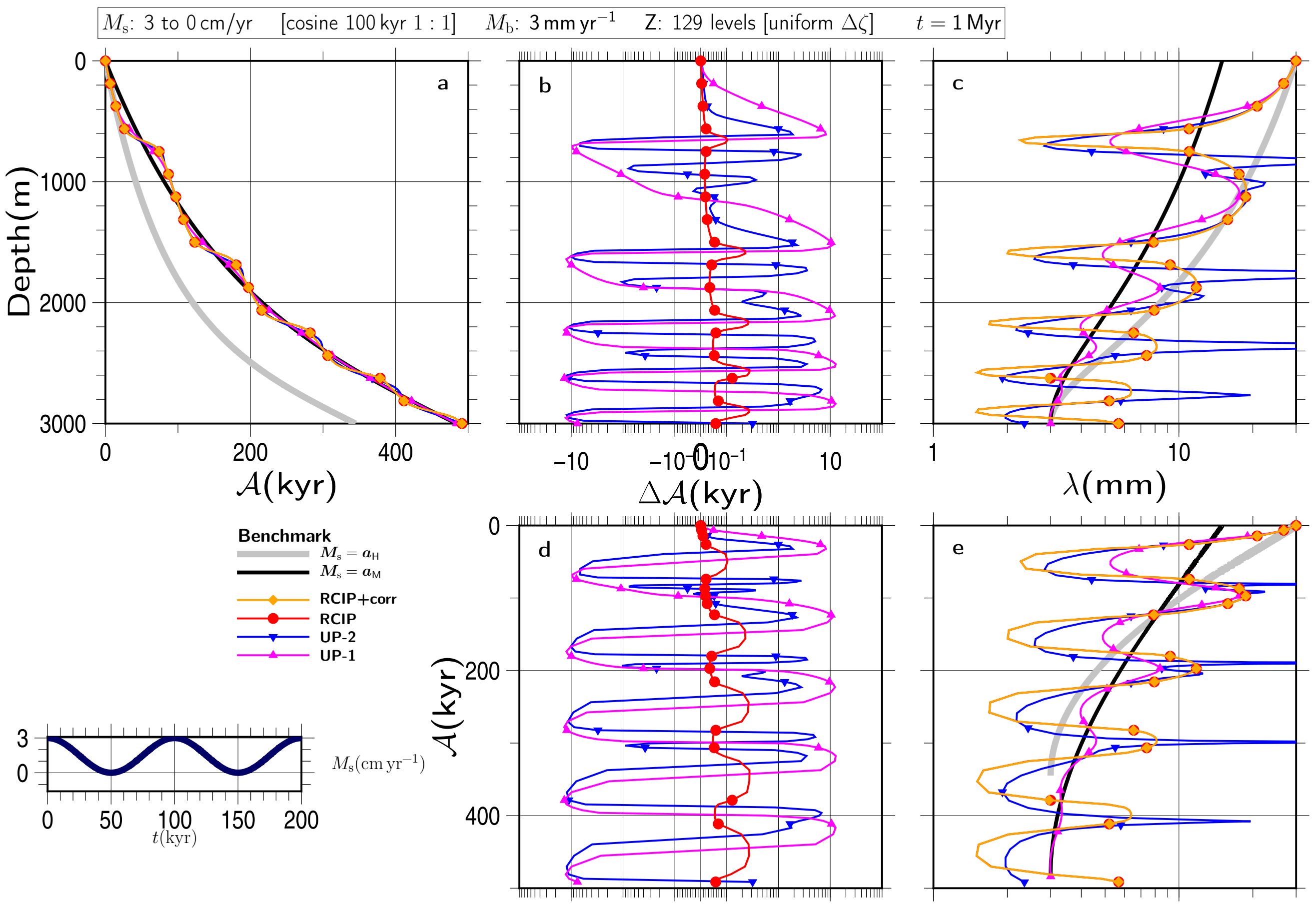

Figure S18

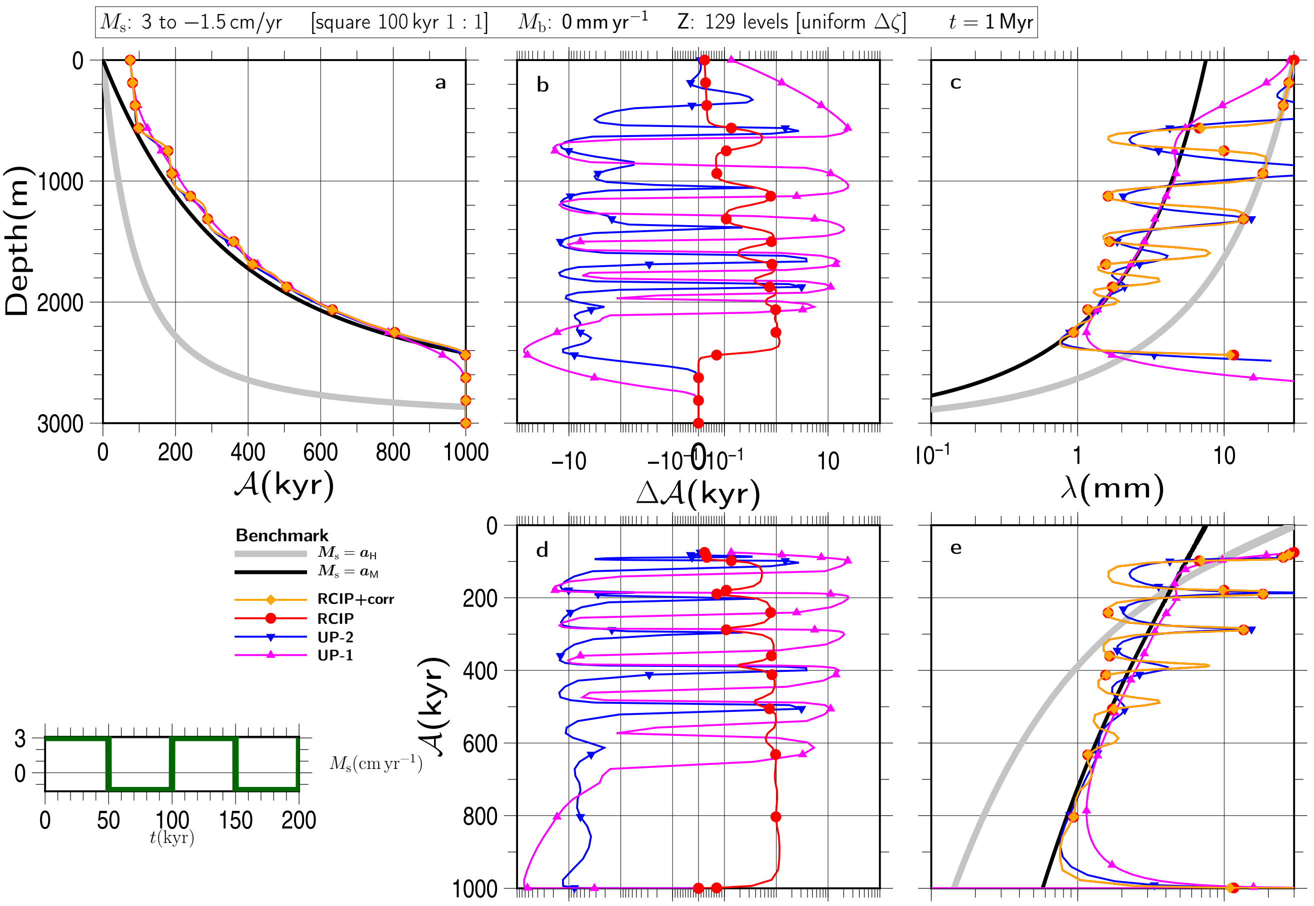

Figure S19

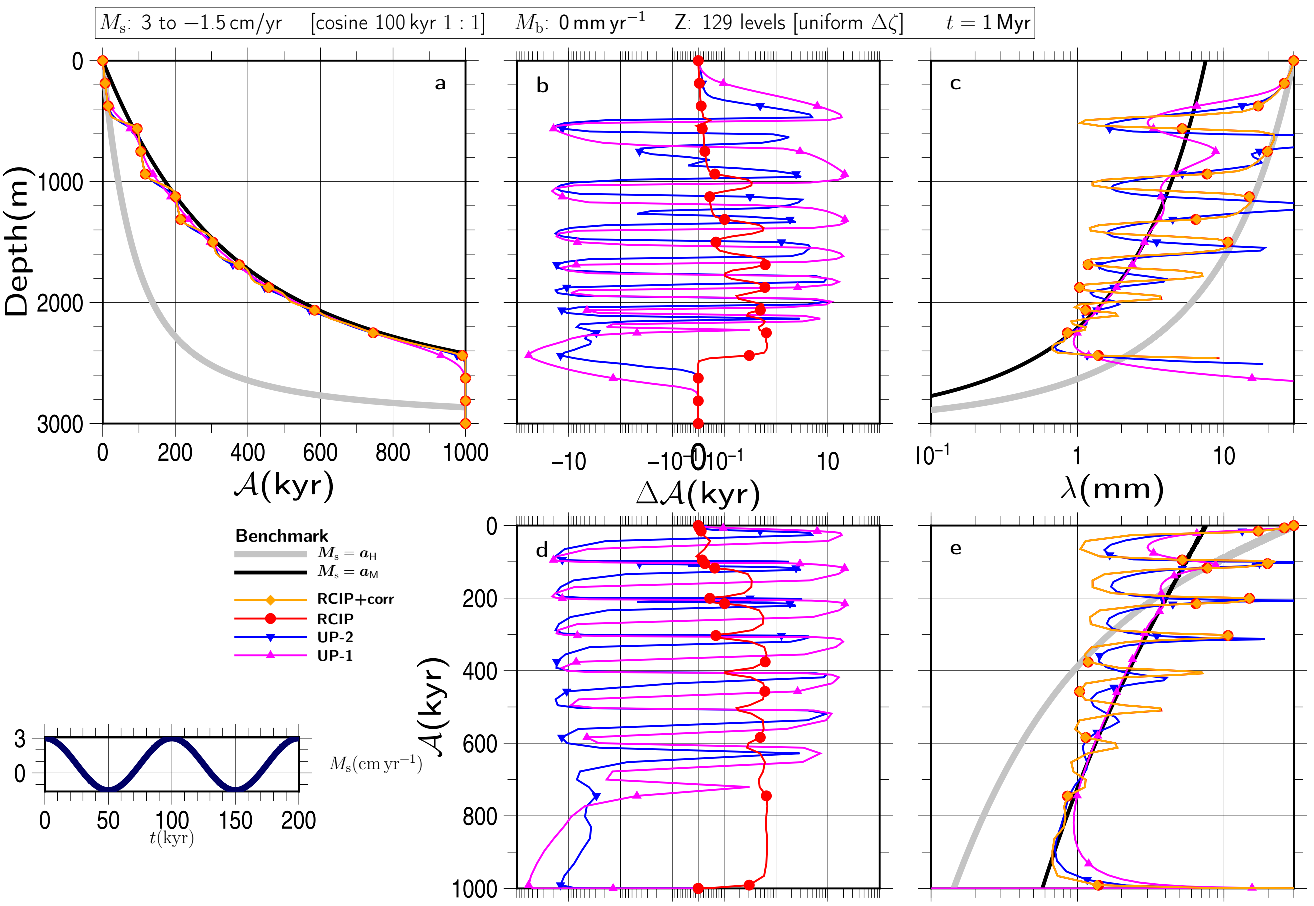

Figure S20

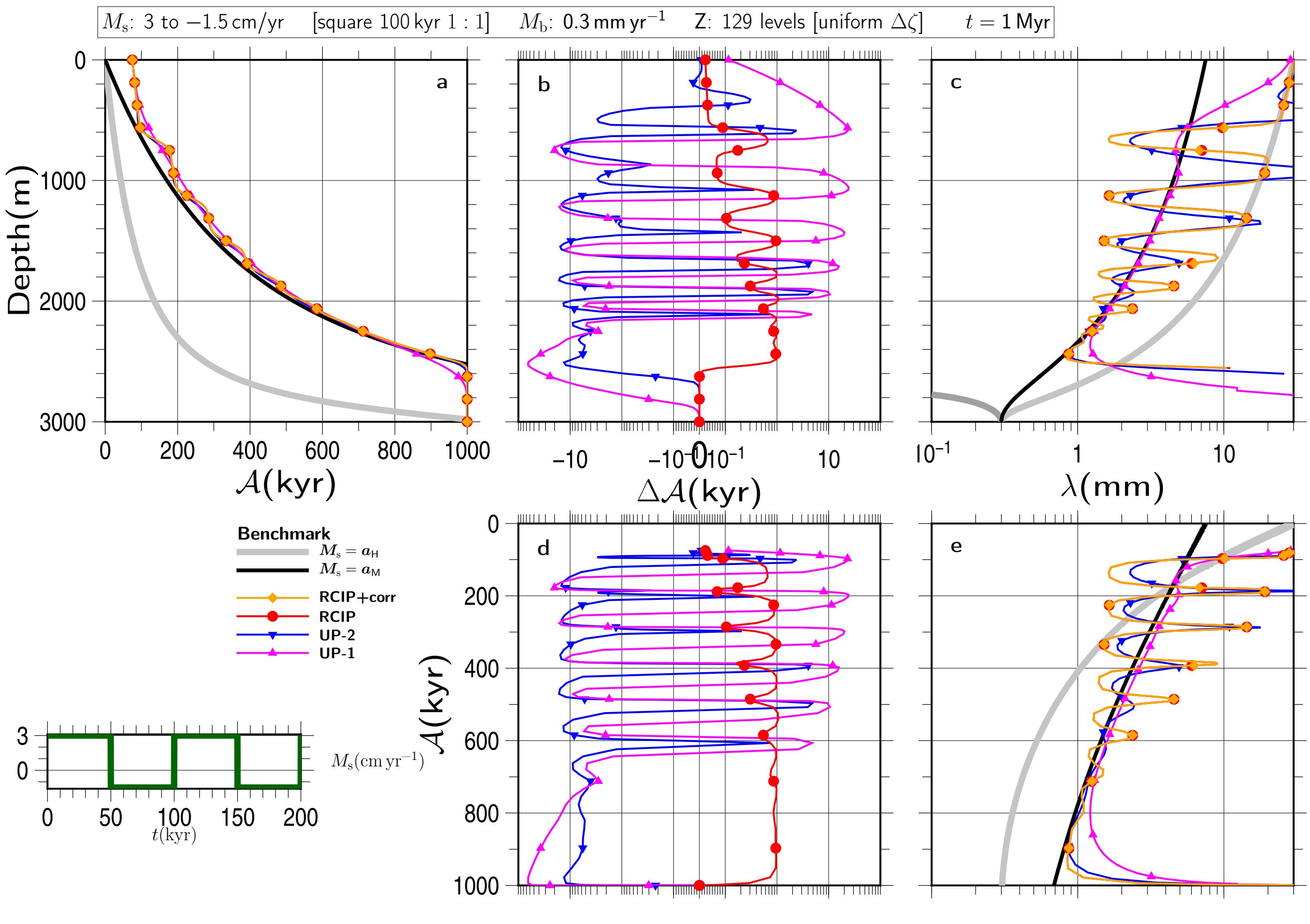

Figure S21

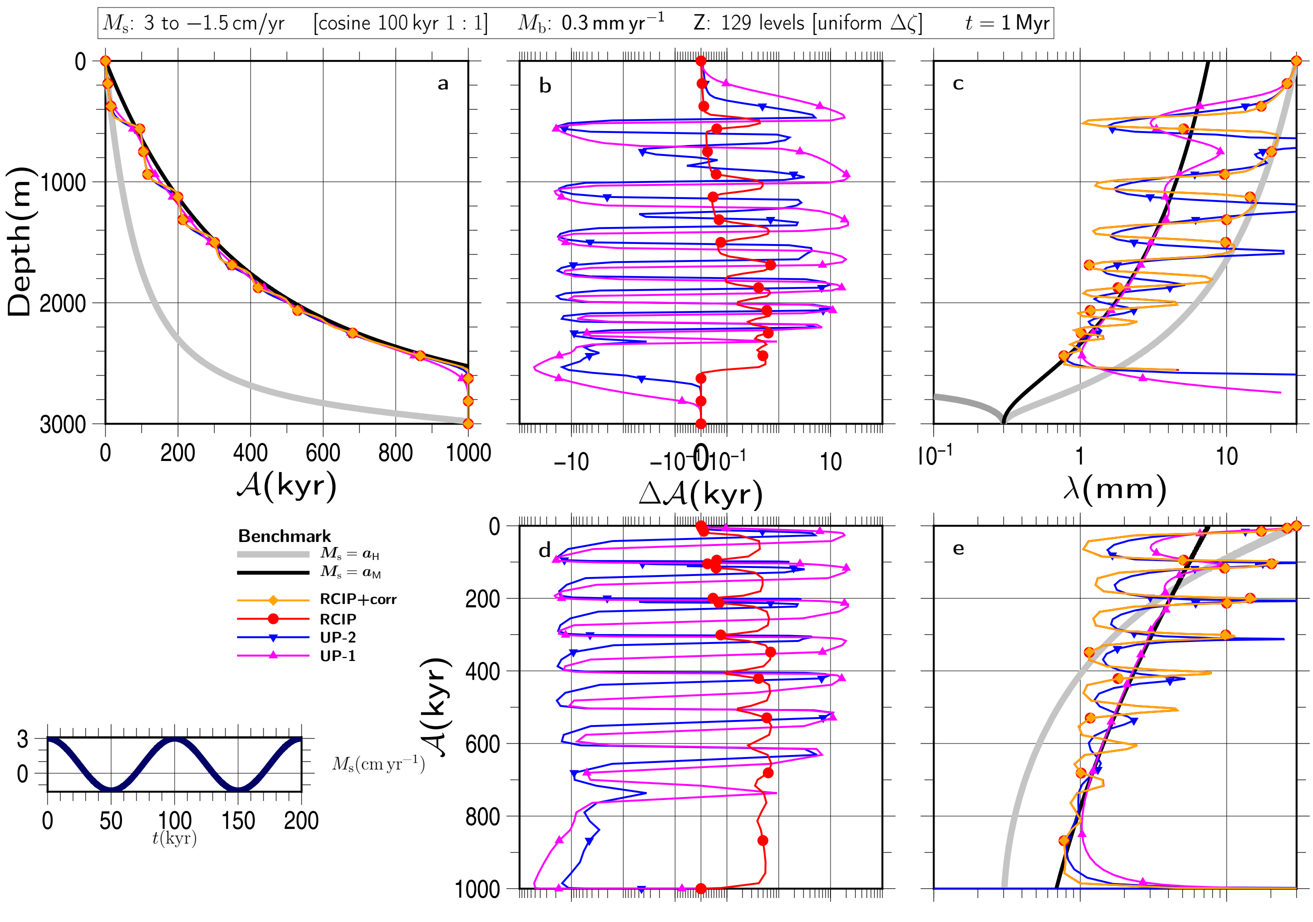

Figure S22

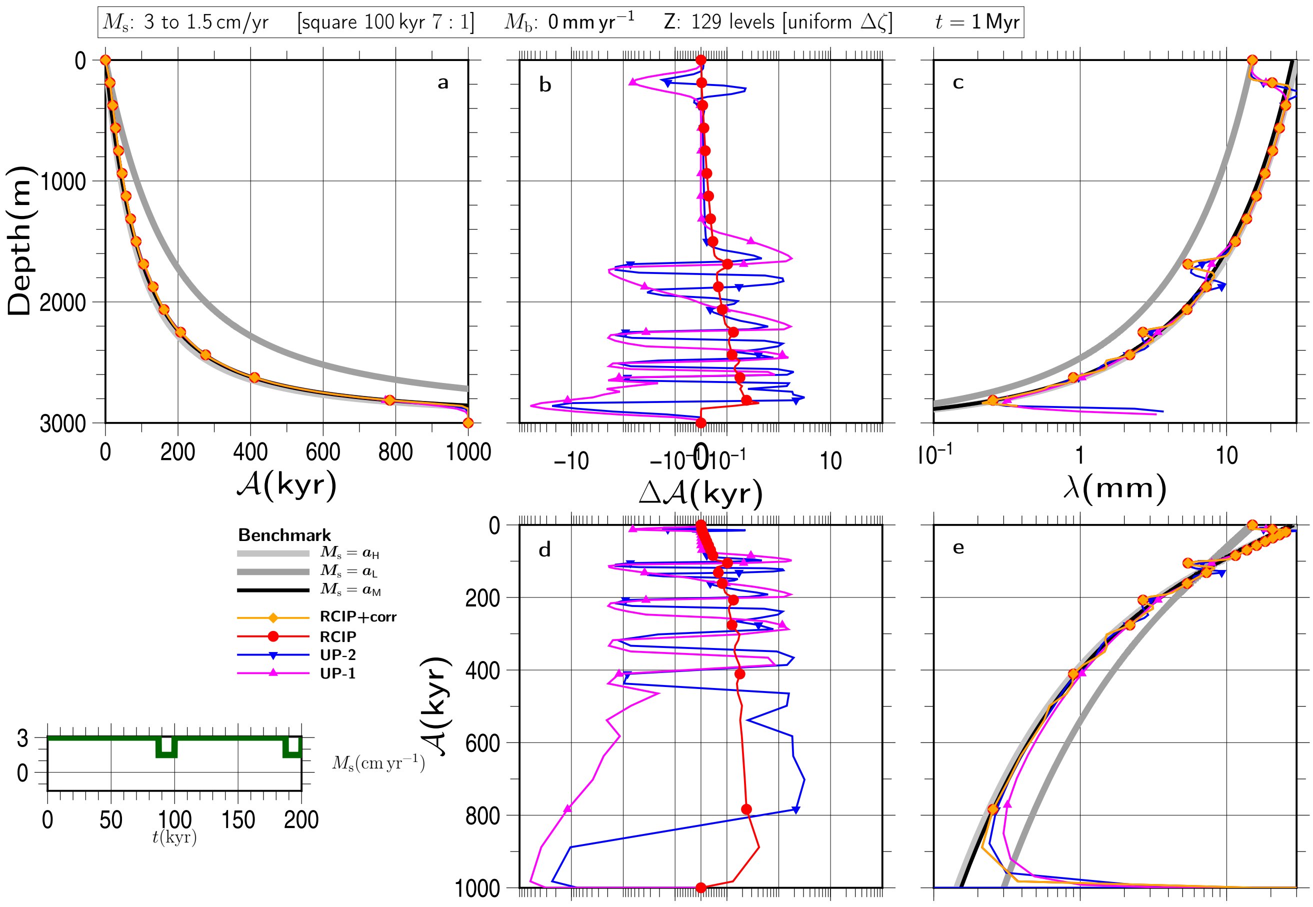

Figure S23

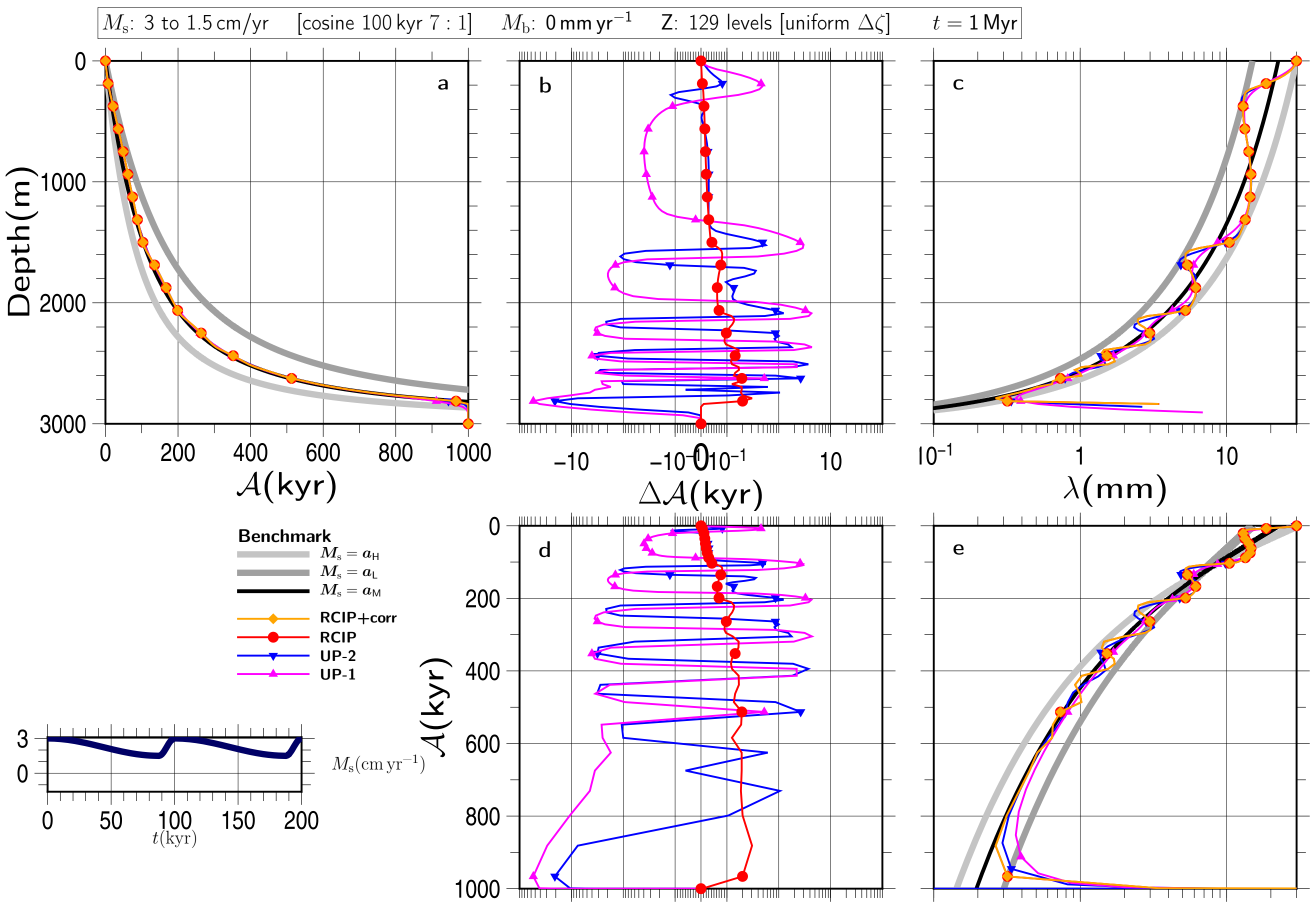

Figure S24

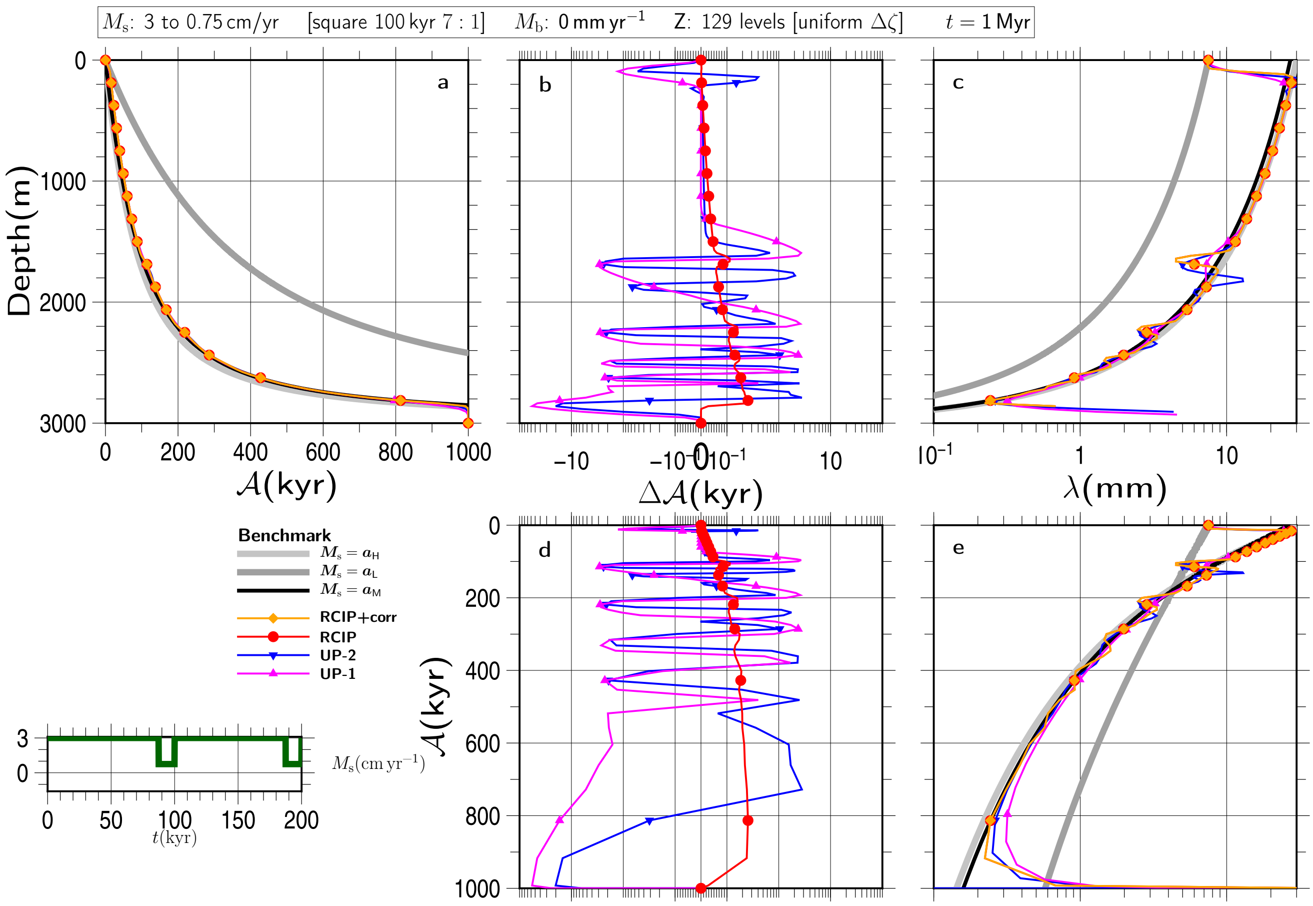

Figure S25

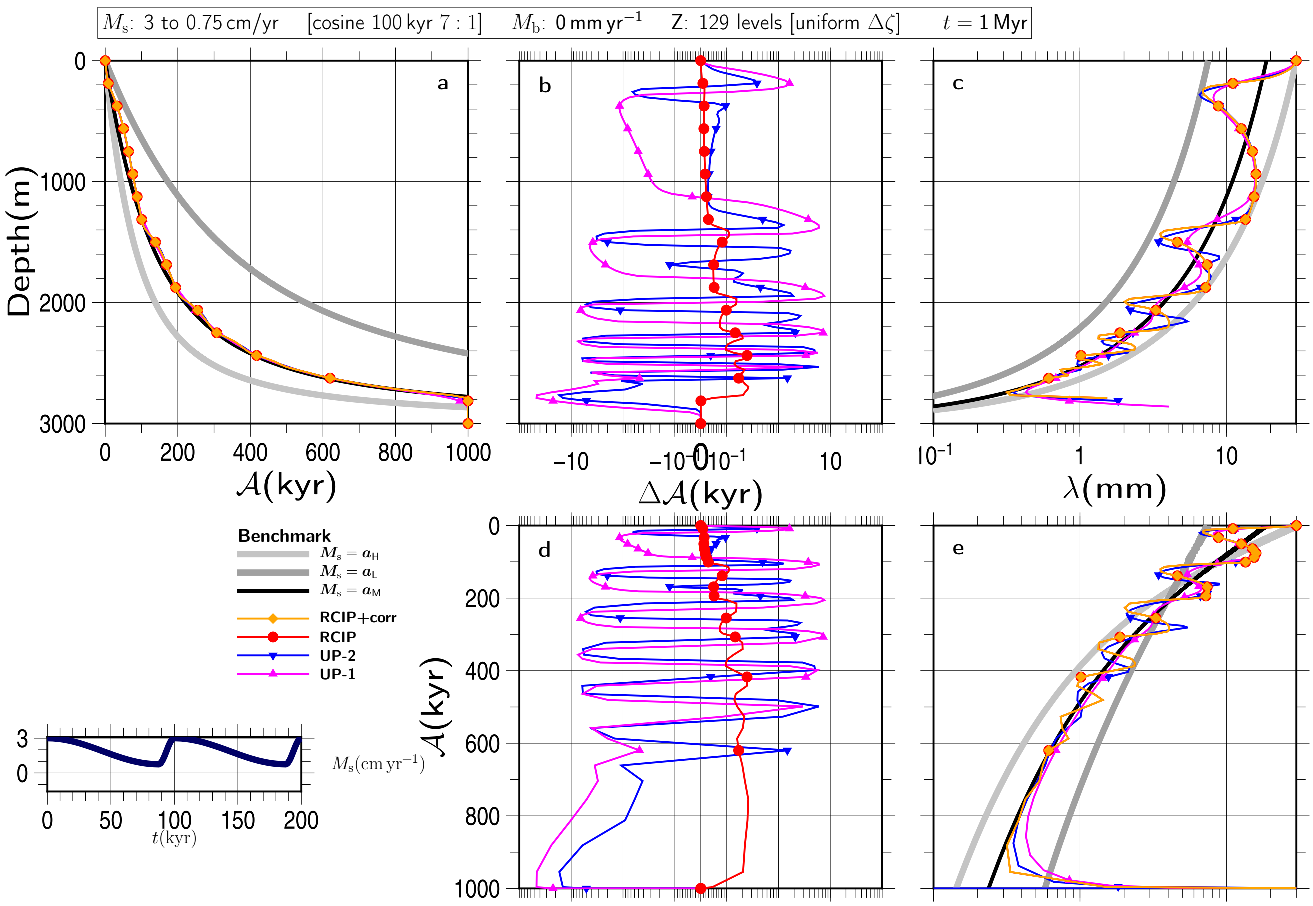

Figure S26

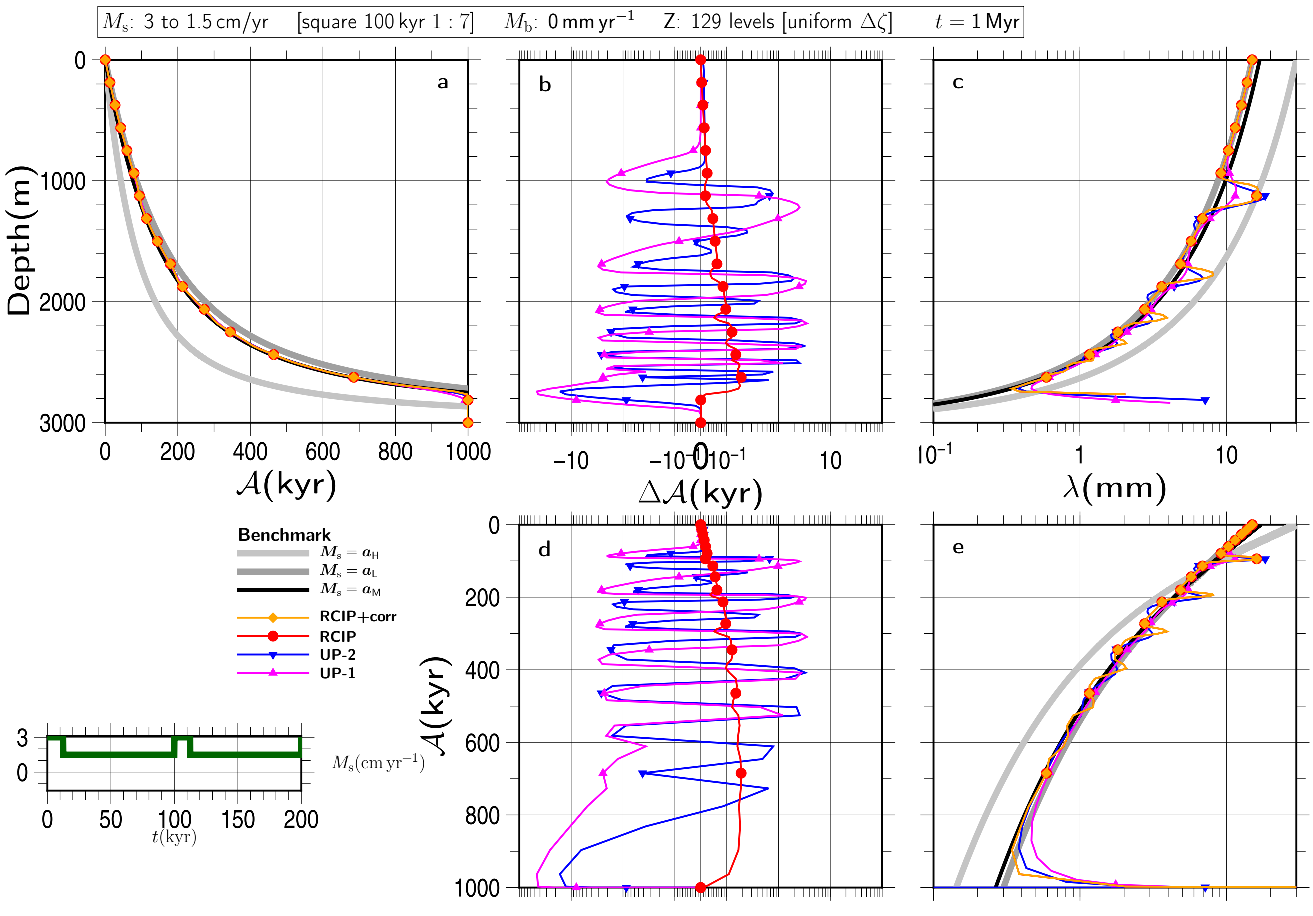

Figure S27

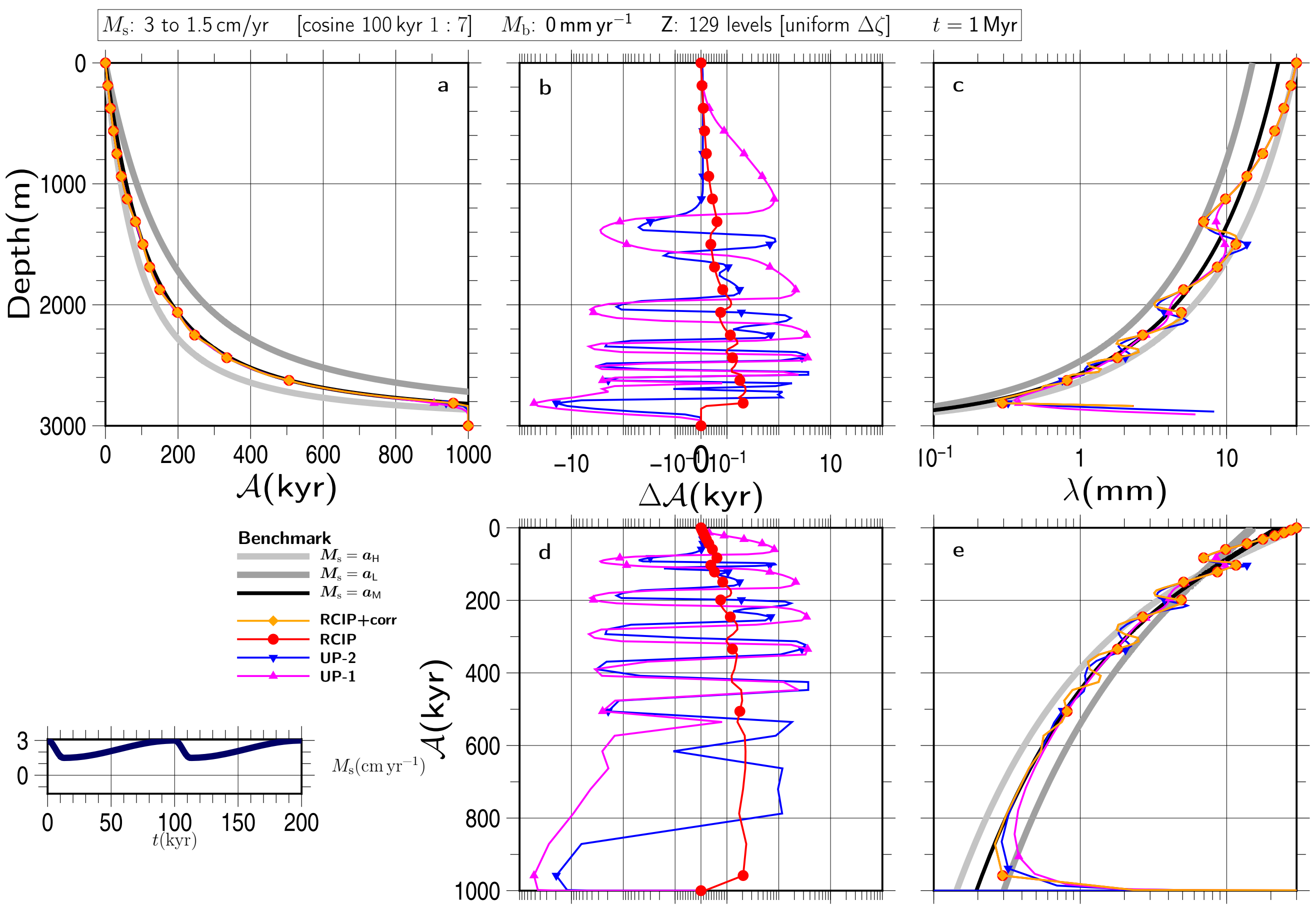

Figure S28

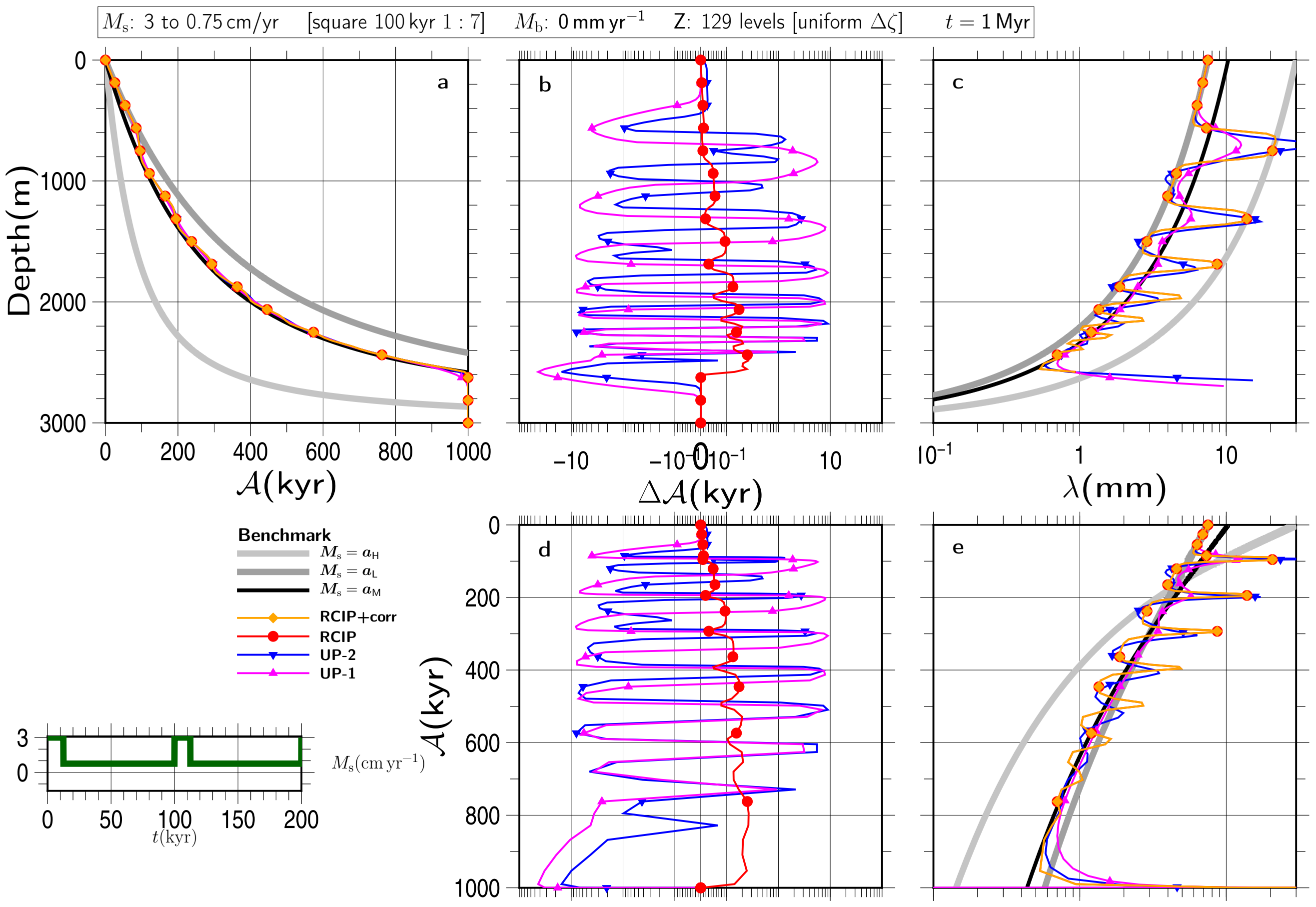

Figure S29

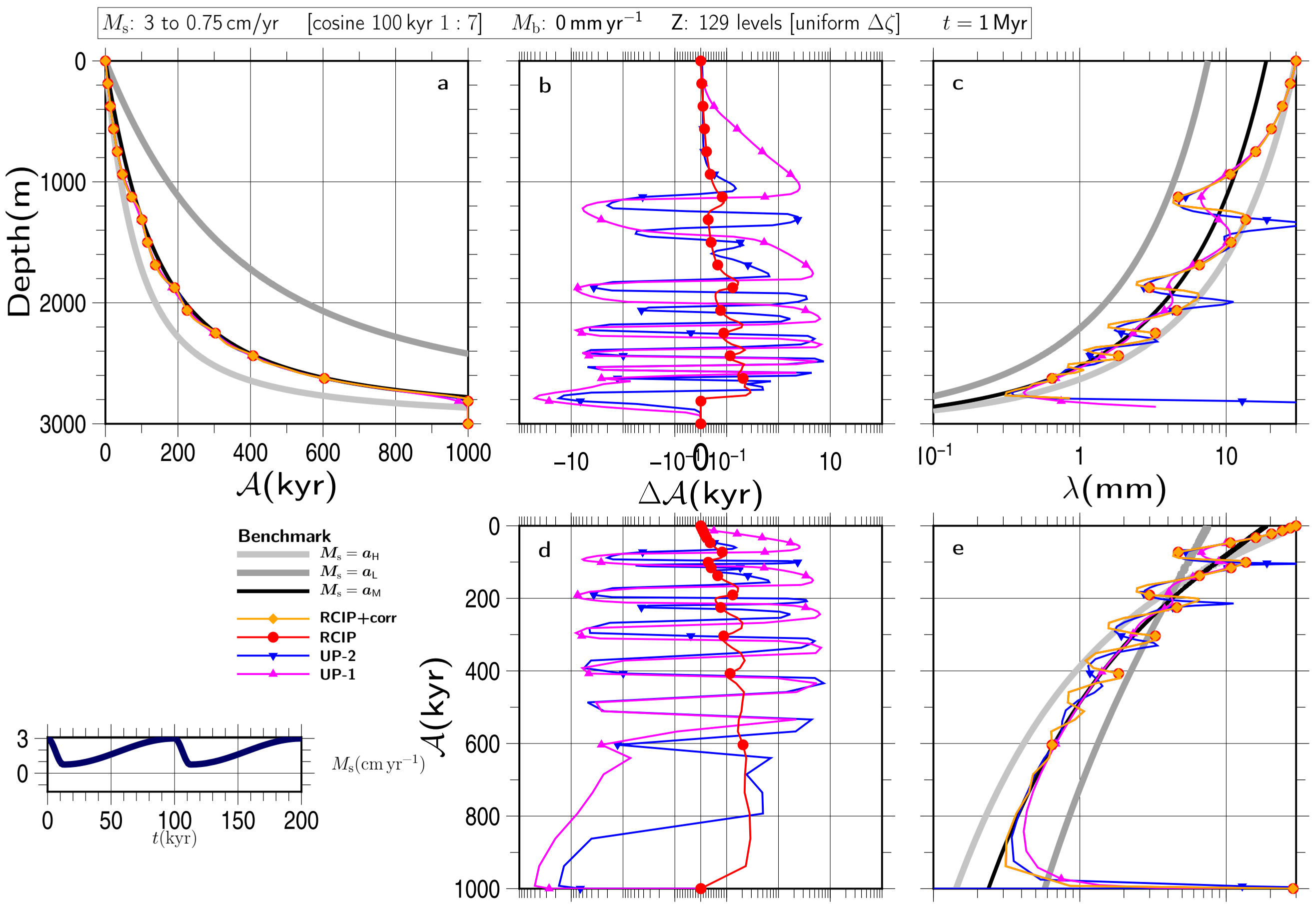

Figure S30

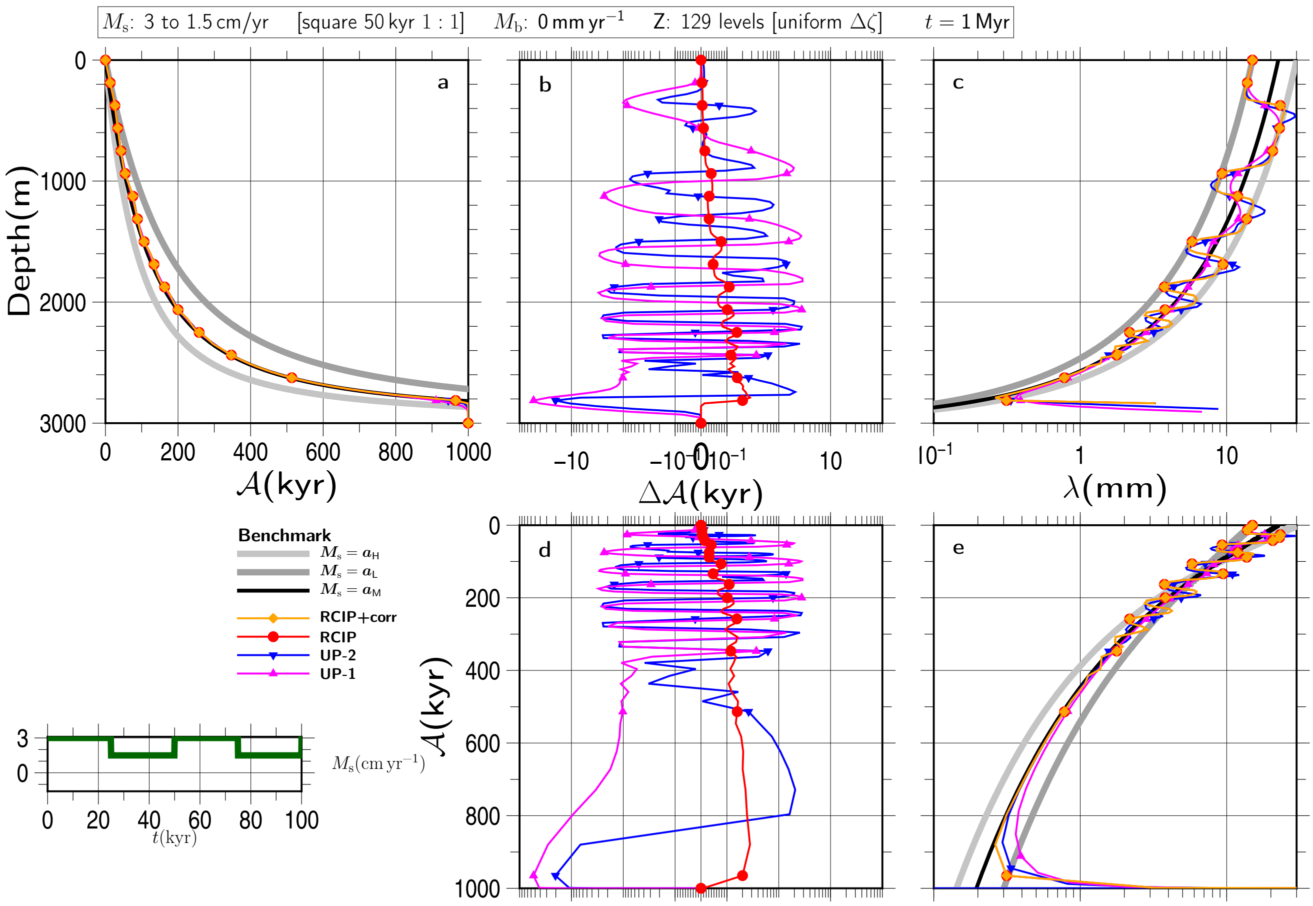

Figure S31

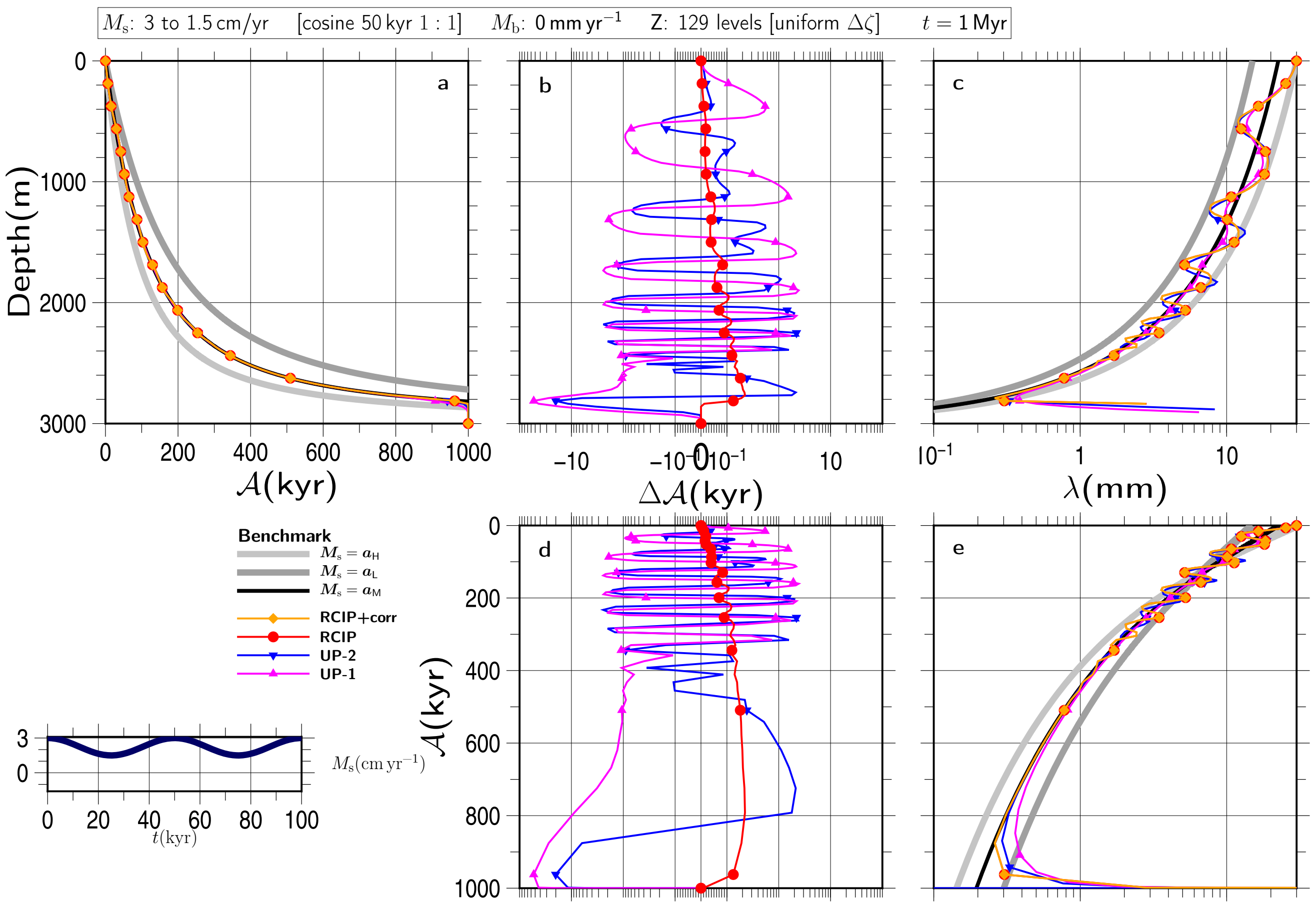

Figure S32

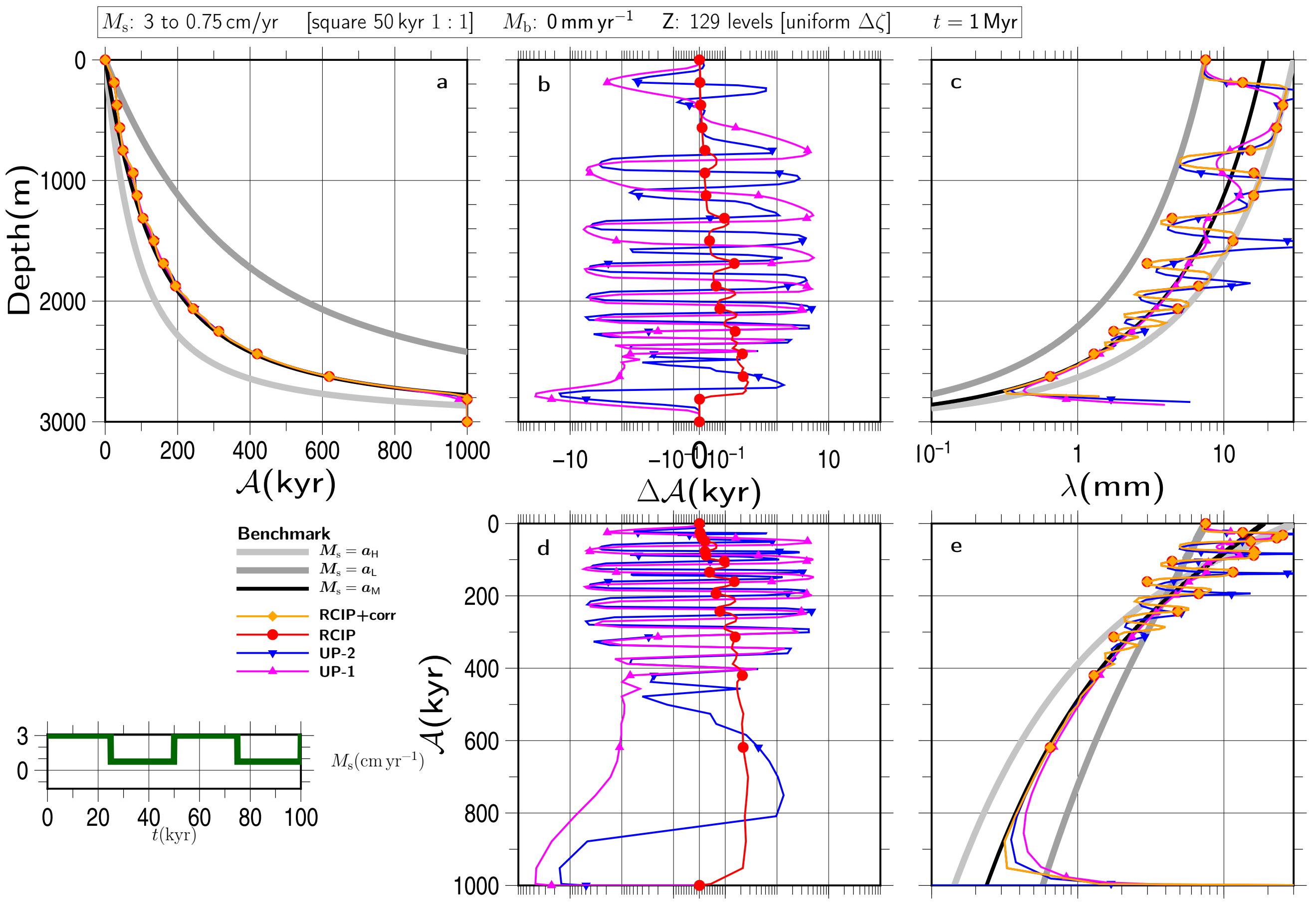

Figure S33

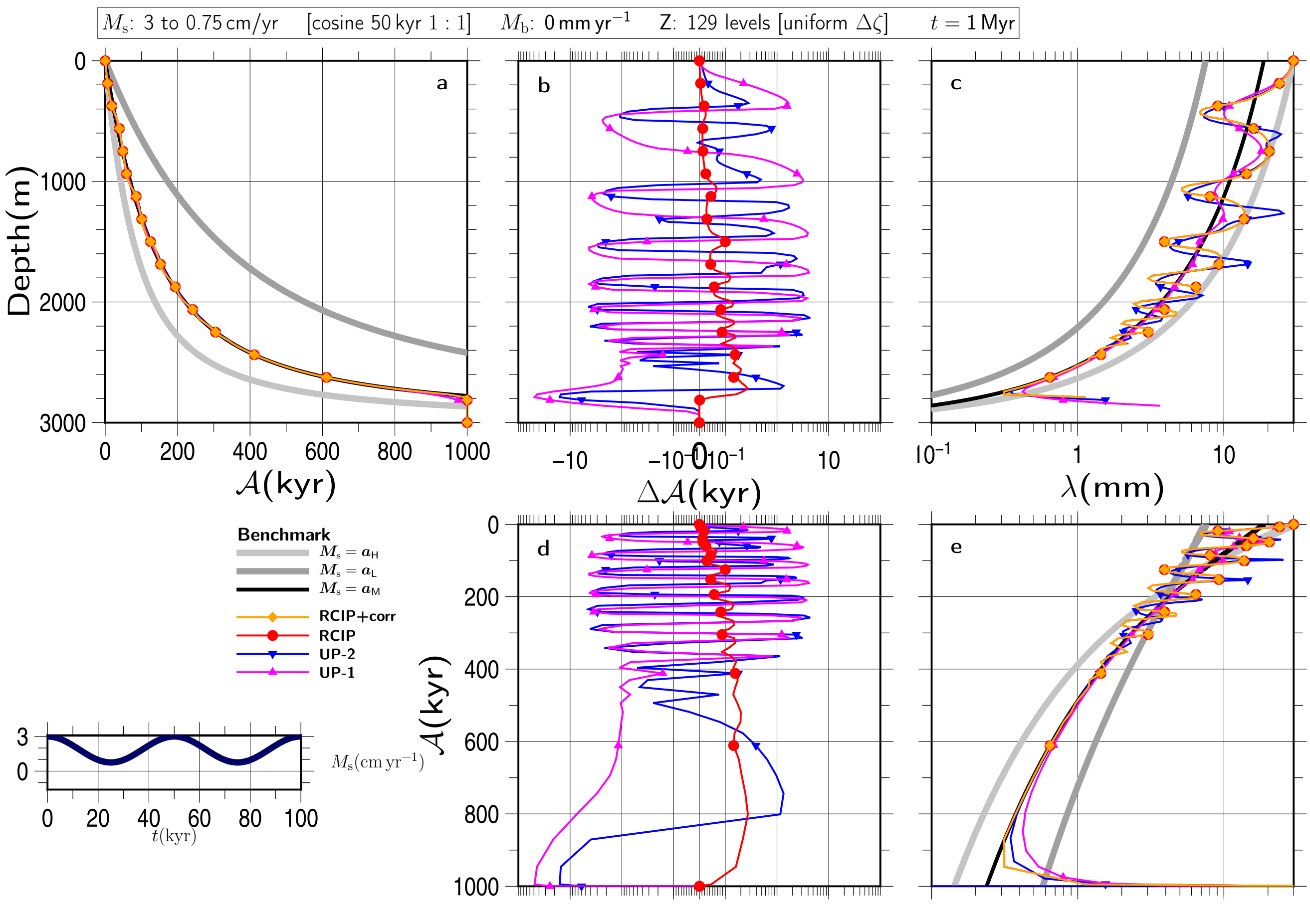

Figure S34

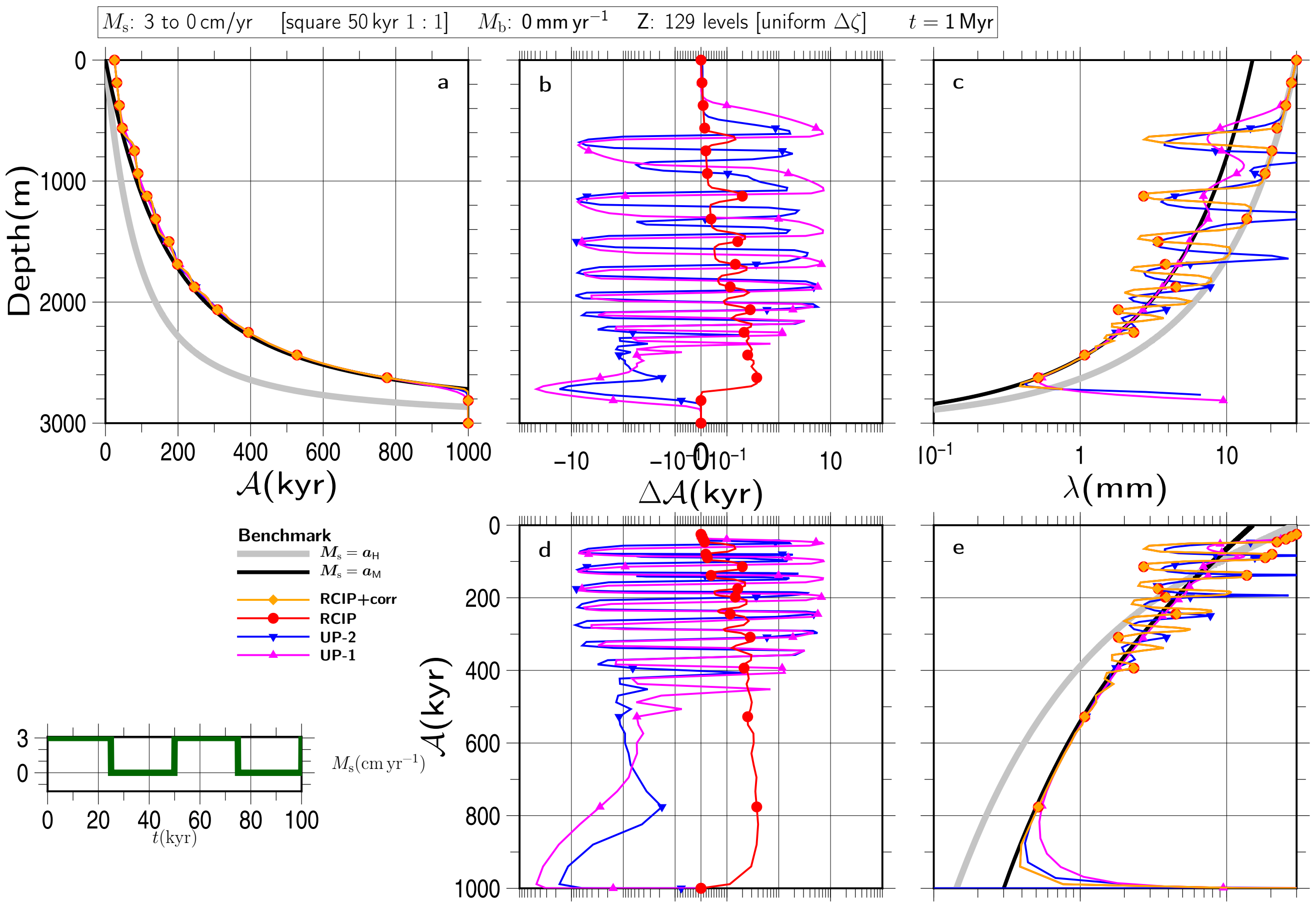

Figure S35

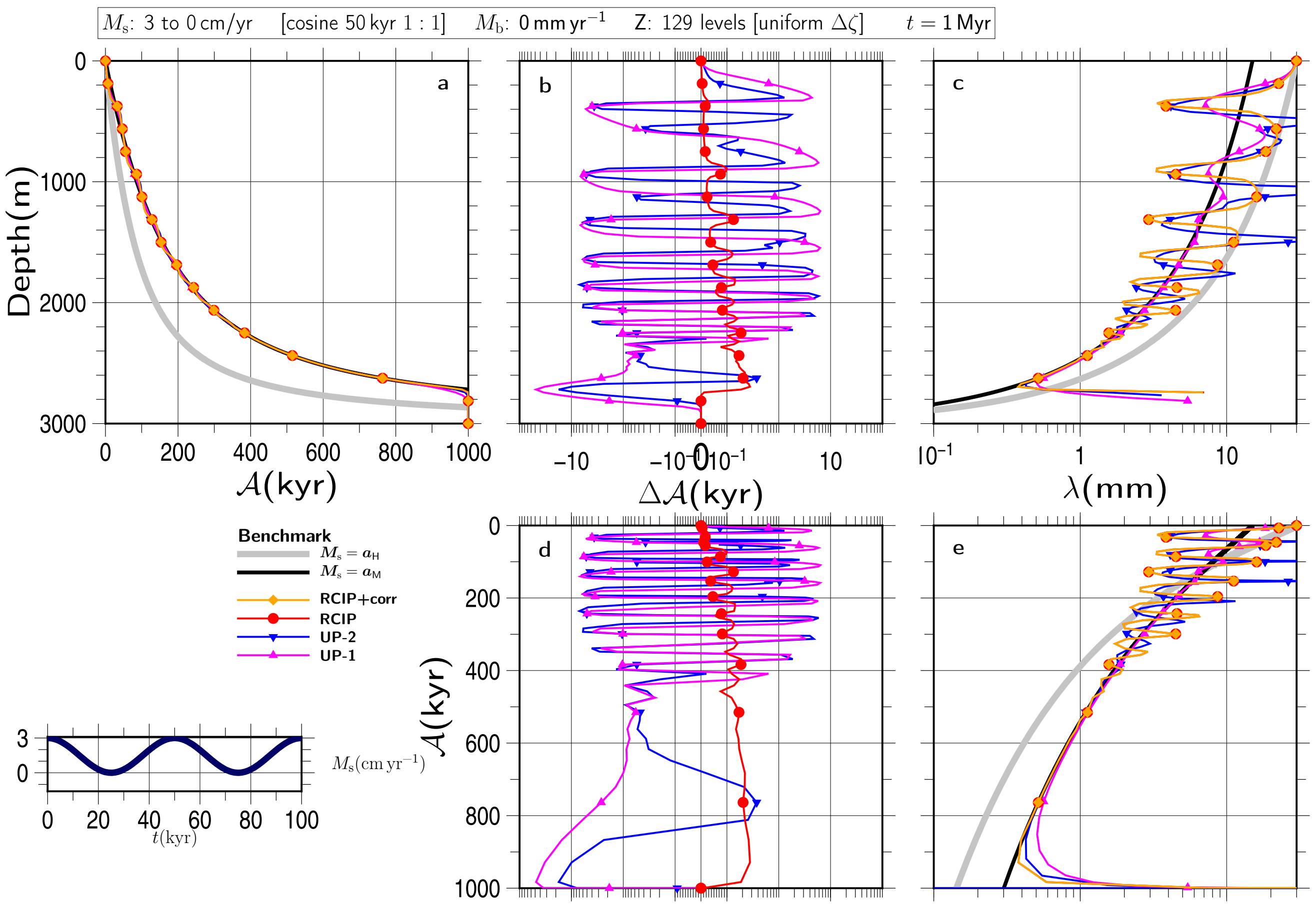

Figure S36

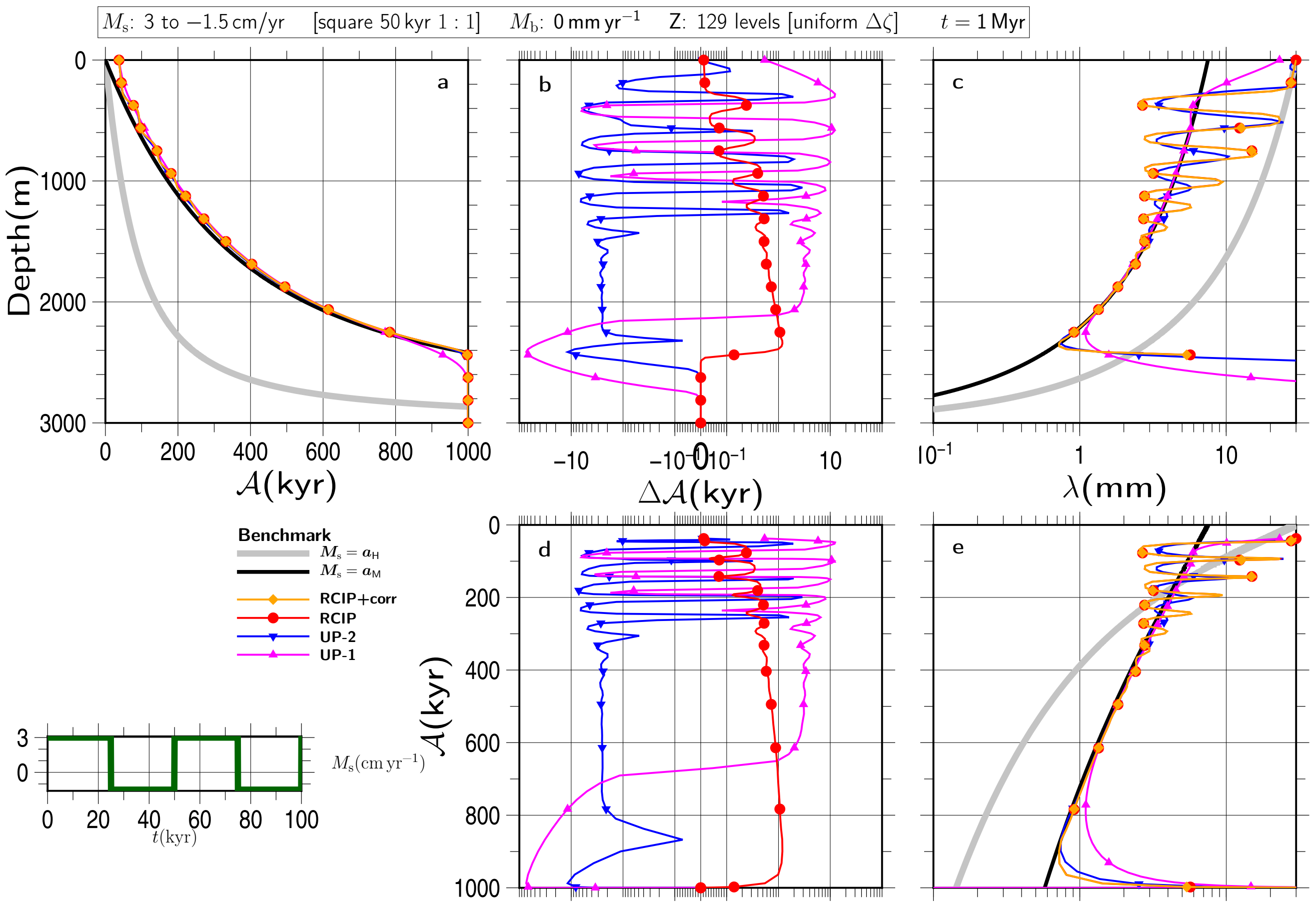

Figure S37

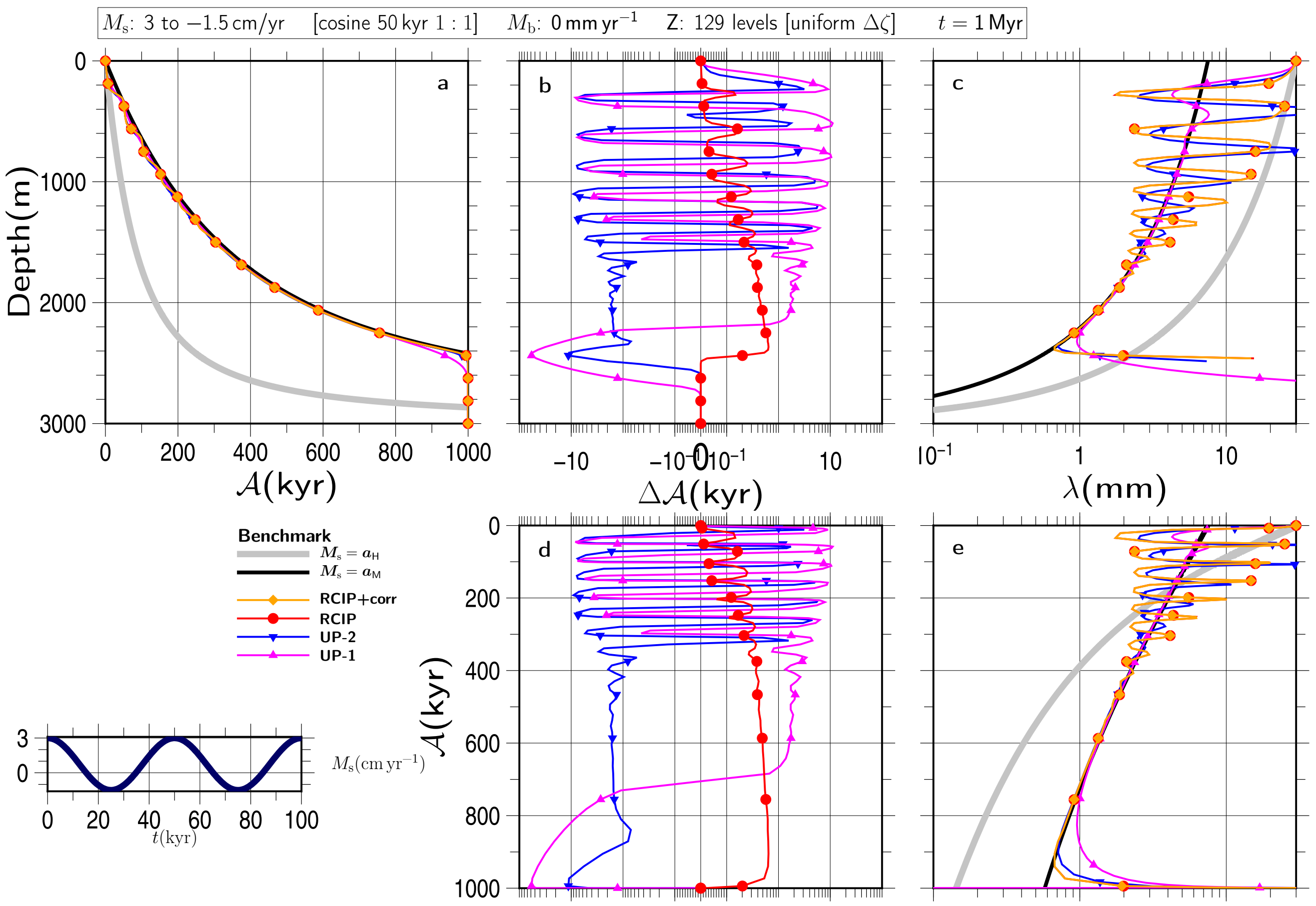

Figure S38

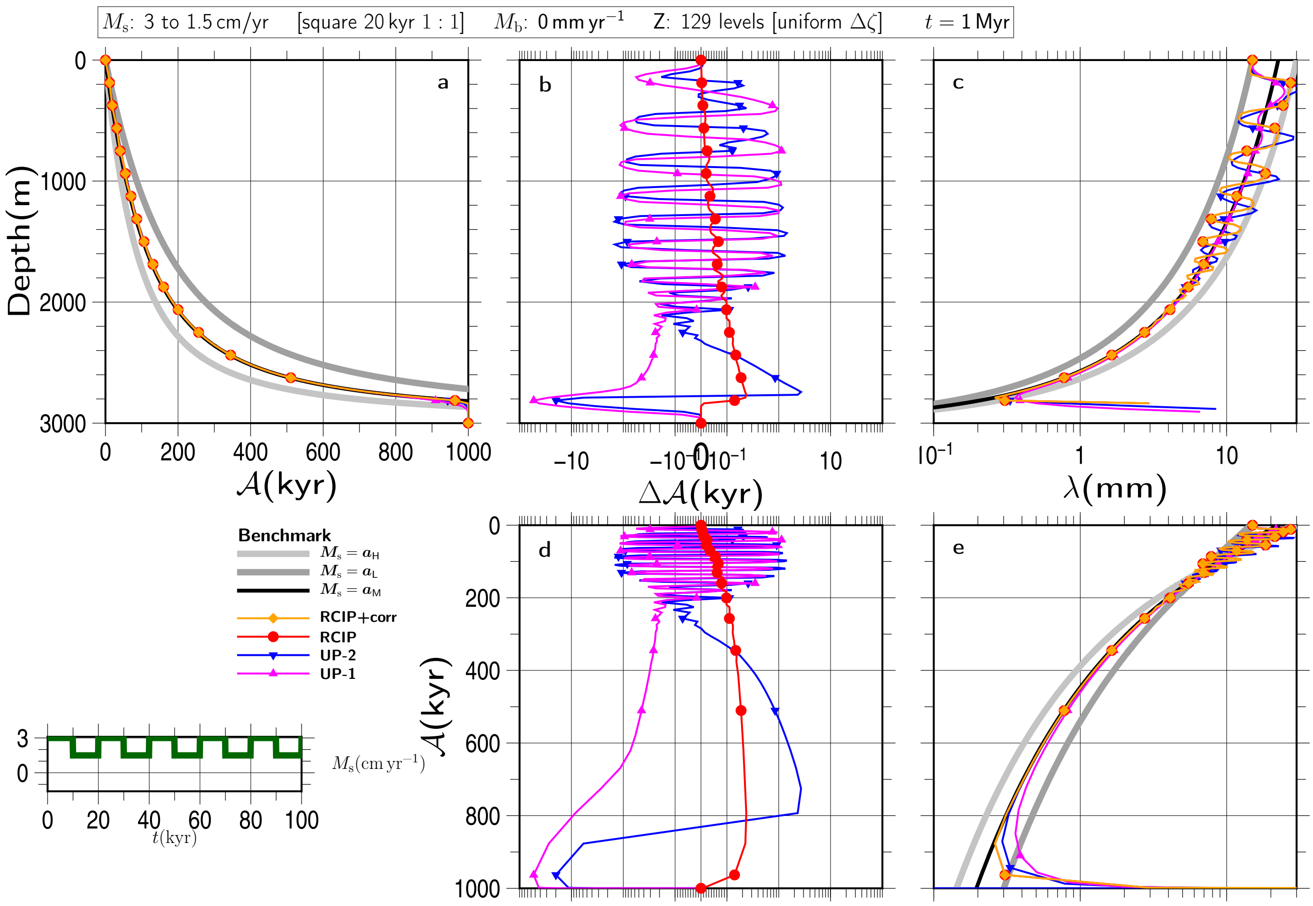

Figure S39

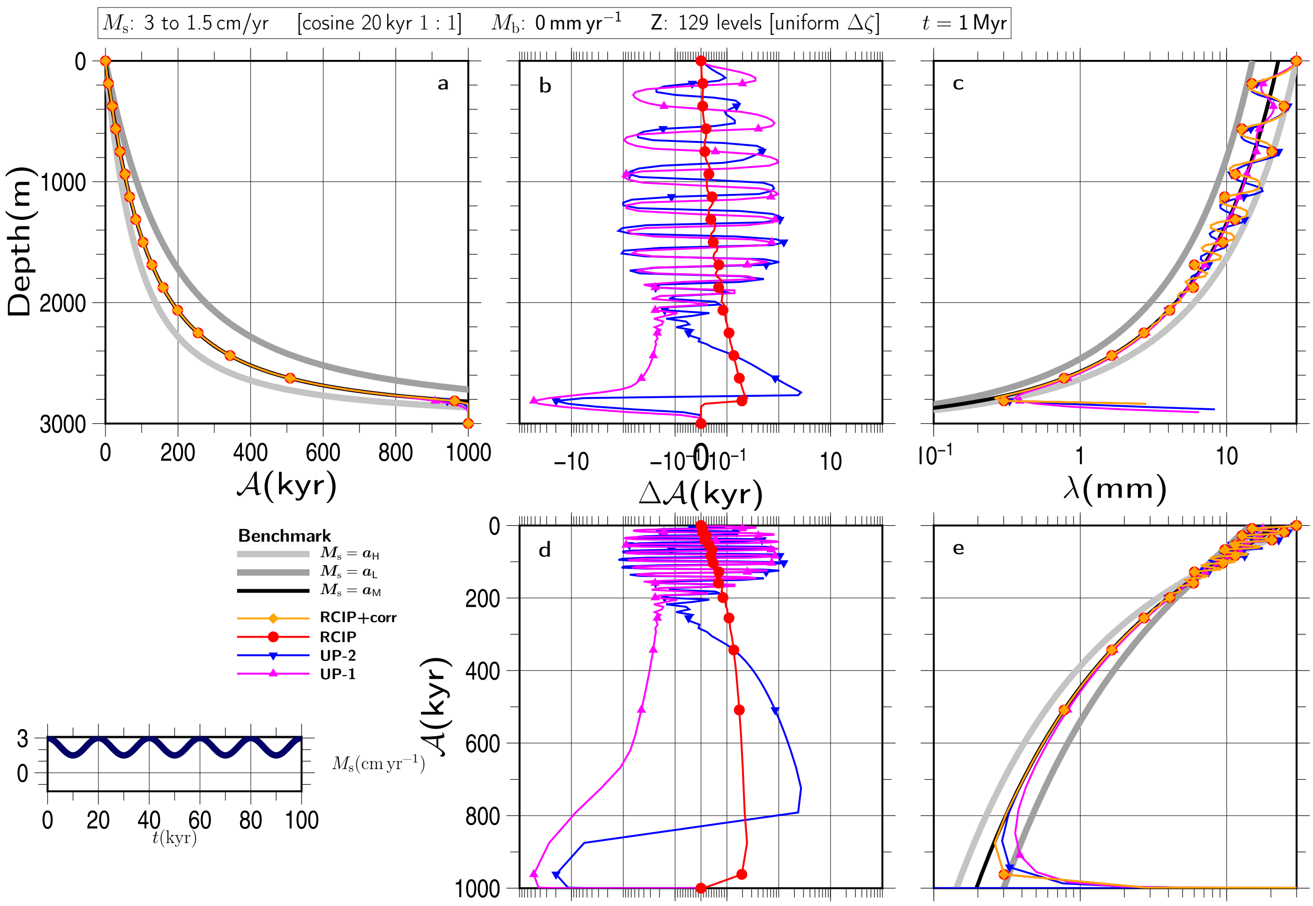

Figure S40

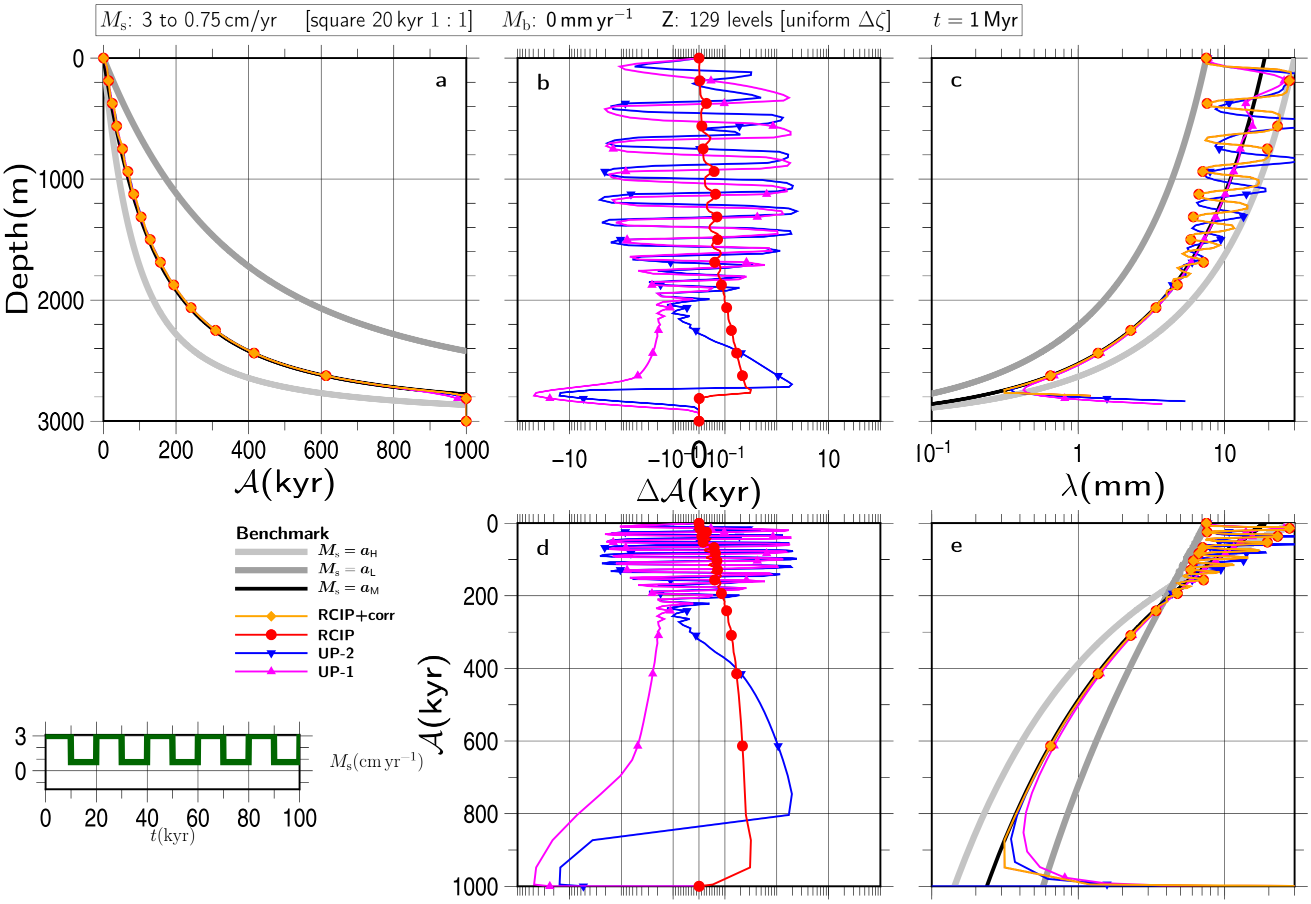

Figure S41

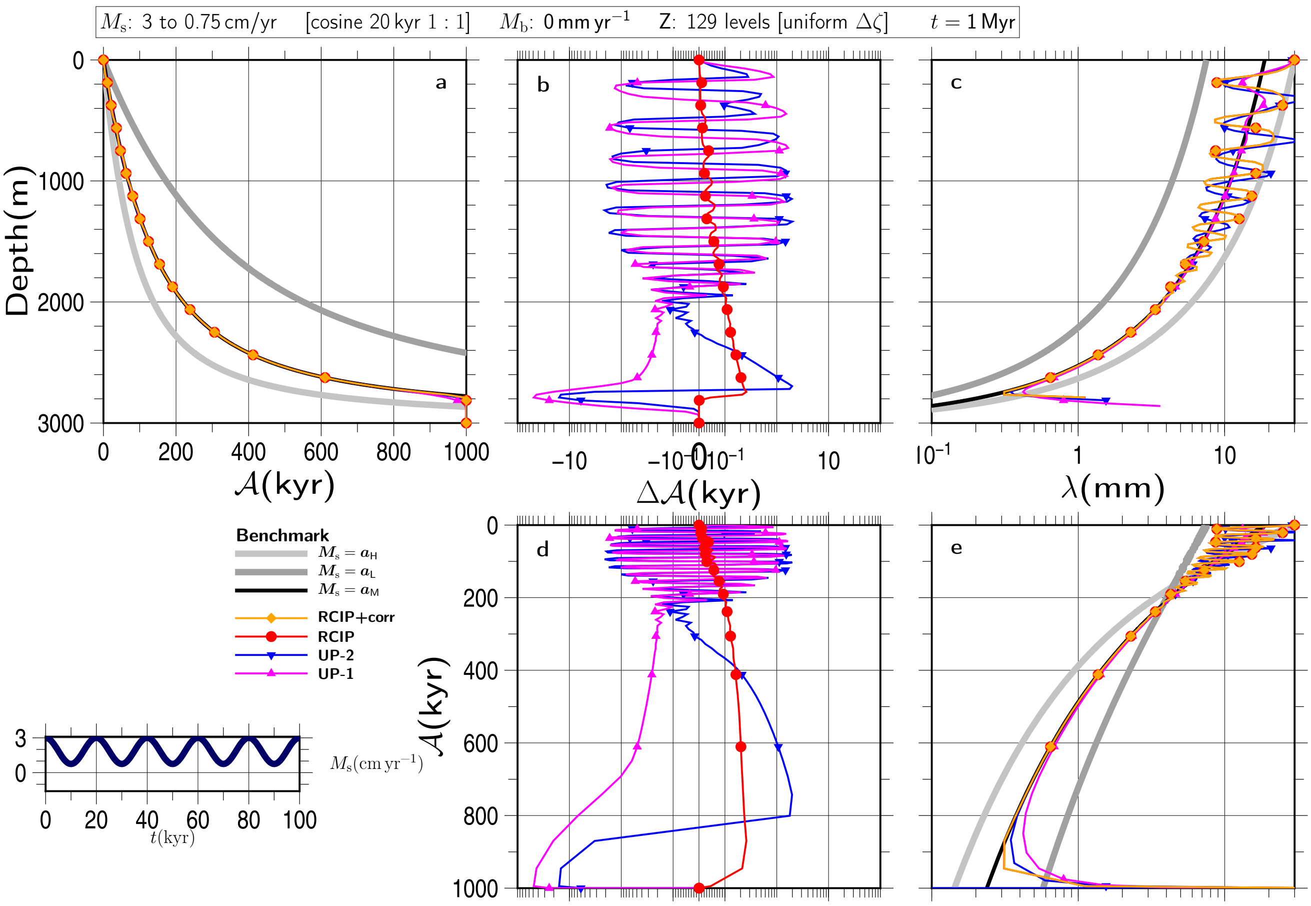

Figure S42

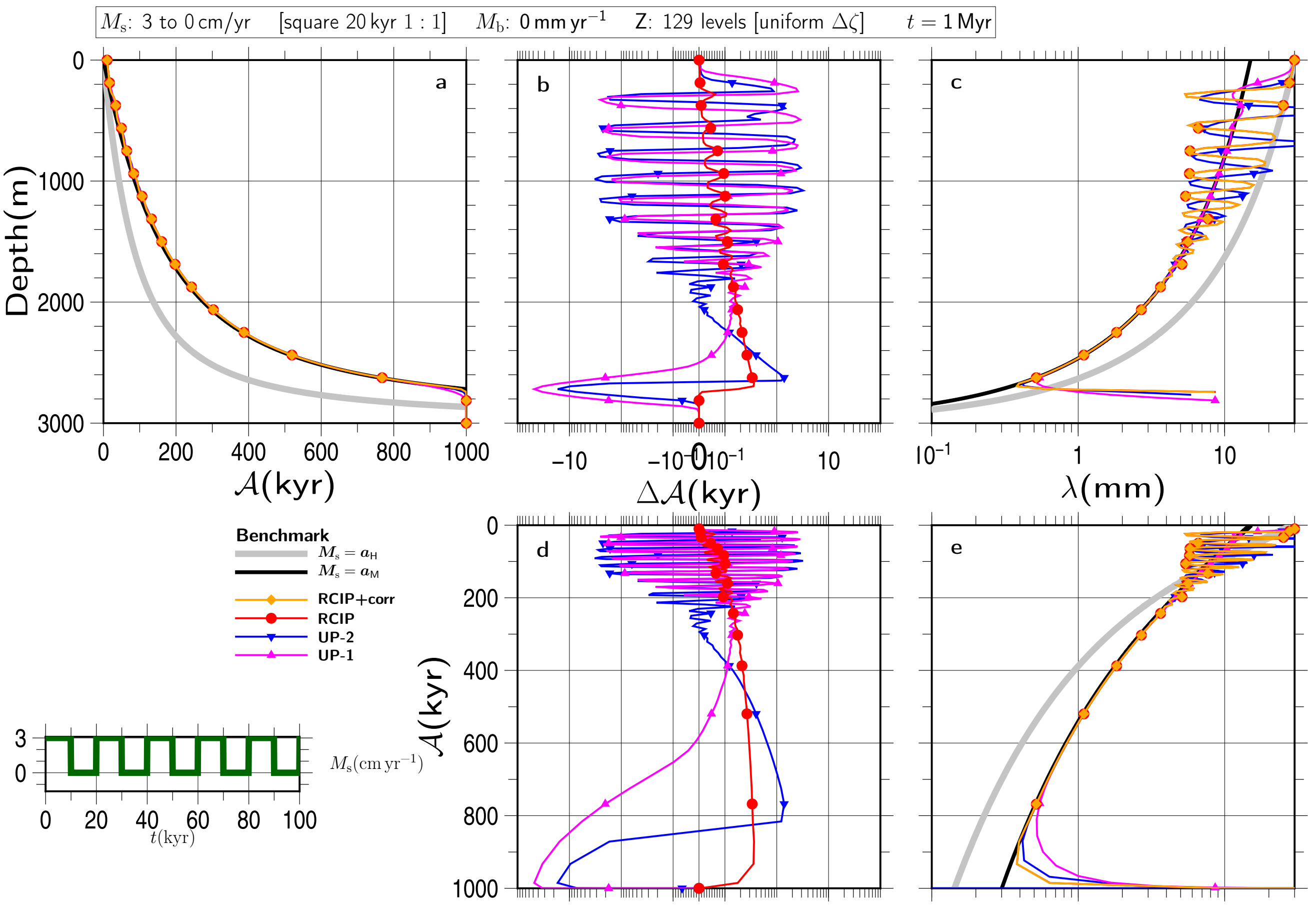

Figure S43

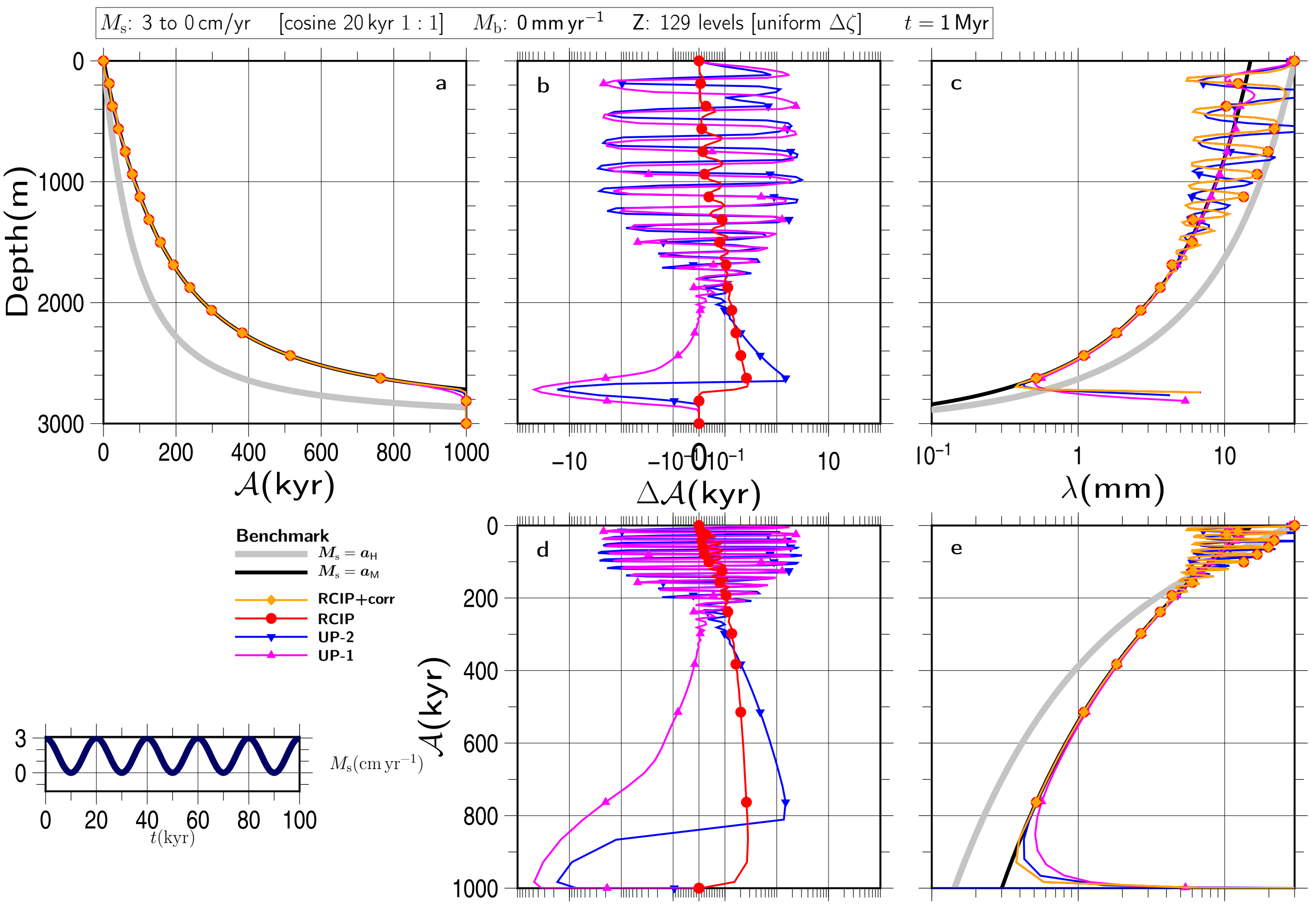

Figure S44

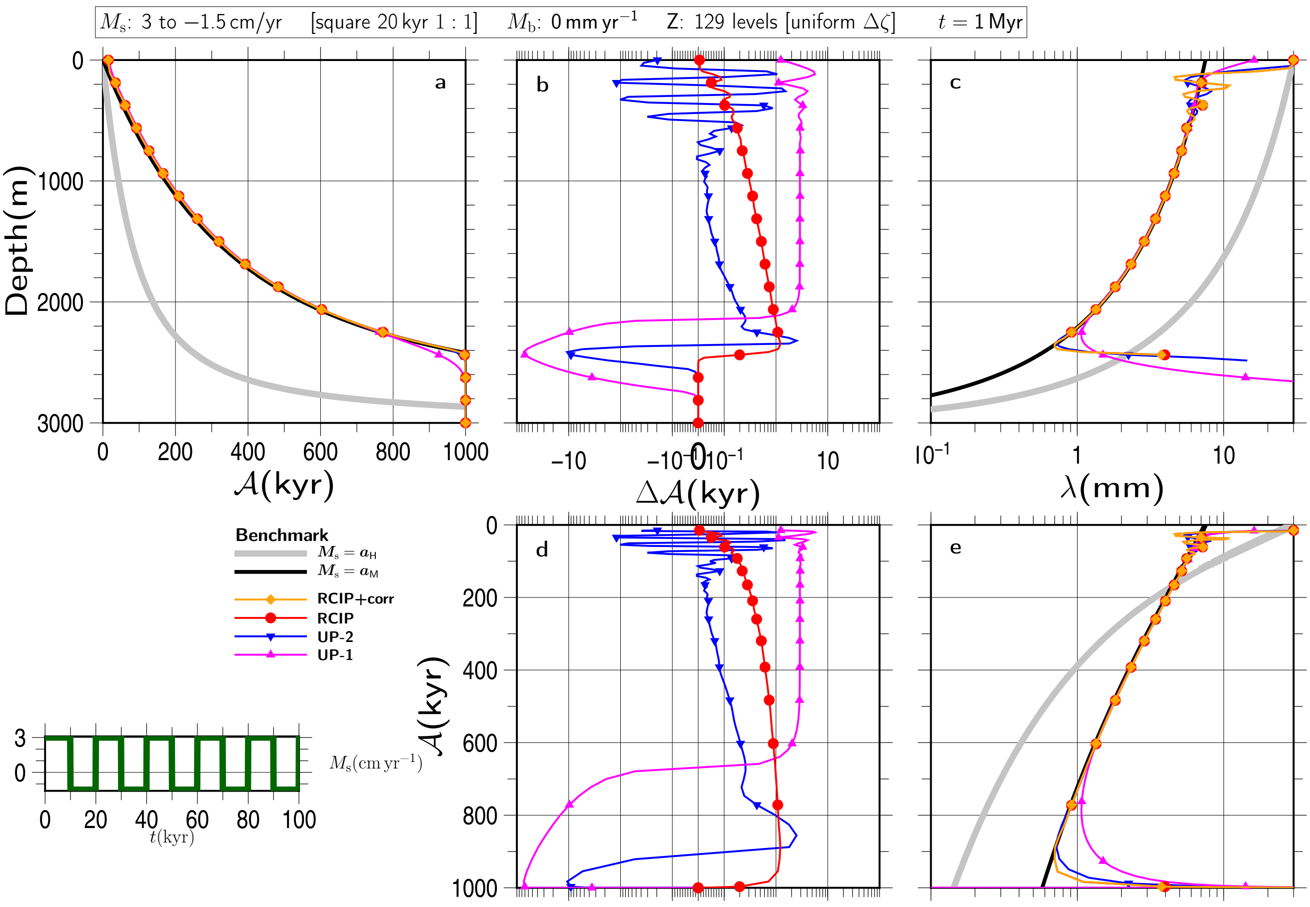

Figure S45

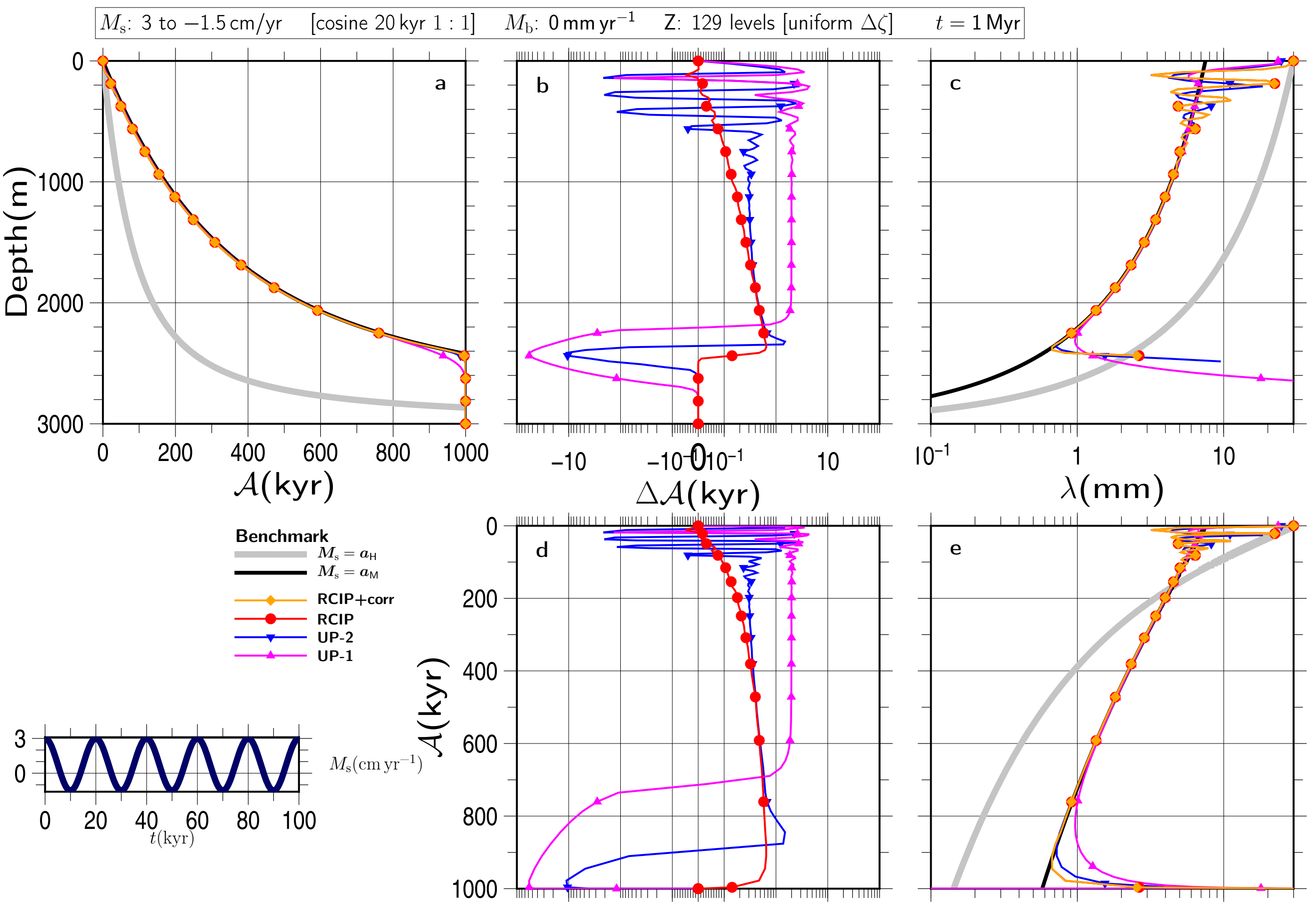

Figure S46

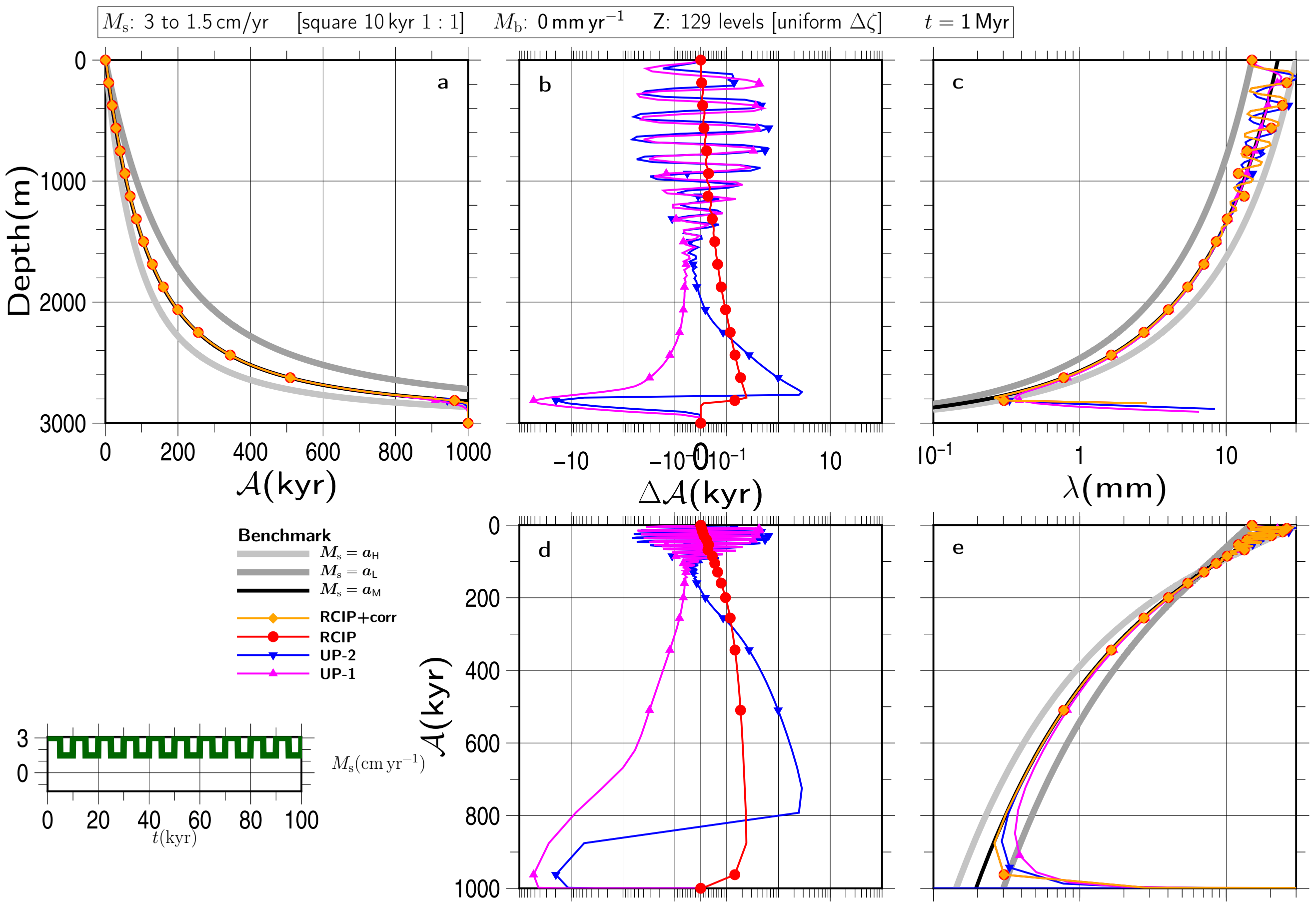

Figure S47

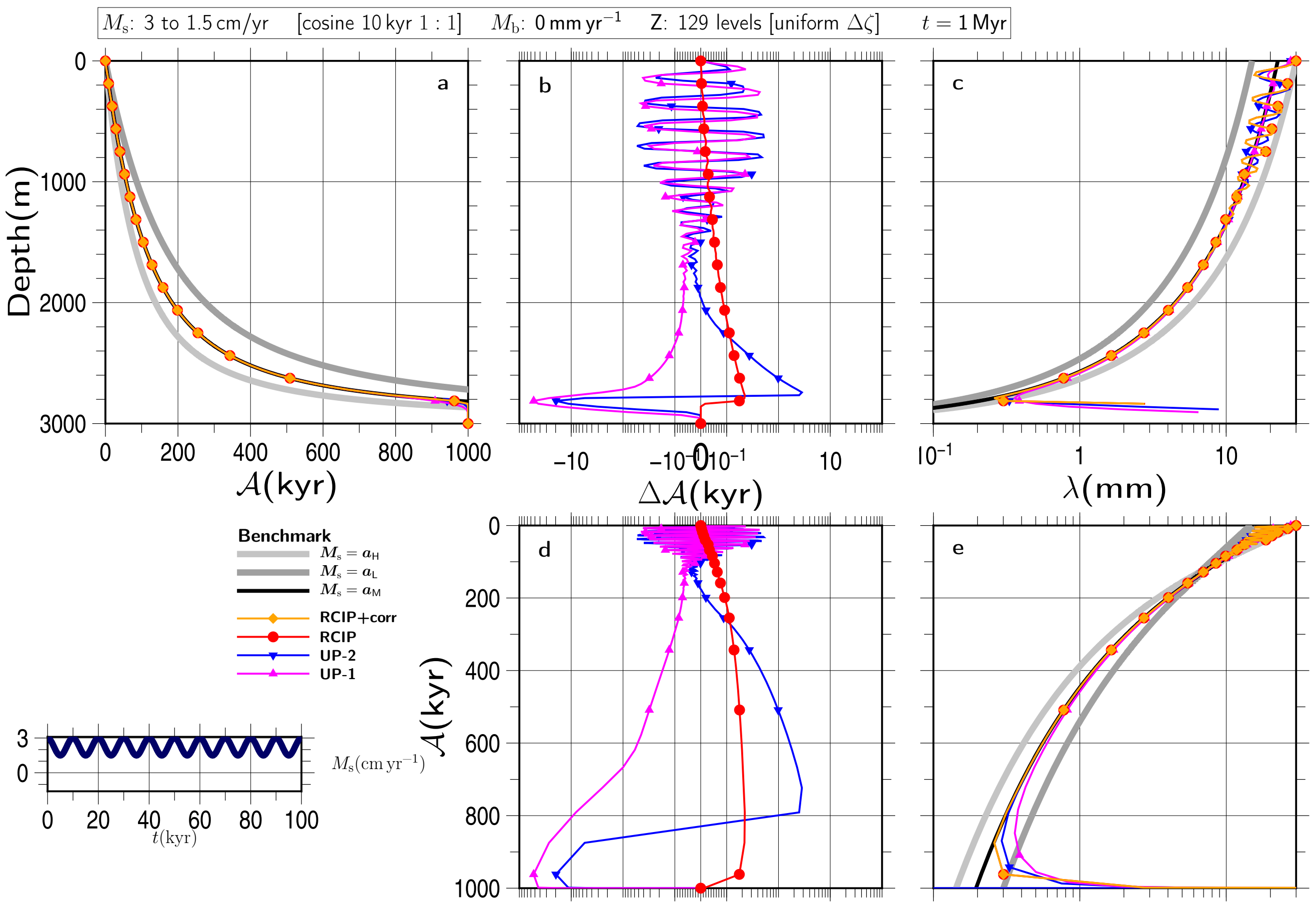

Figure S48

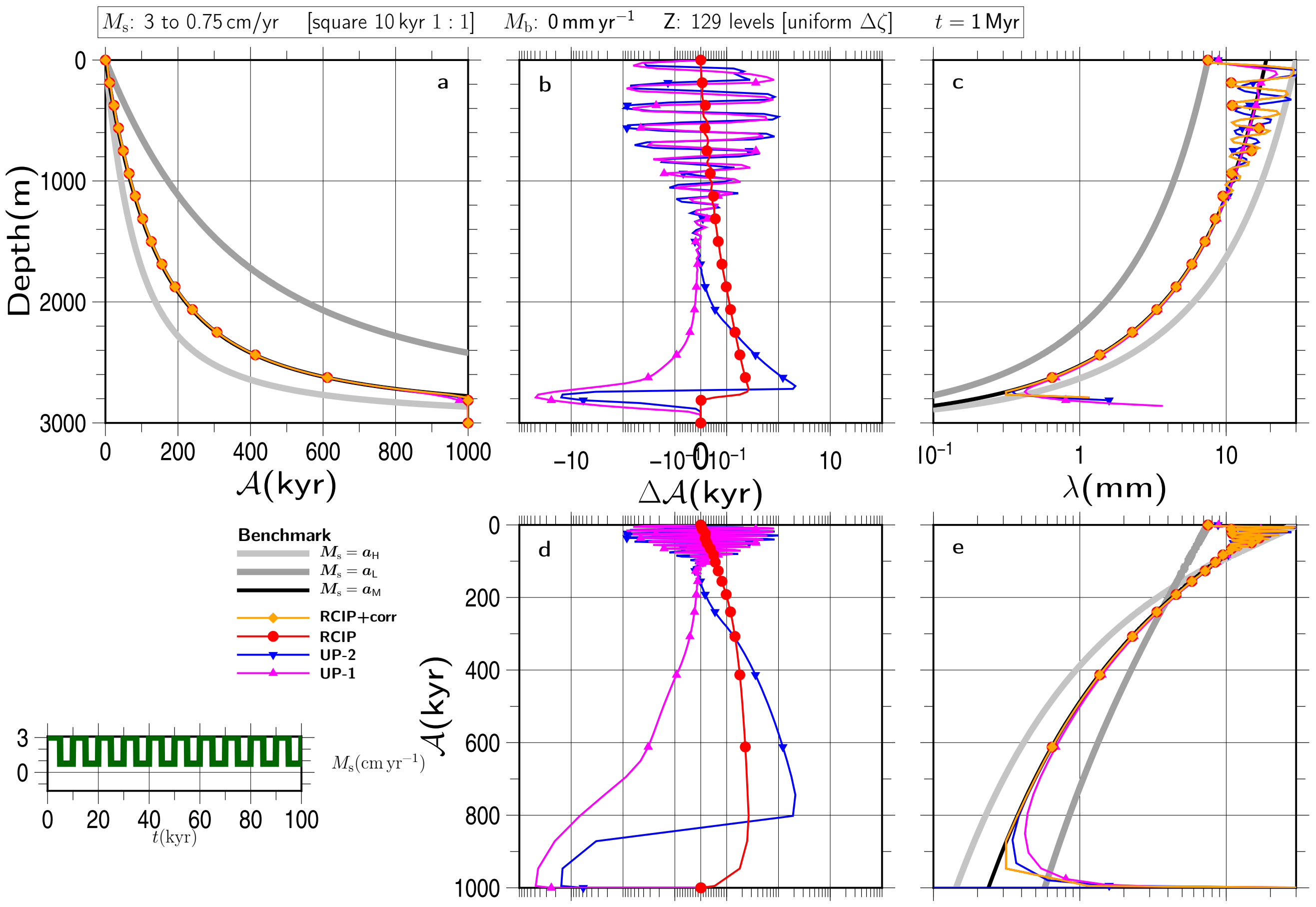

Figure S49

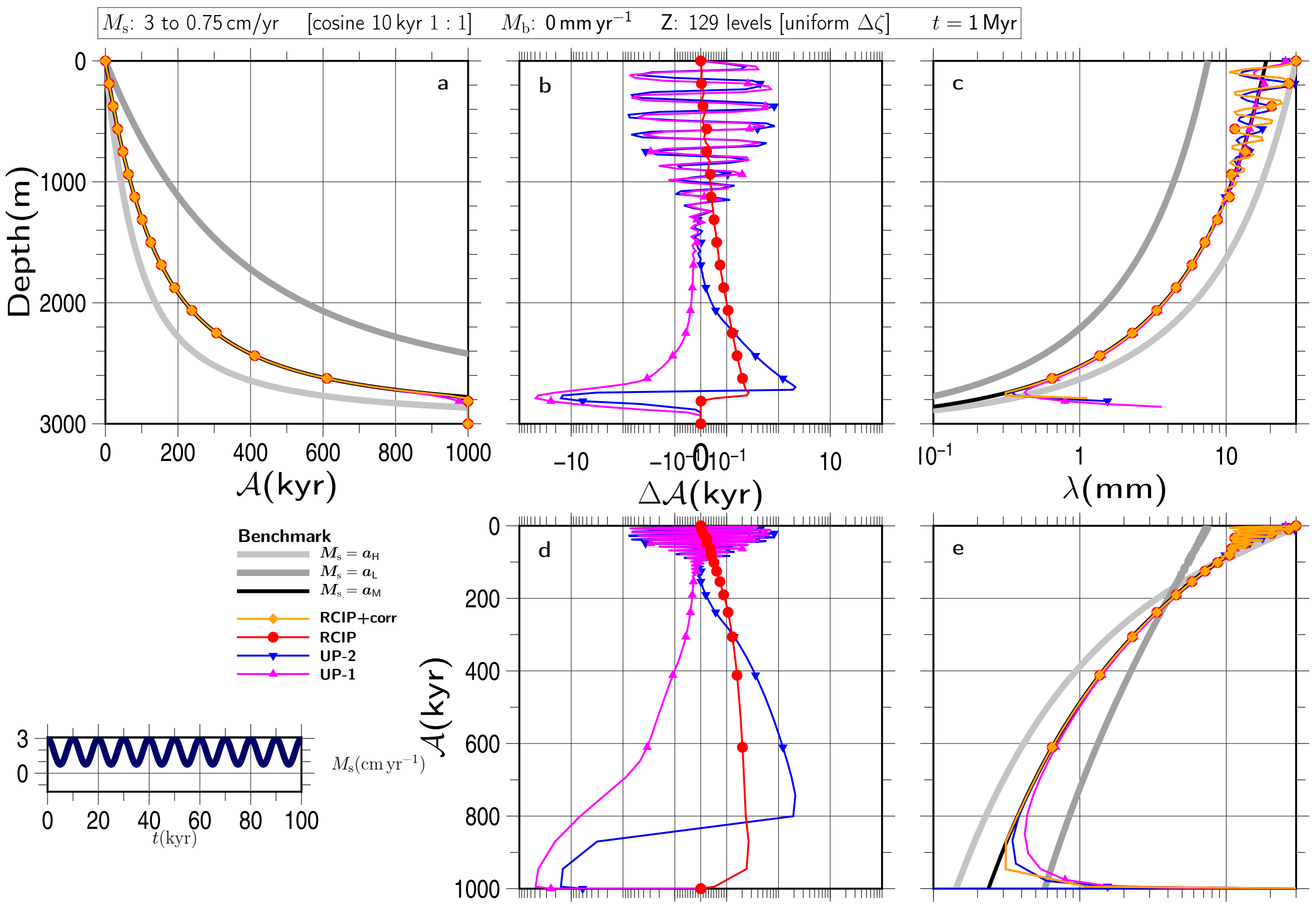

Figure S50

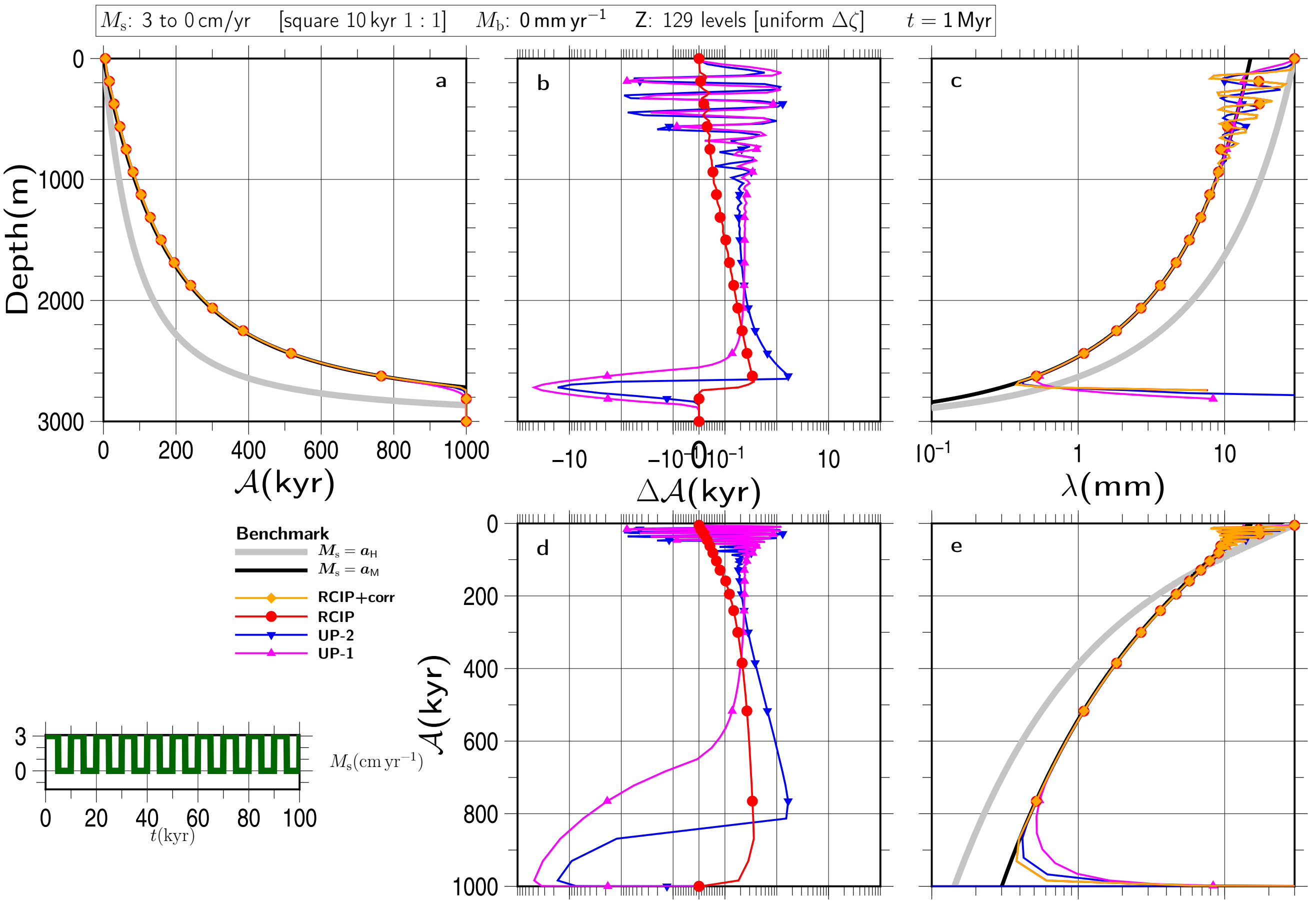

Figure S51

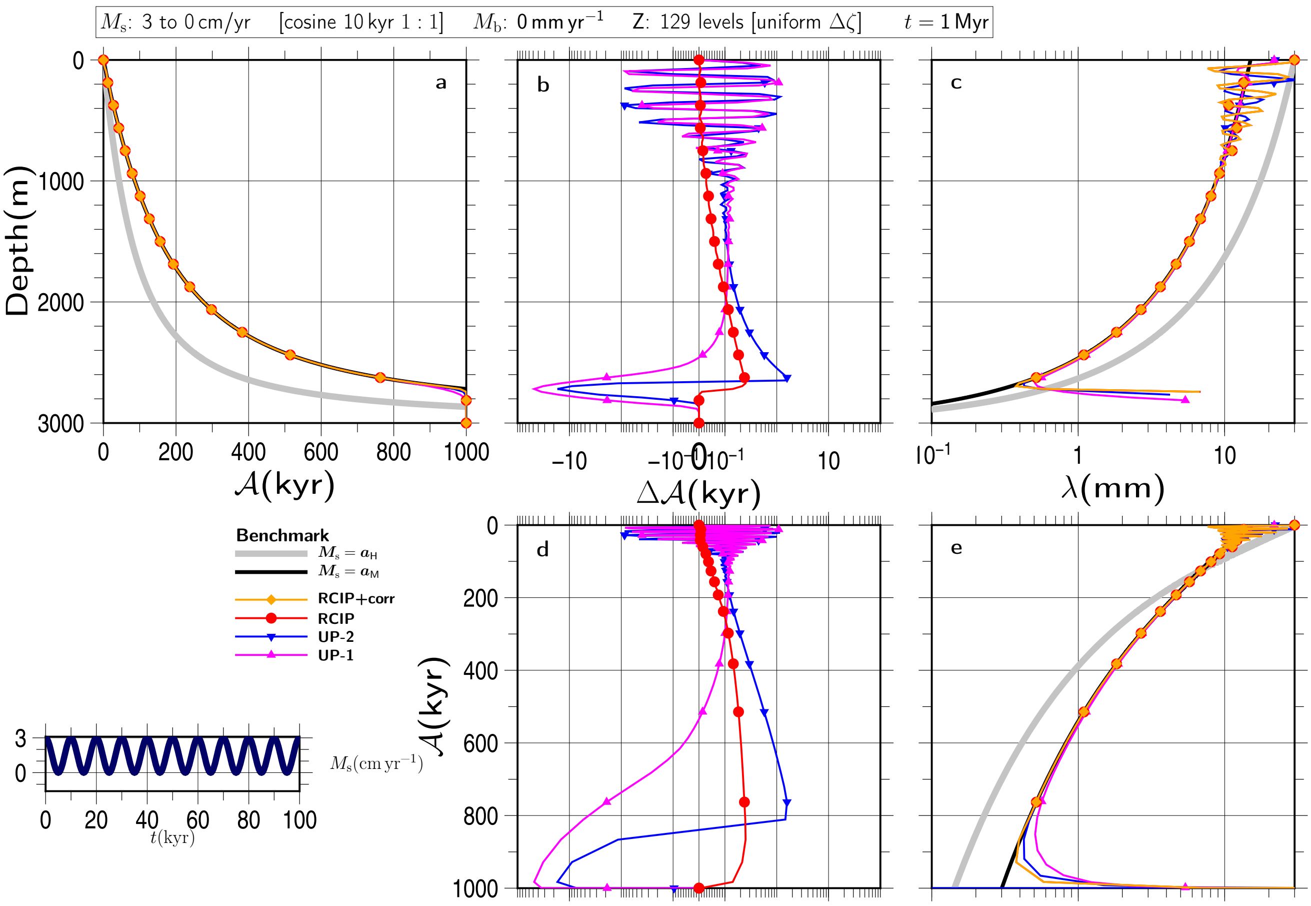

Figure S52

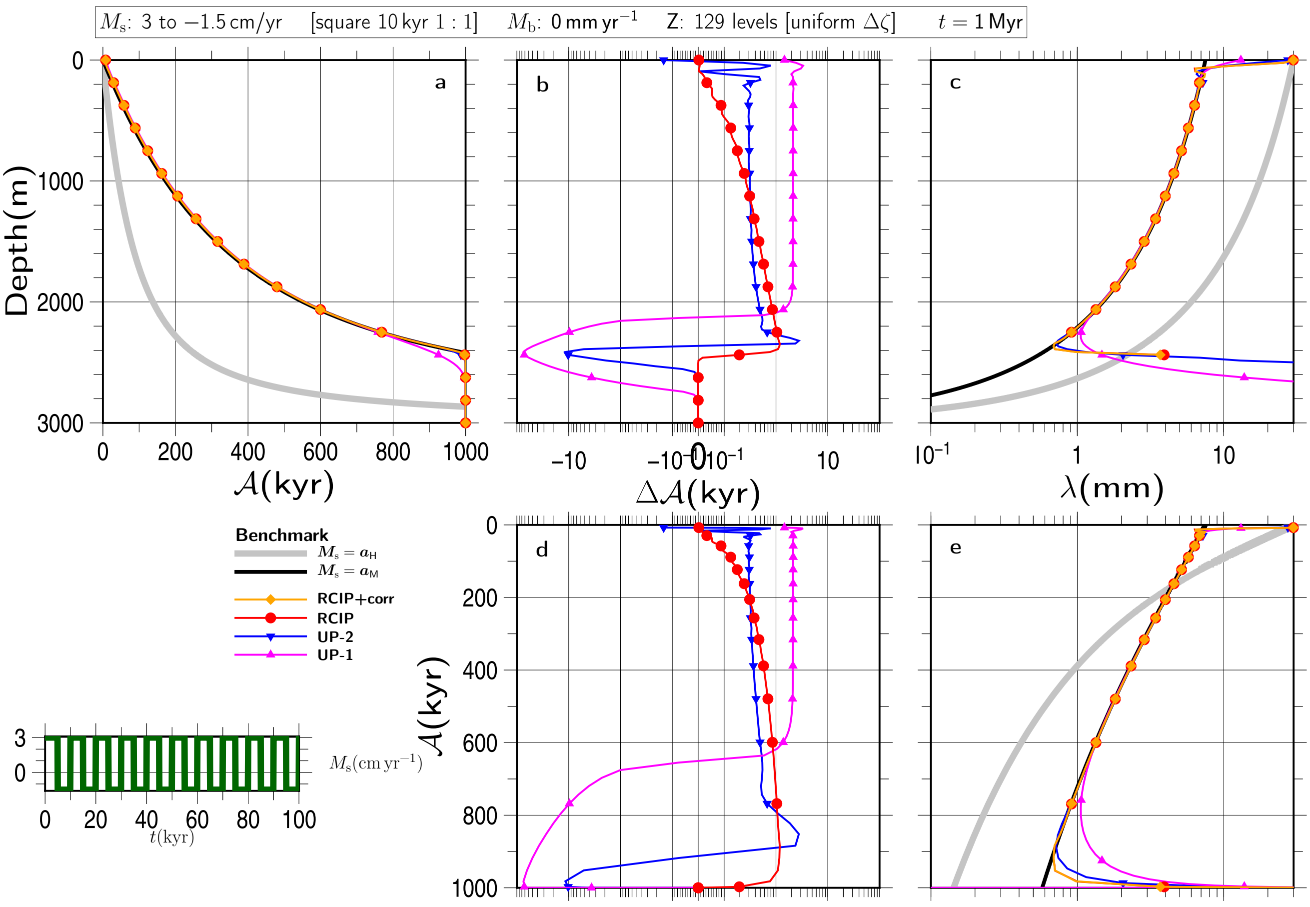

Figure S53

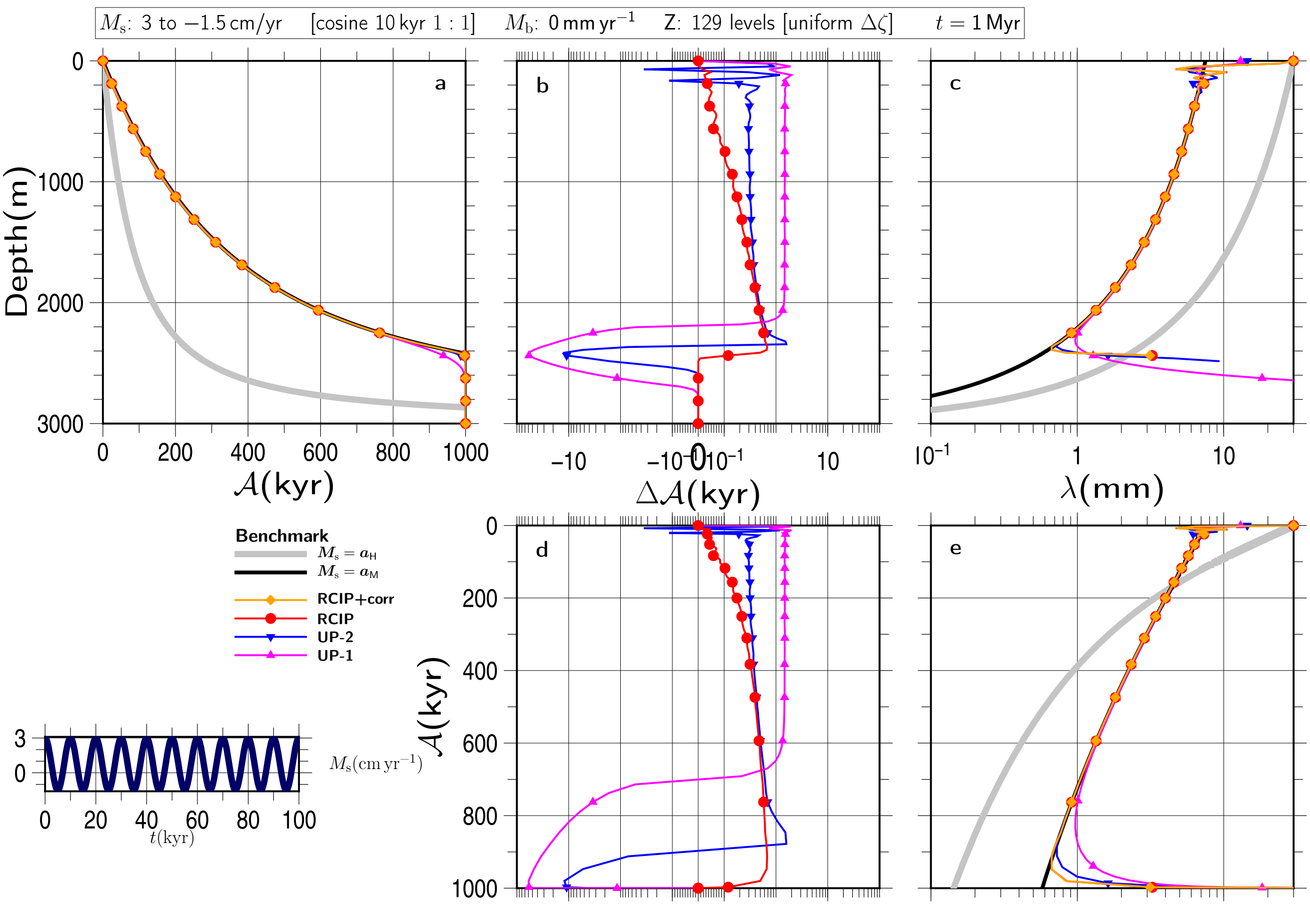

Figure S54

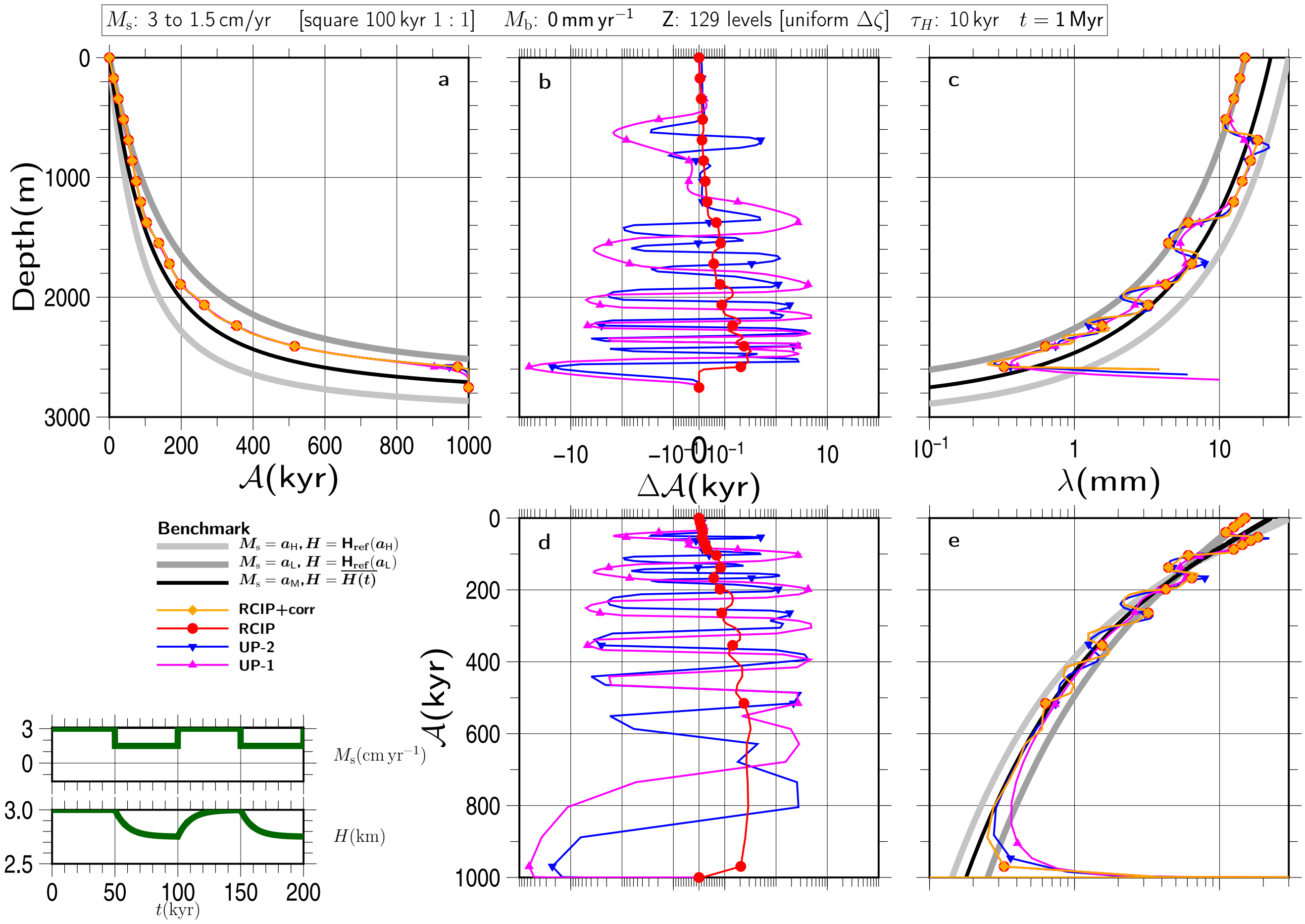

Figure S55

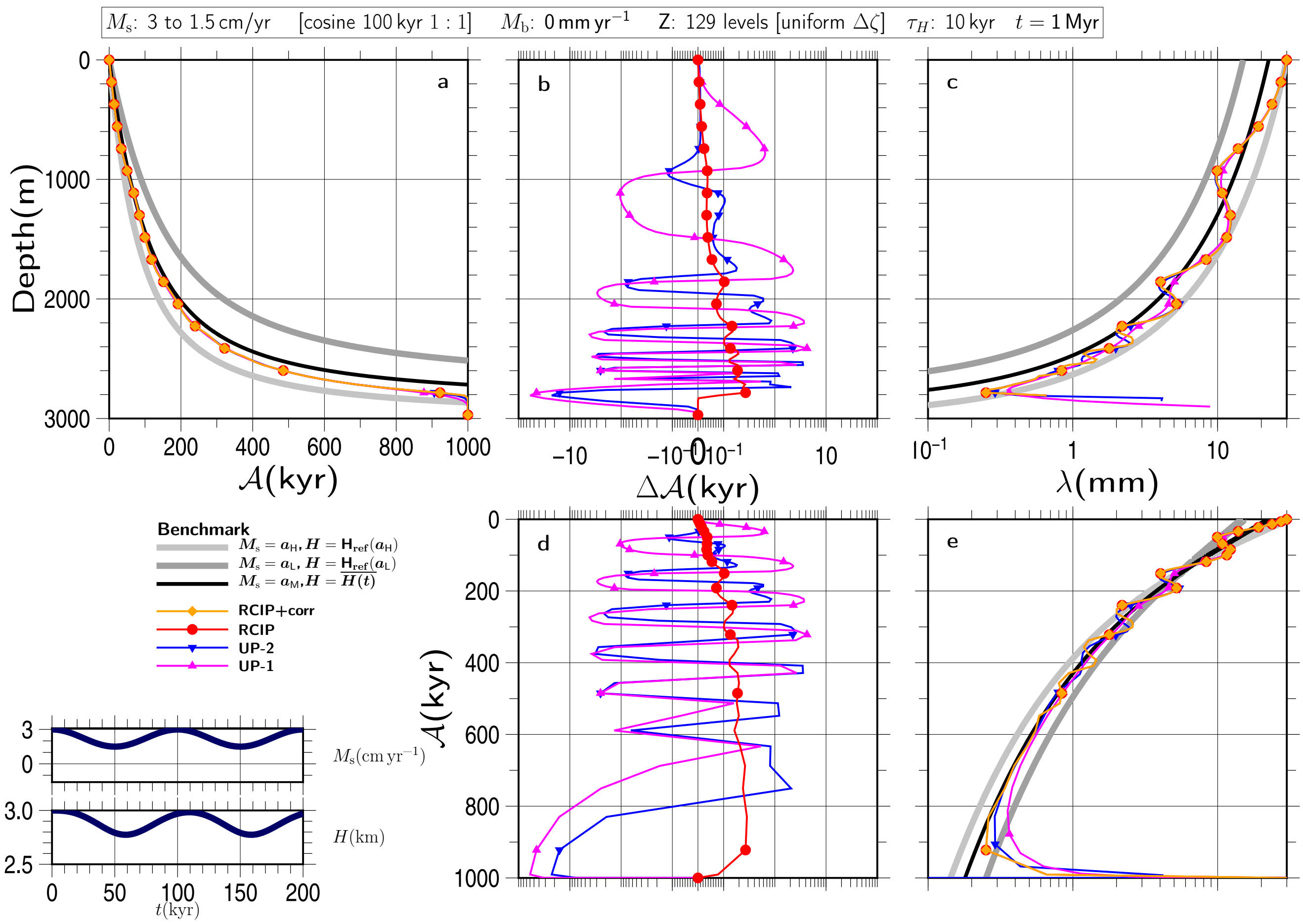

Figure S56

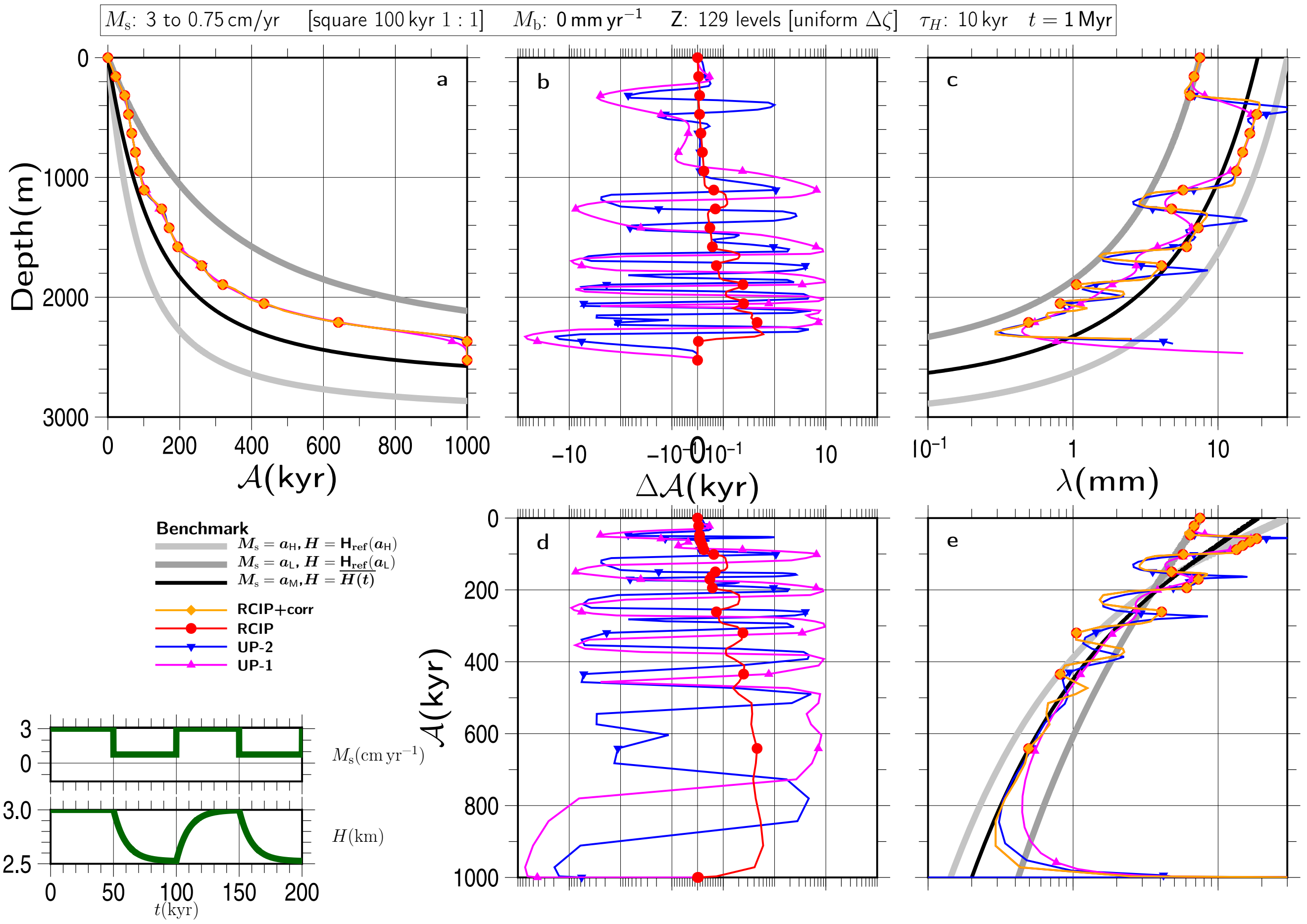

Figure S57

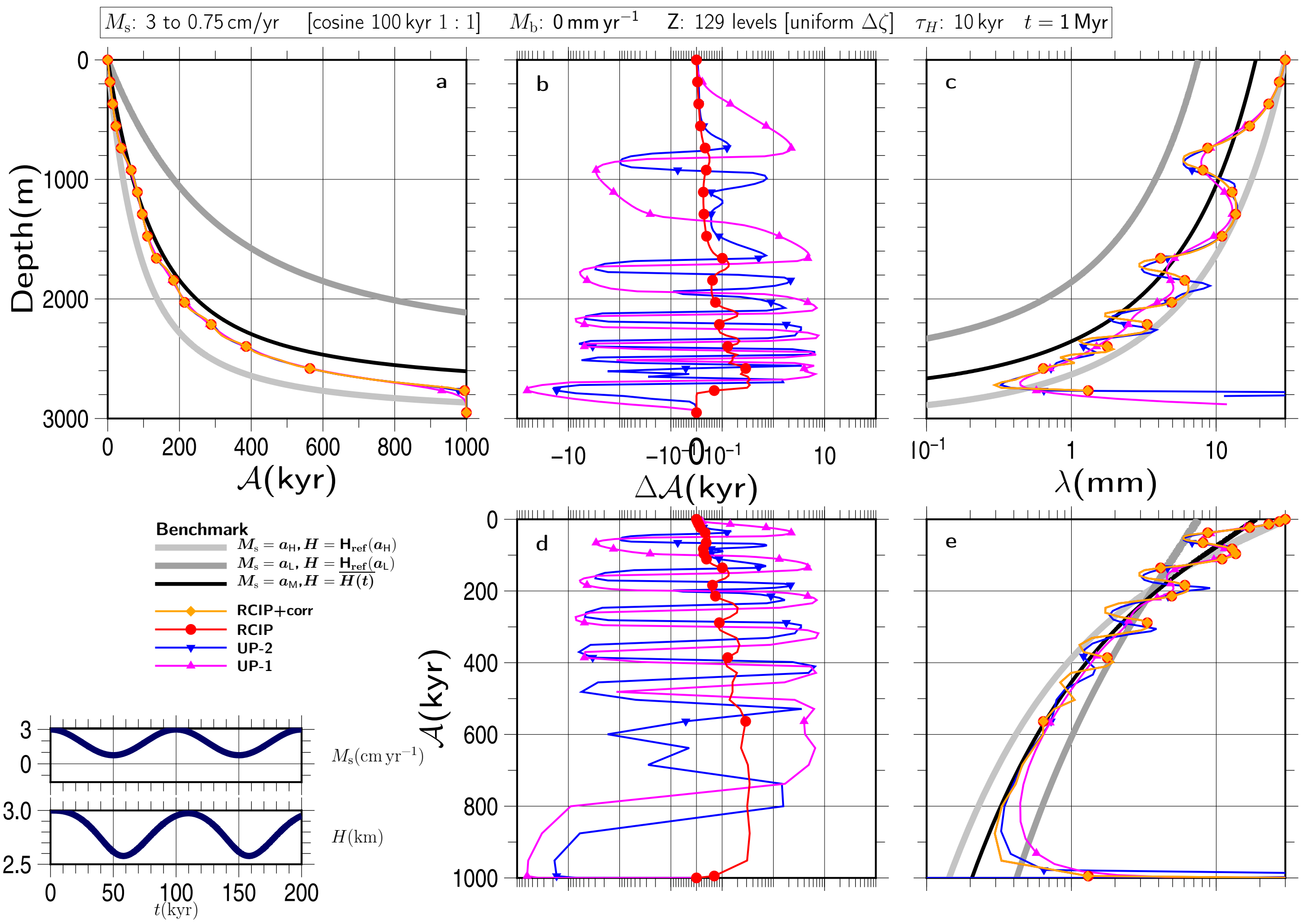

Figure S58

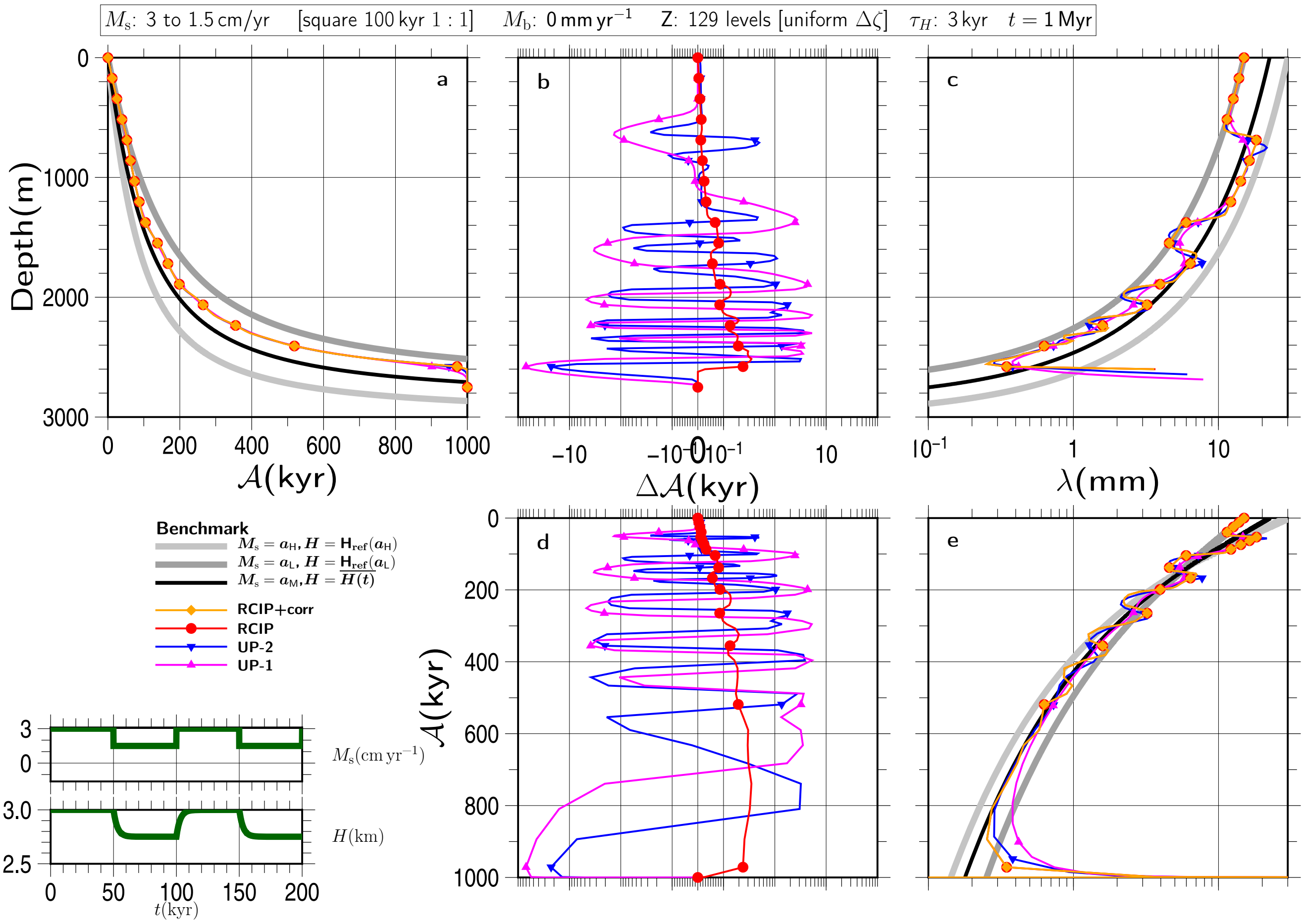

Figure S59

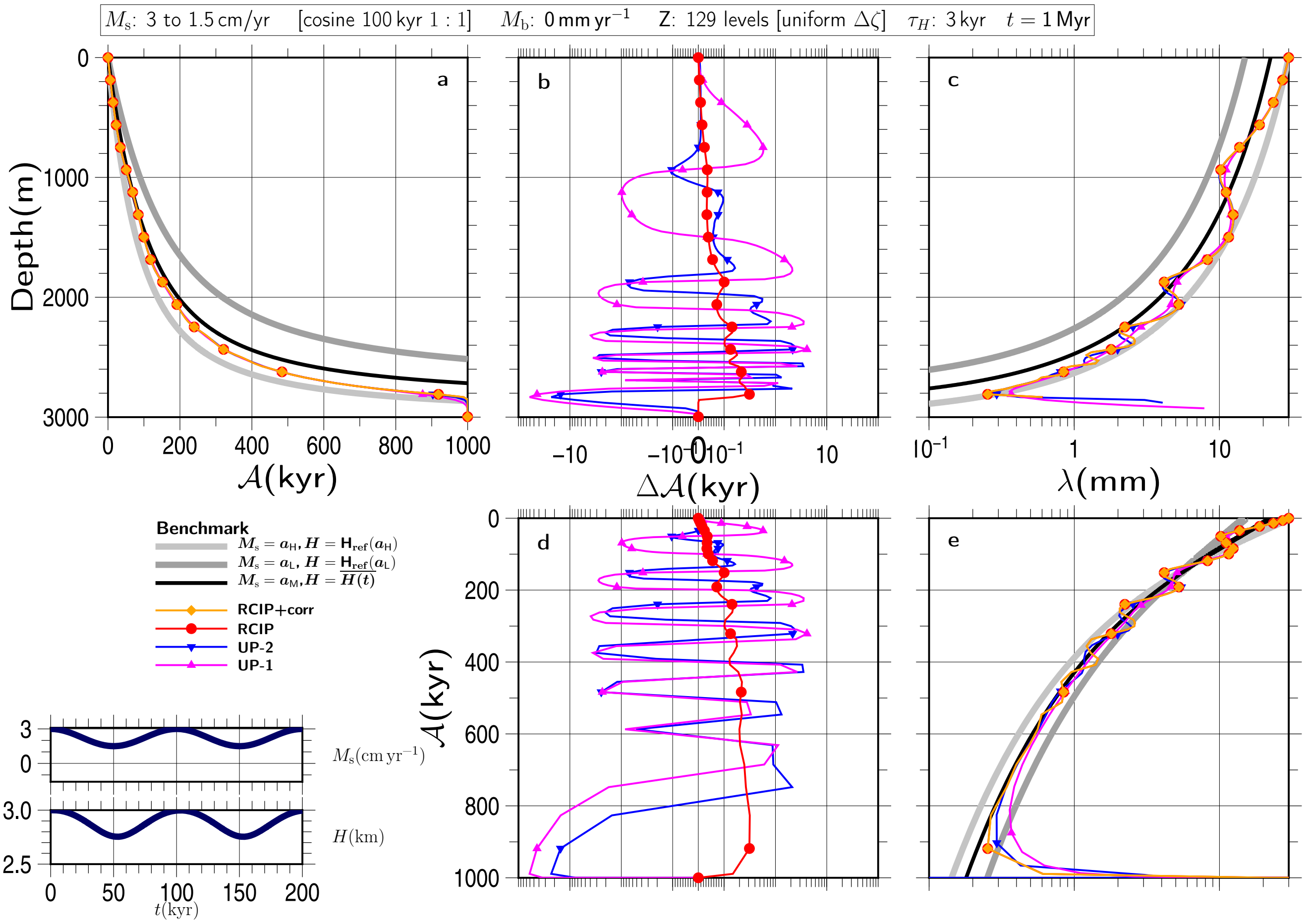

Figure S60

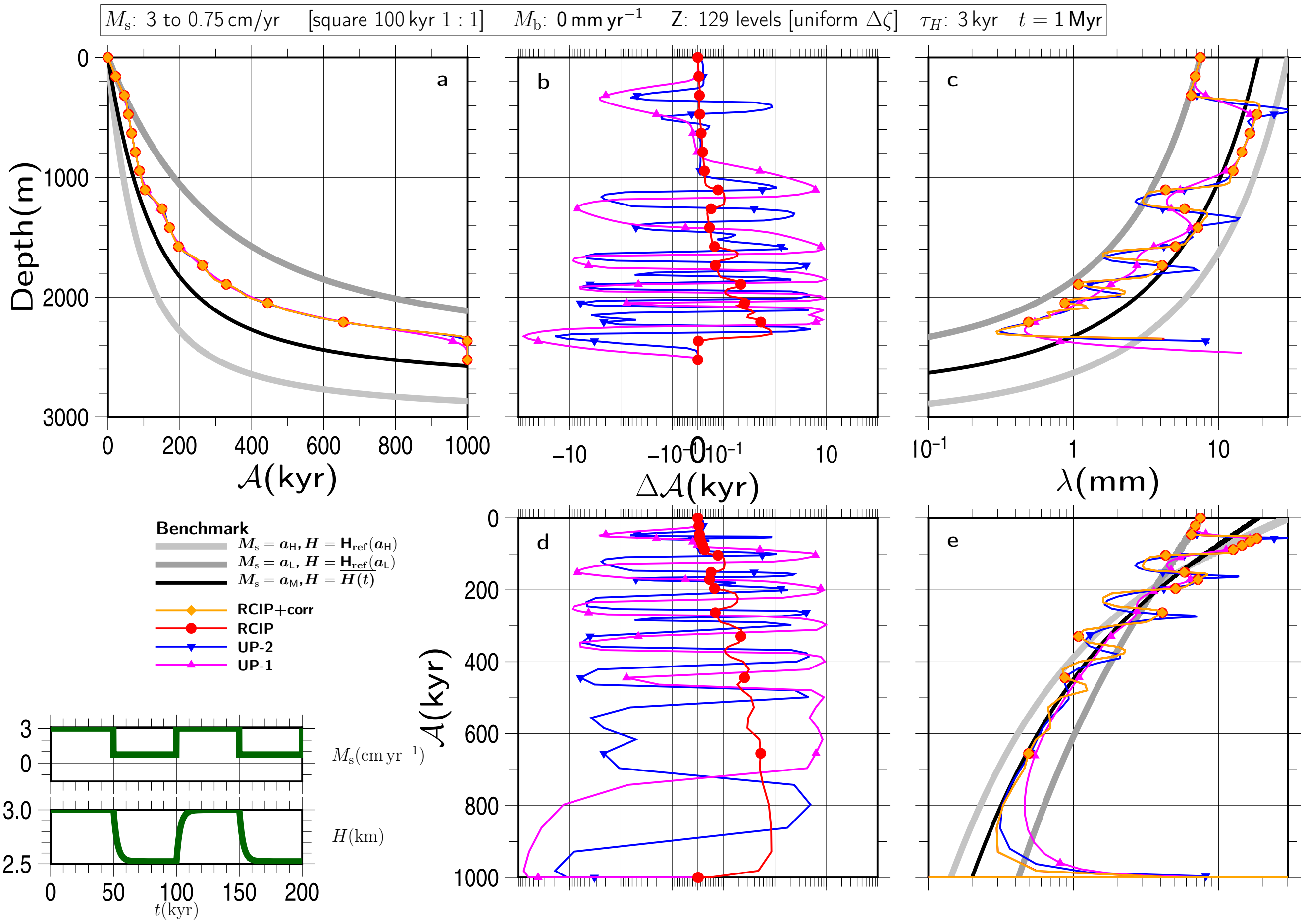

Figure S61

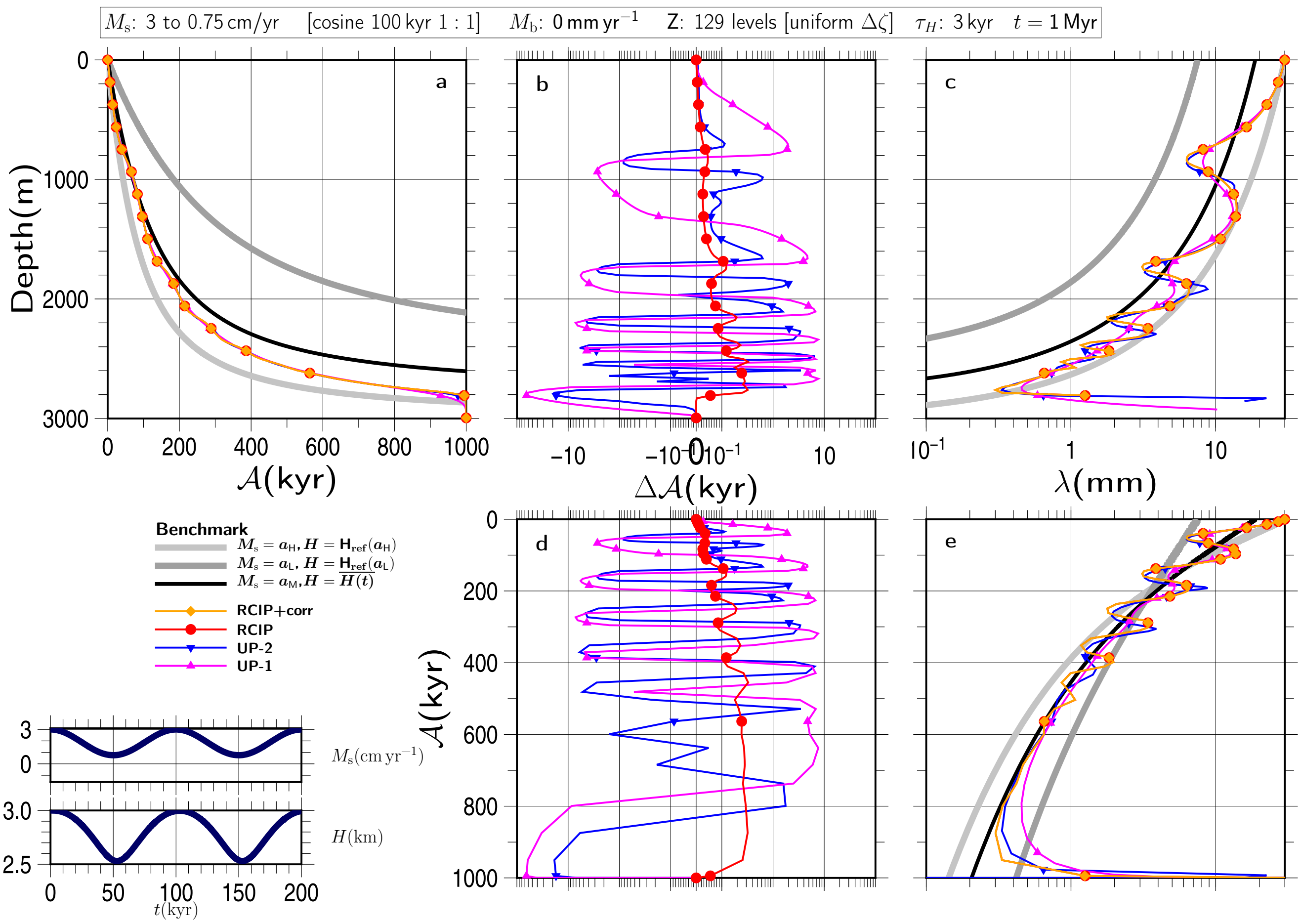

Figure S62

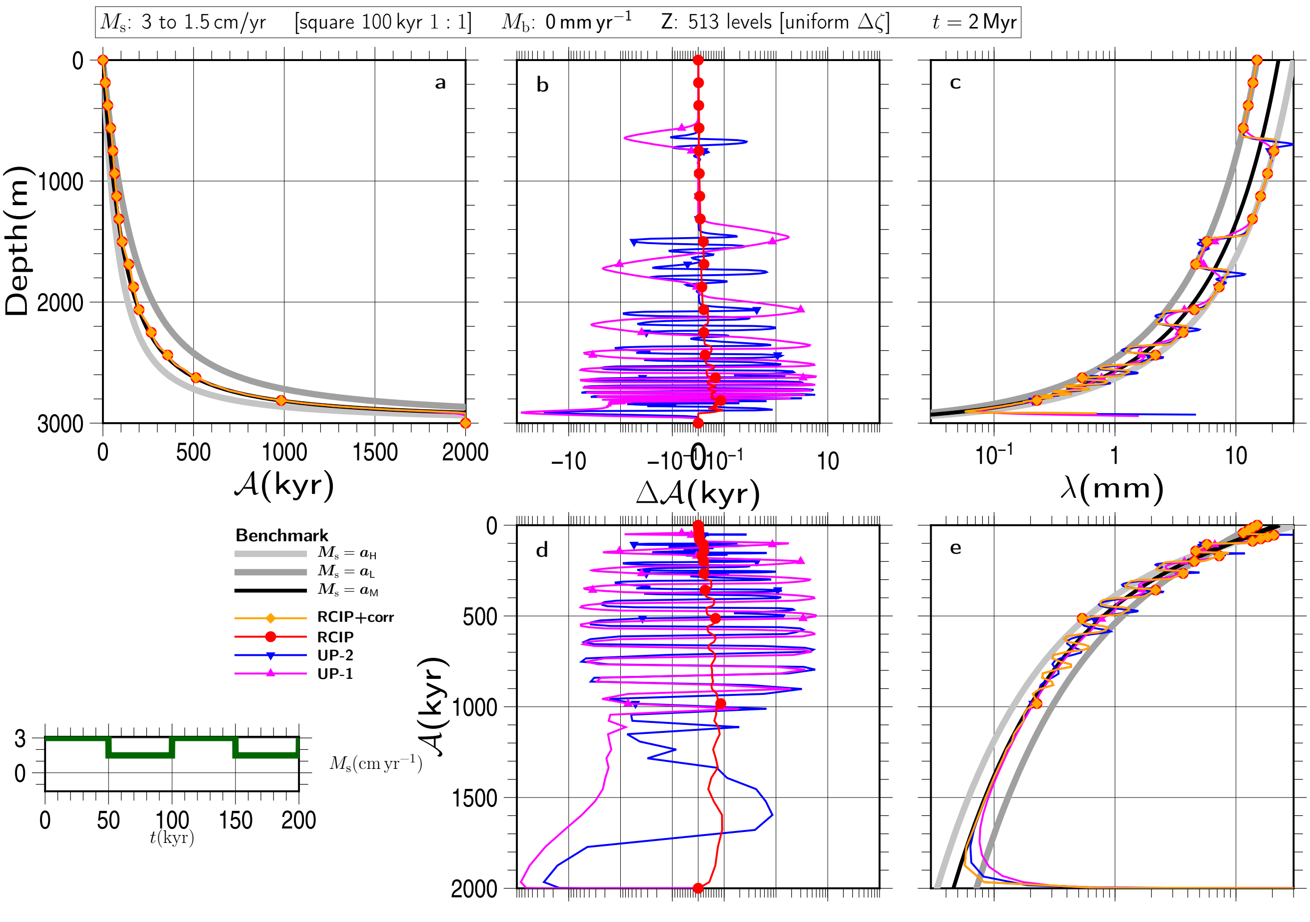

Figure S63

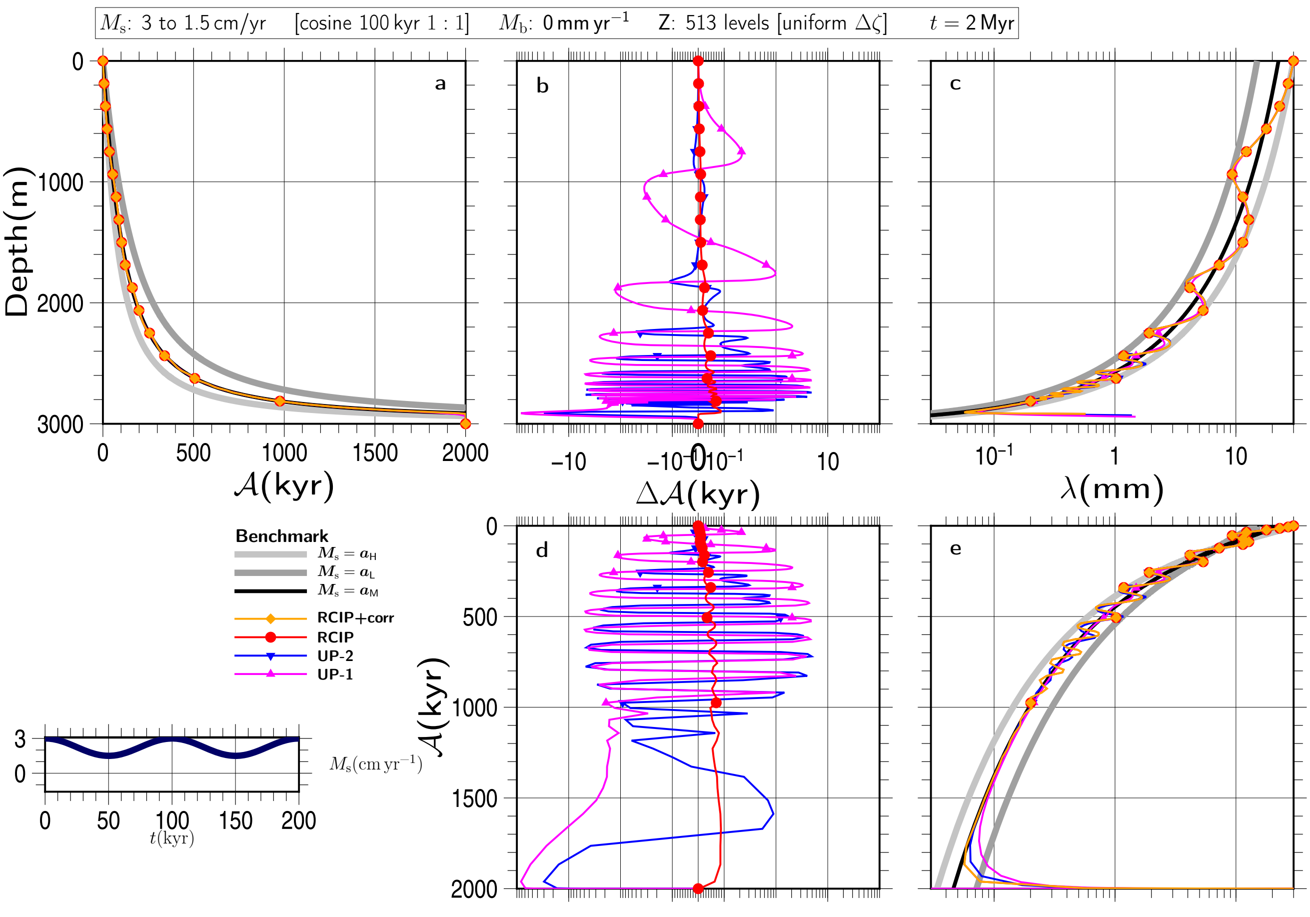

Figure S64

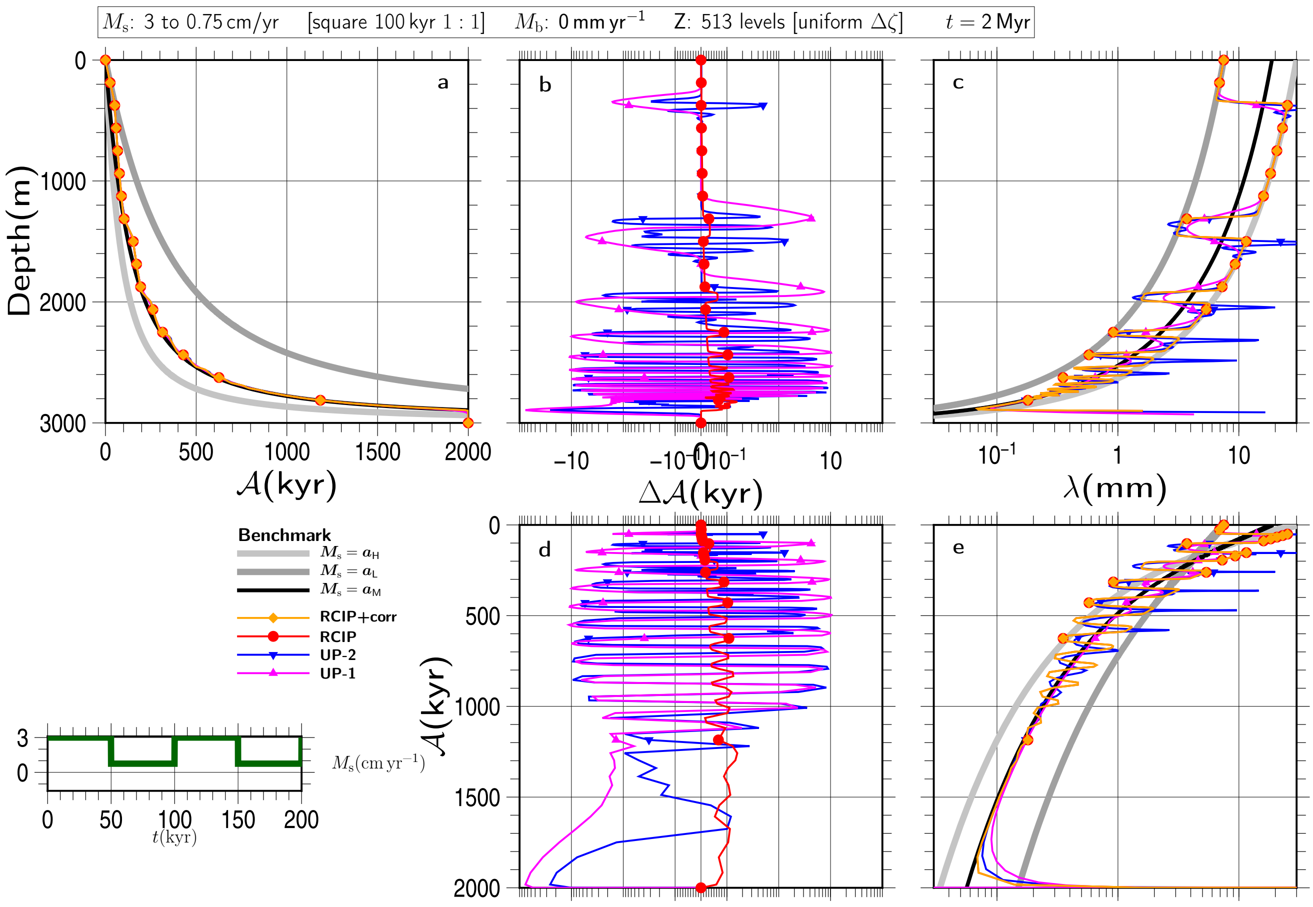

Figure S65

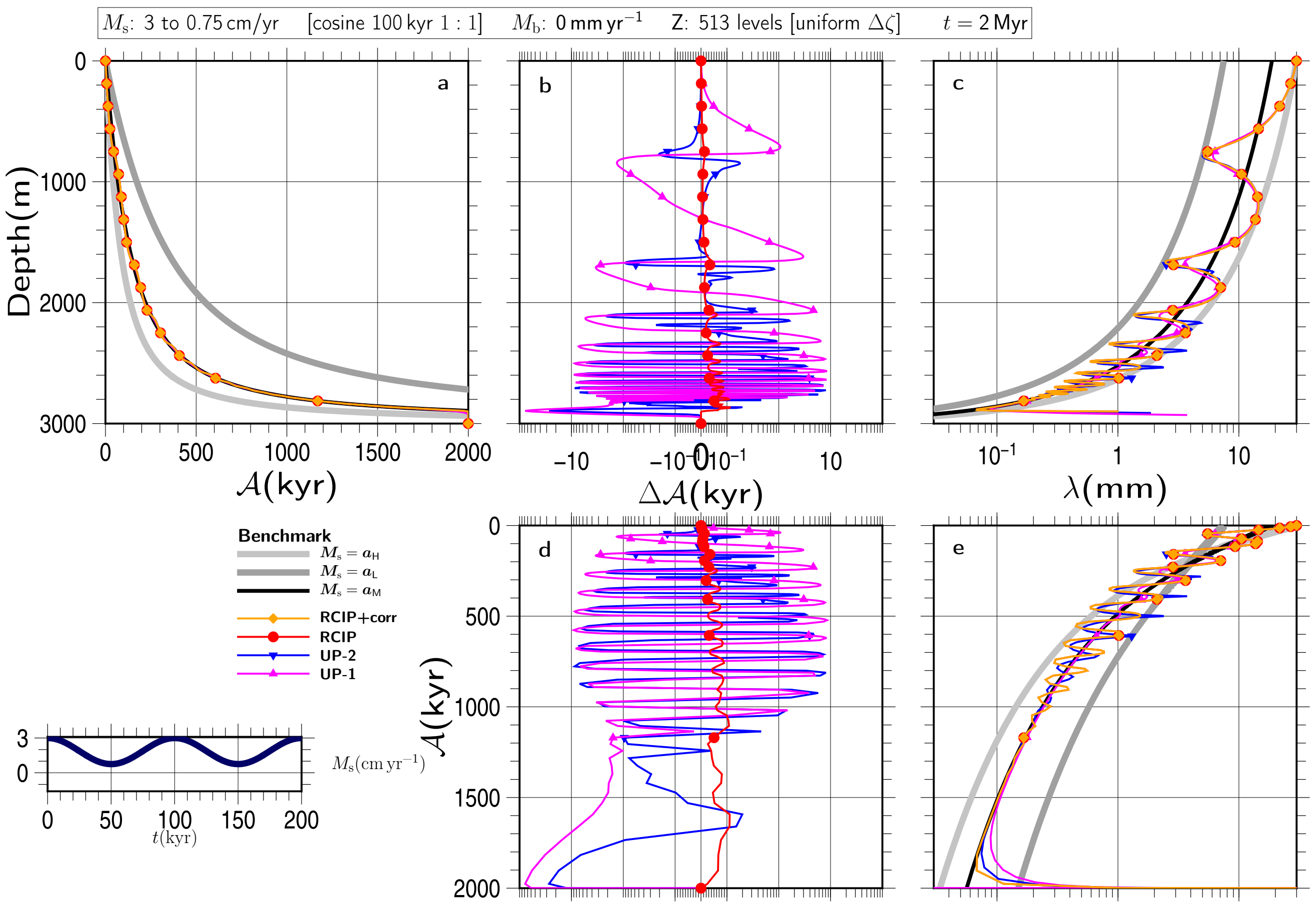

Figure S66

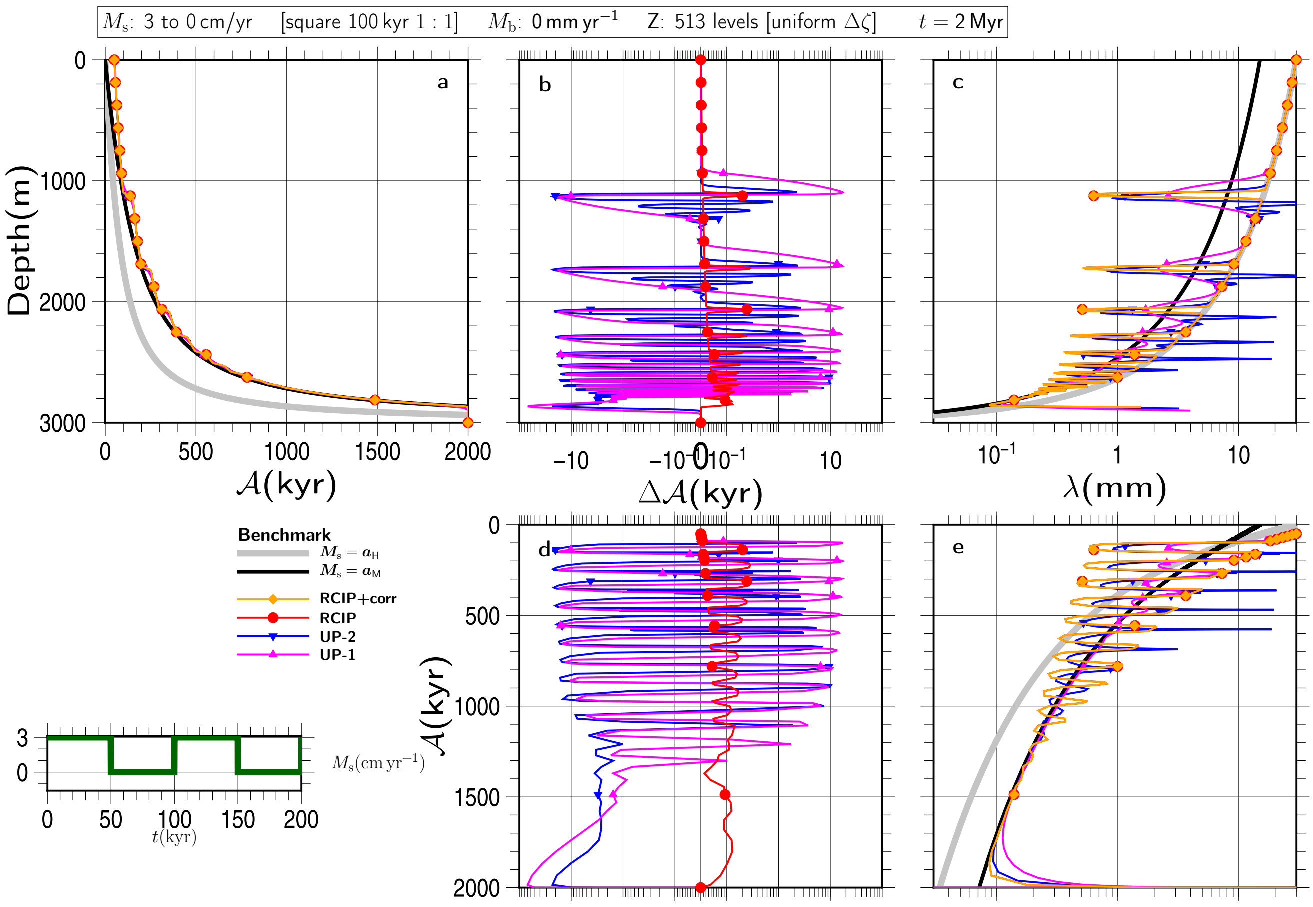

Figure S67

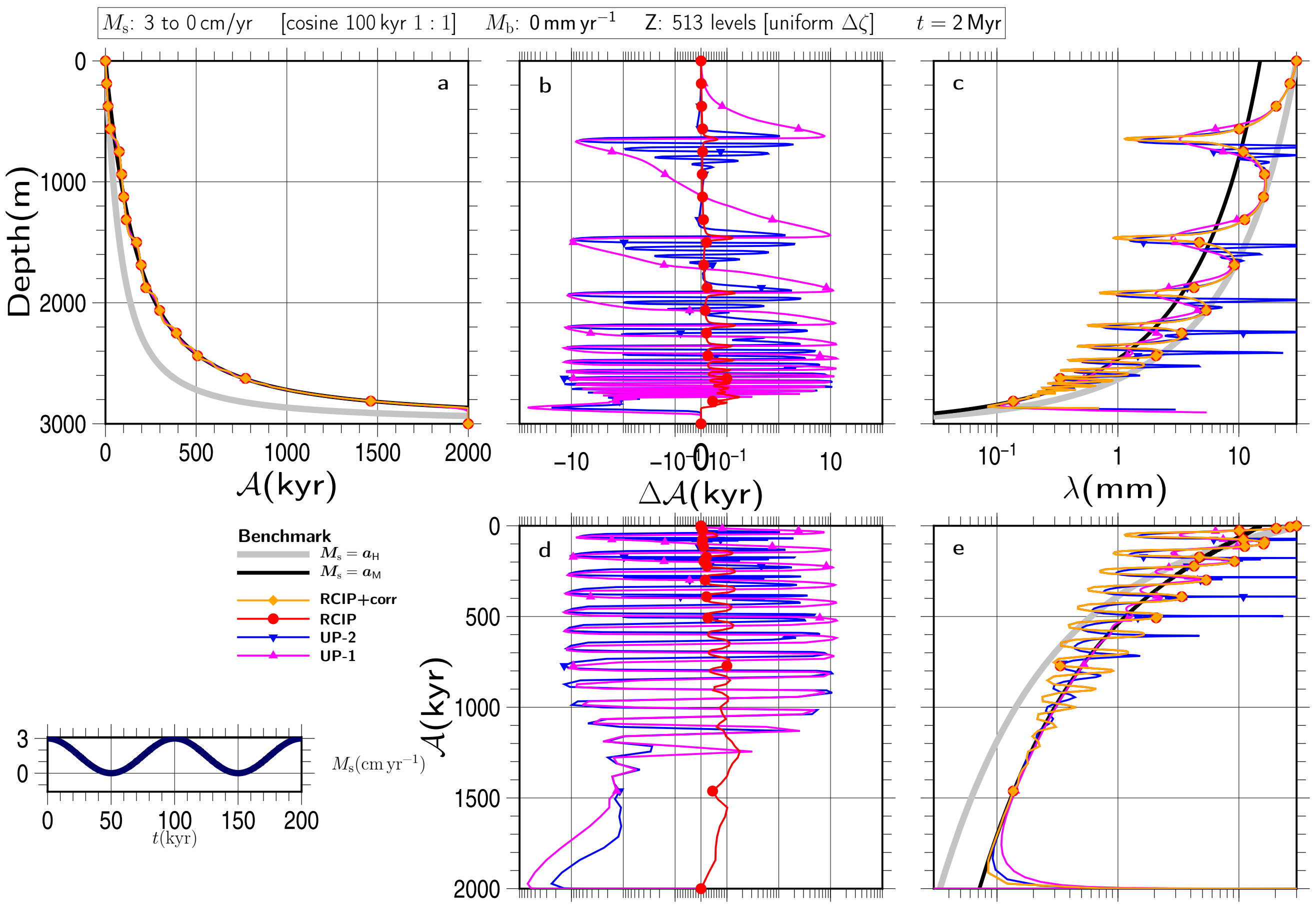

Figure S68

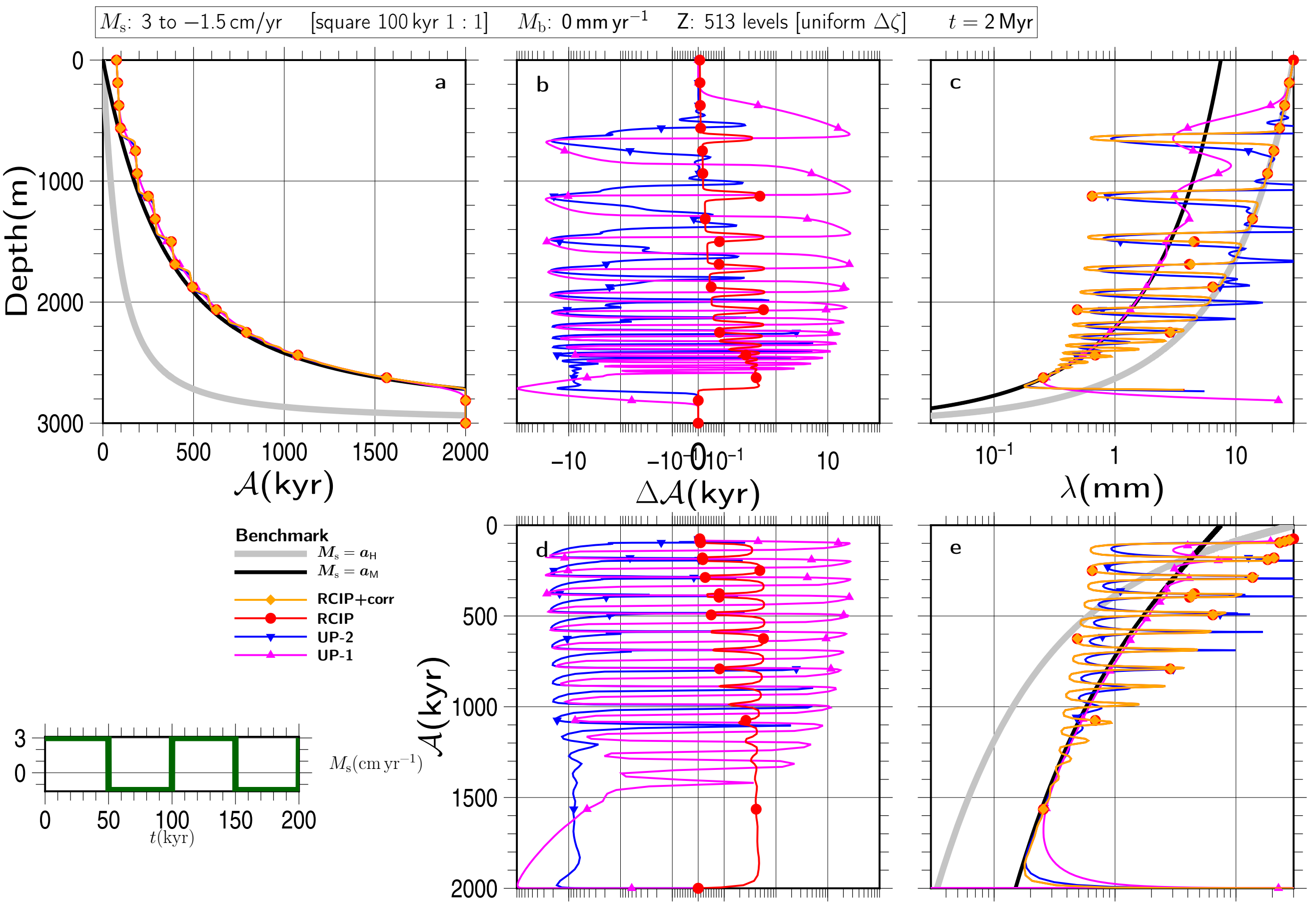

Figure S69

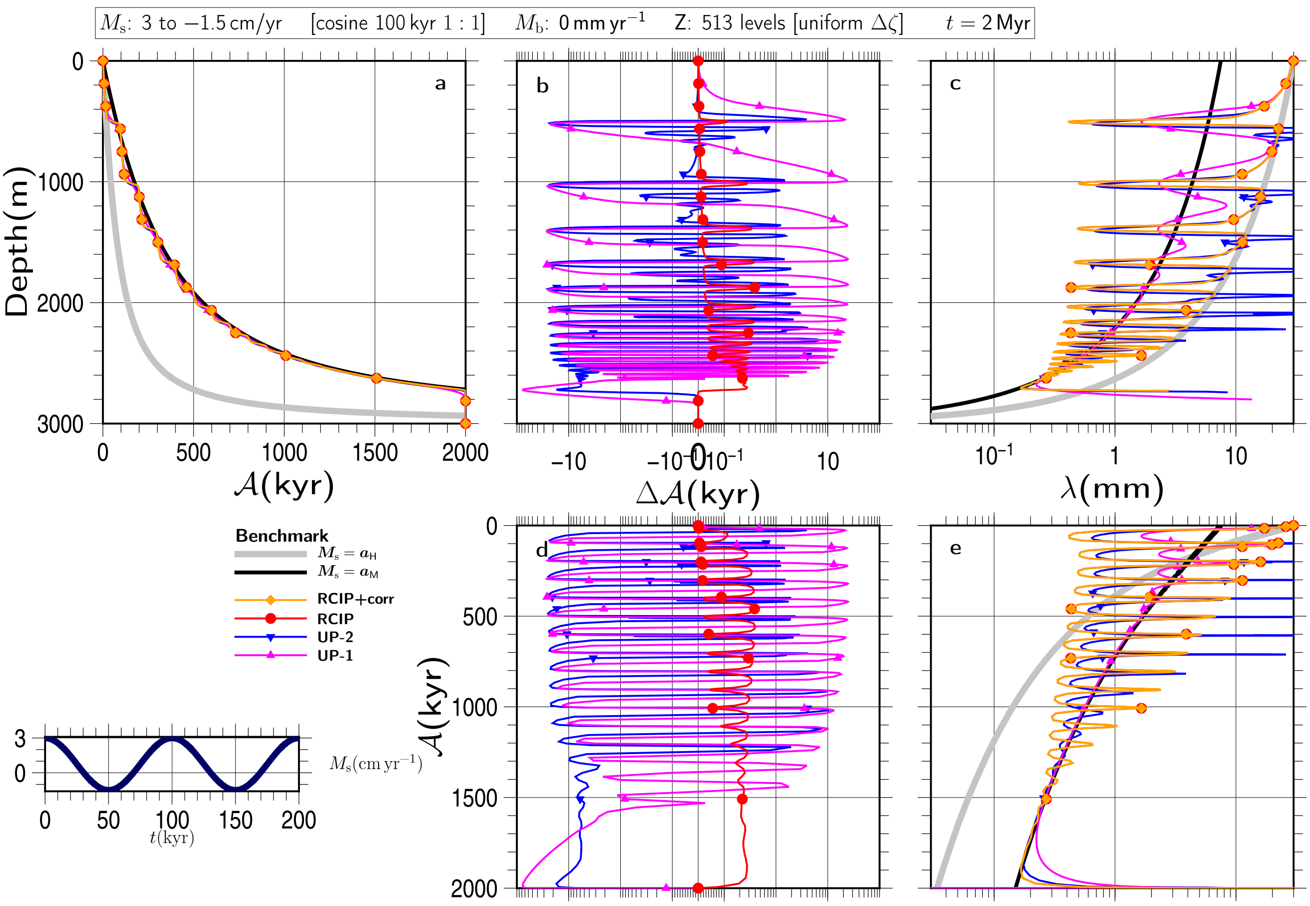

Figure S70

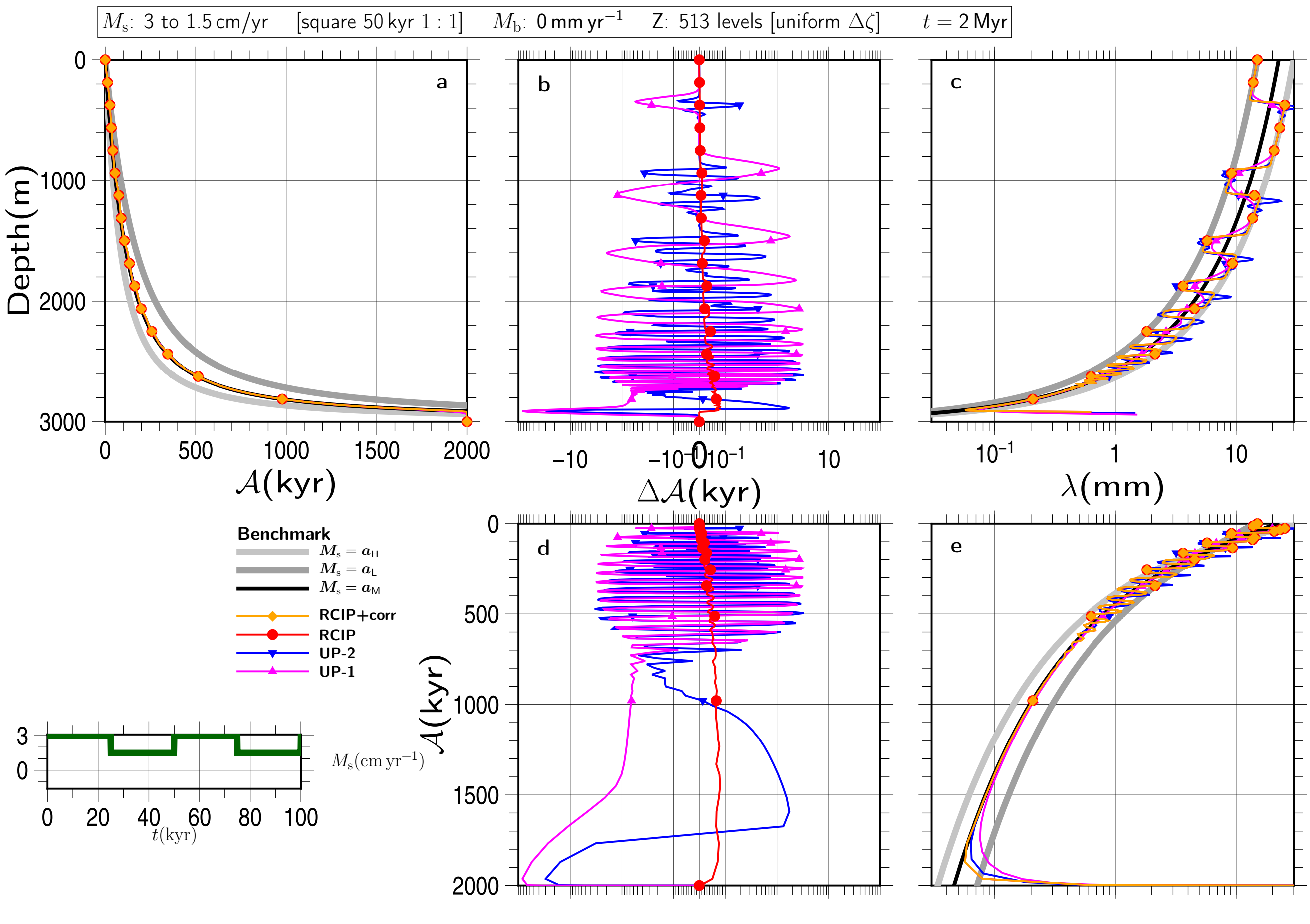

Figure S71

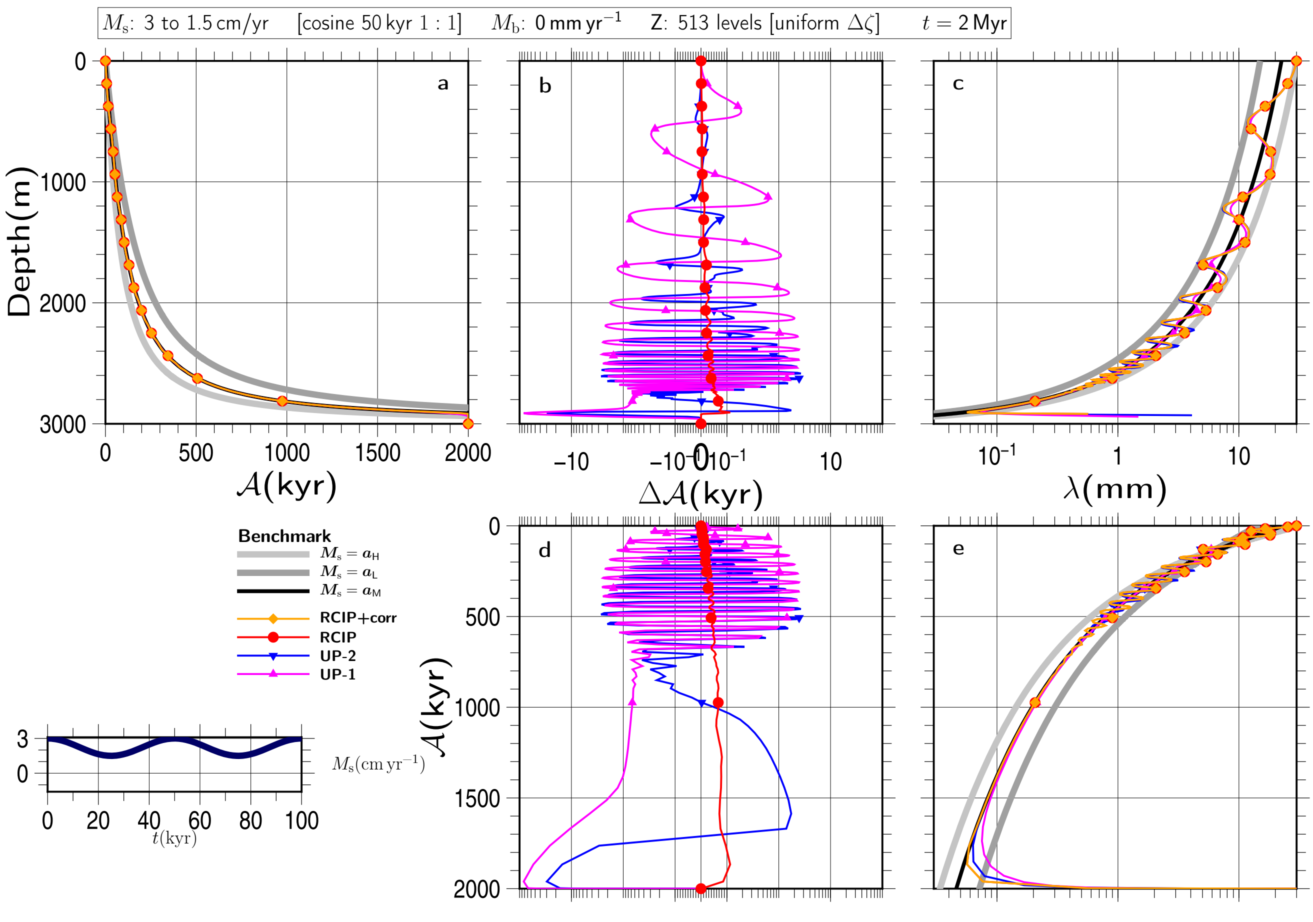

Figure S72

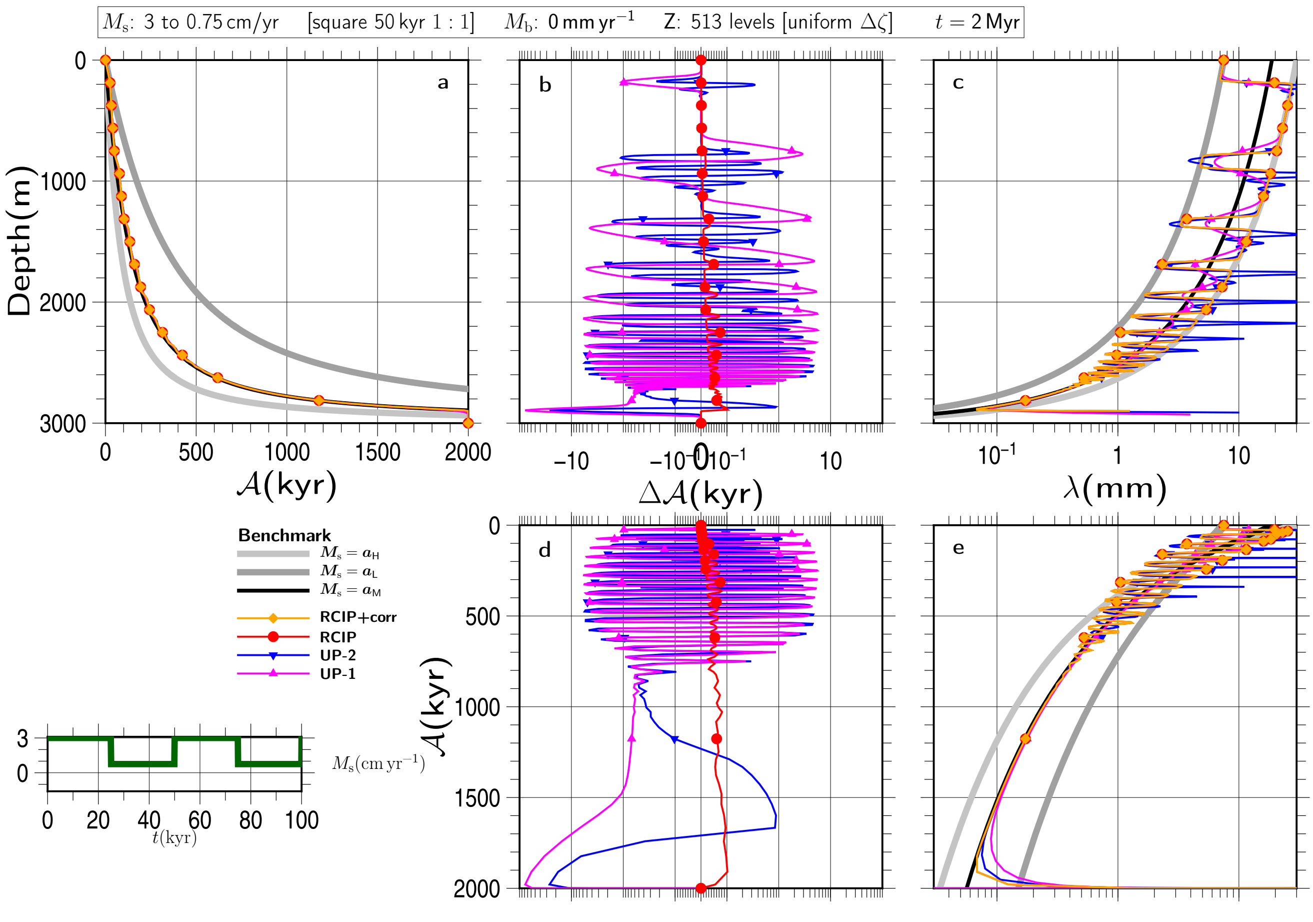

Figure S73

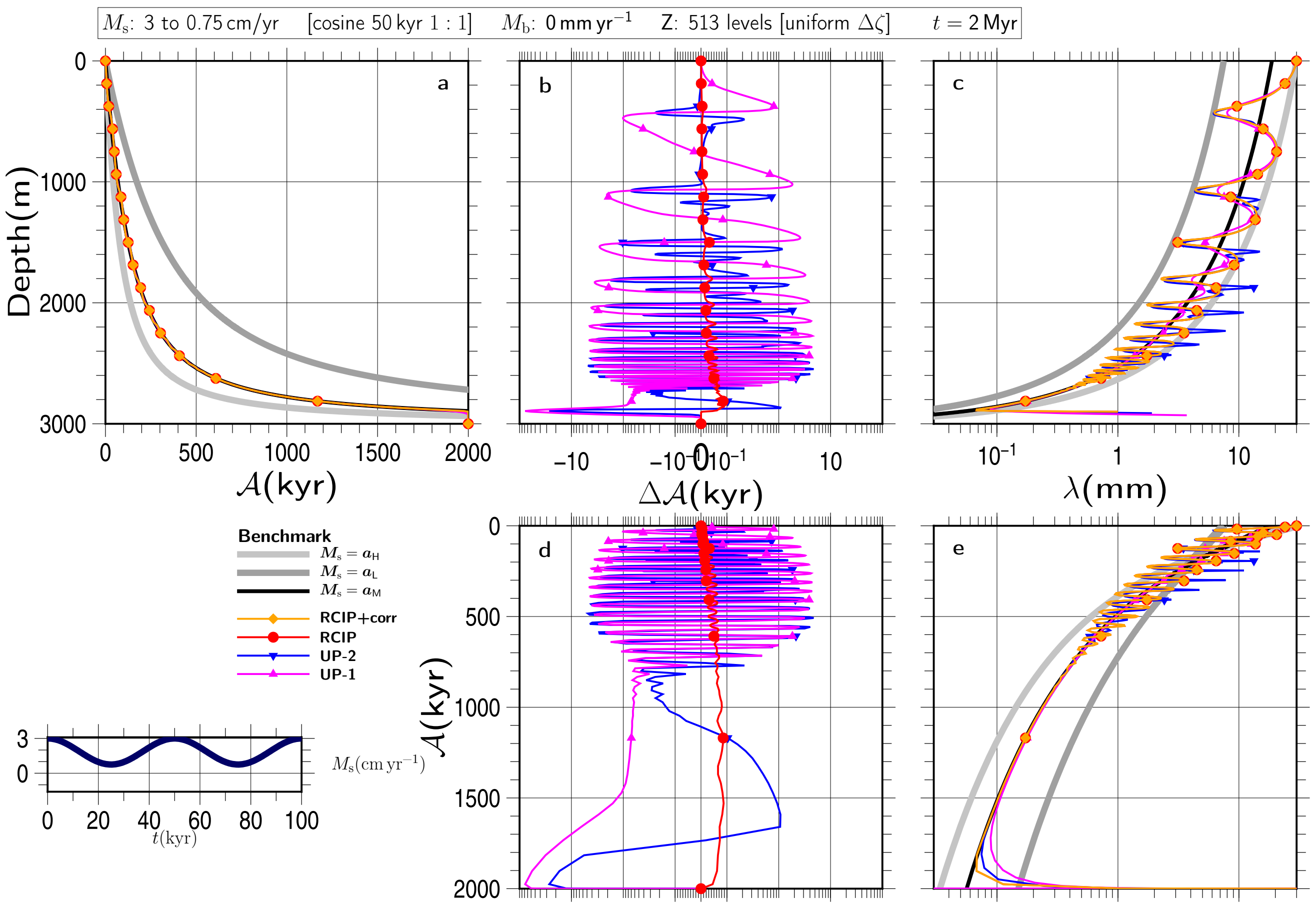

Figure S74

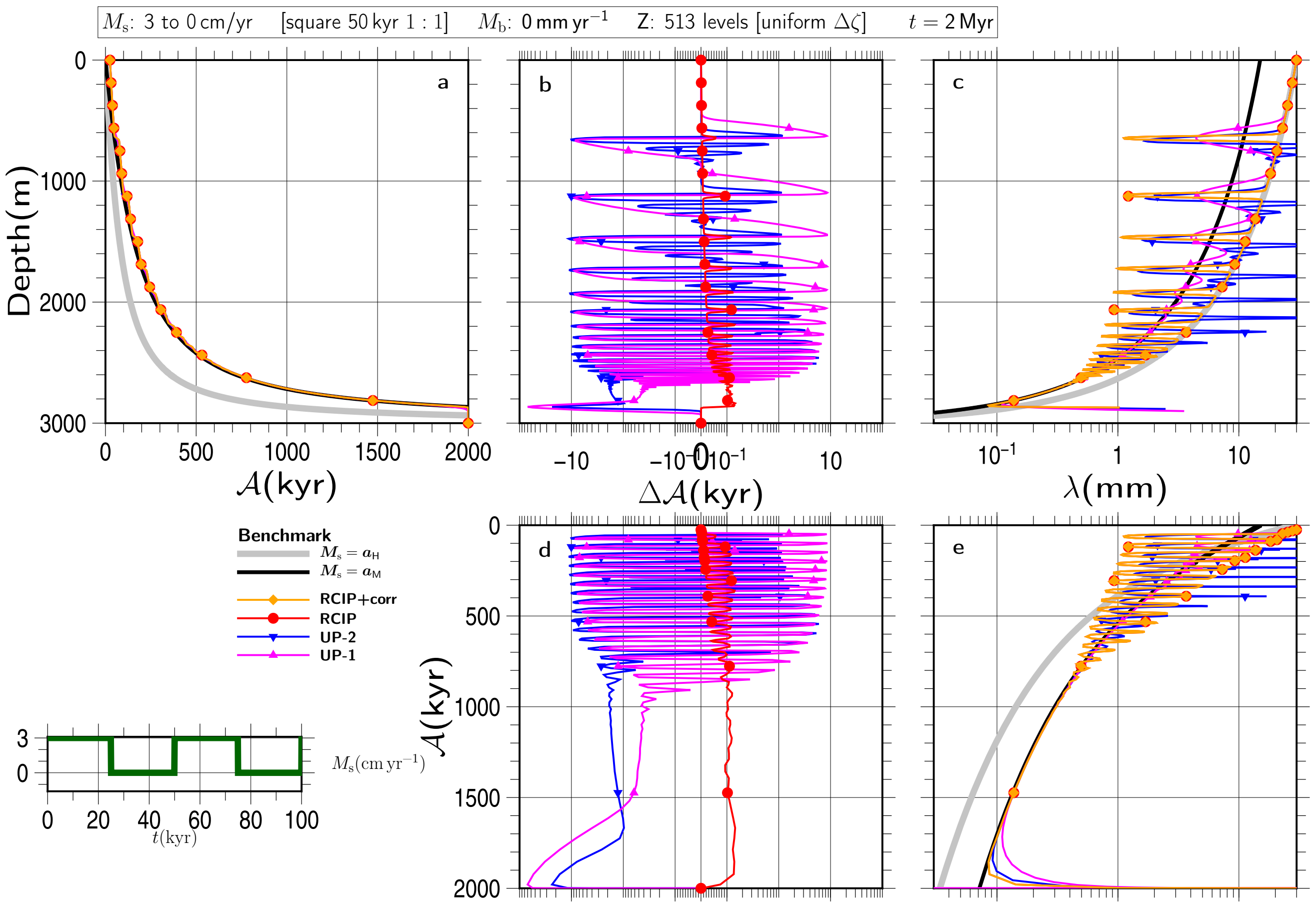

Figure S75

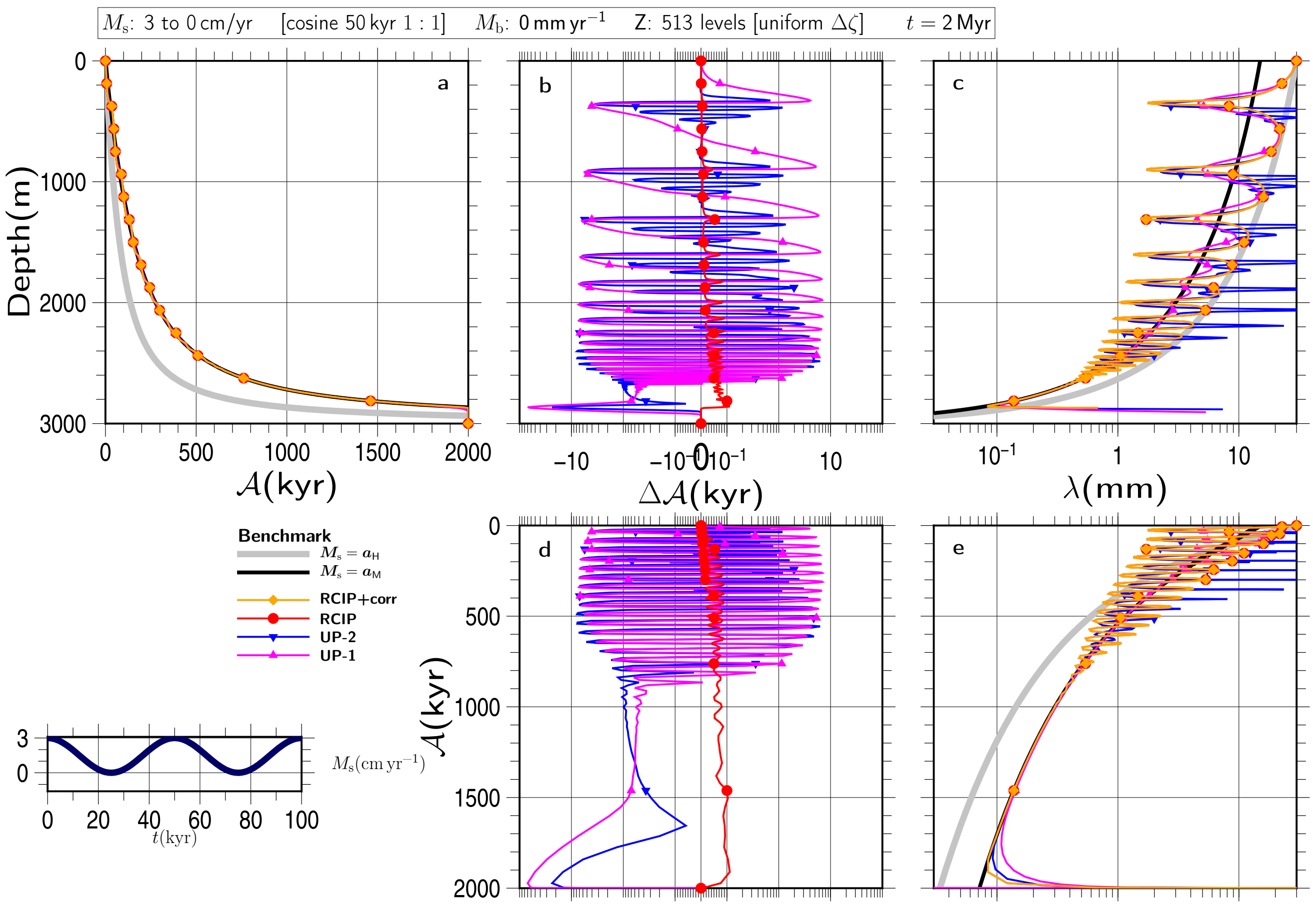

Figure S76

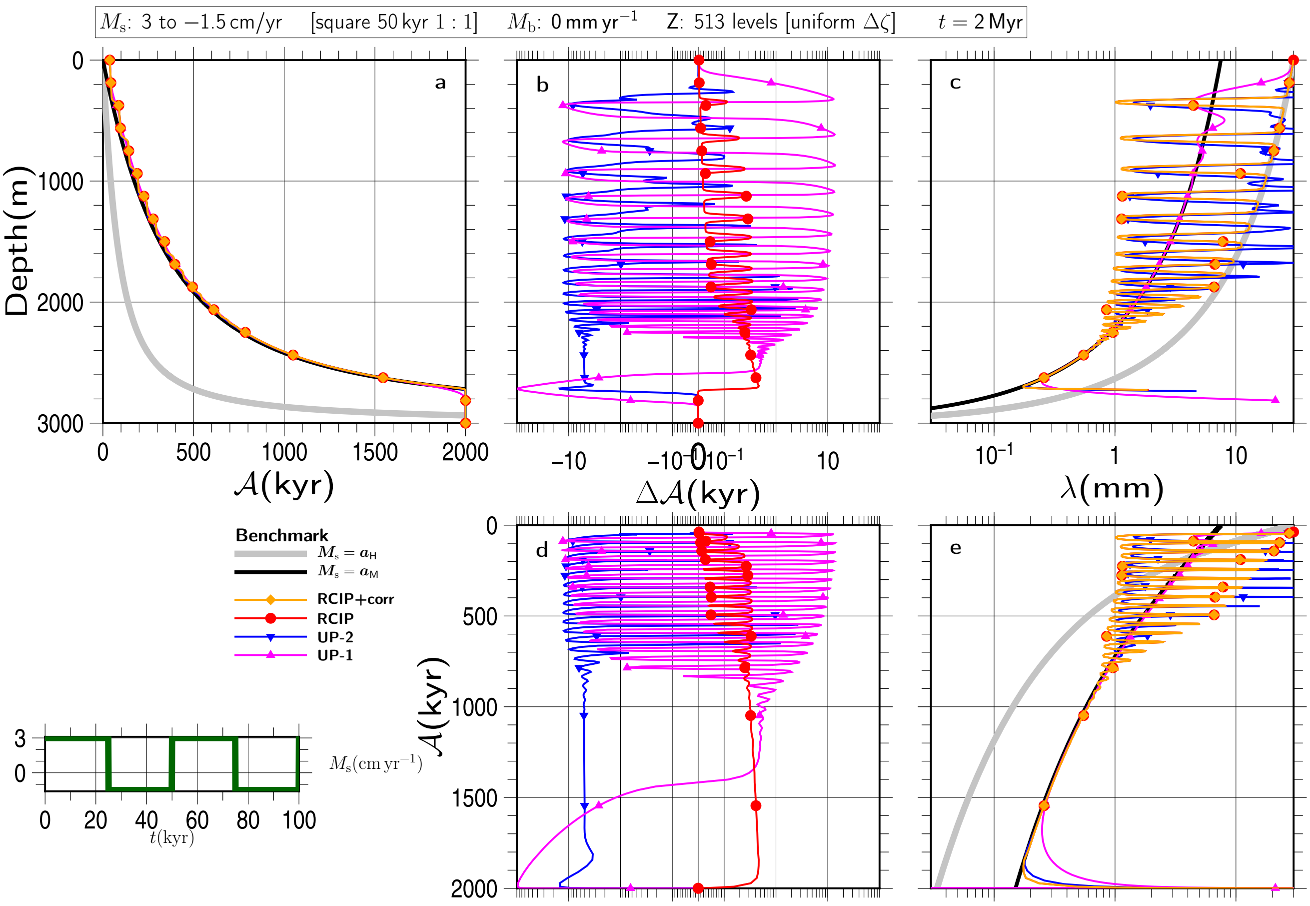

Figure S77

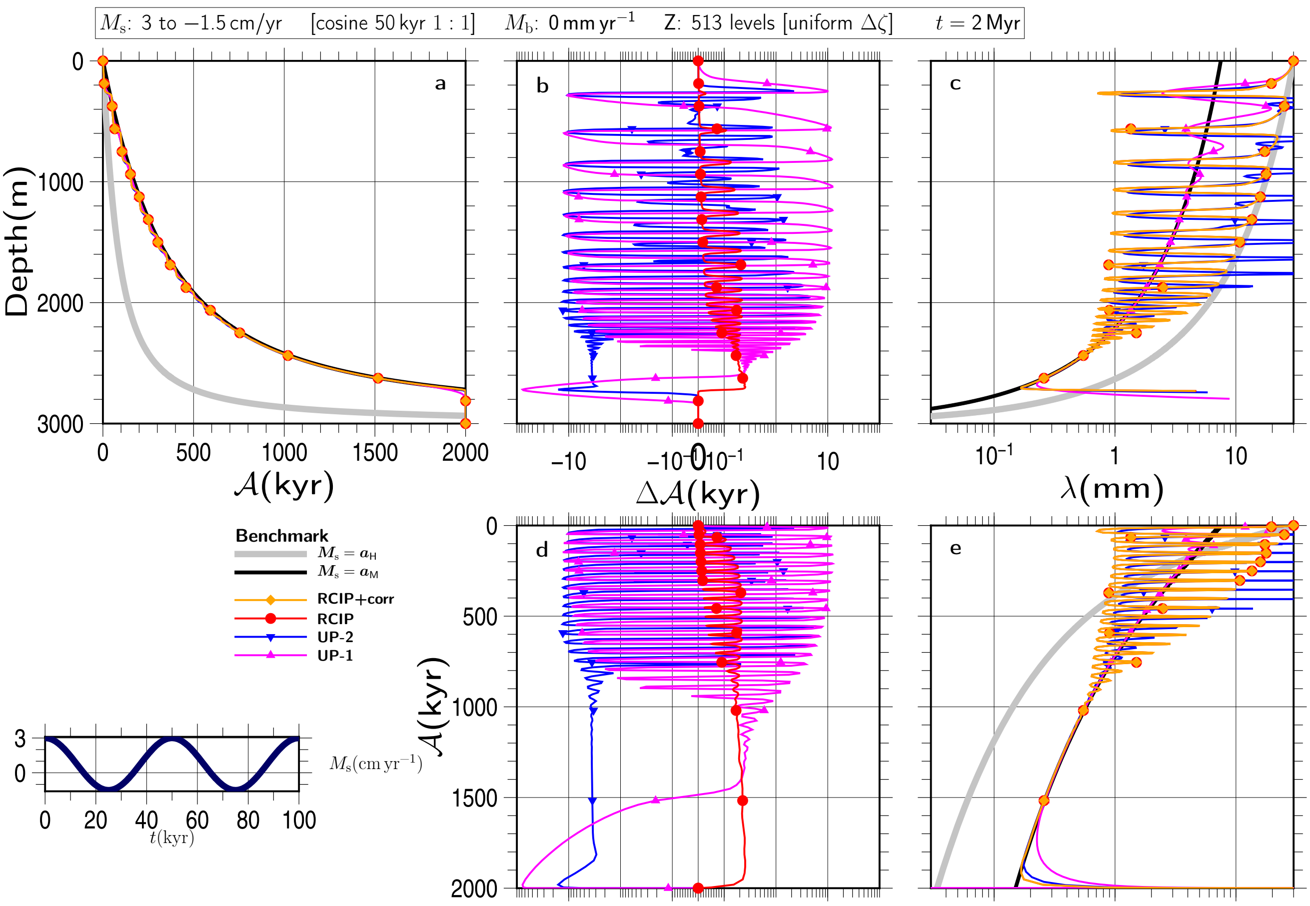

Figure S78

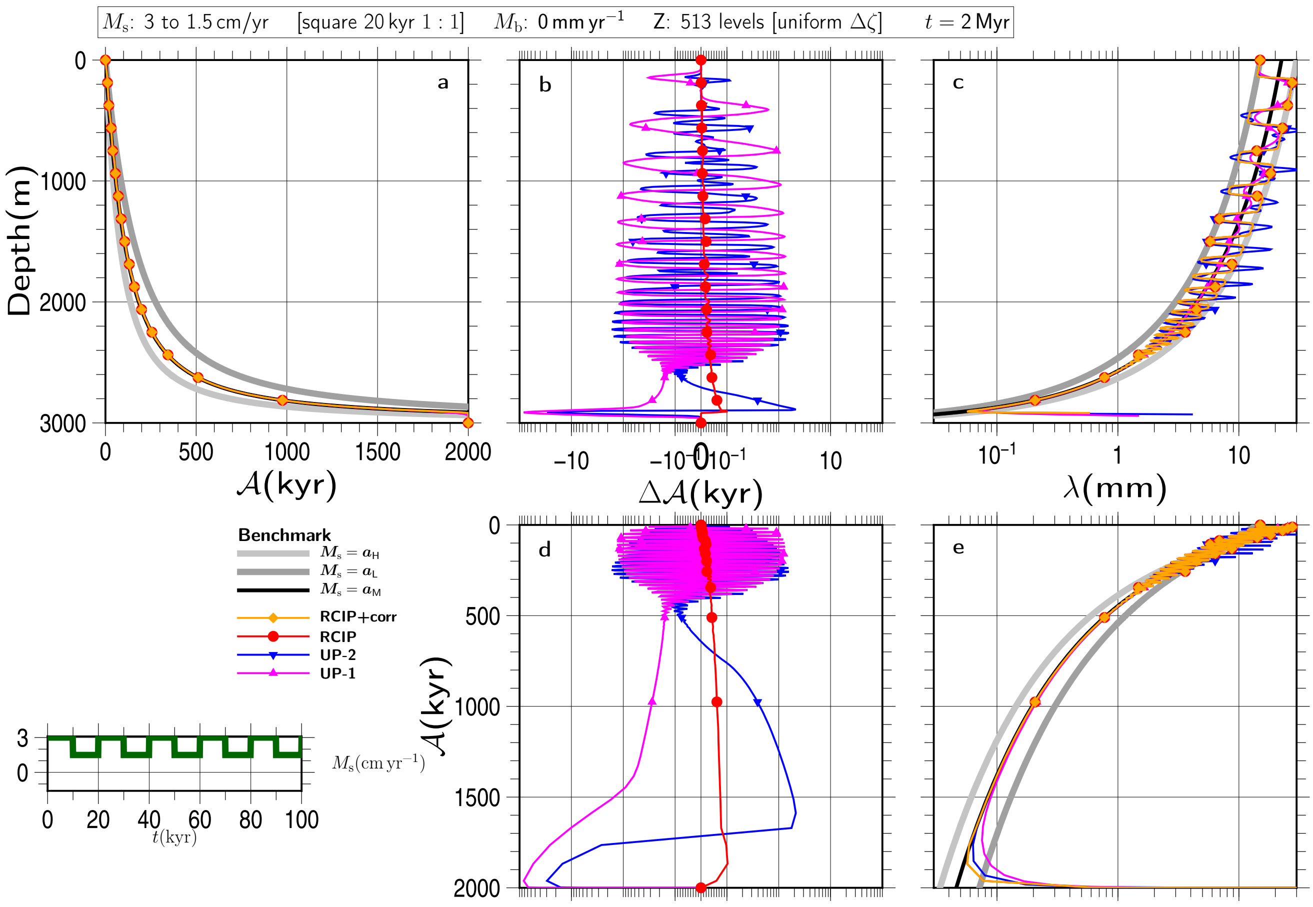

Figure S79

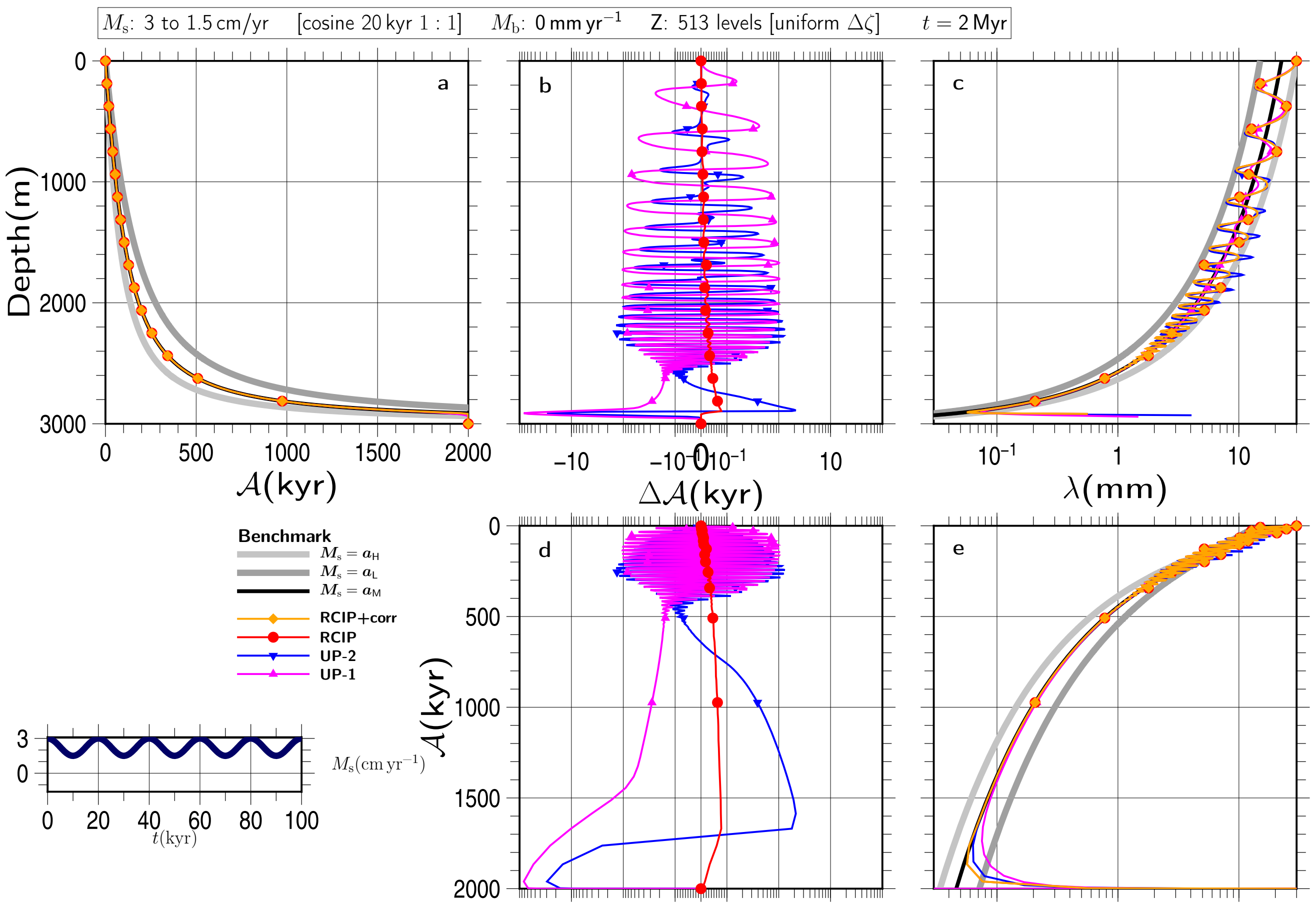

Figure S80

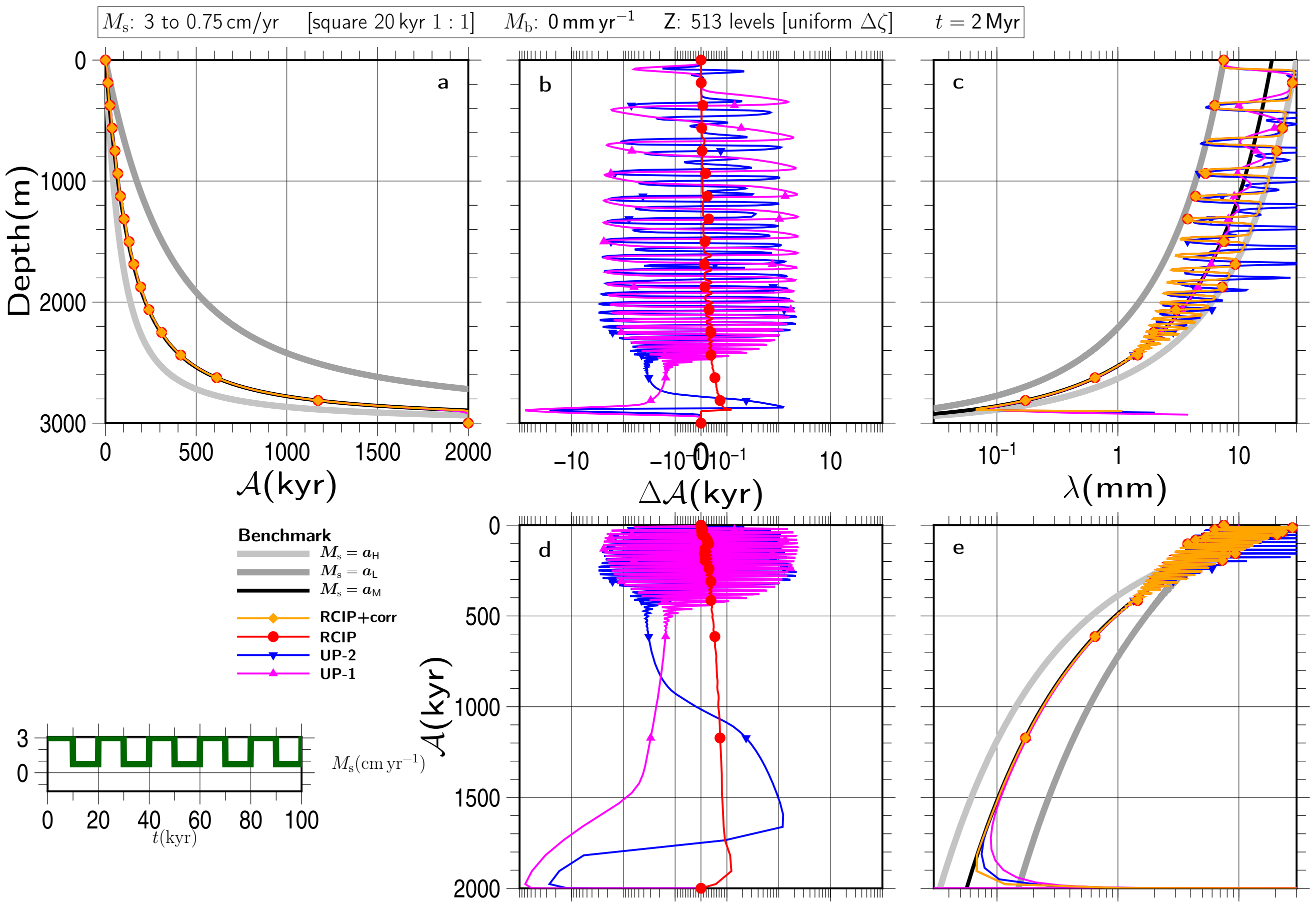

Figure S81

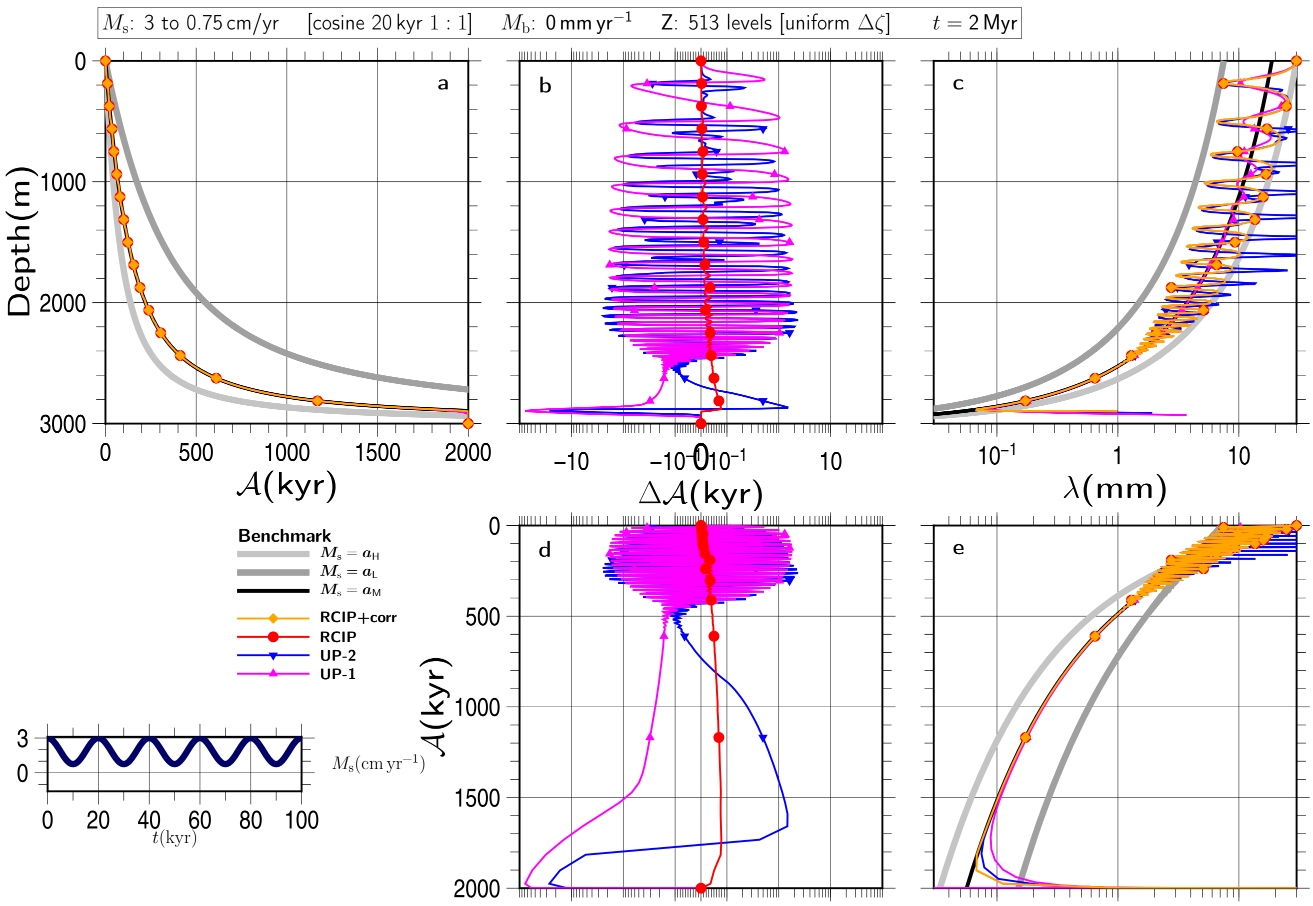

Figure S82

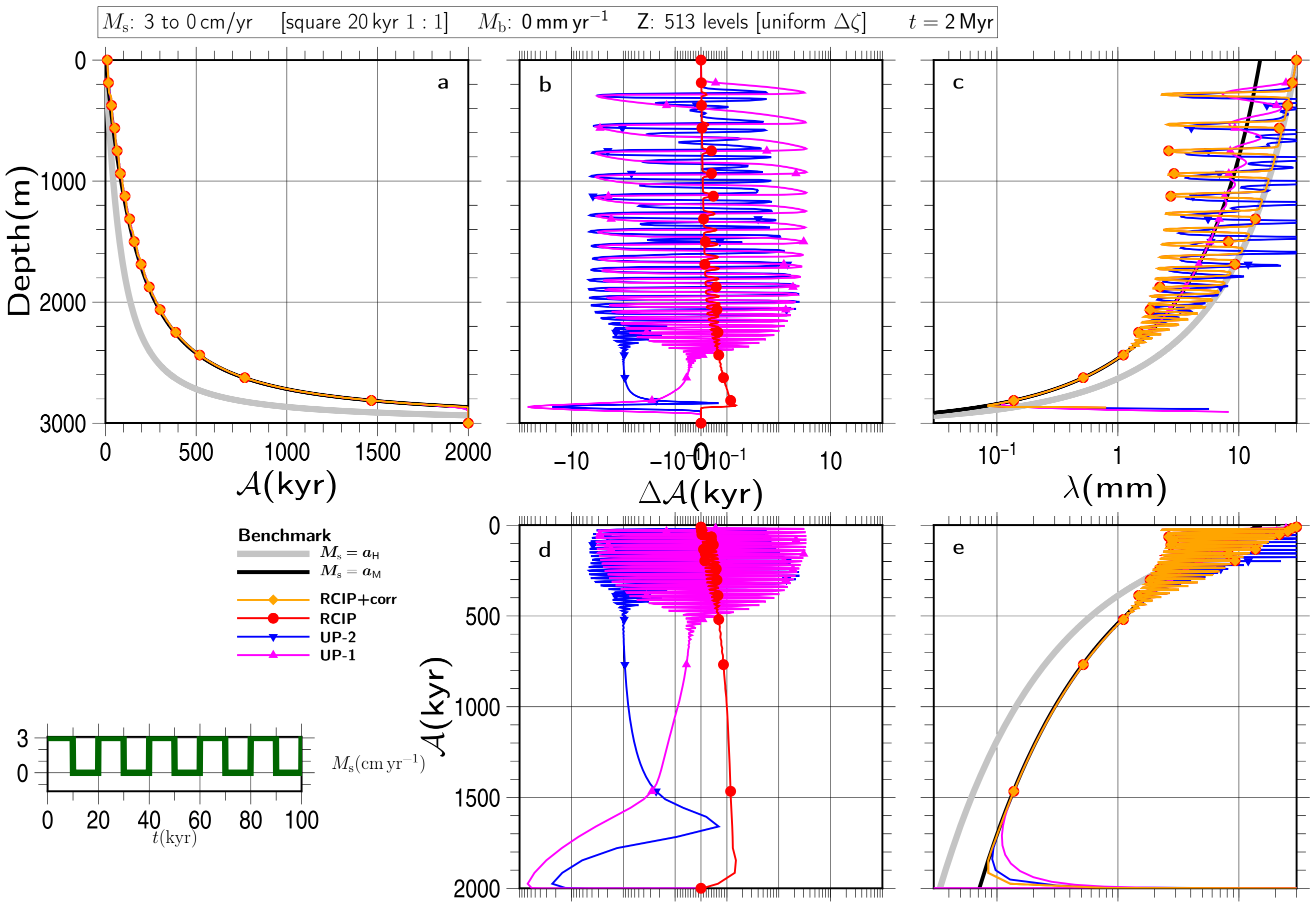

Figure S83

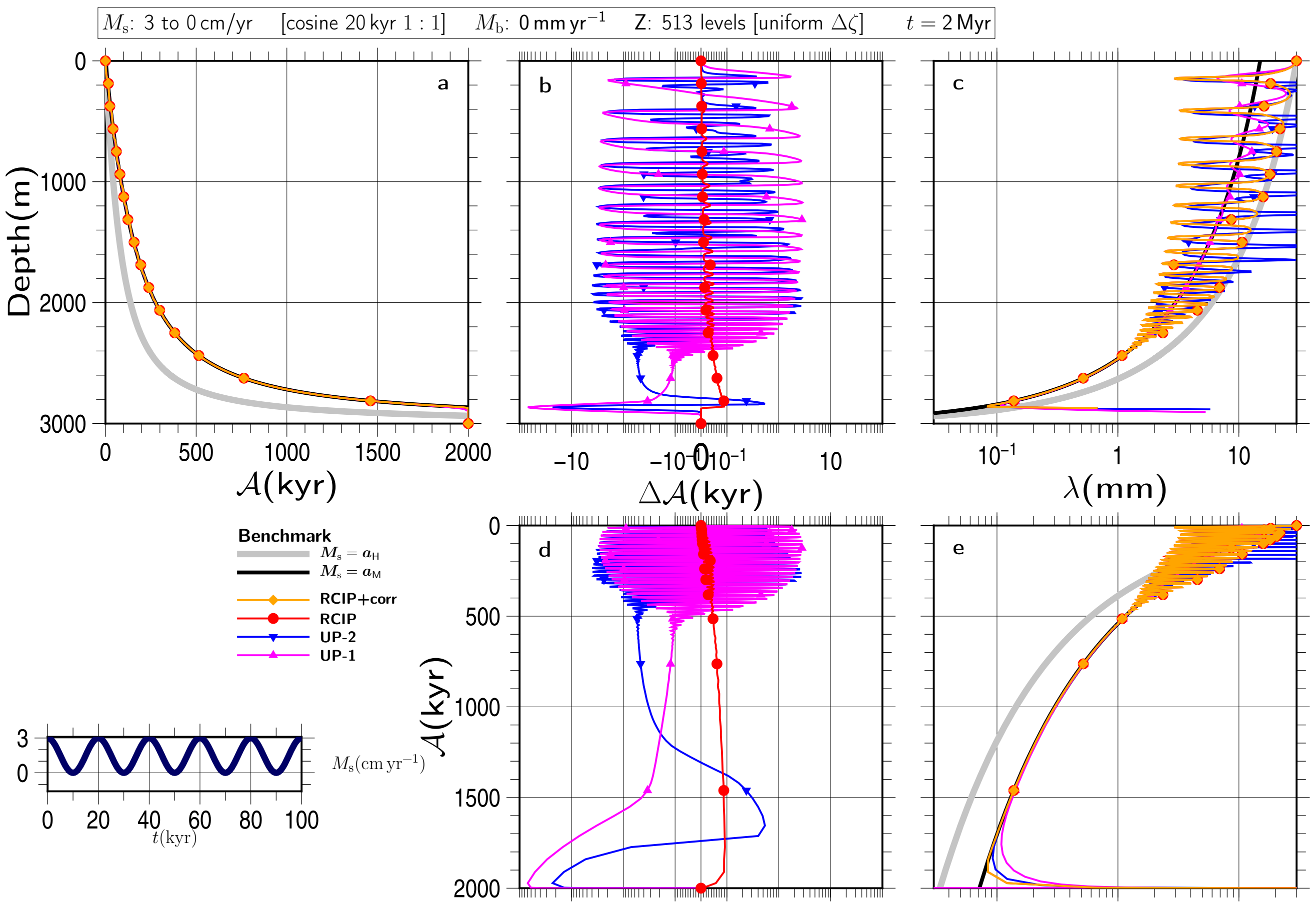

Figure S84

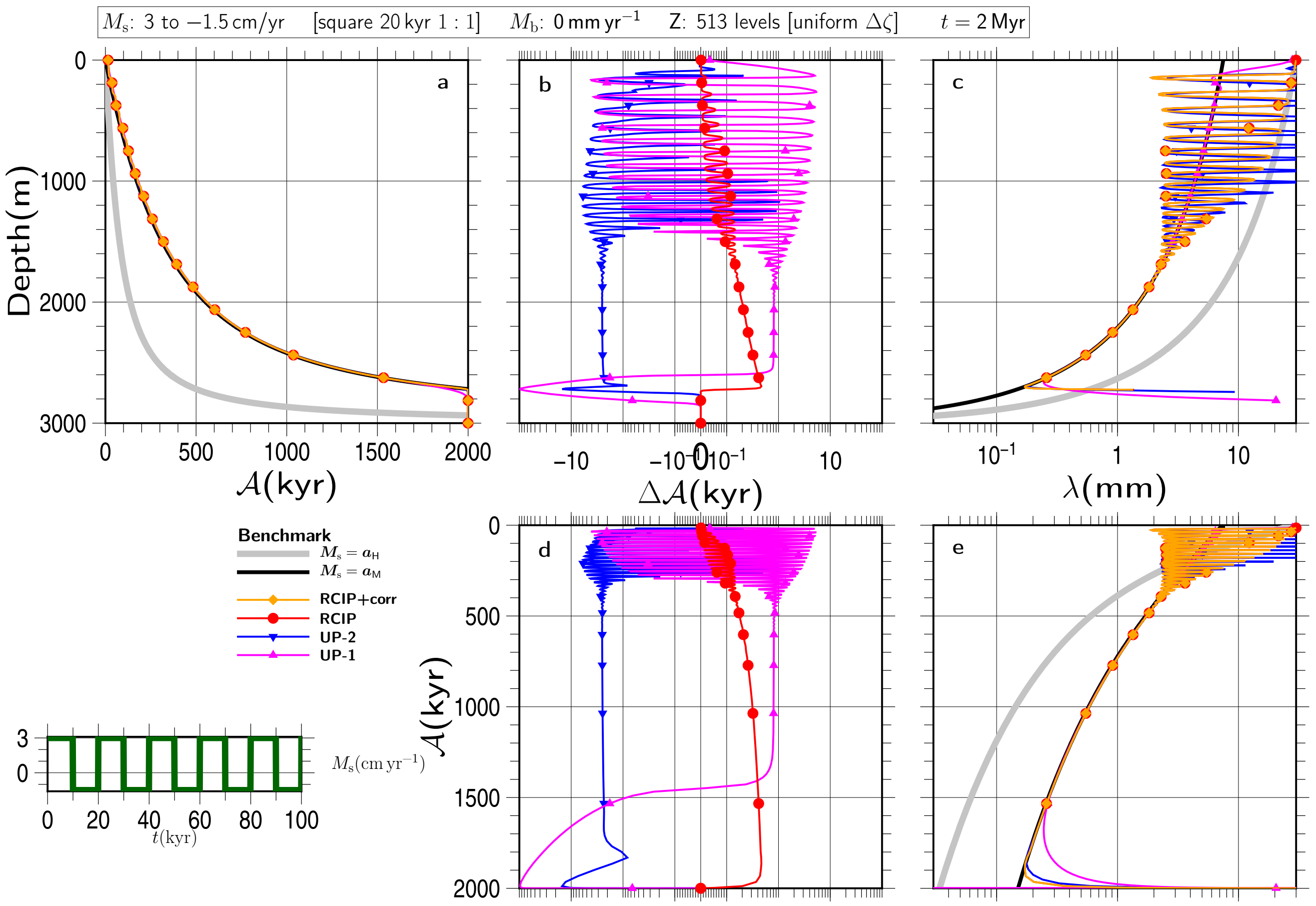

Figure S85

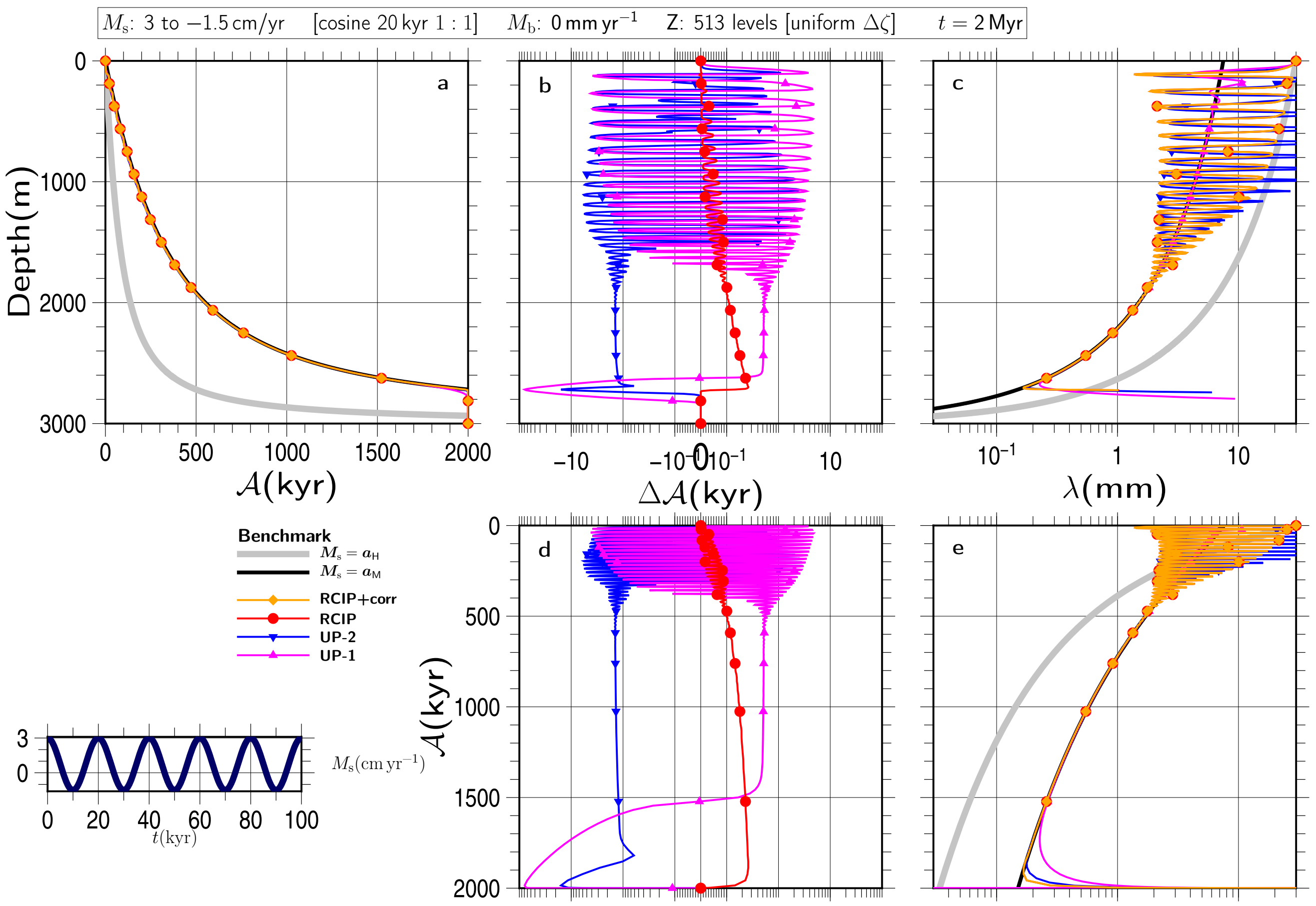

Figure S86

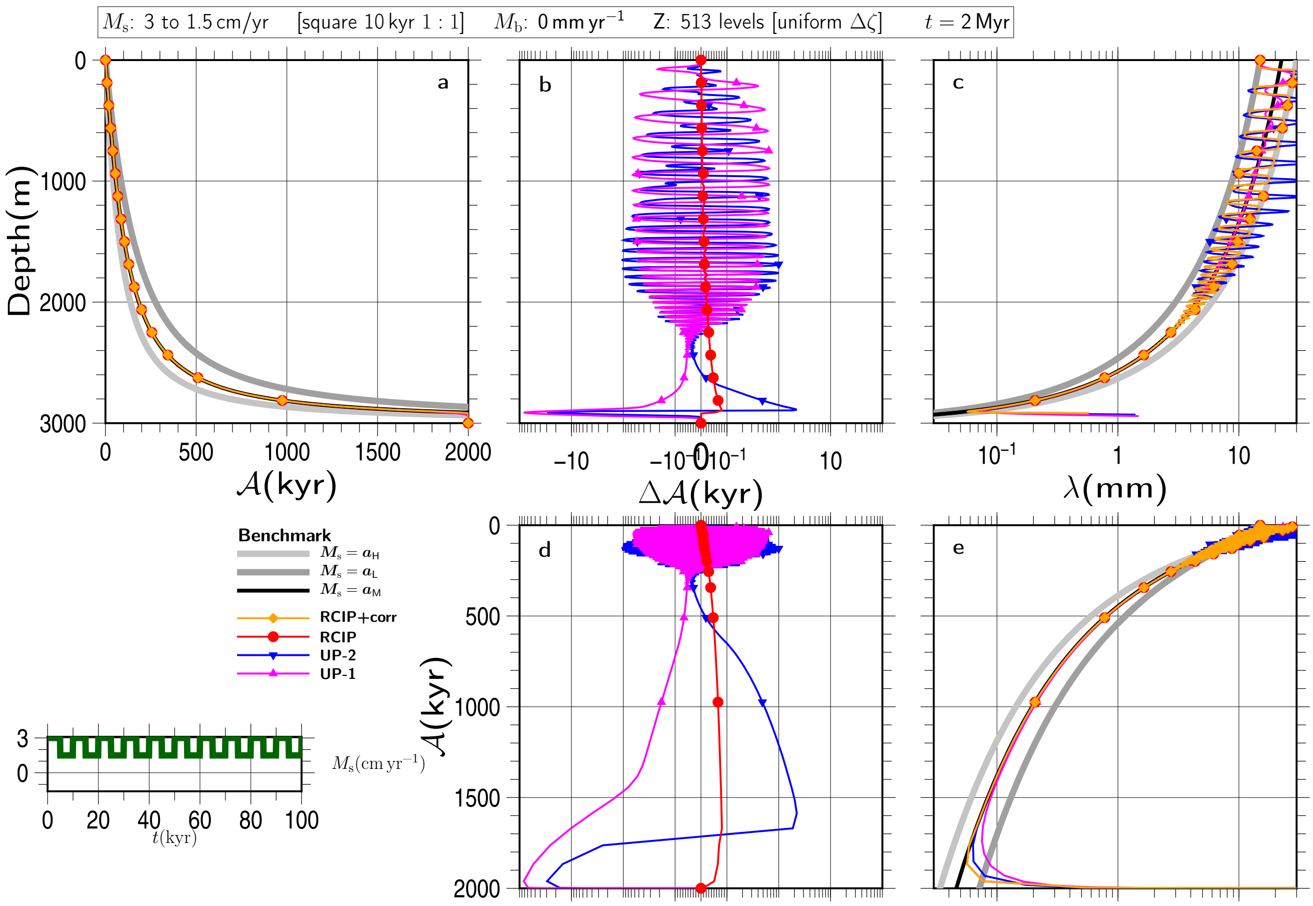

Figure S87

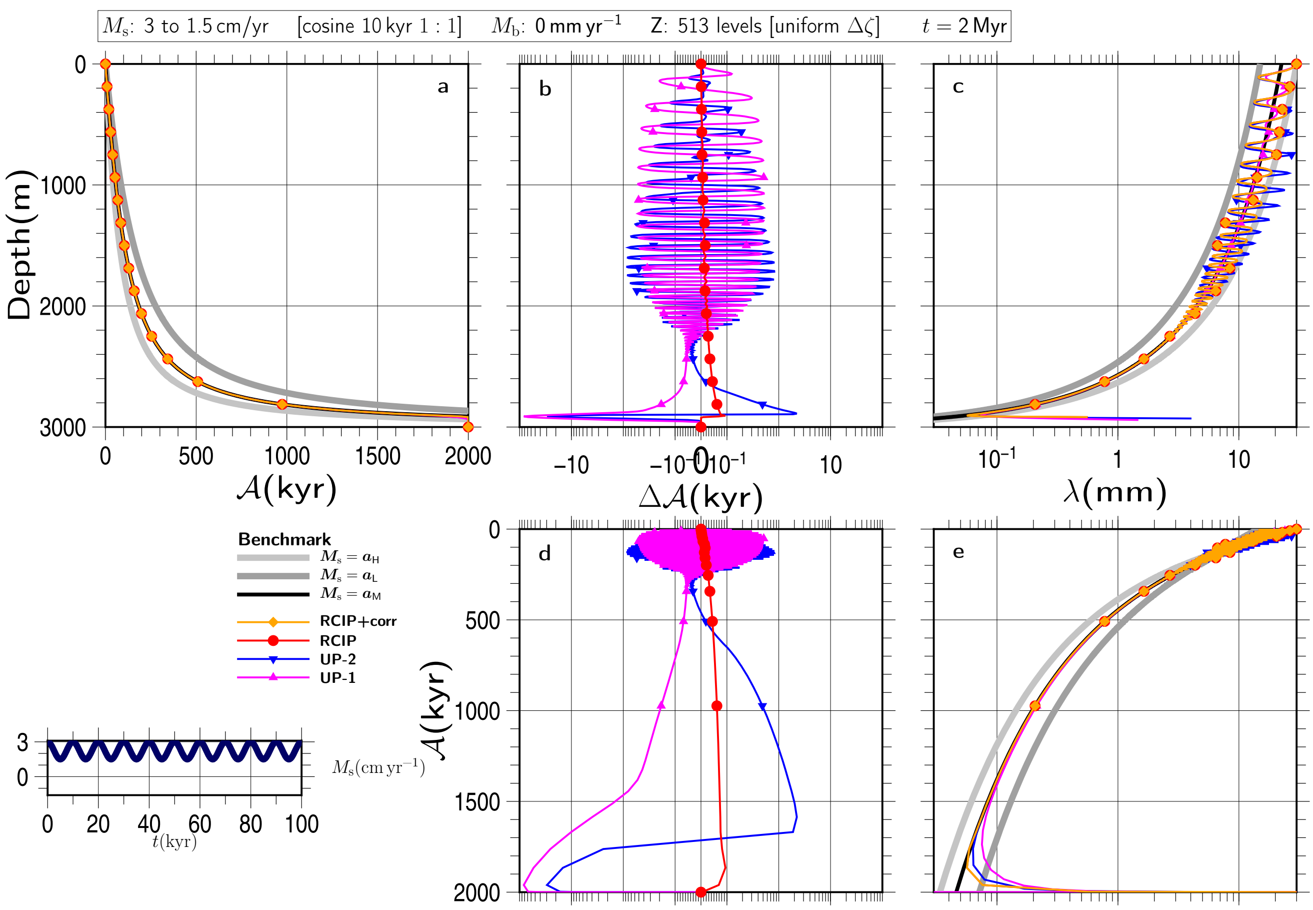

Figure S88

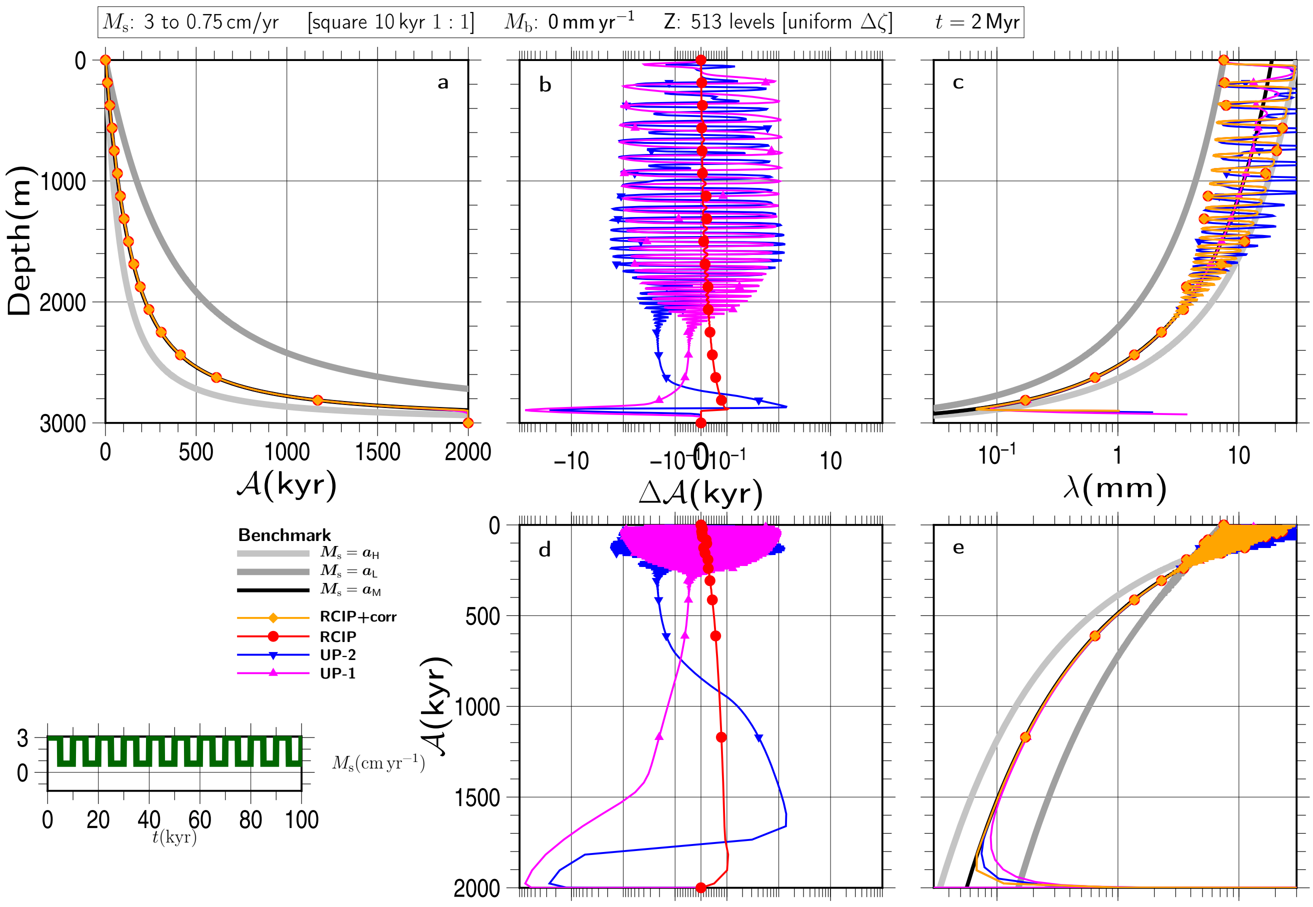

Figure S89

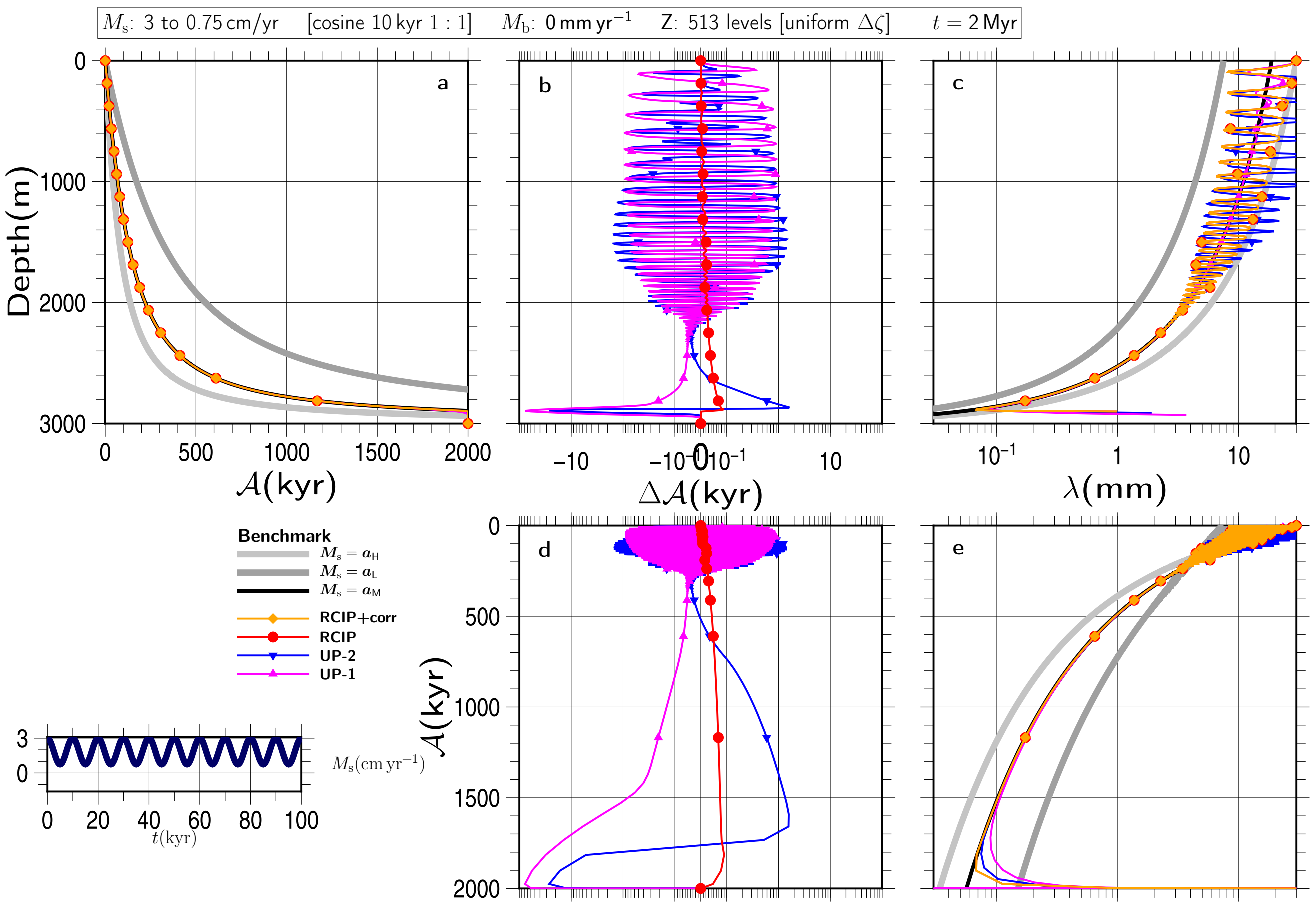

Figure S90

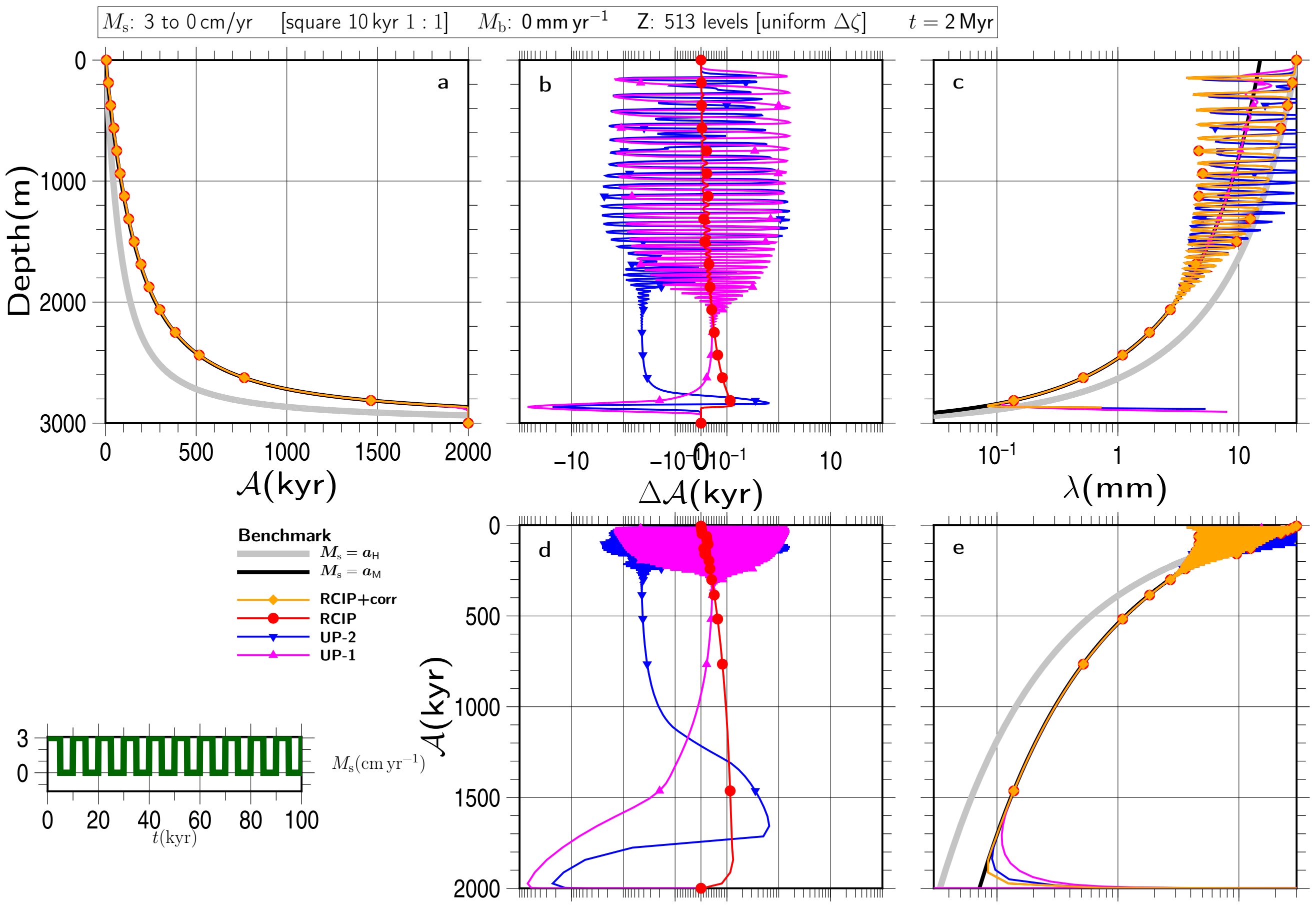

Figure S91

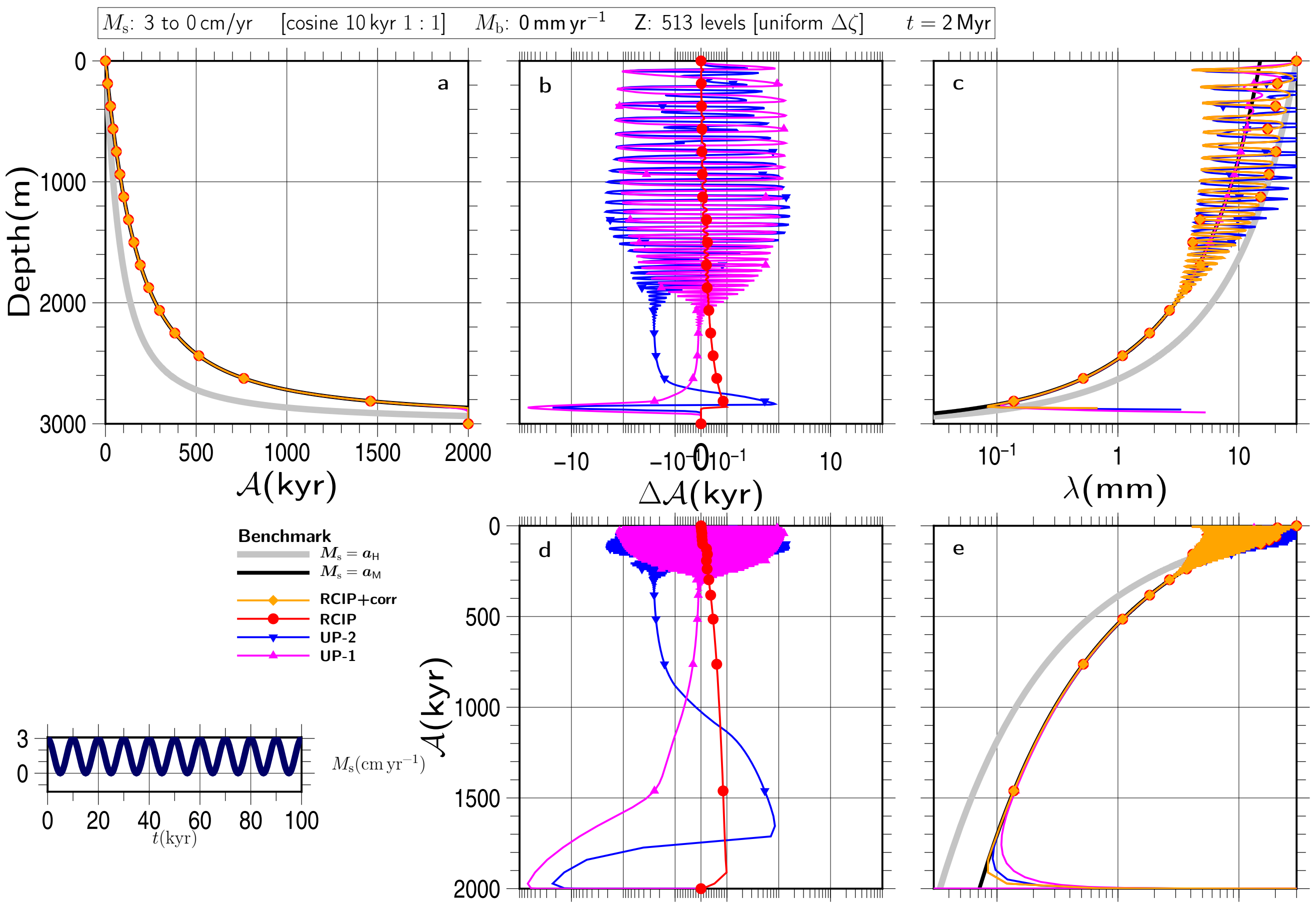

Figure S92

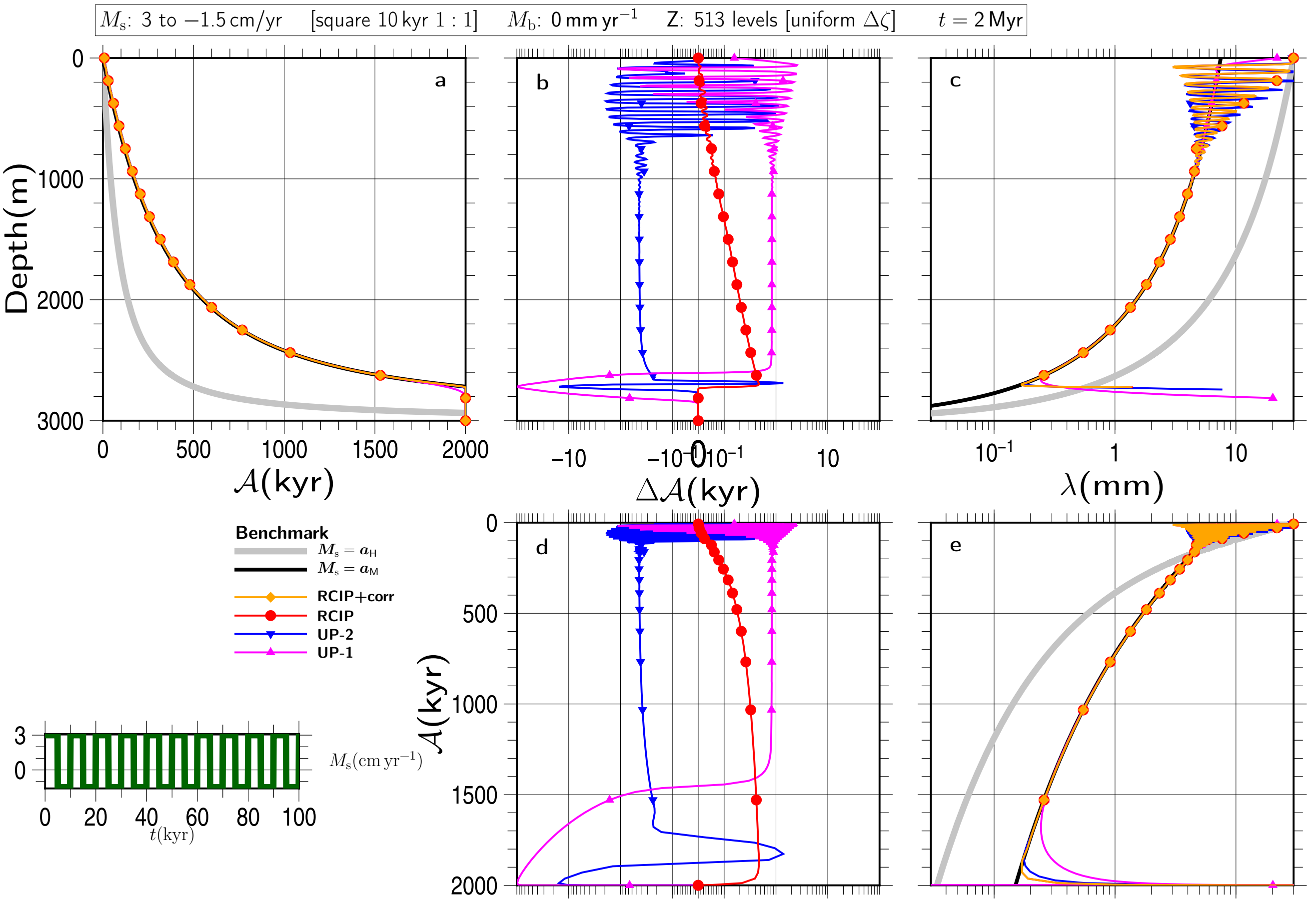

Figure S93

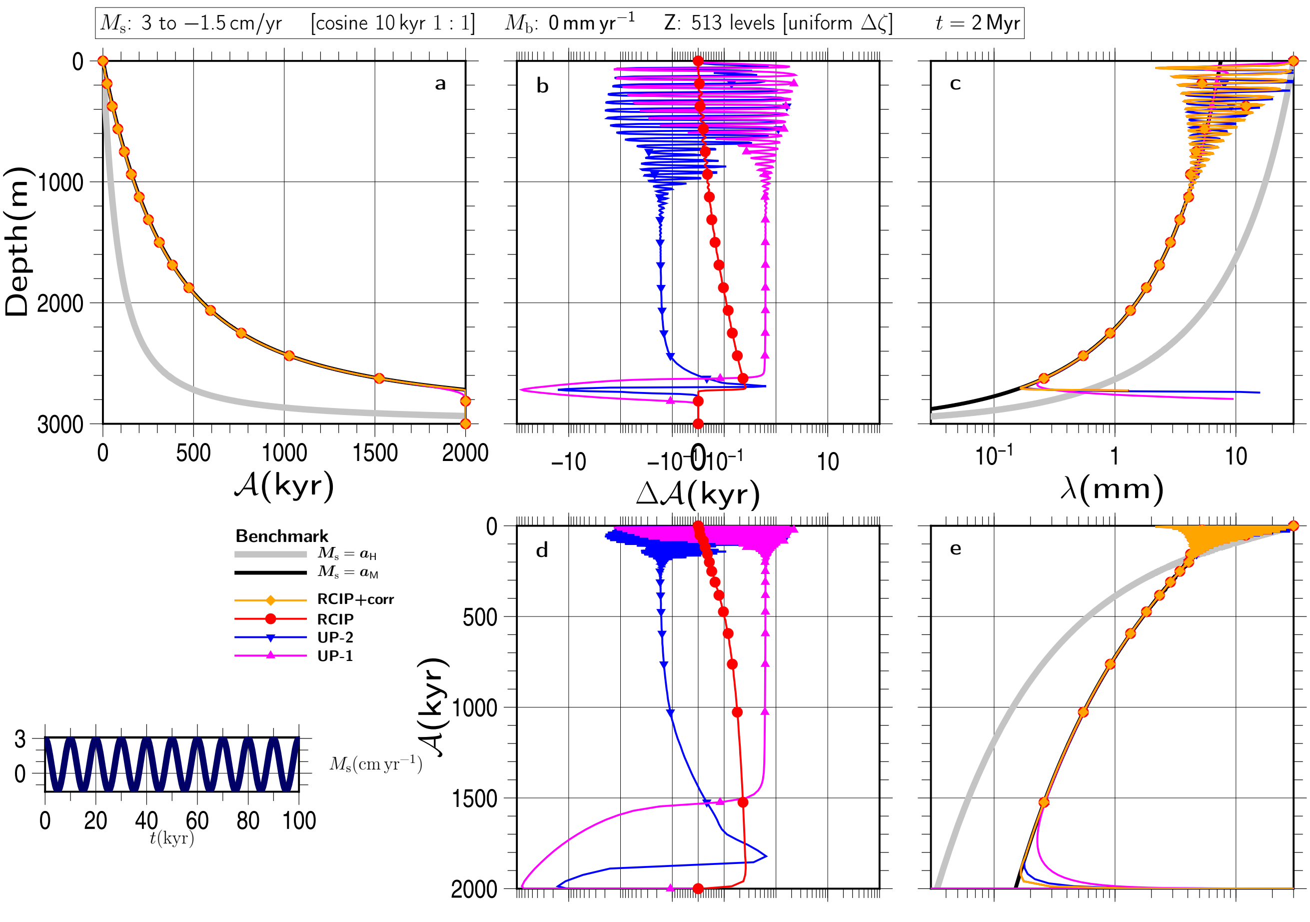

Figure S94

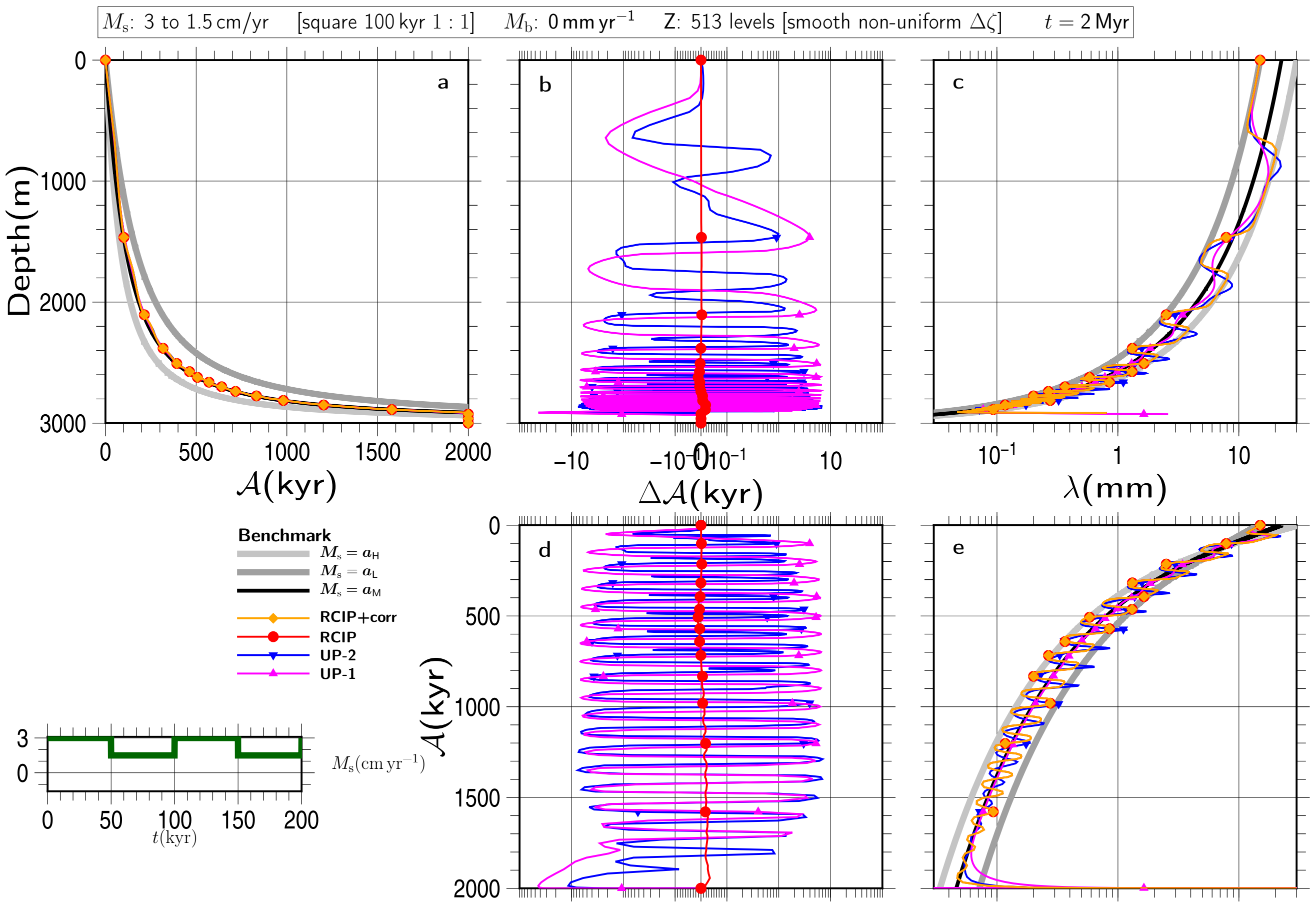

Figure S95

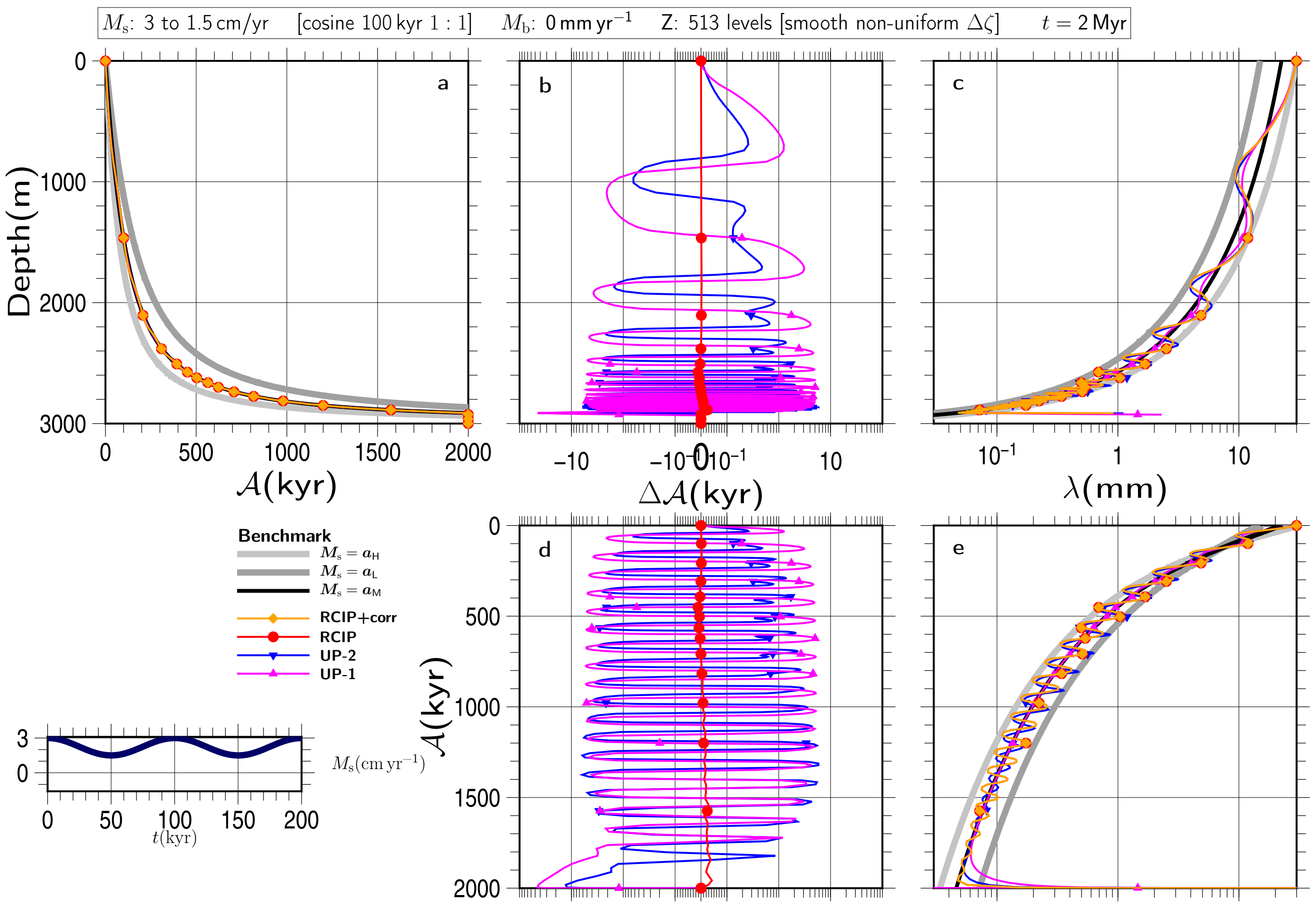

Figure S96

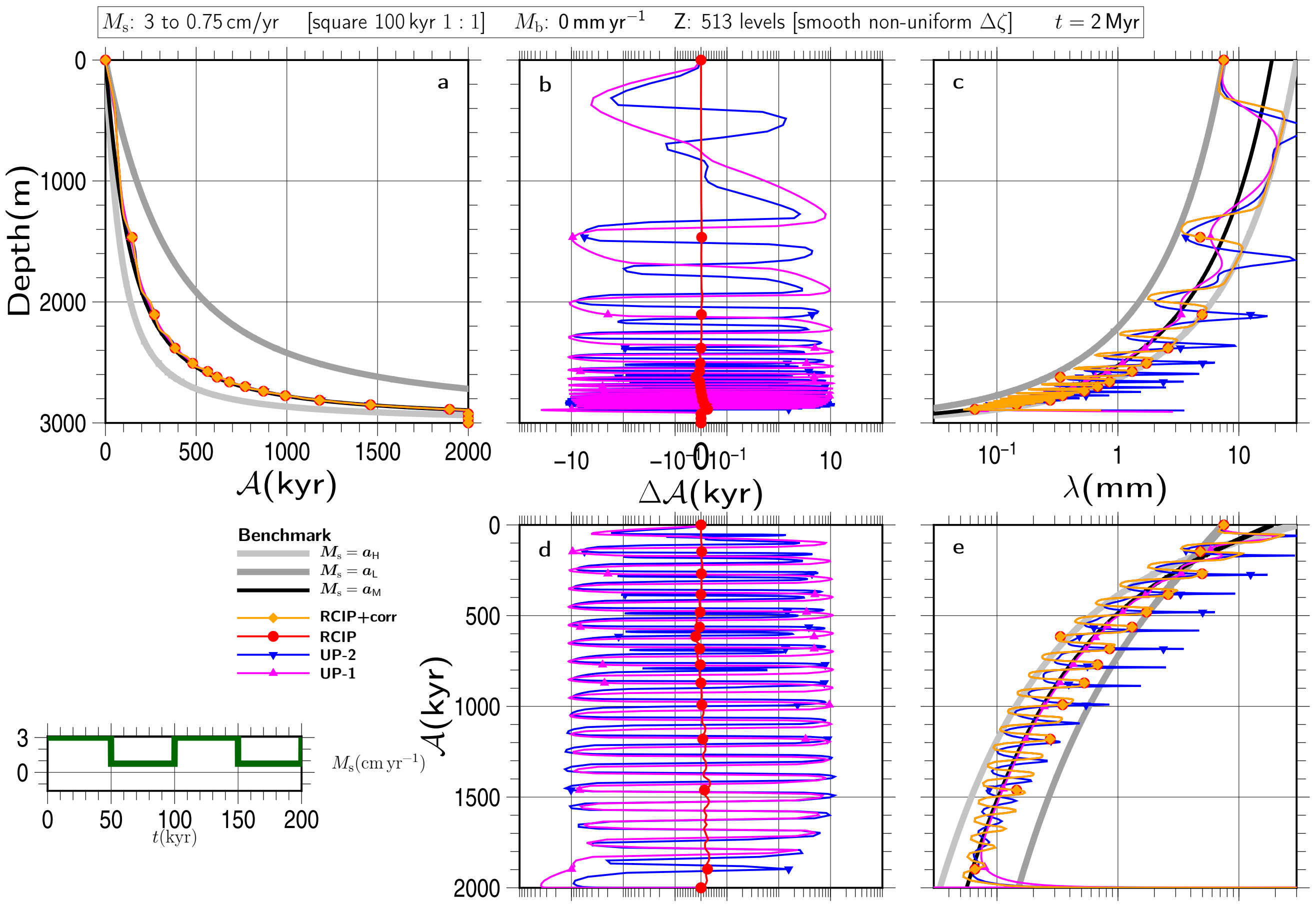

Figure S97

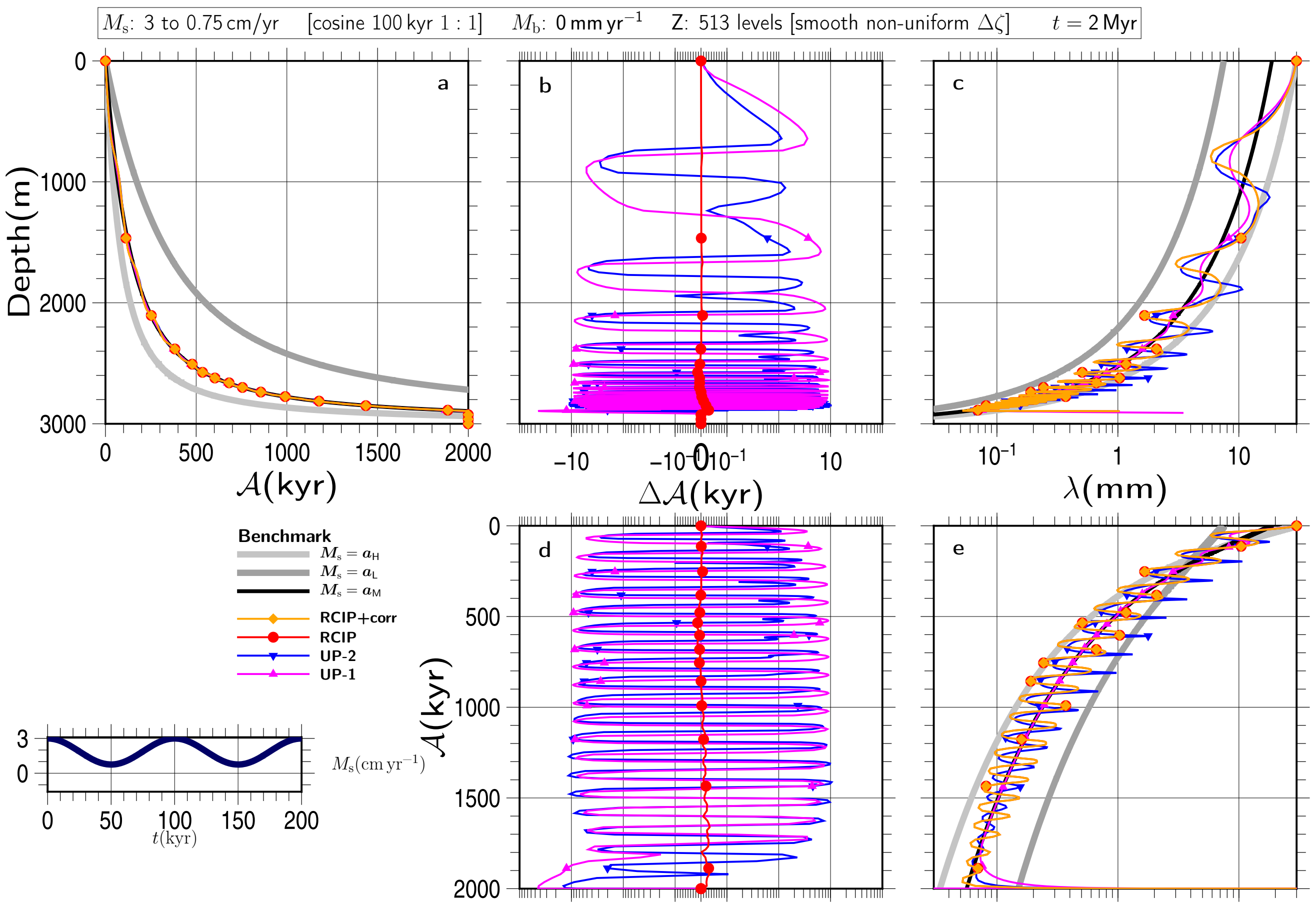

Figure S98

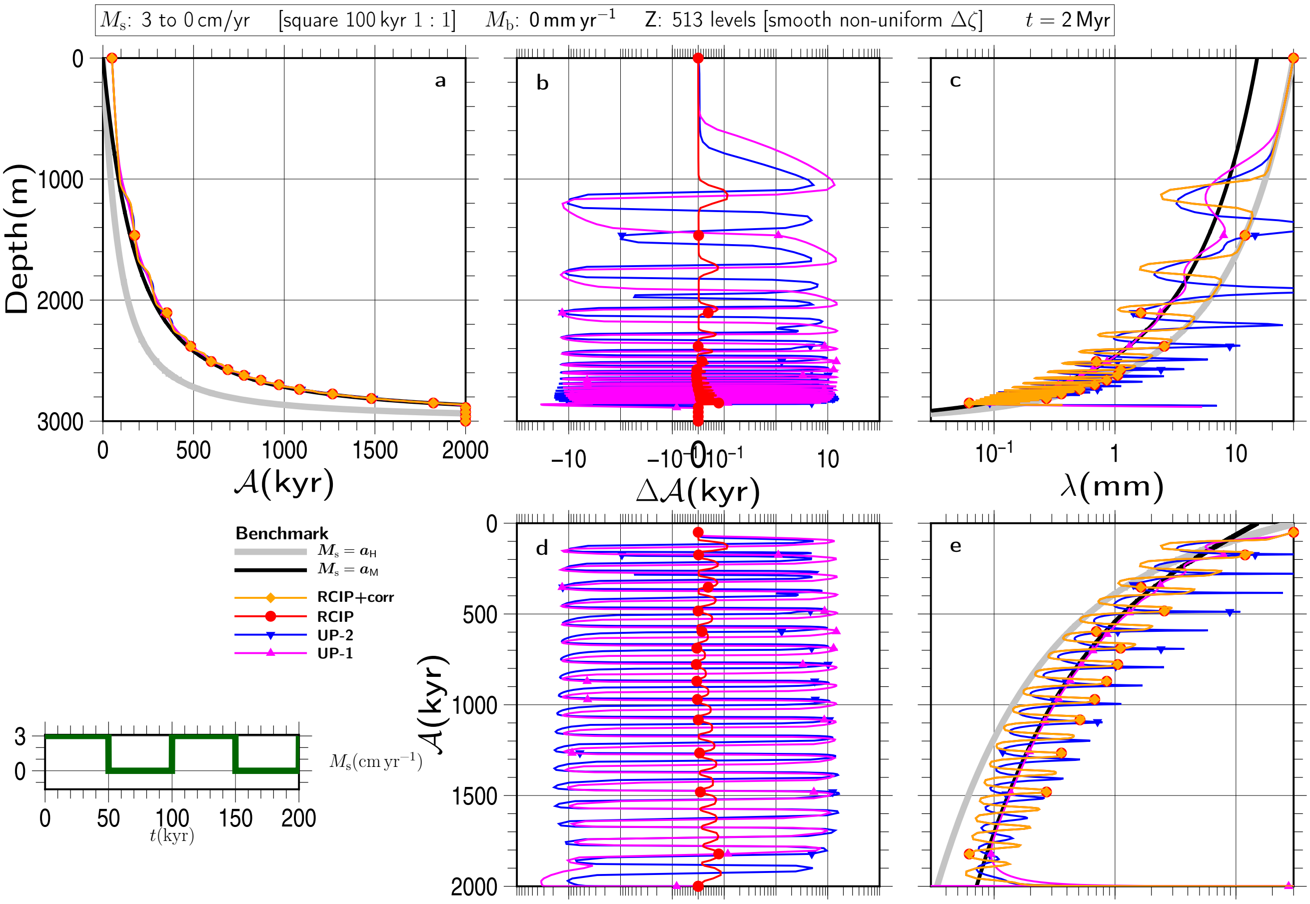

Figure S99

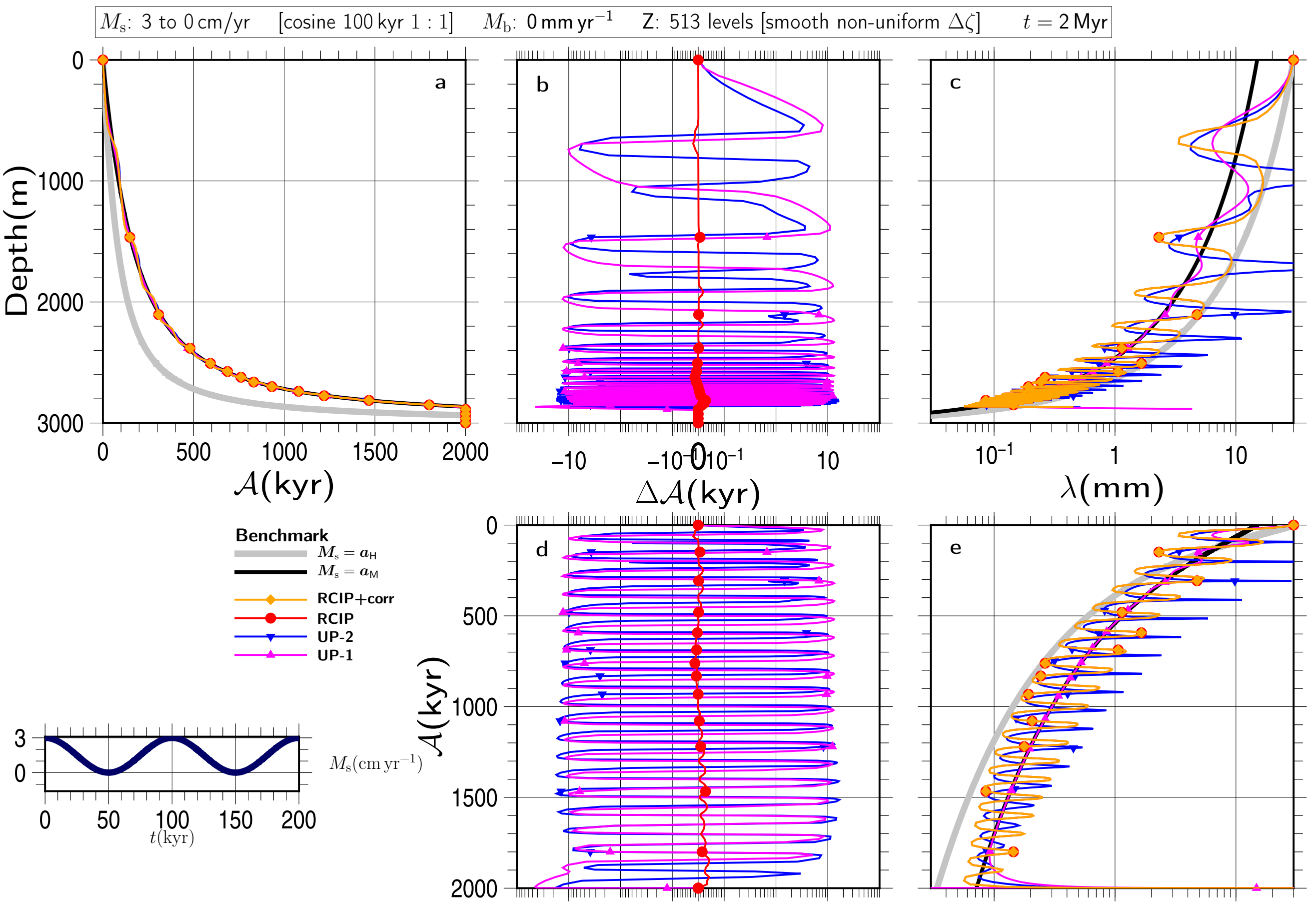

Figure S100

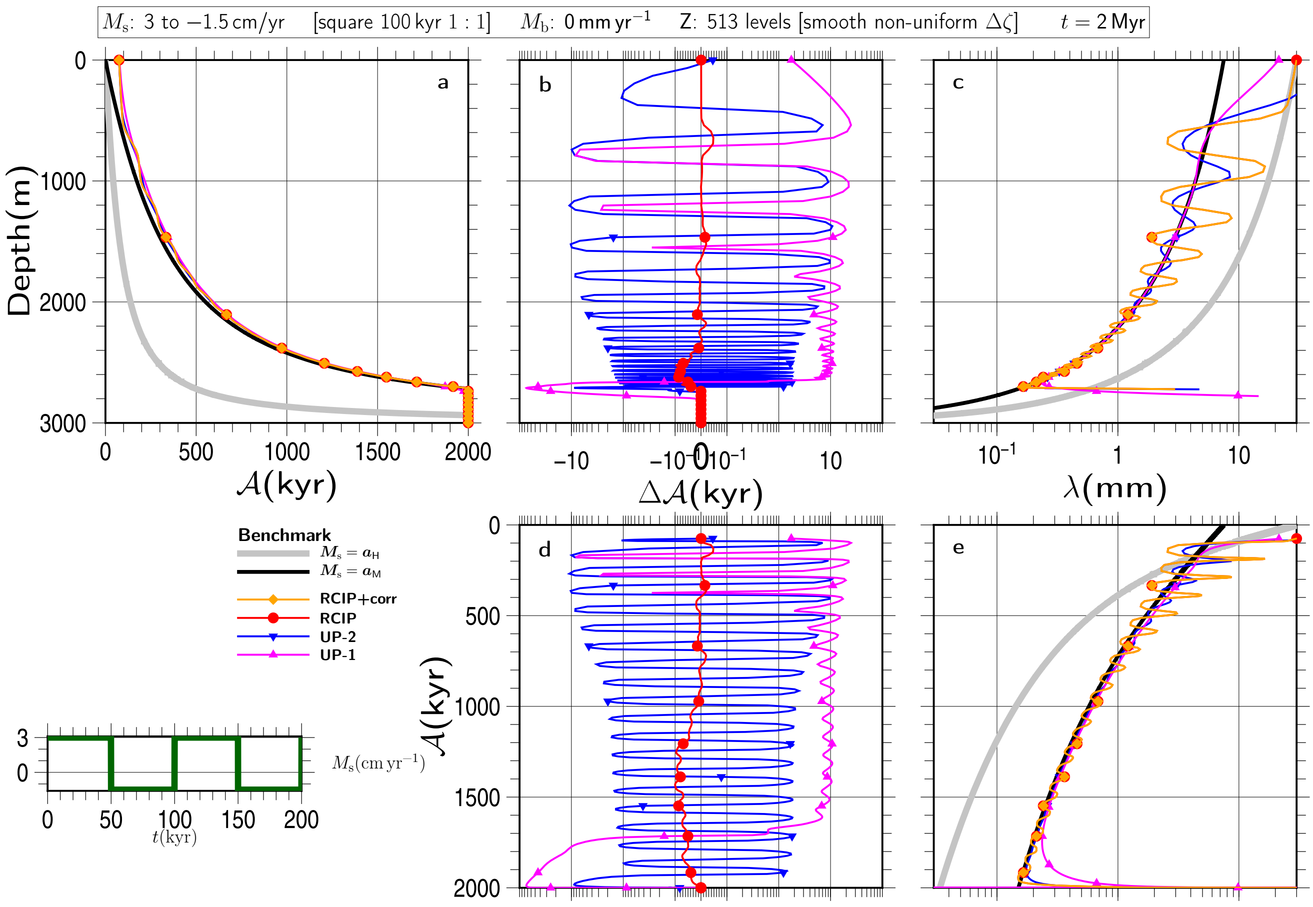

Figure S101

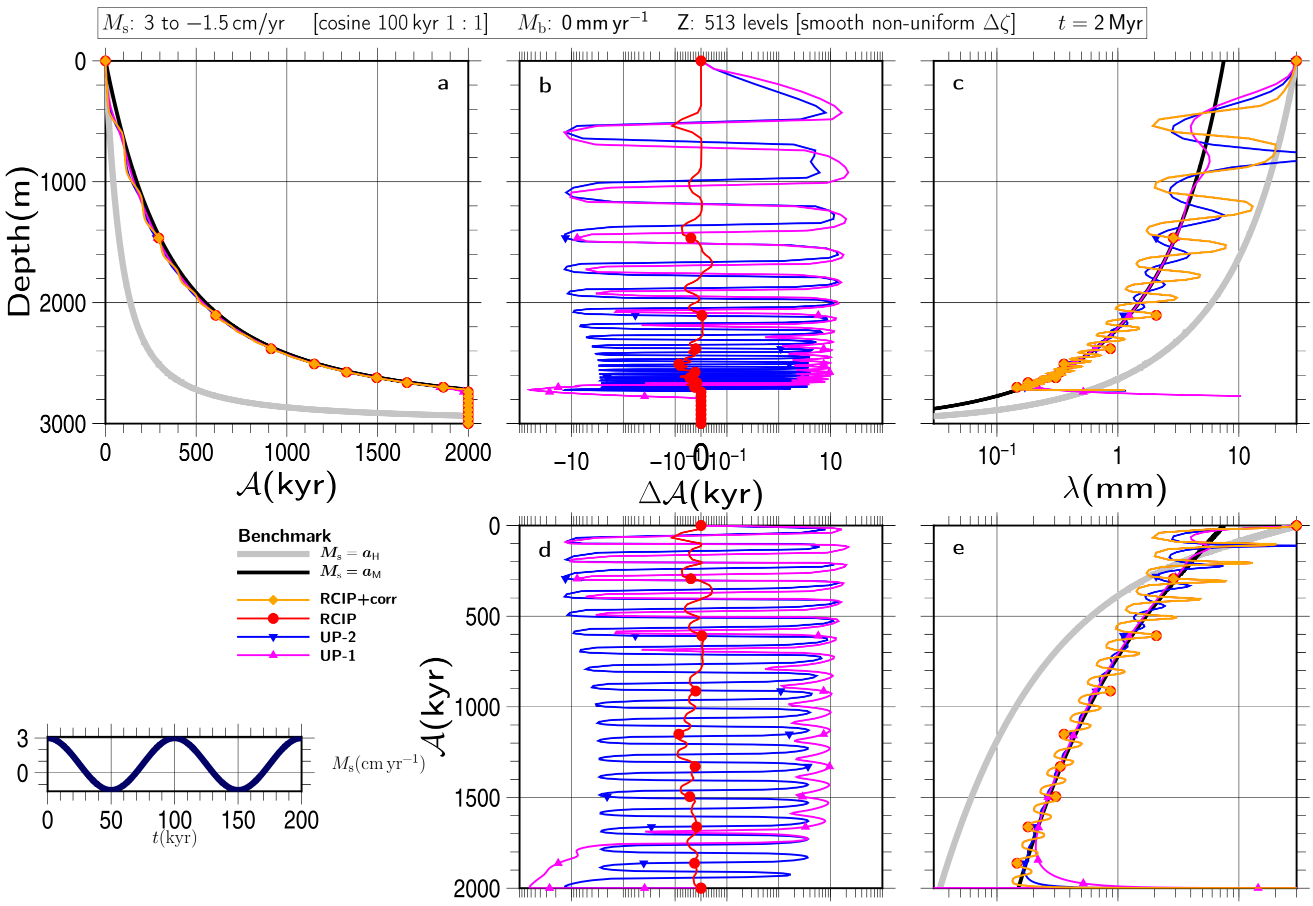

Figure S102

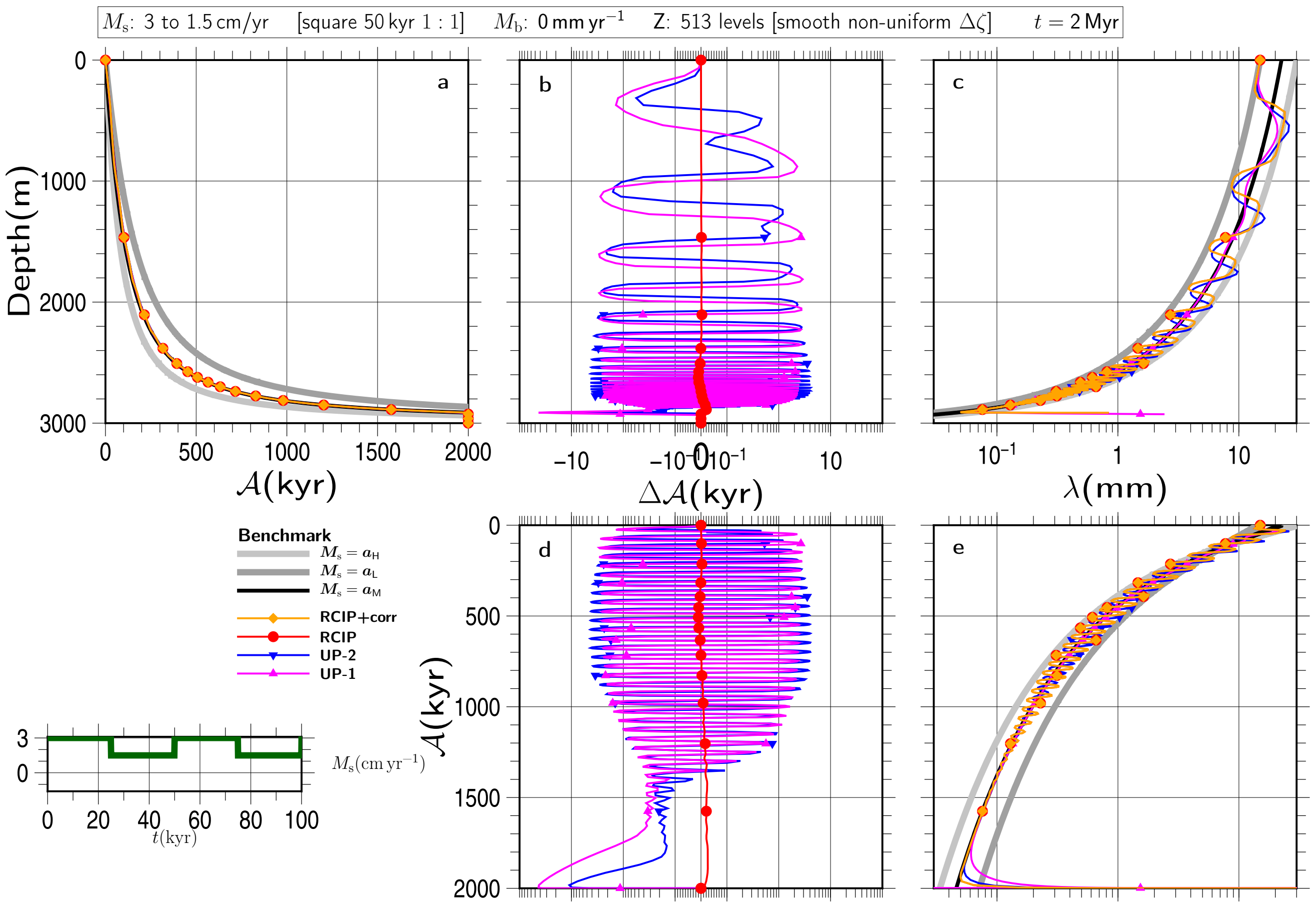

Figure S103

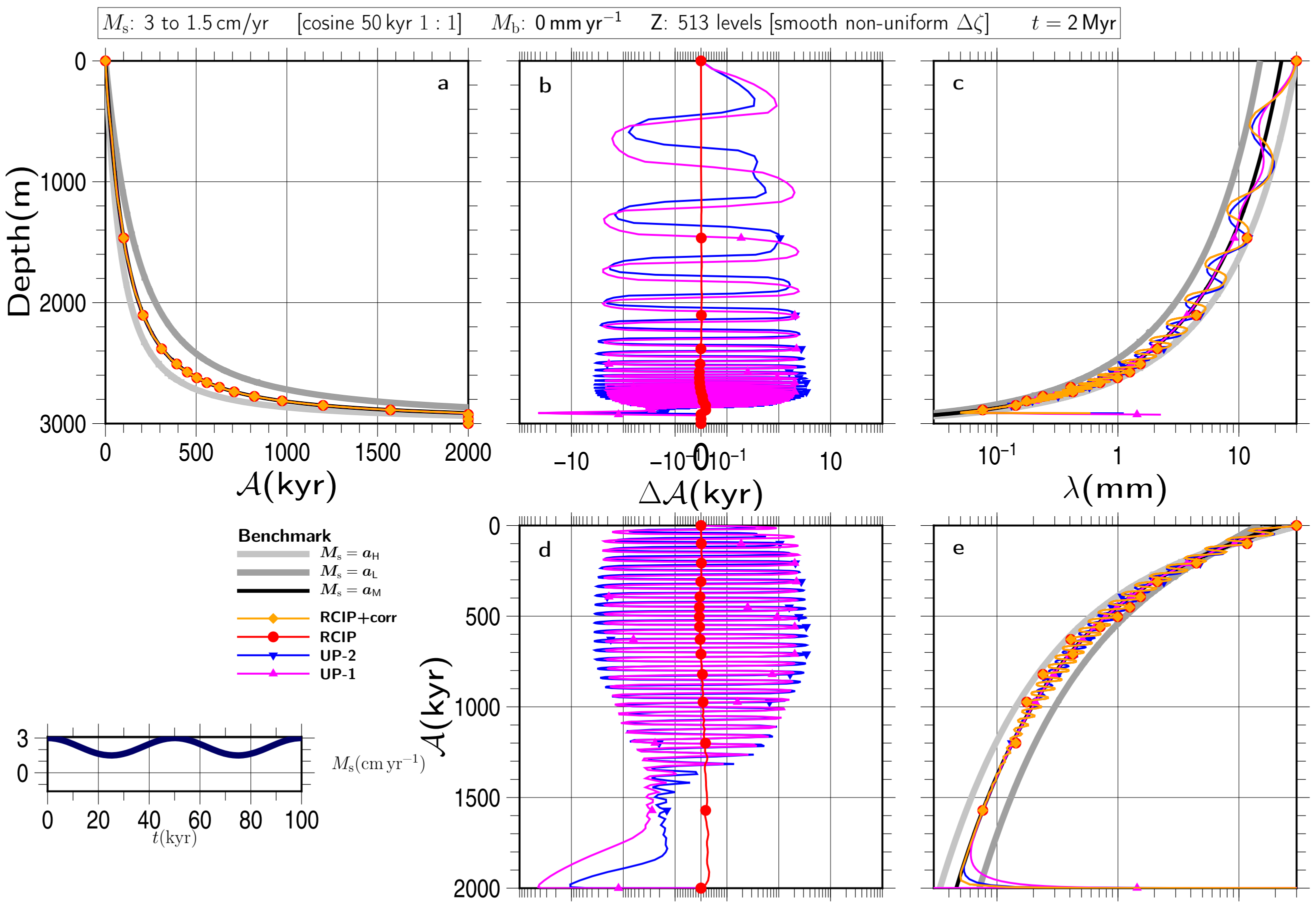

Figure S104

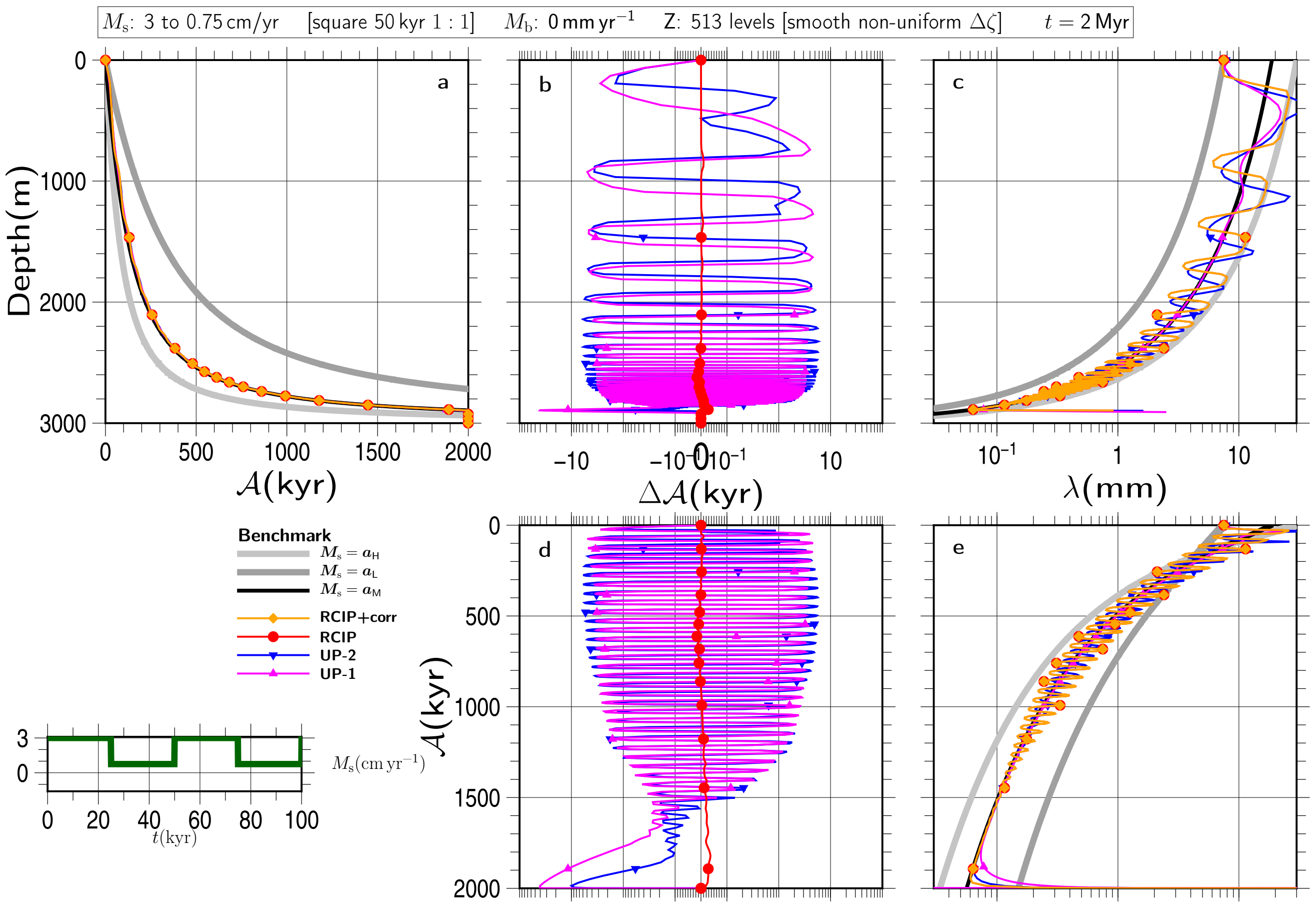

Figure S105

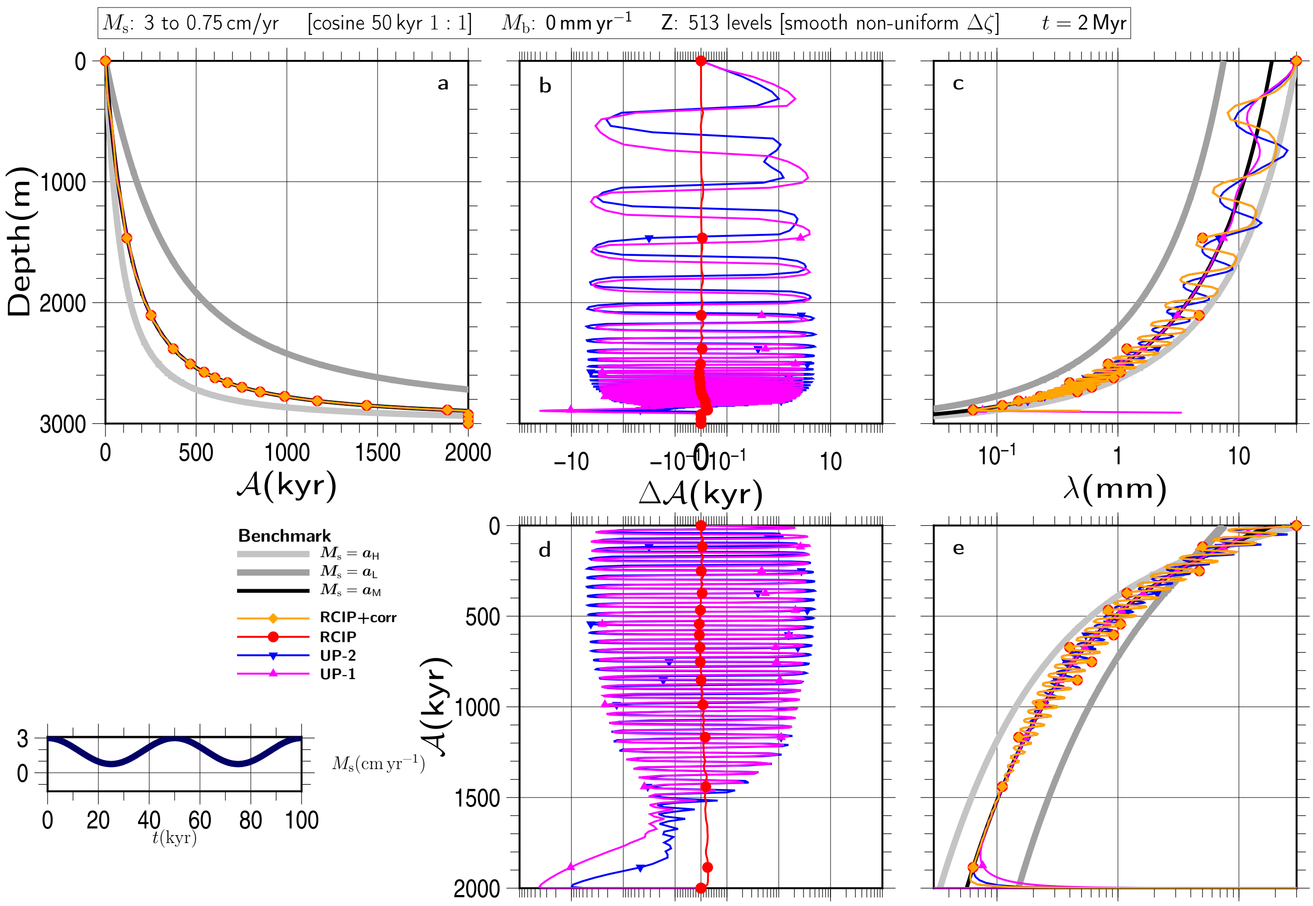

Figure S106

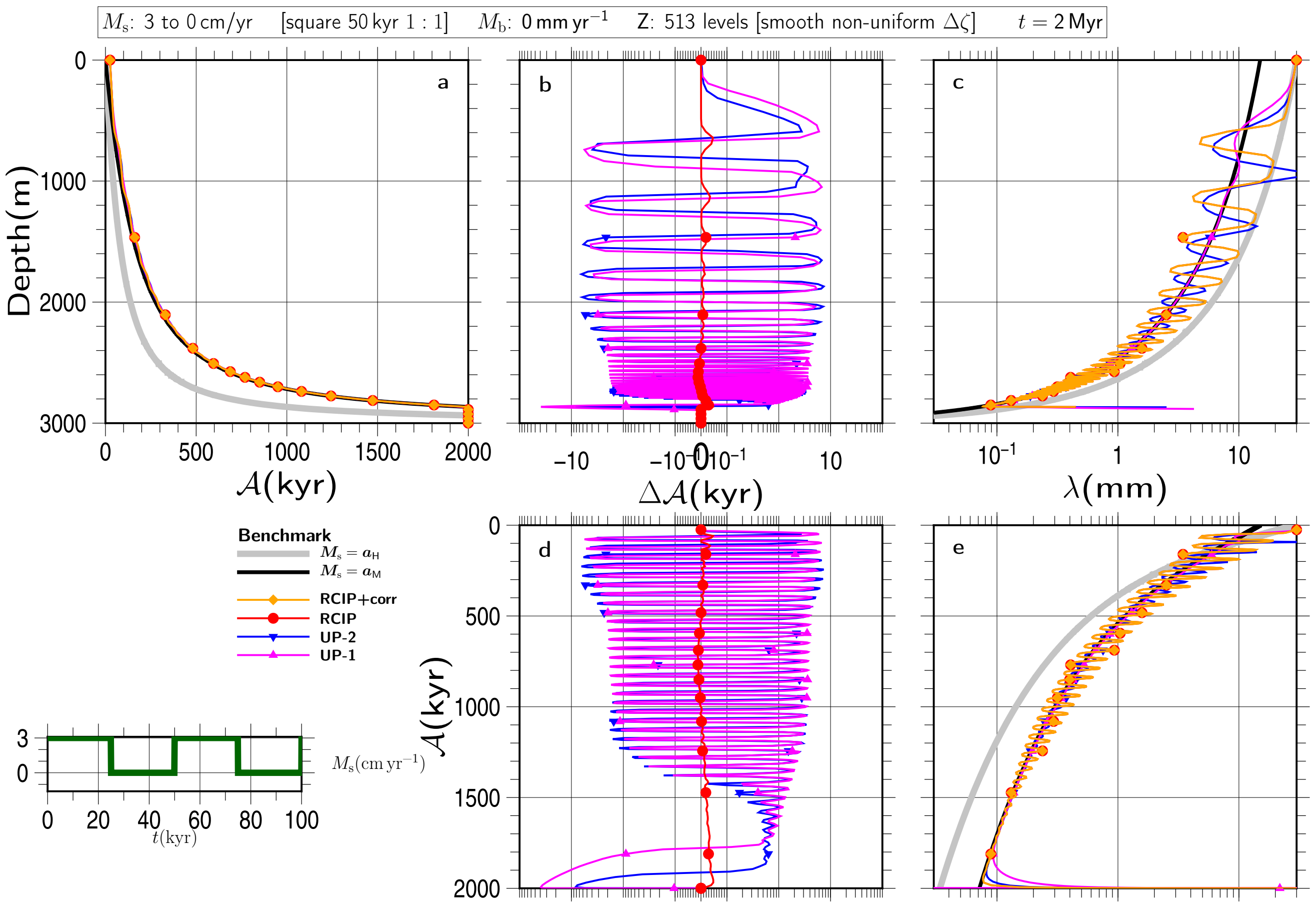

Figure S107

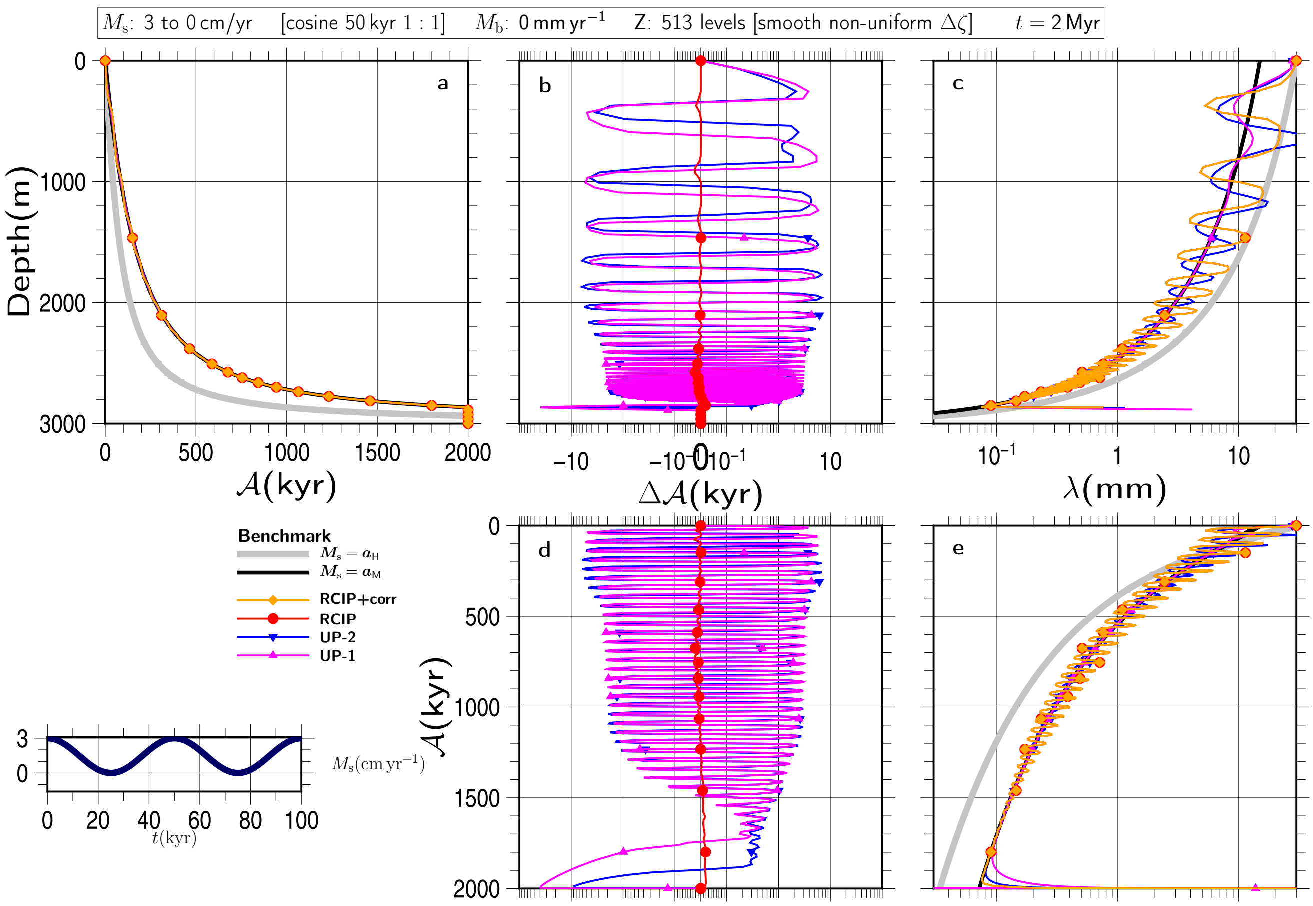

Figure S108

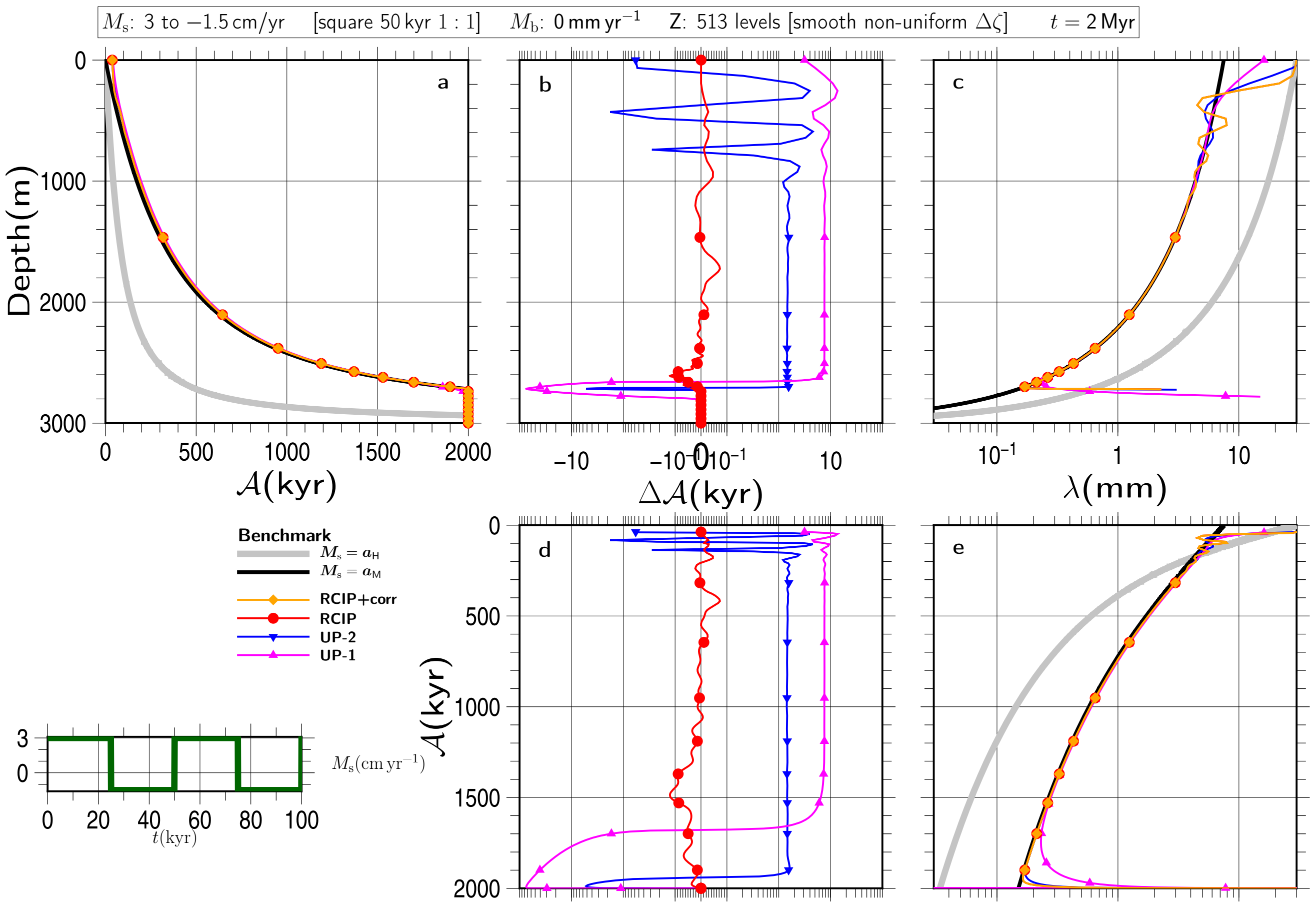

Figure S109

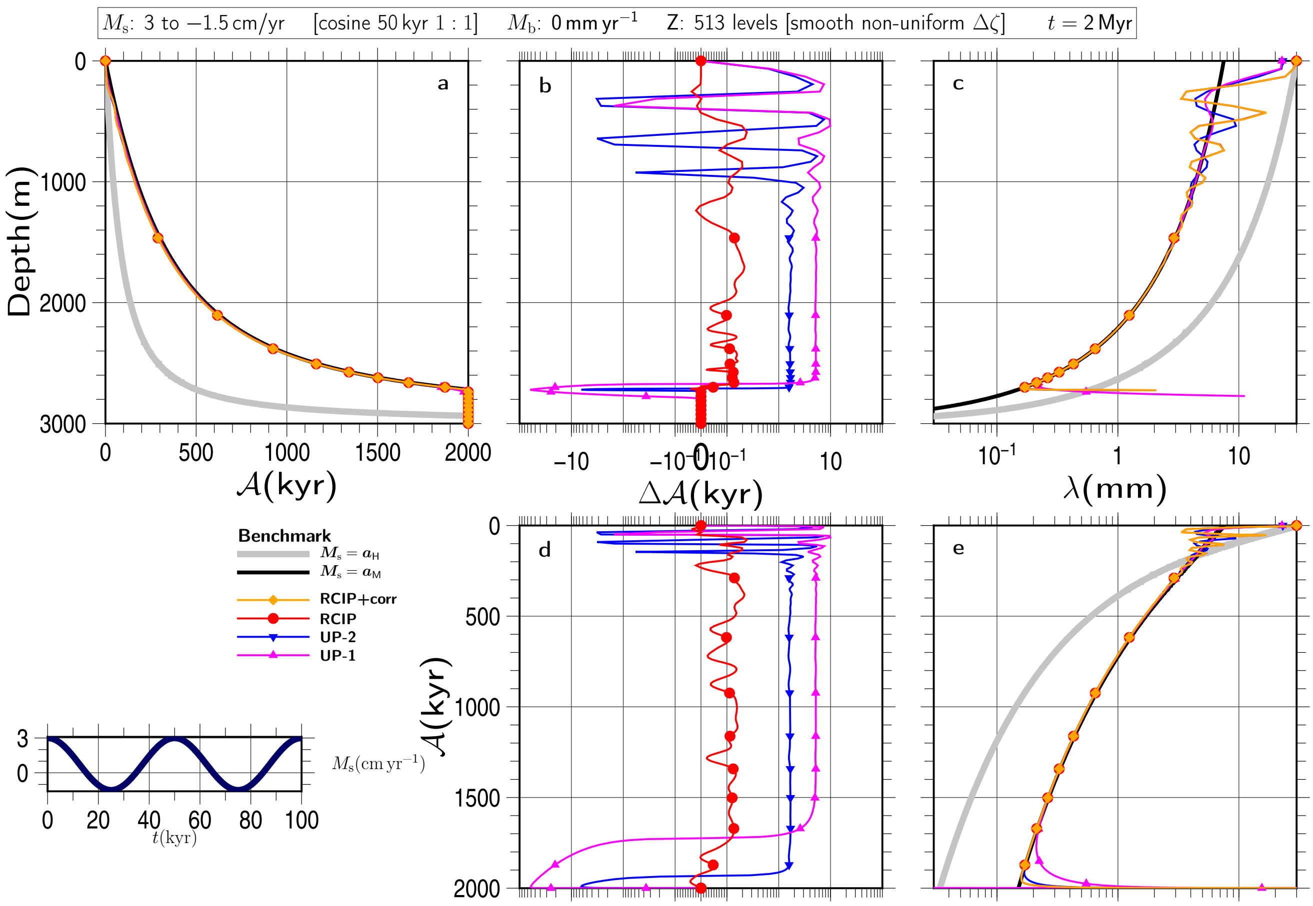

Figure S110

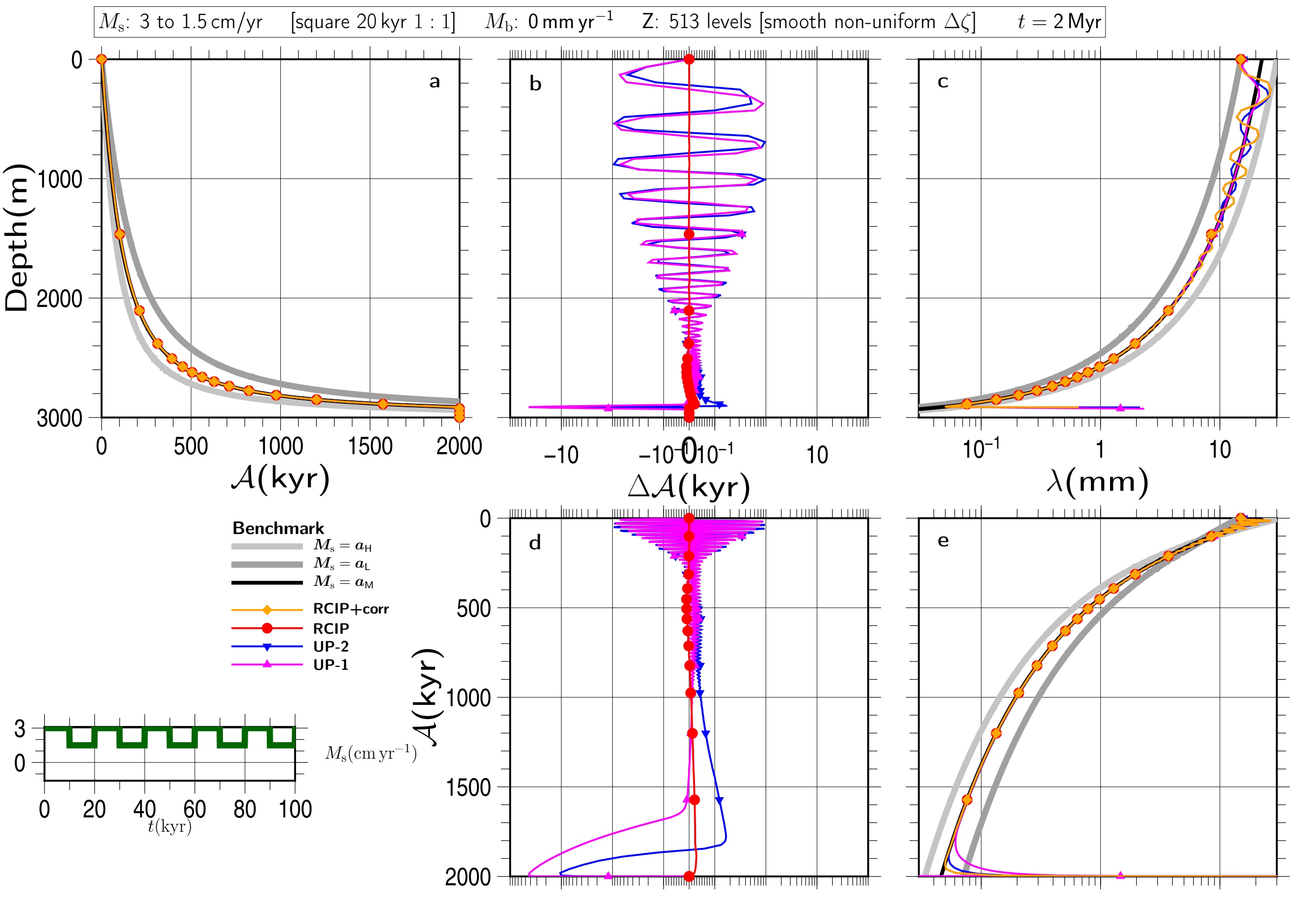

Figure S111

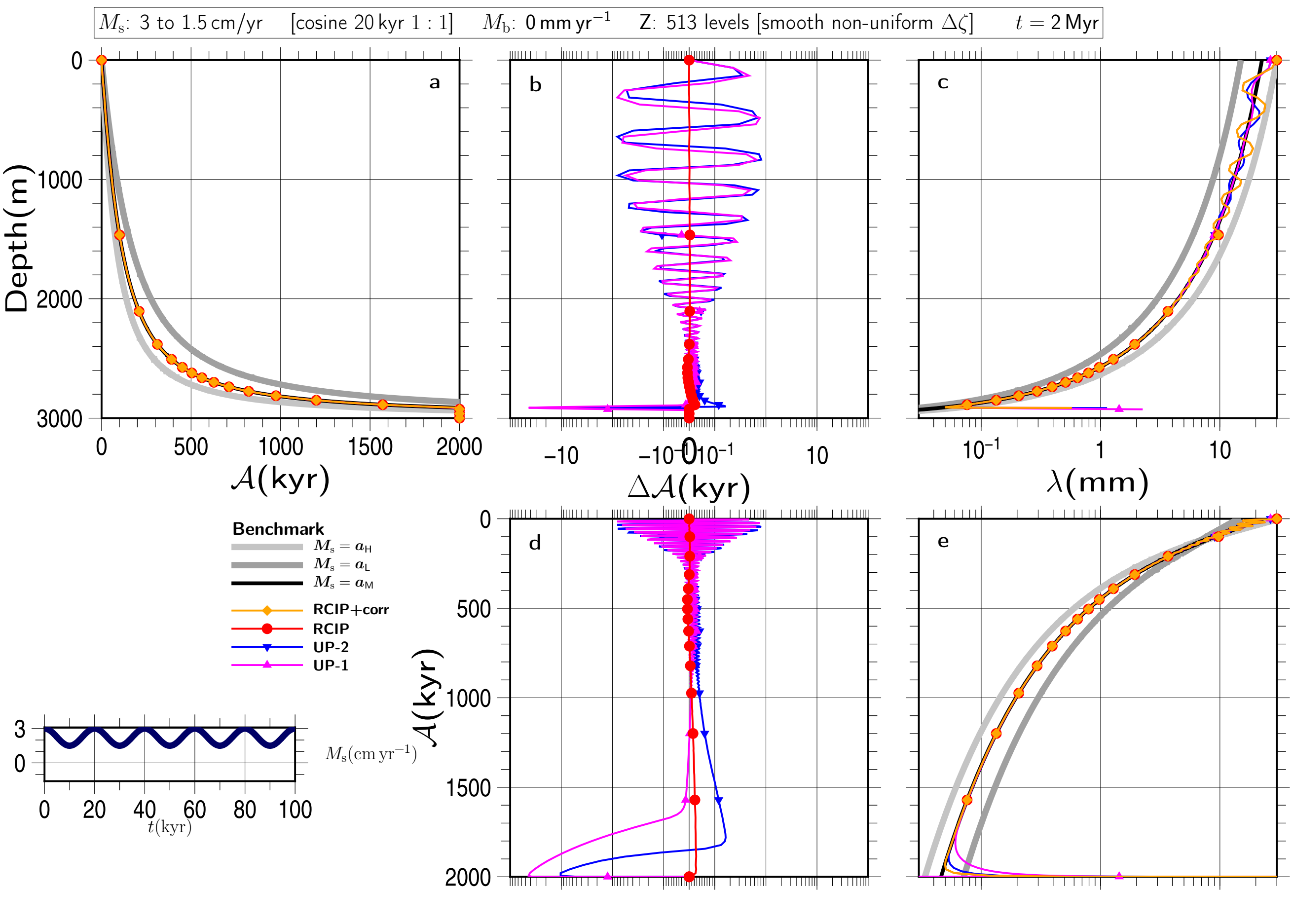

Figure S112

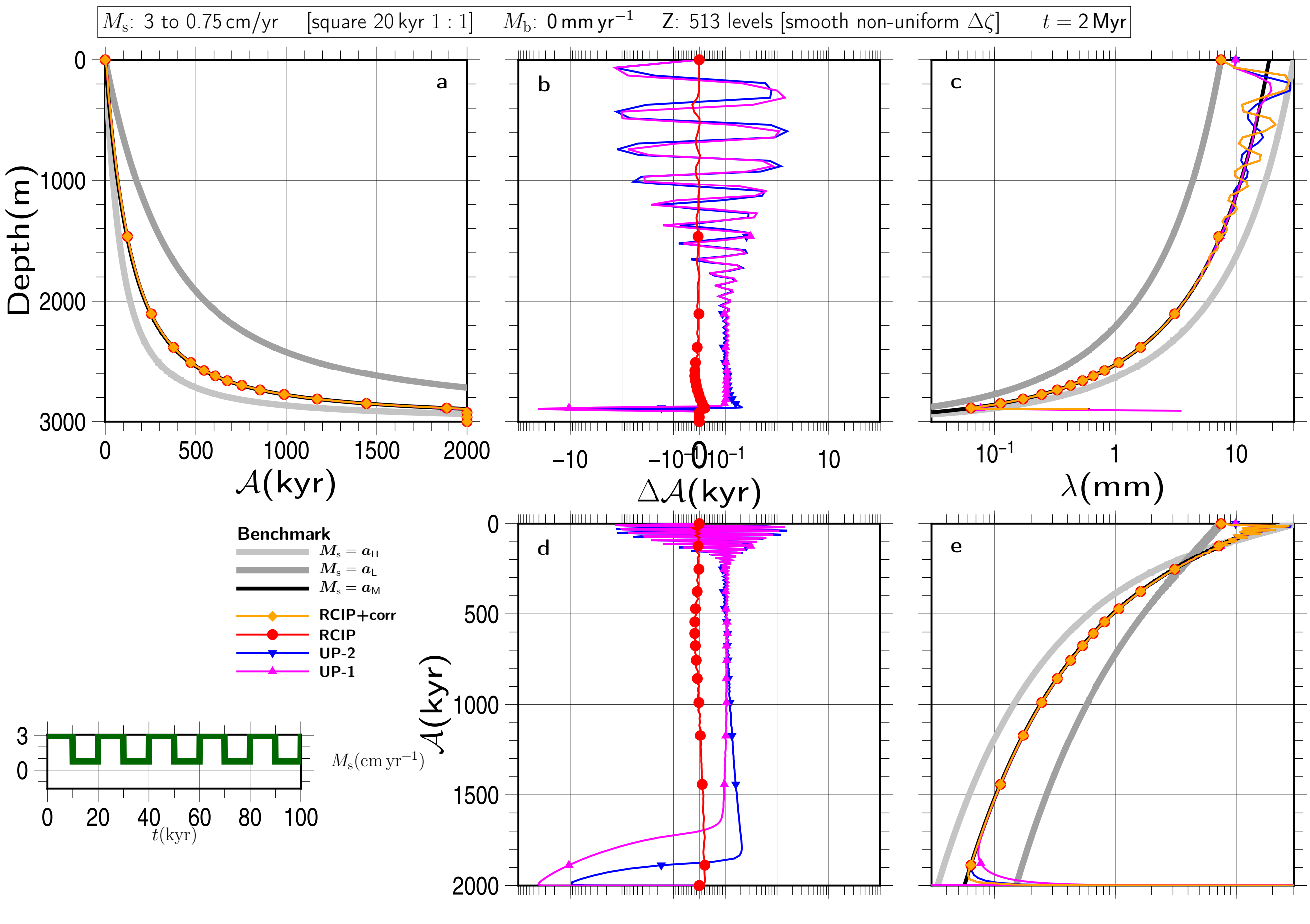

Figure S113

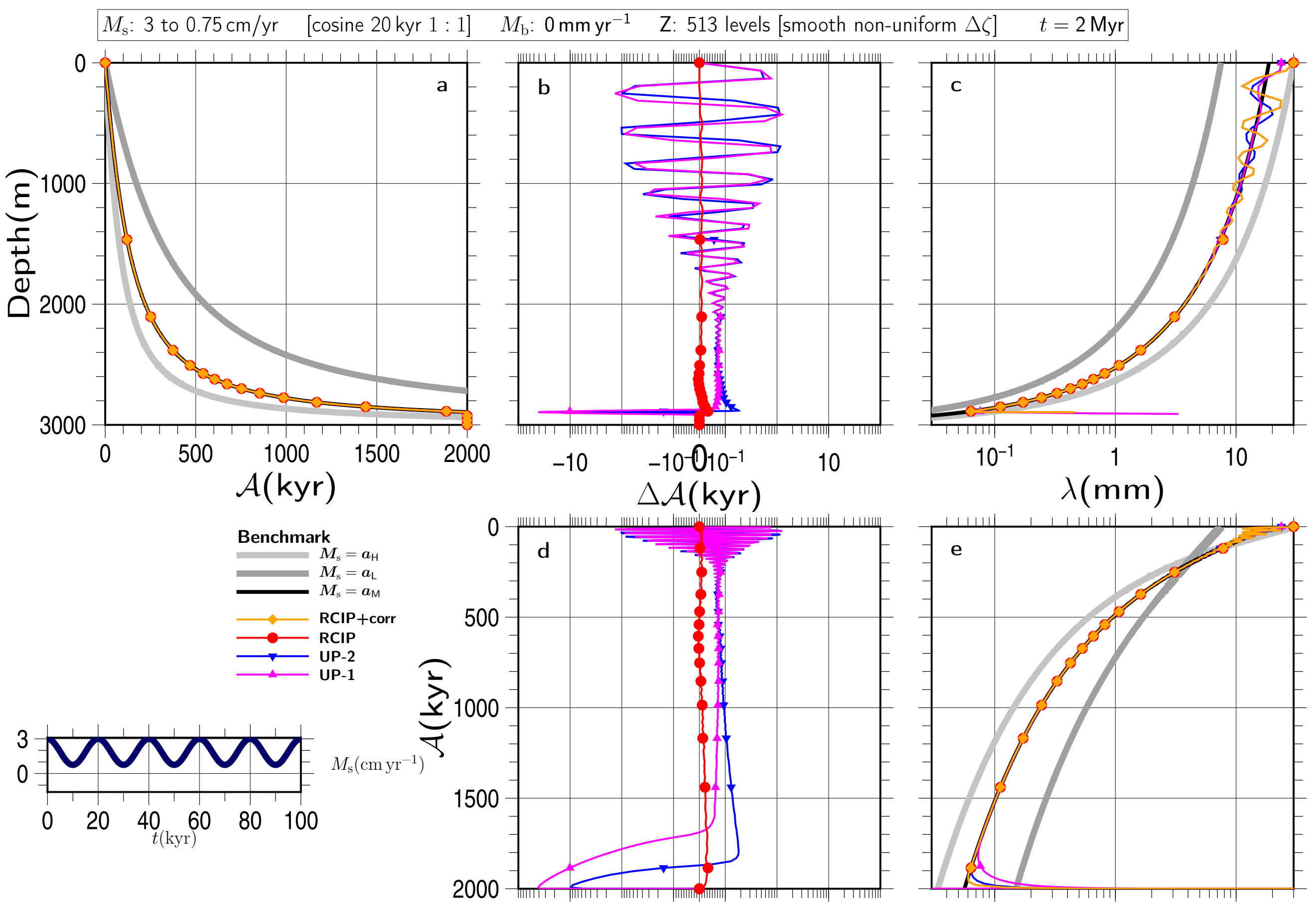

Figure S114

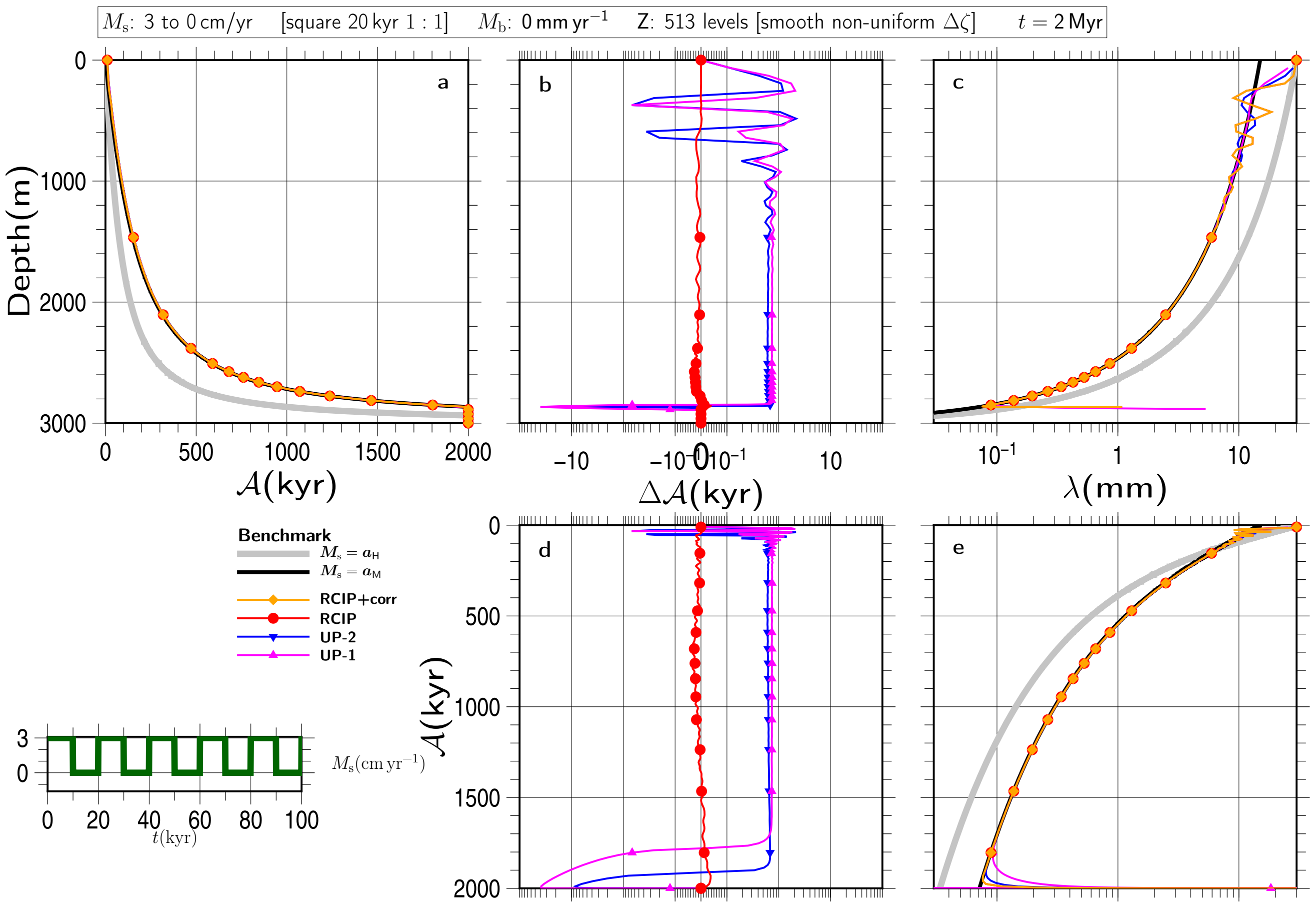

Figure S115

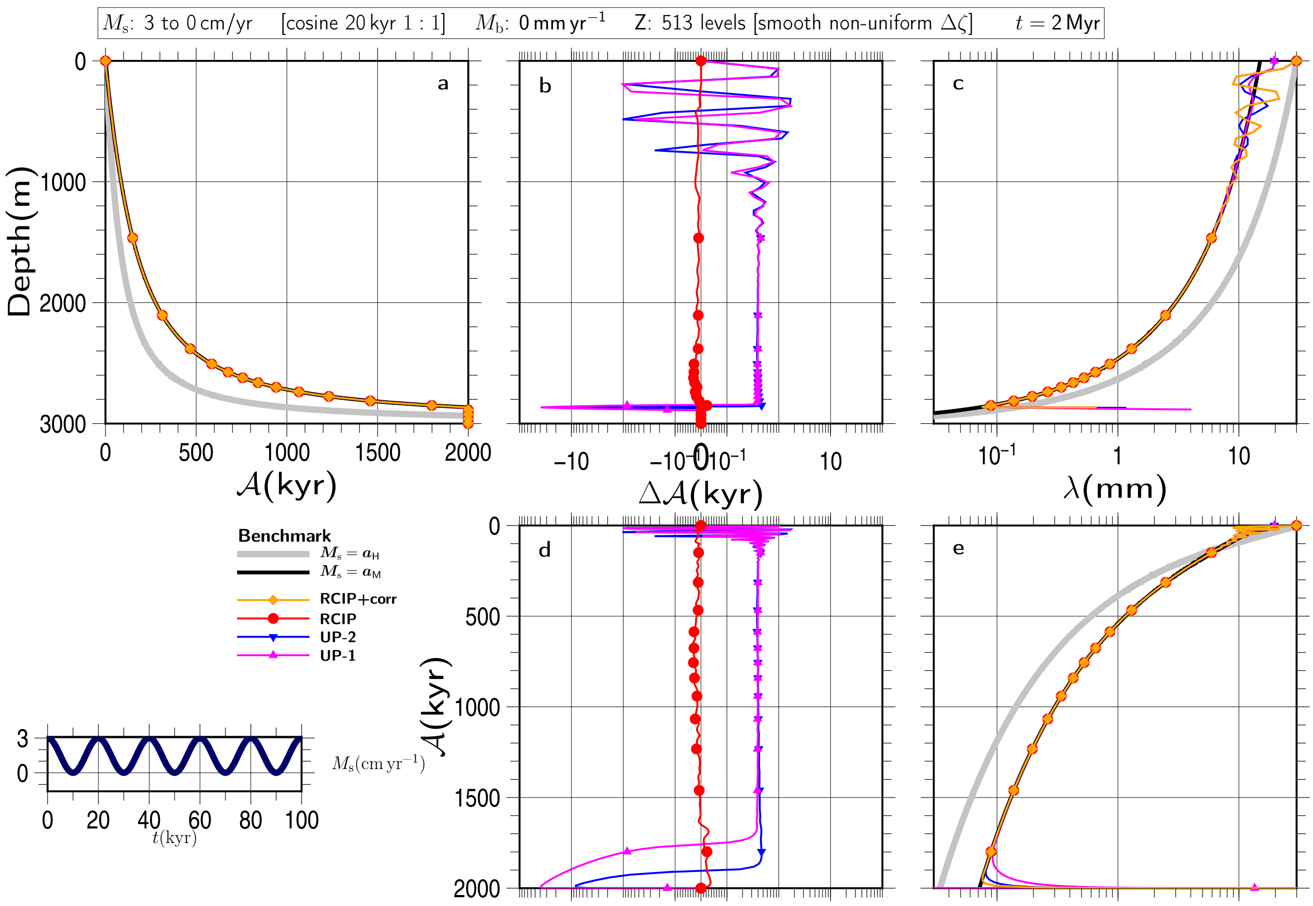

Figure S116

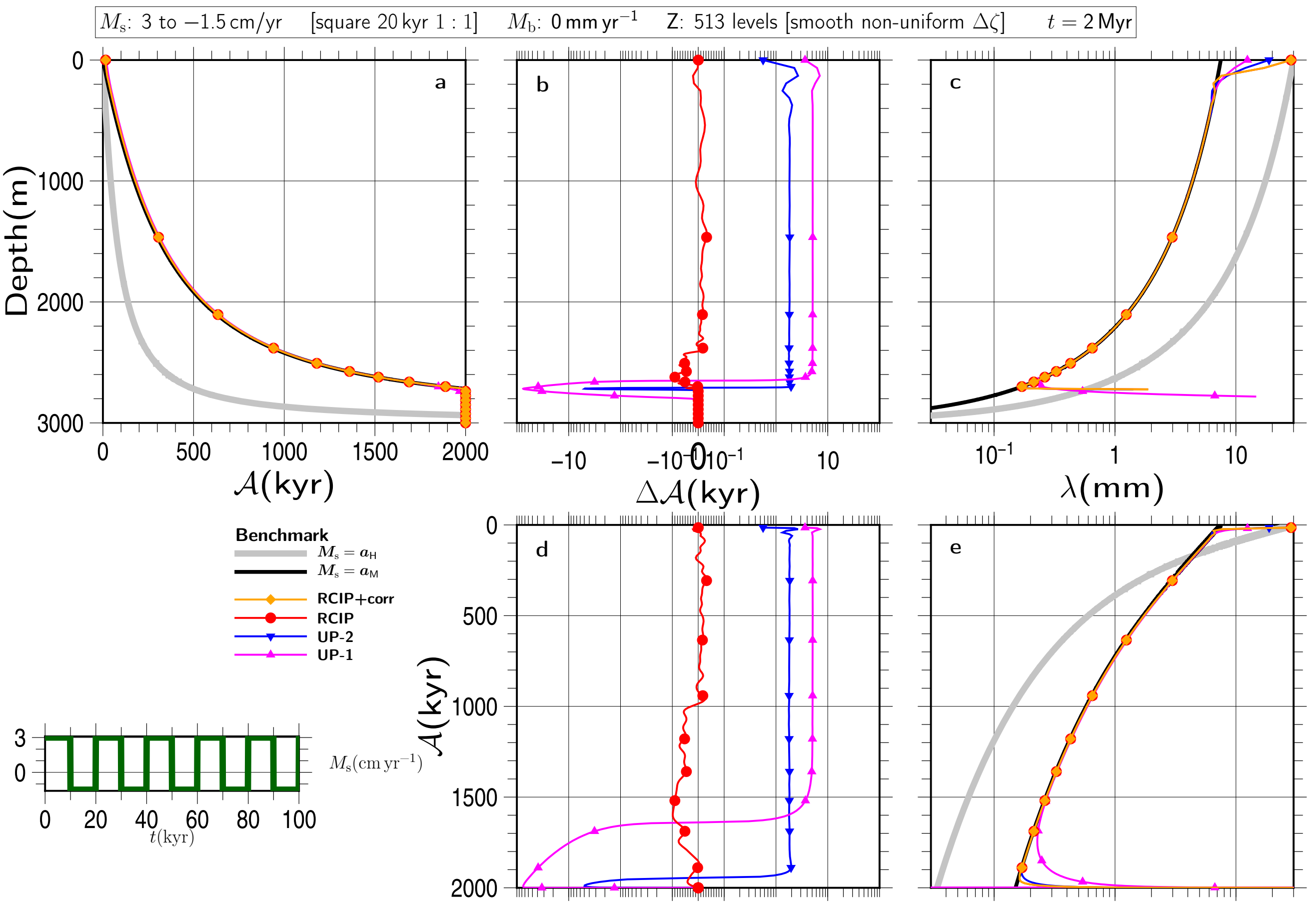

Figure S117

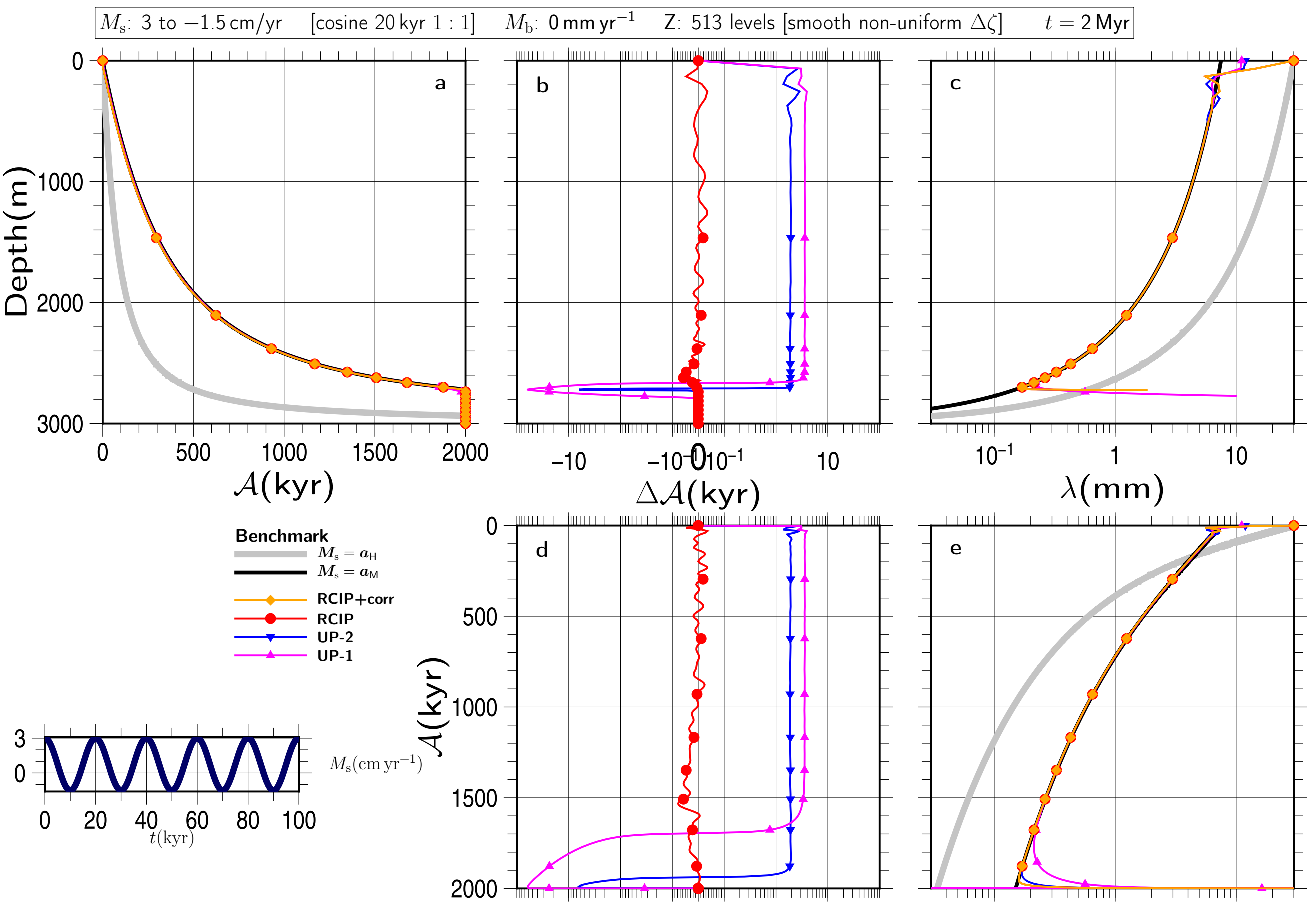

Figure S118

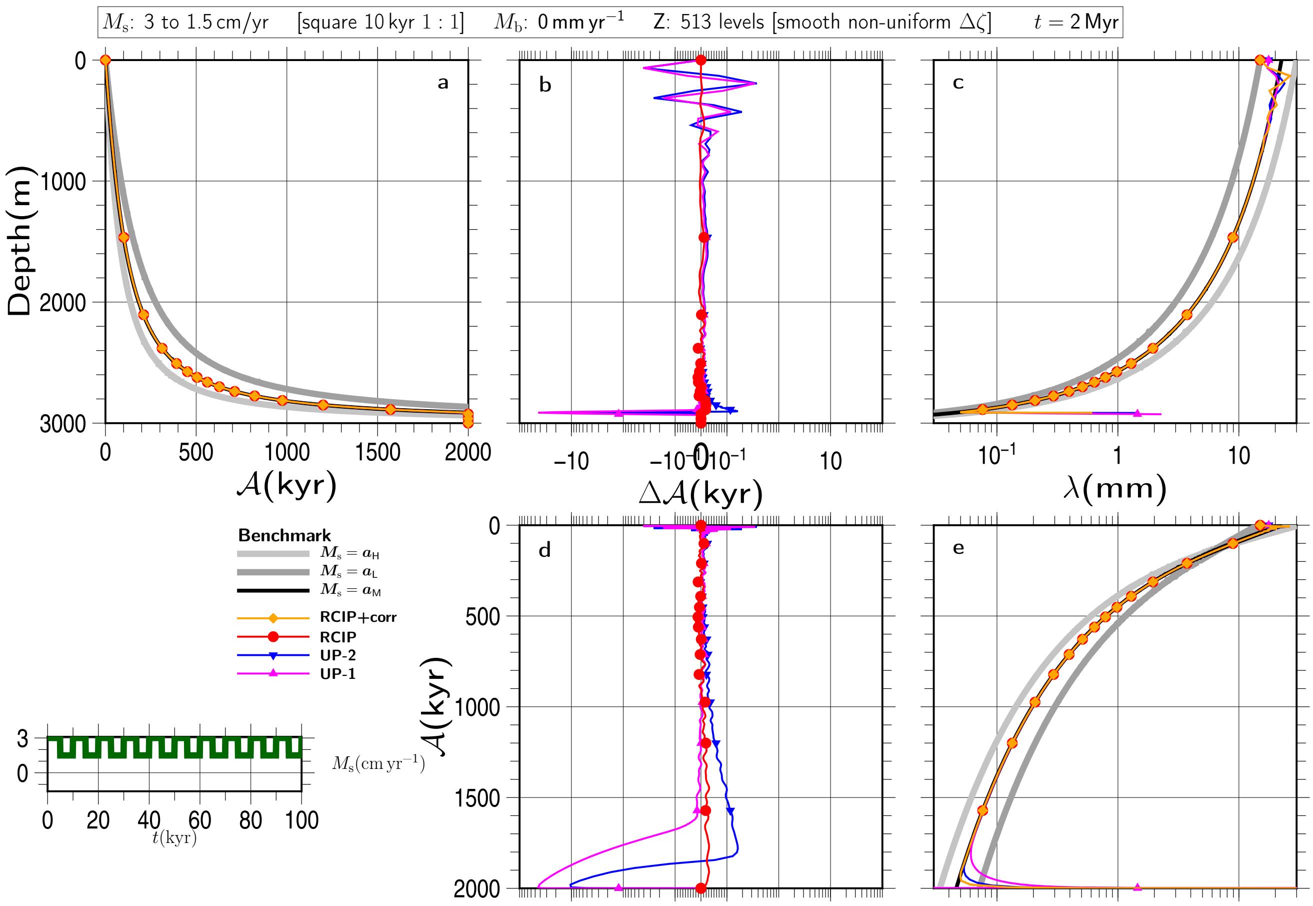

Figure S119

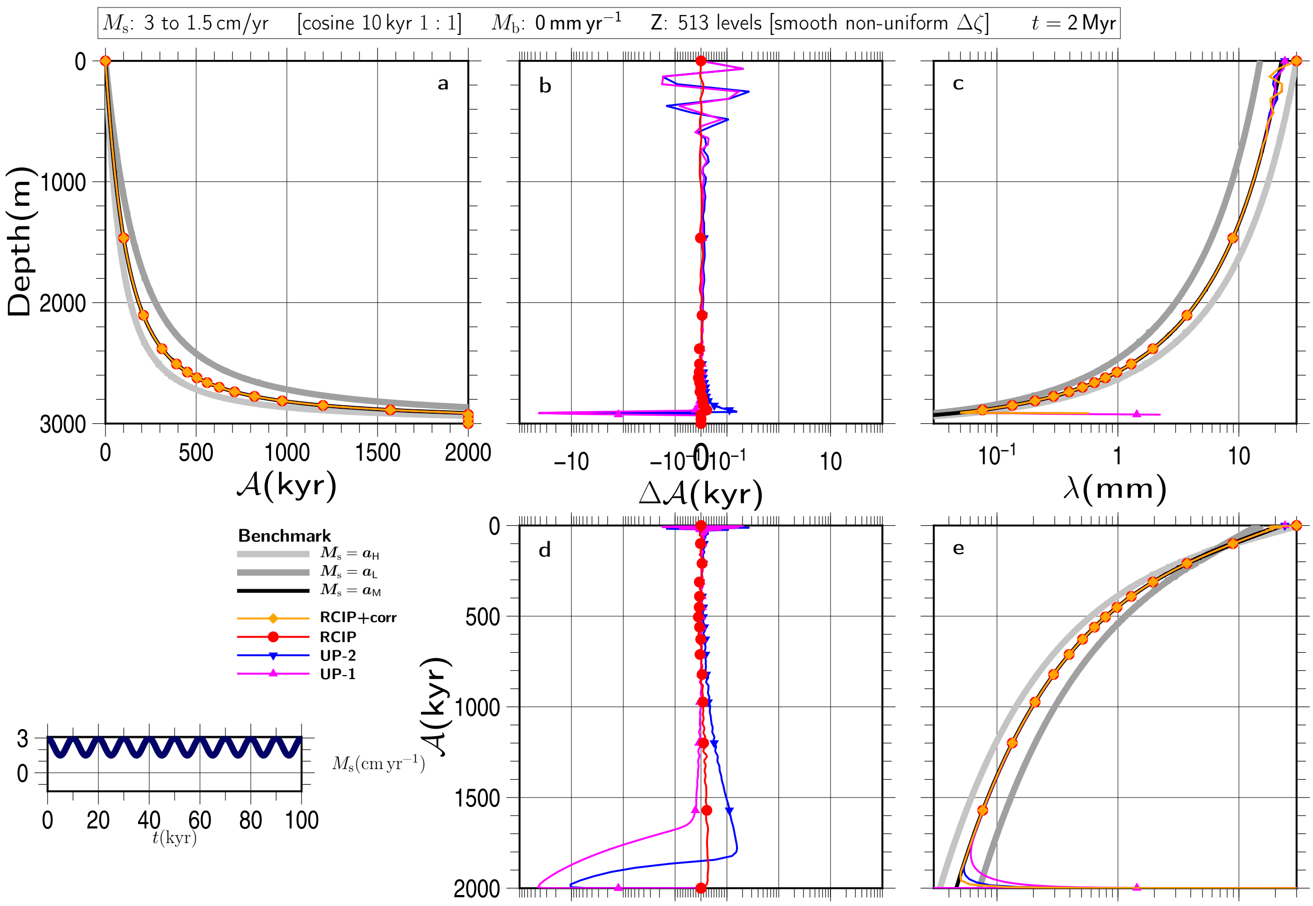

Figure S120

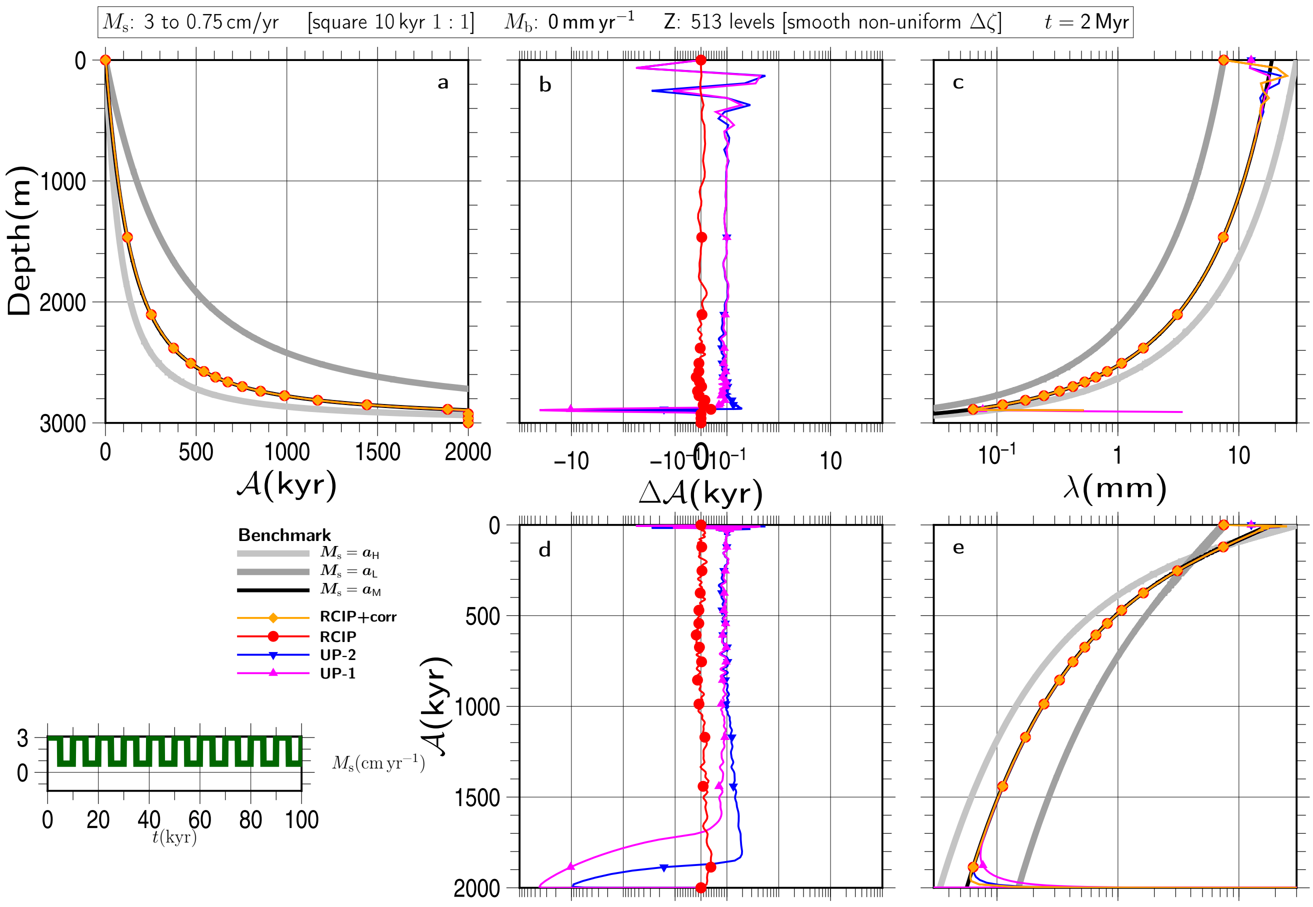

Figure S121

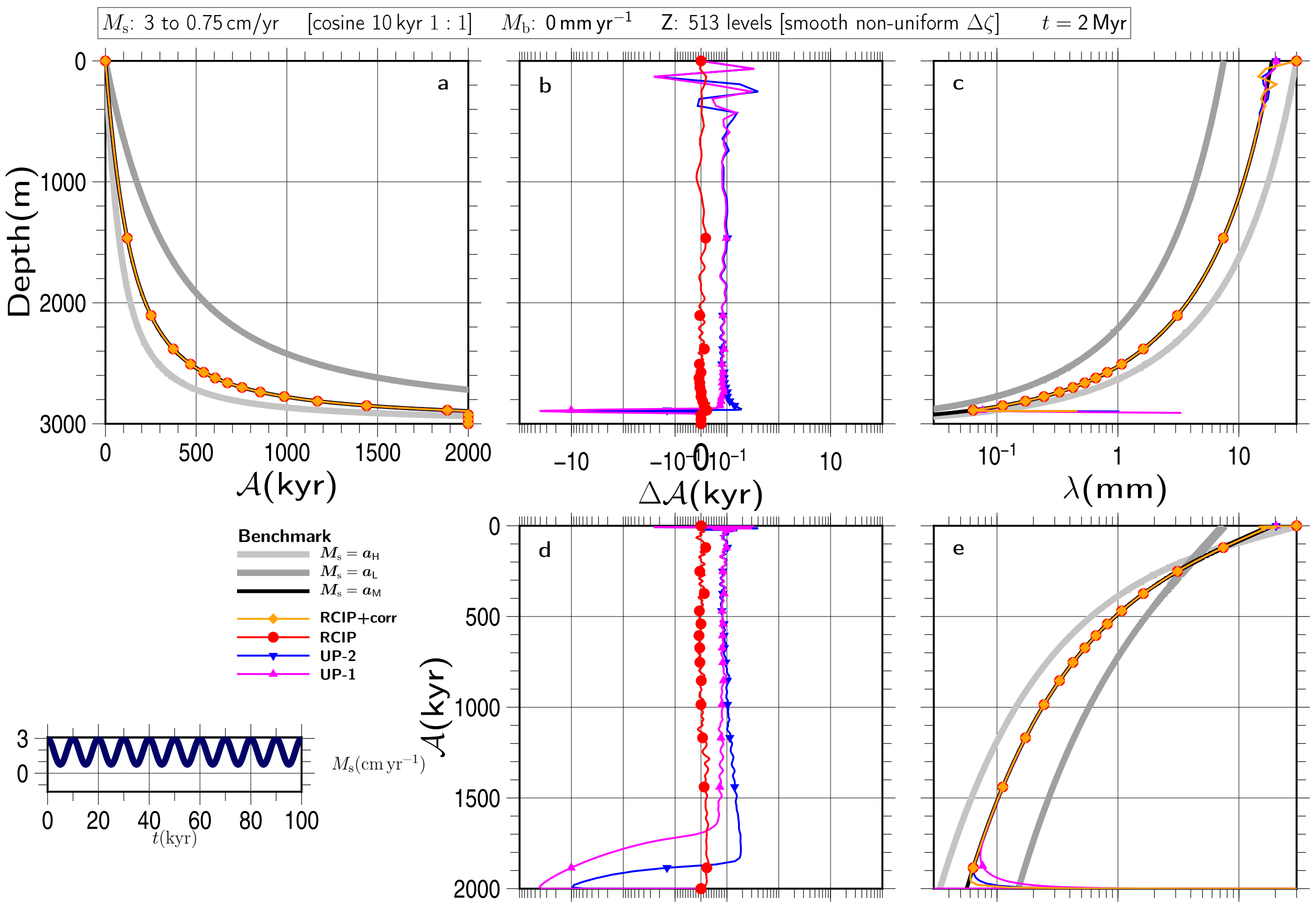

Figure S122

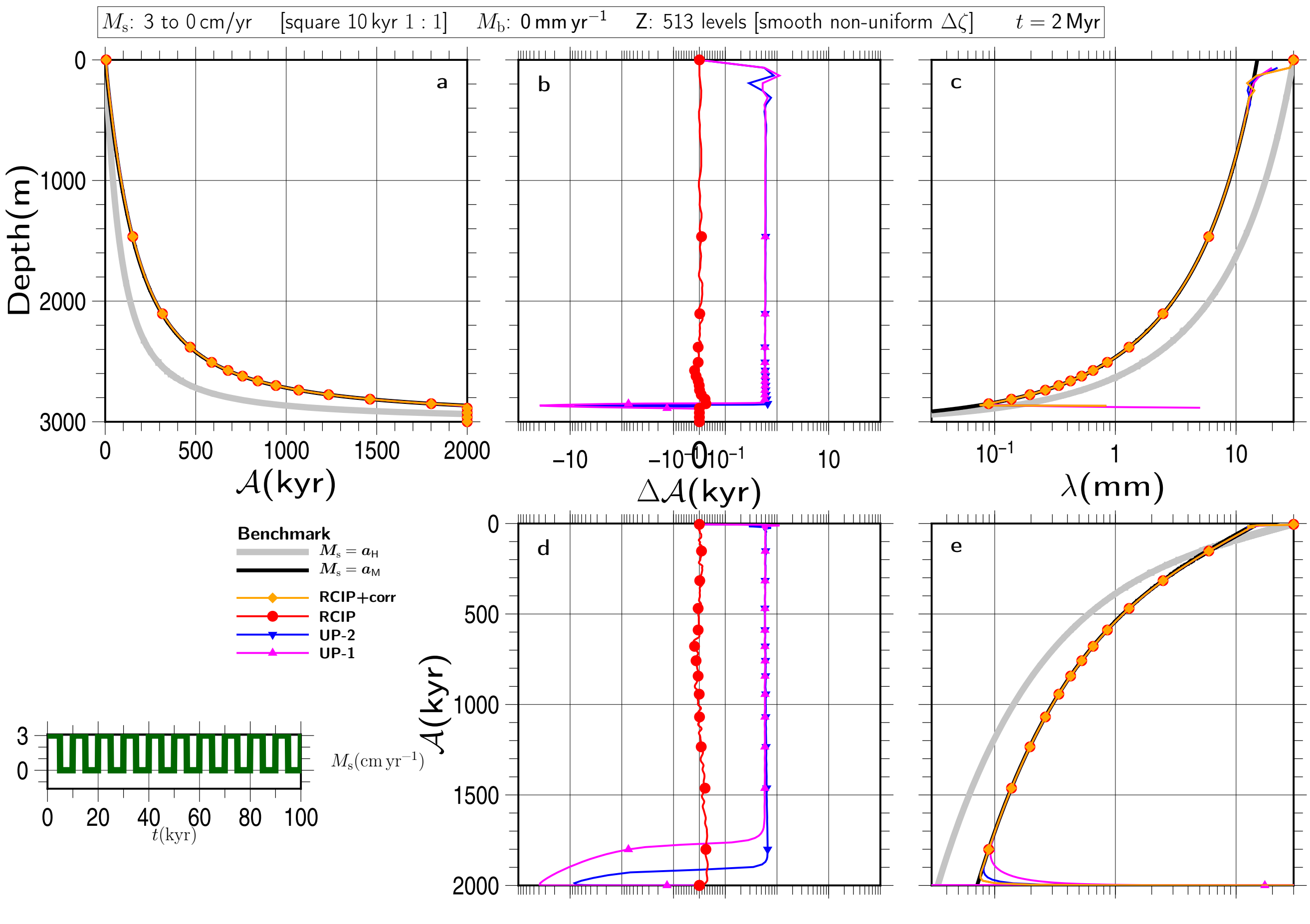

Figure S123

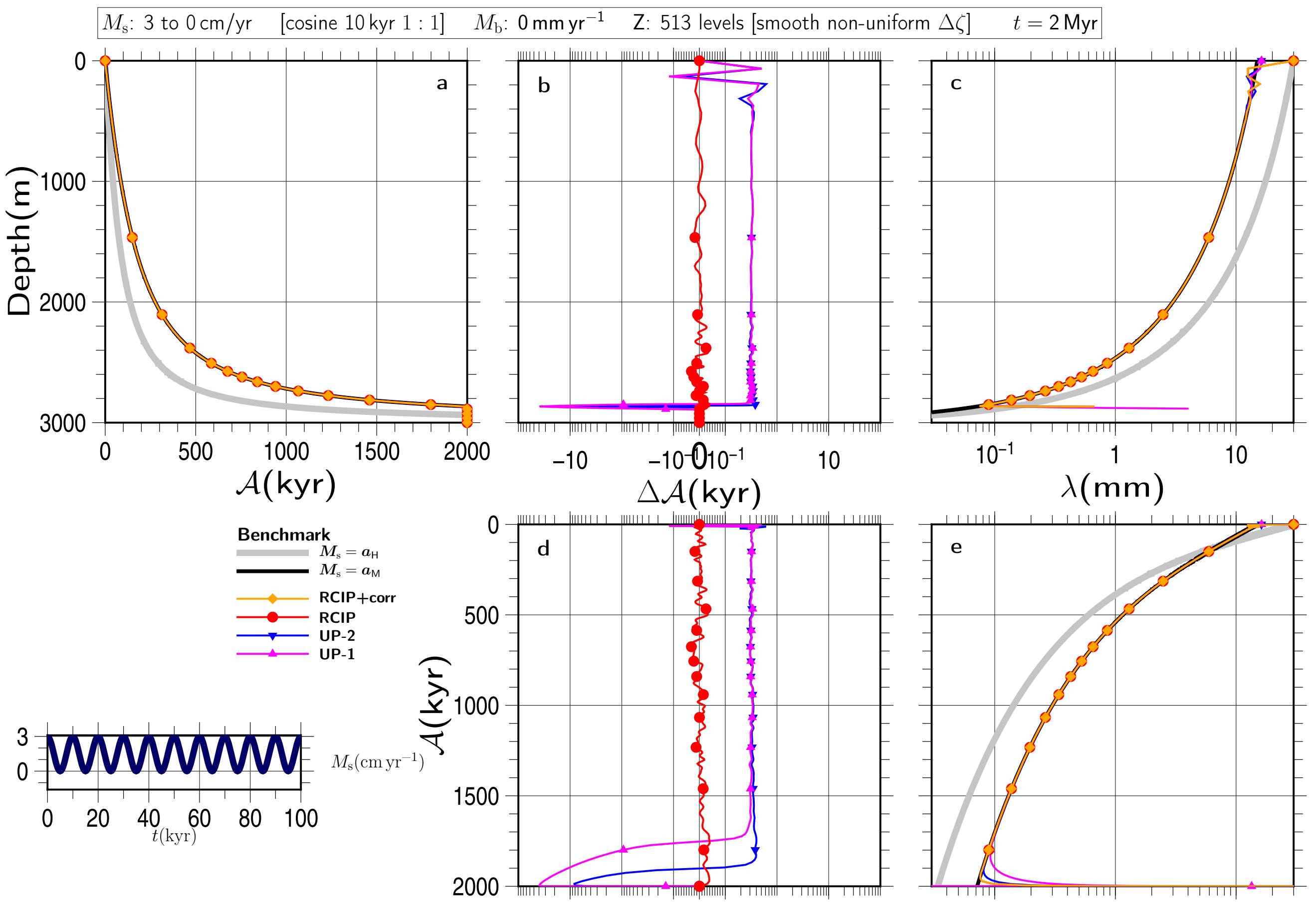

Figure S124

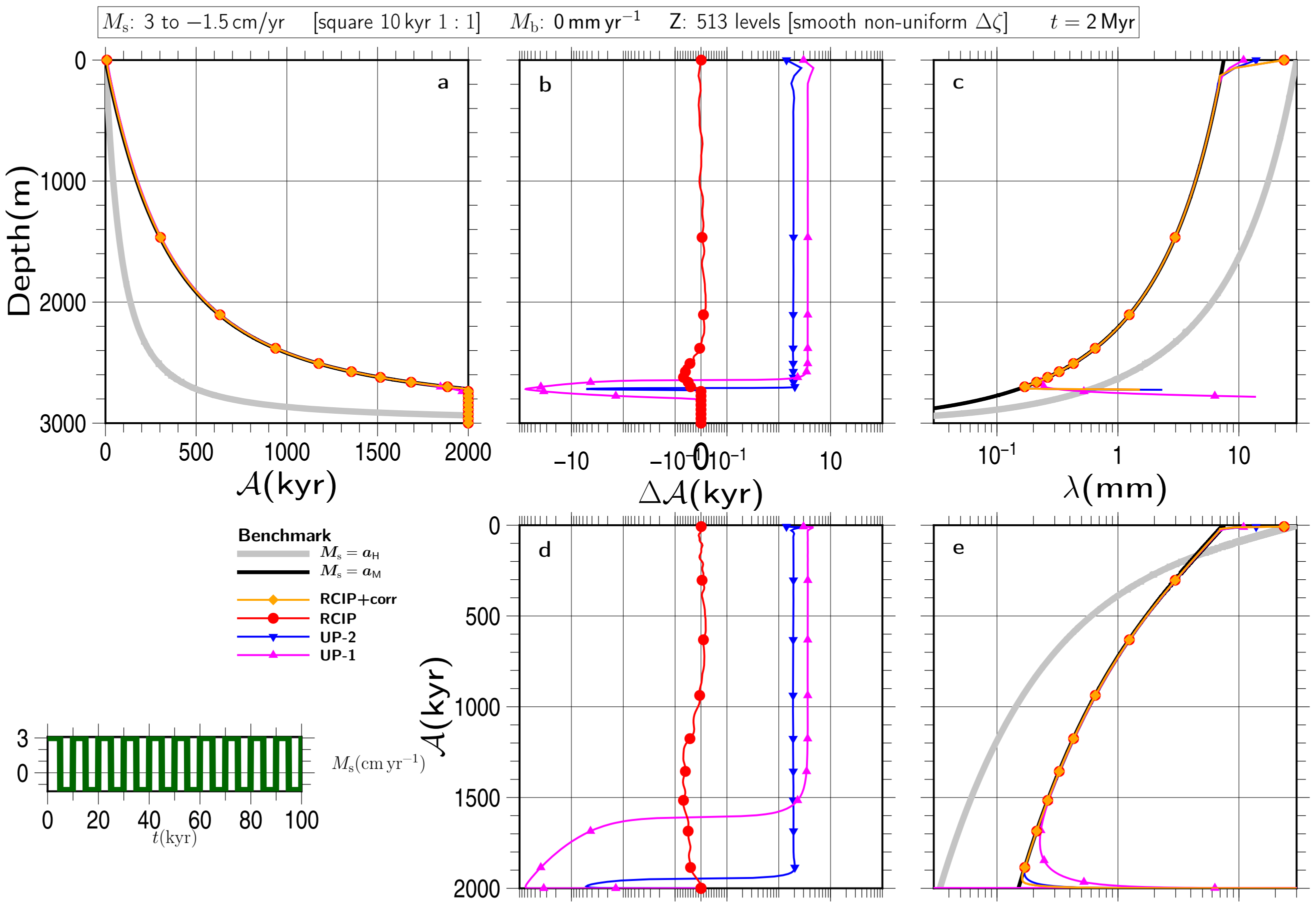

Figure S125

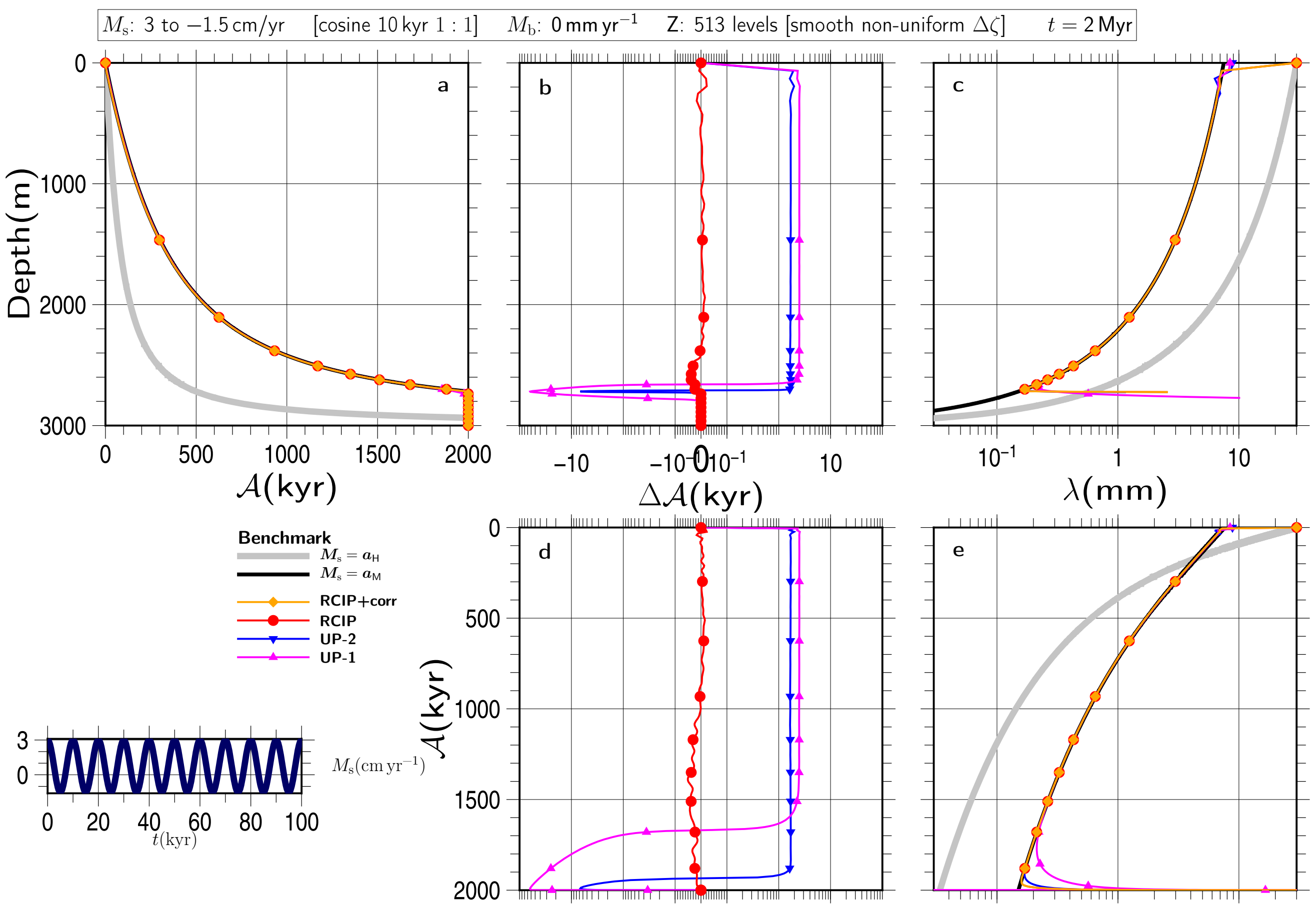

Figure S126

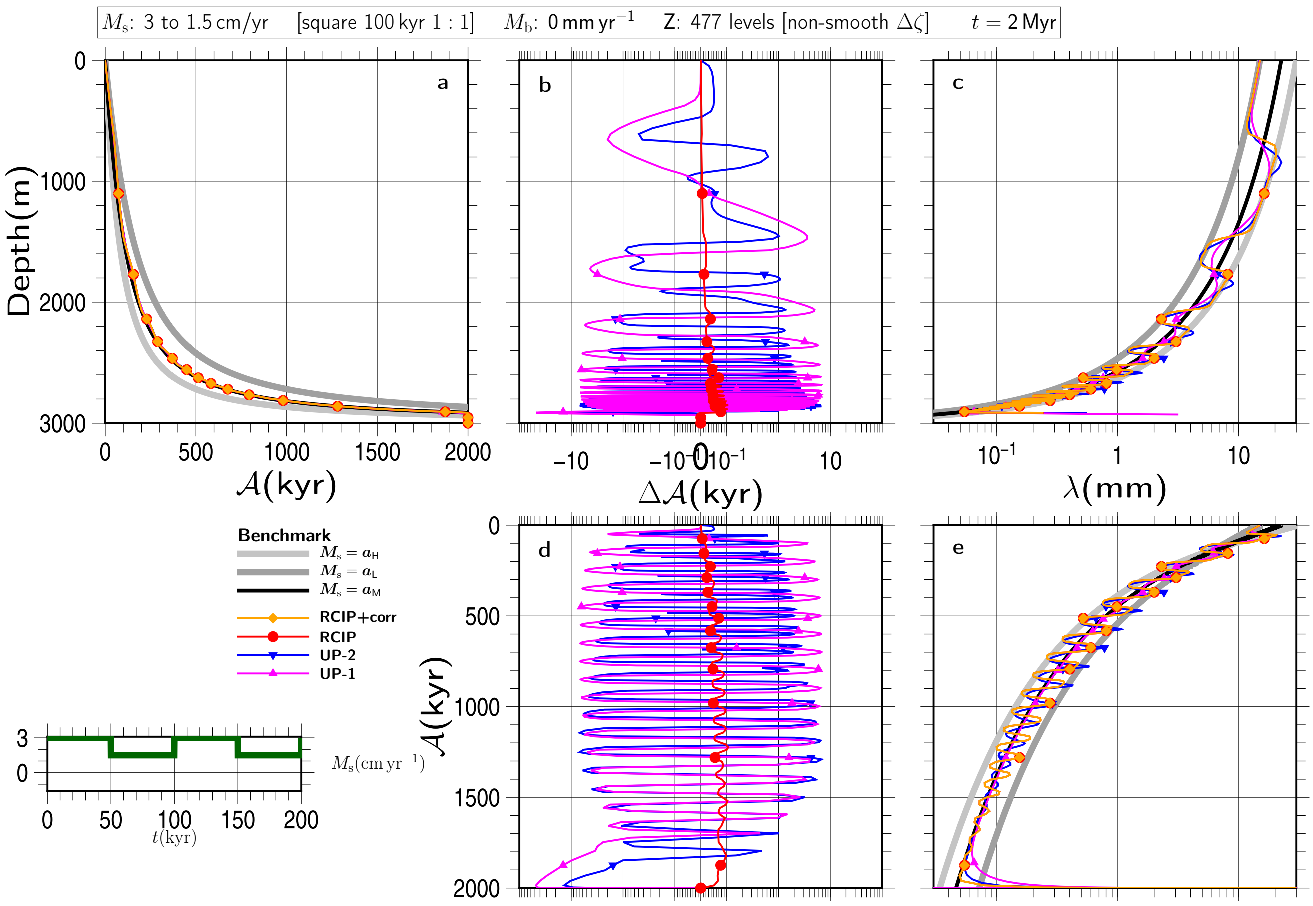

Figure S127

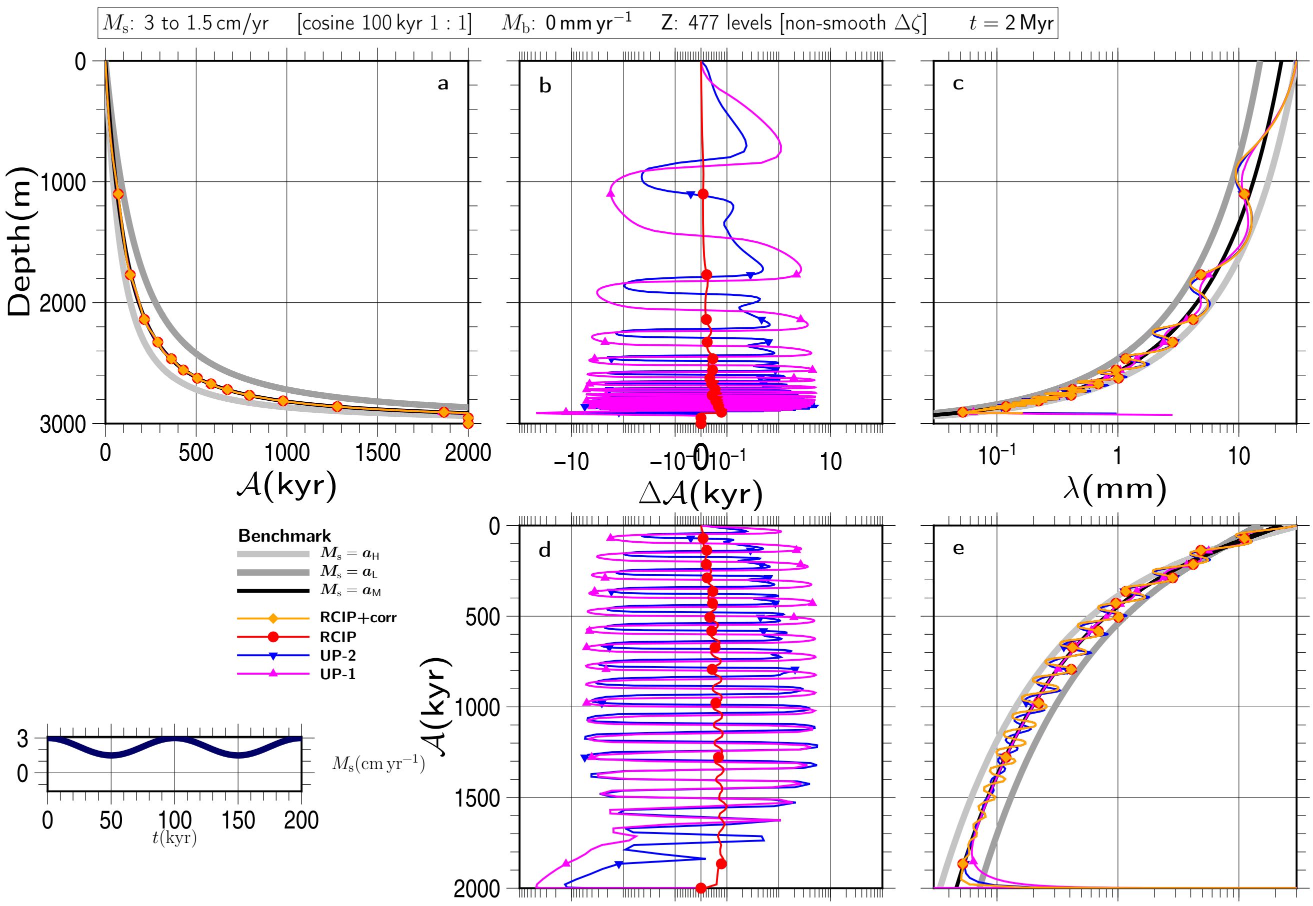

Figure S128

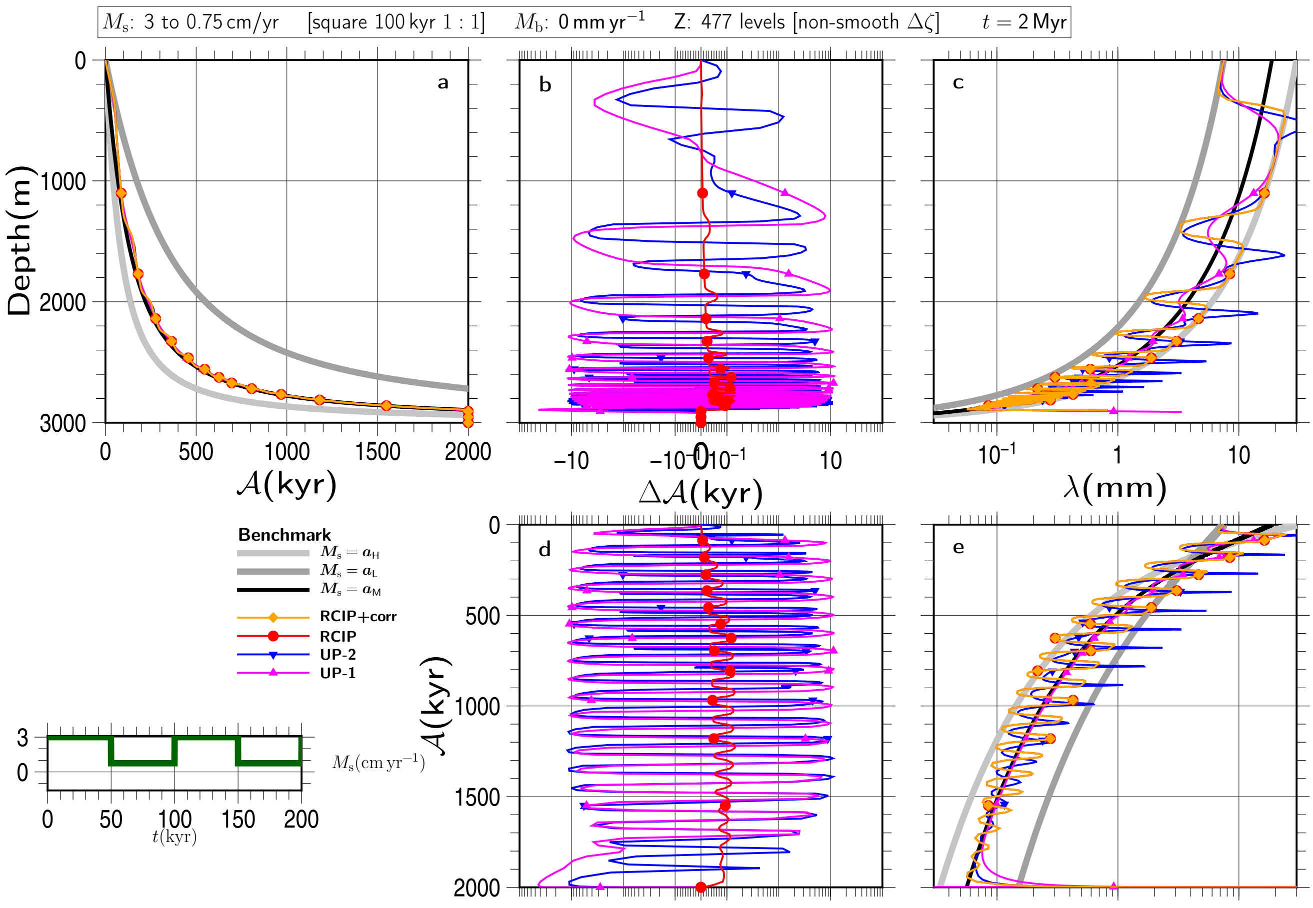

Figure S129

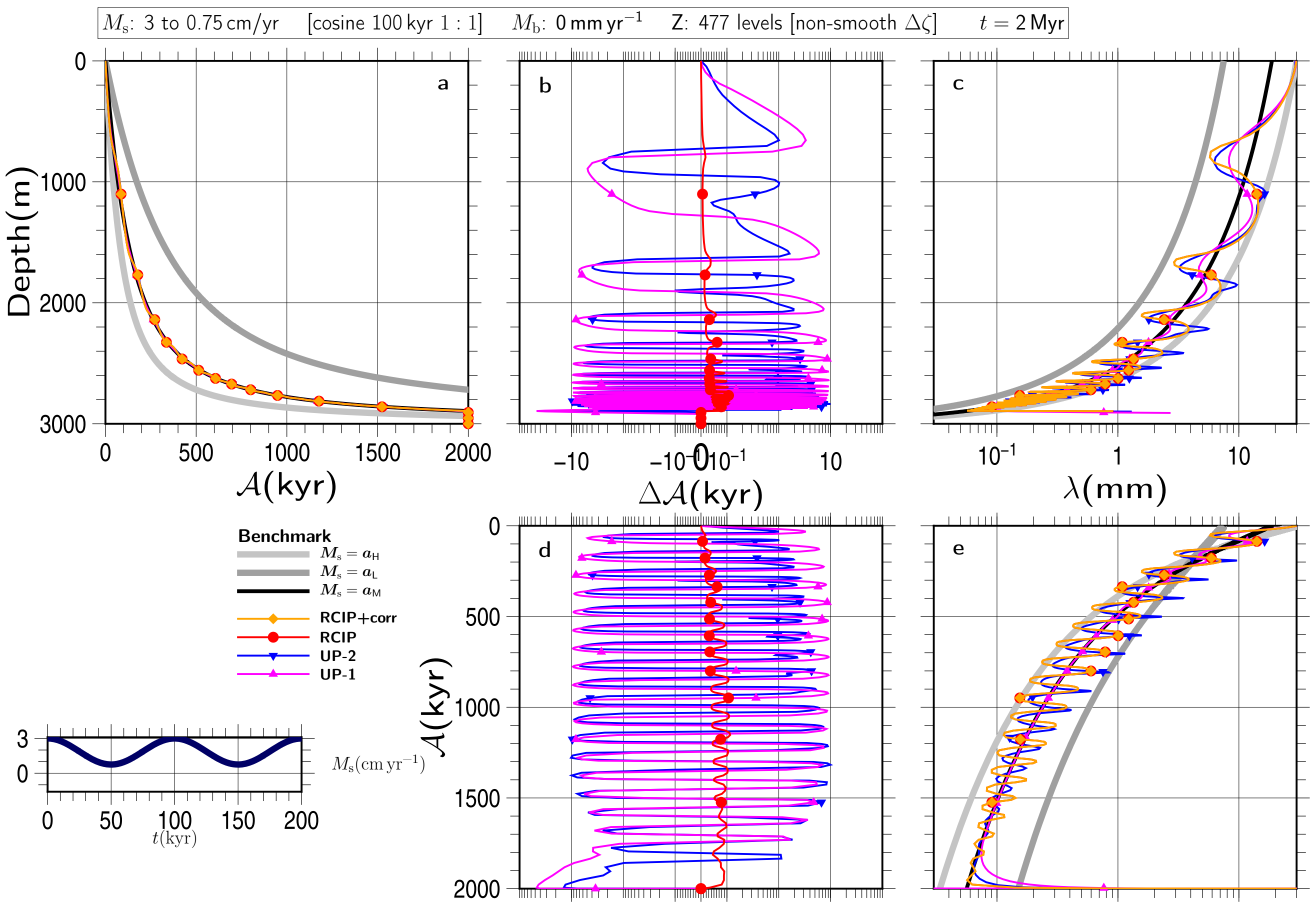

Figure S130

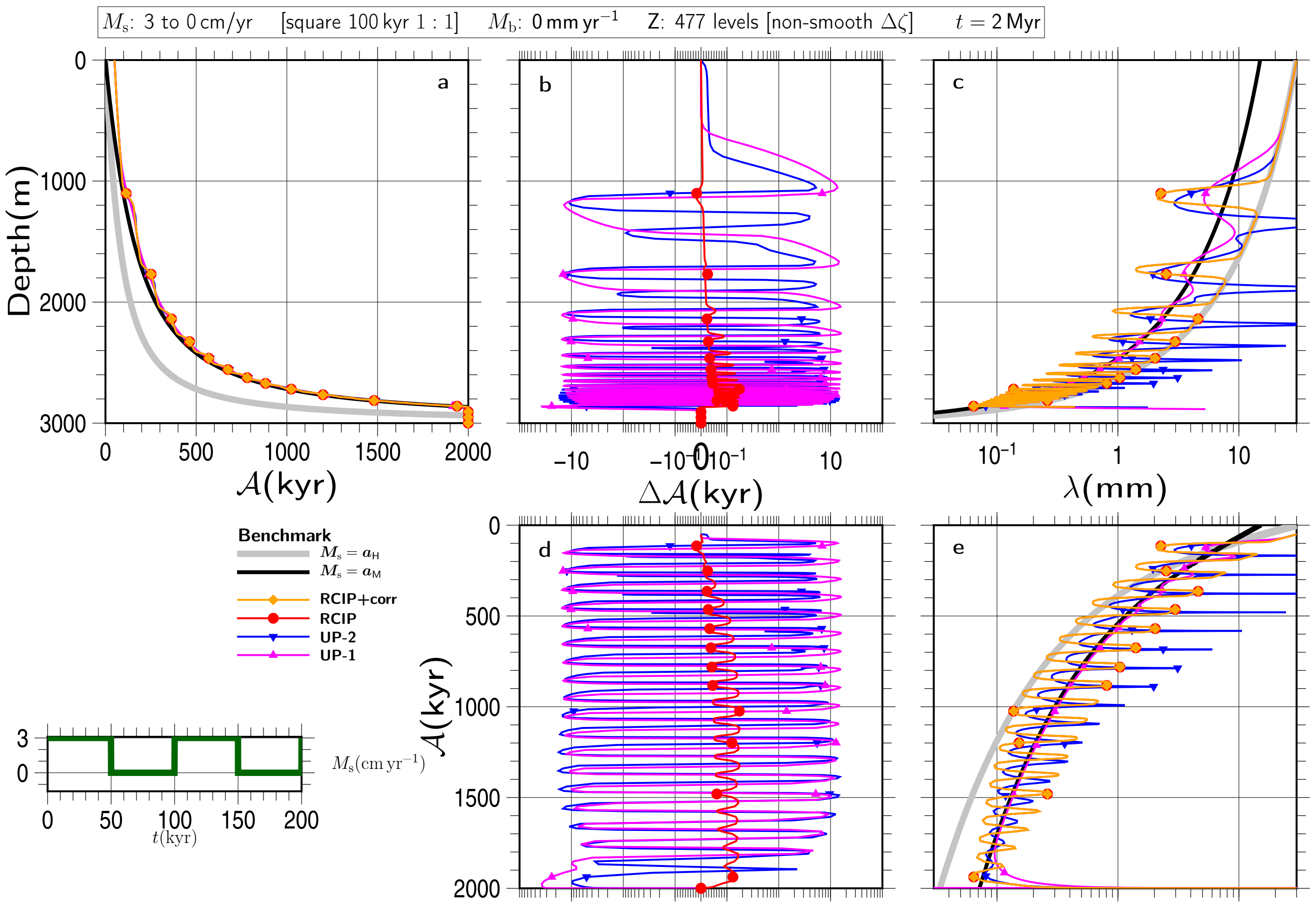

Figure S131

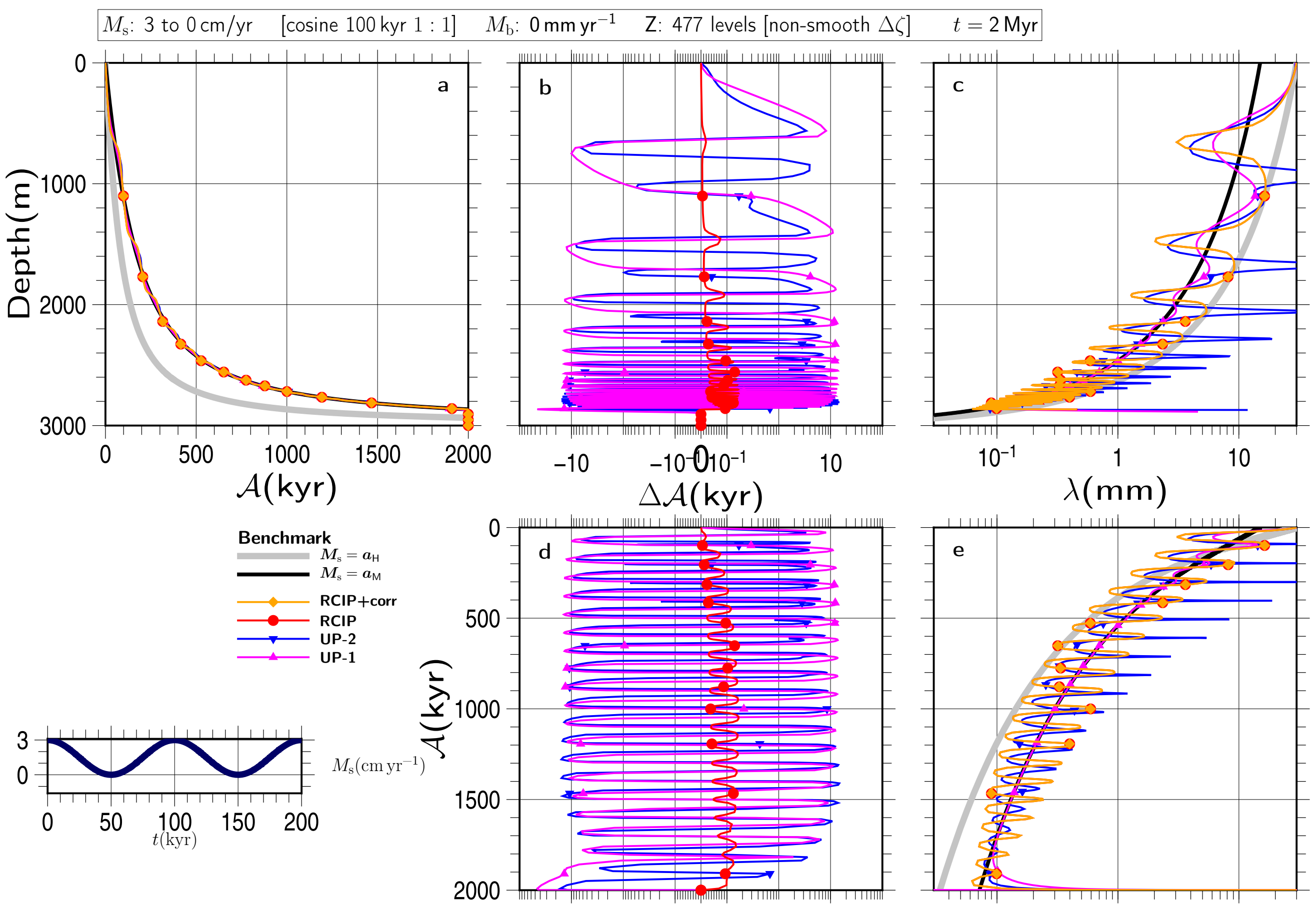

Figure S132

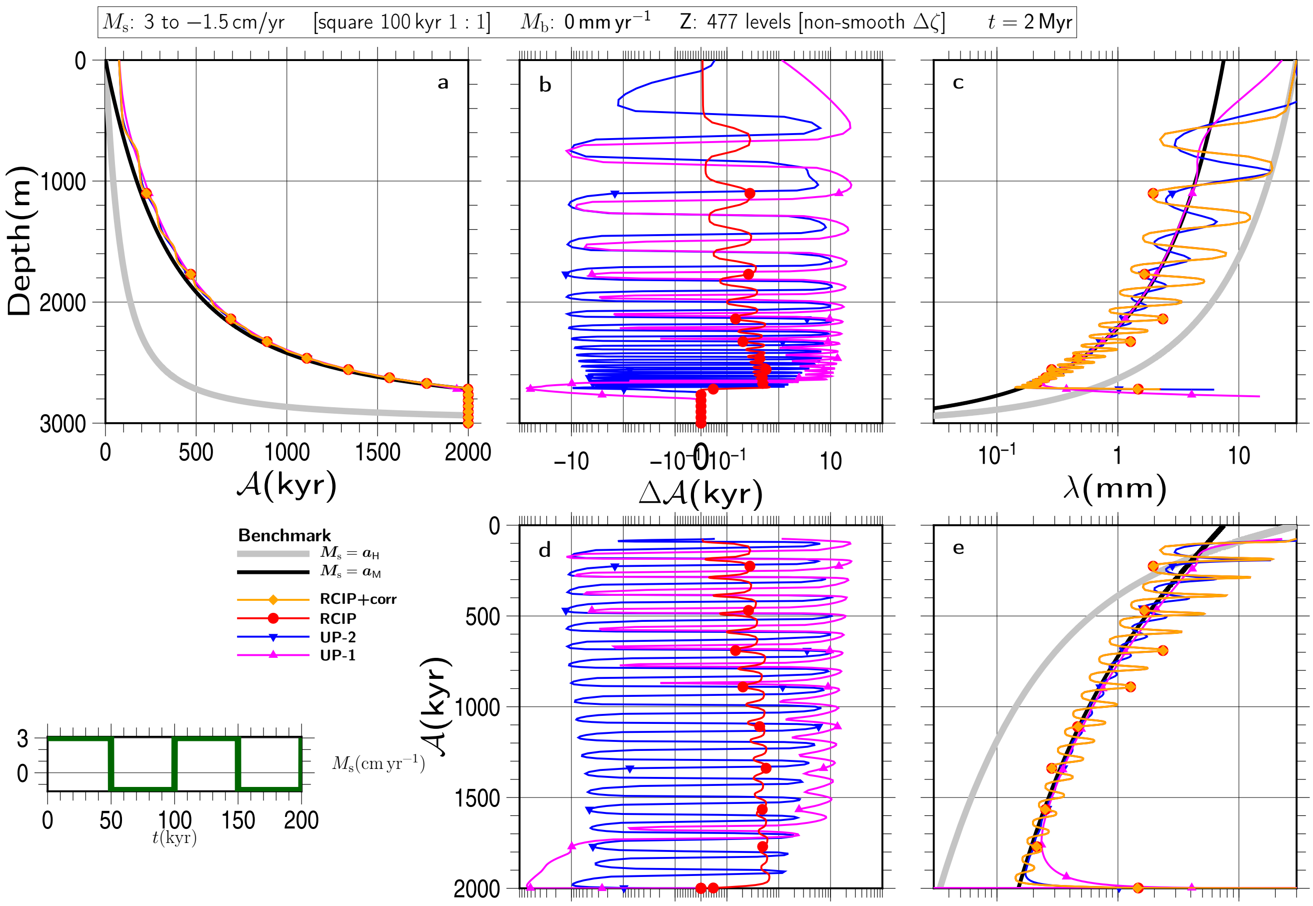

Figure S133

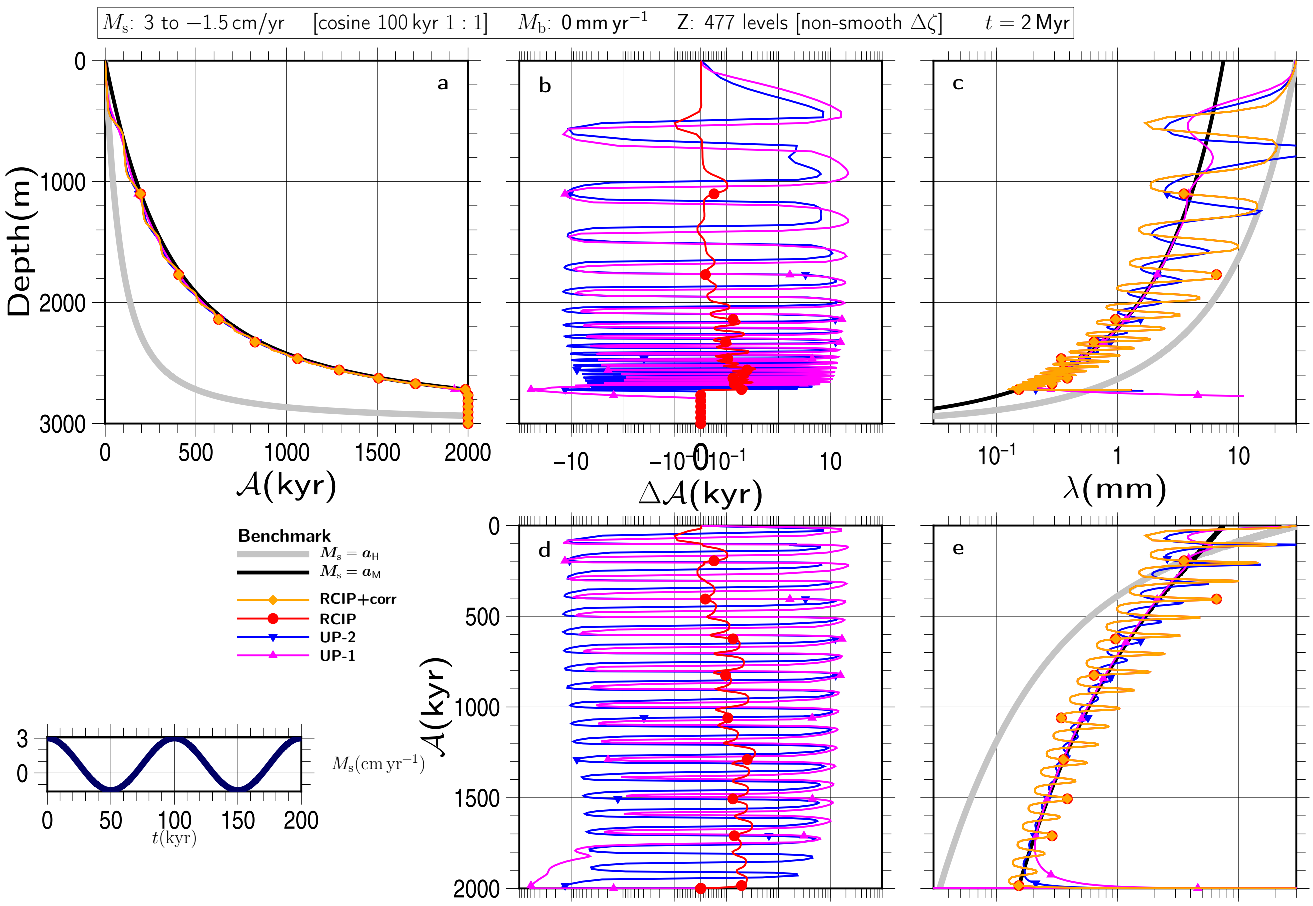

Figure S134

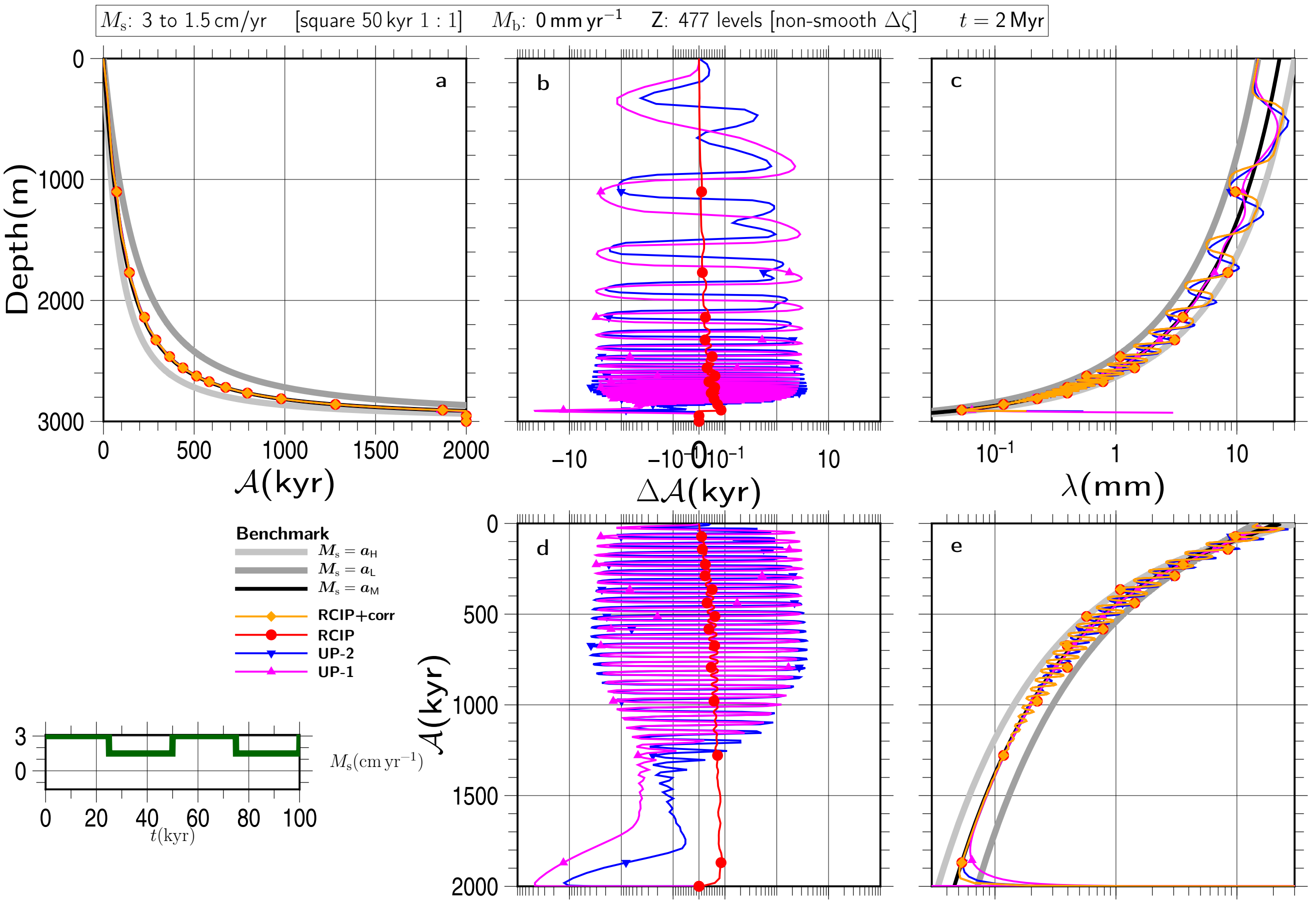

Figure S135

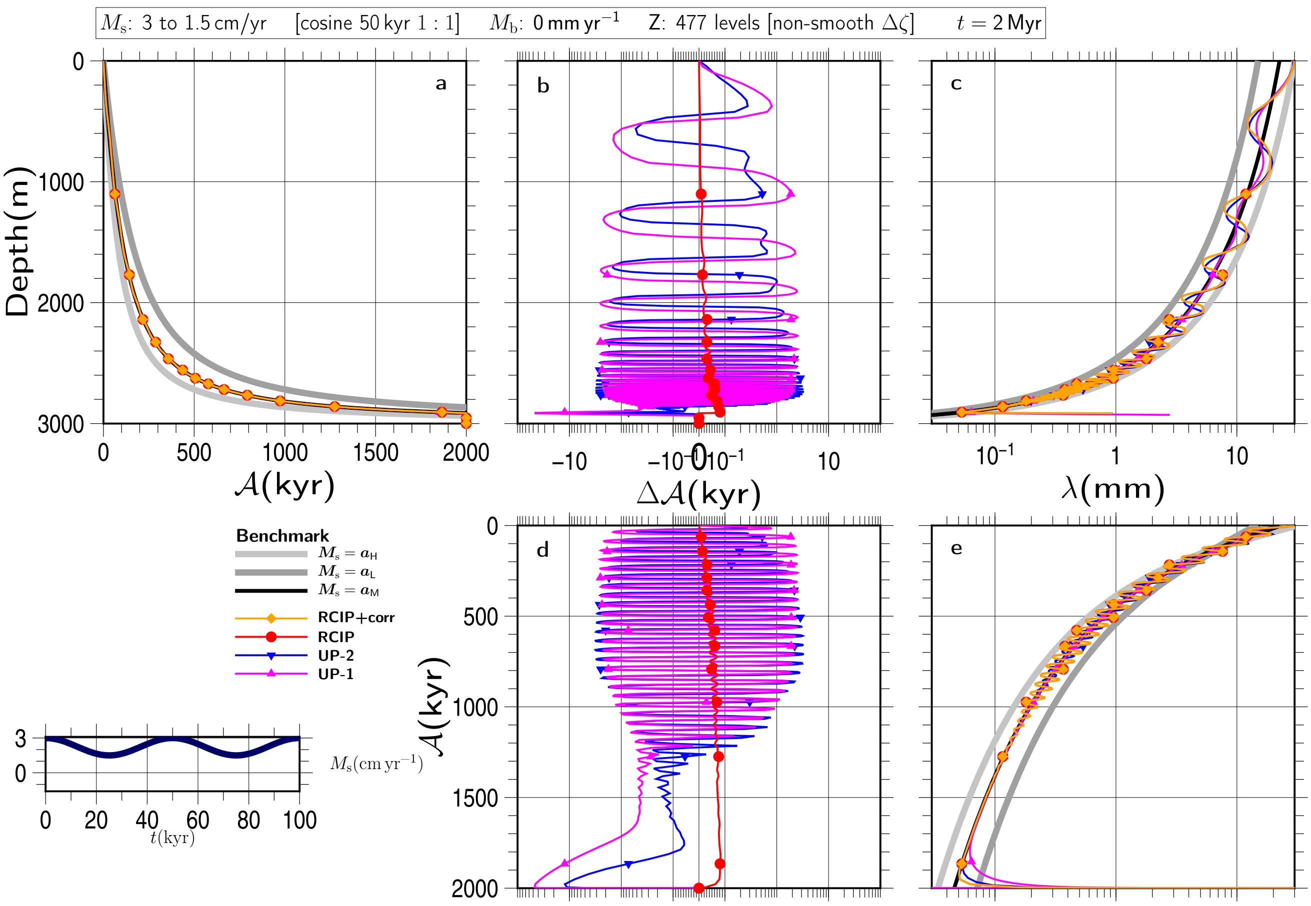

Figure S136

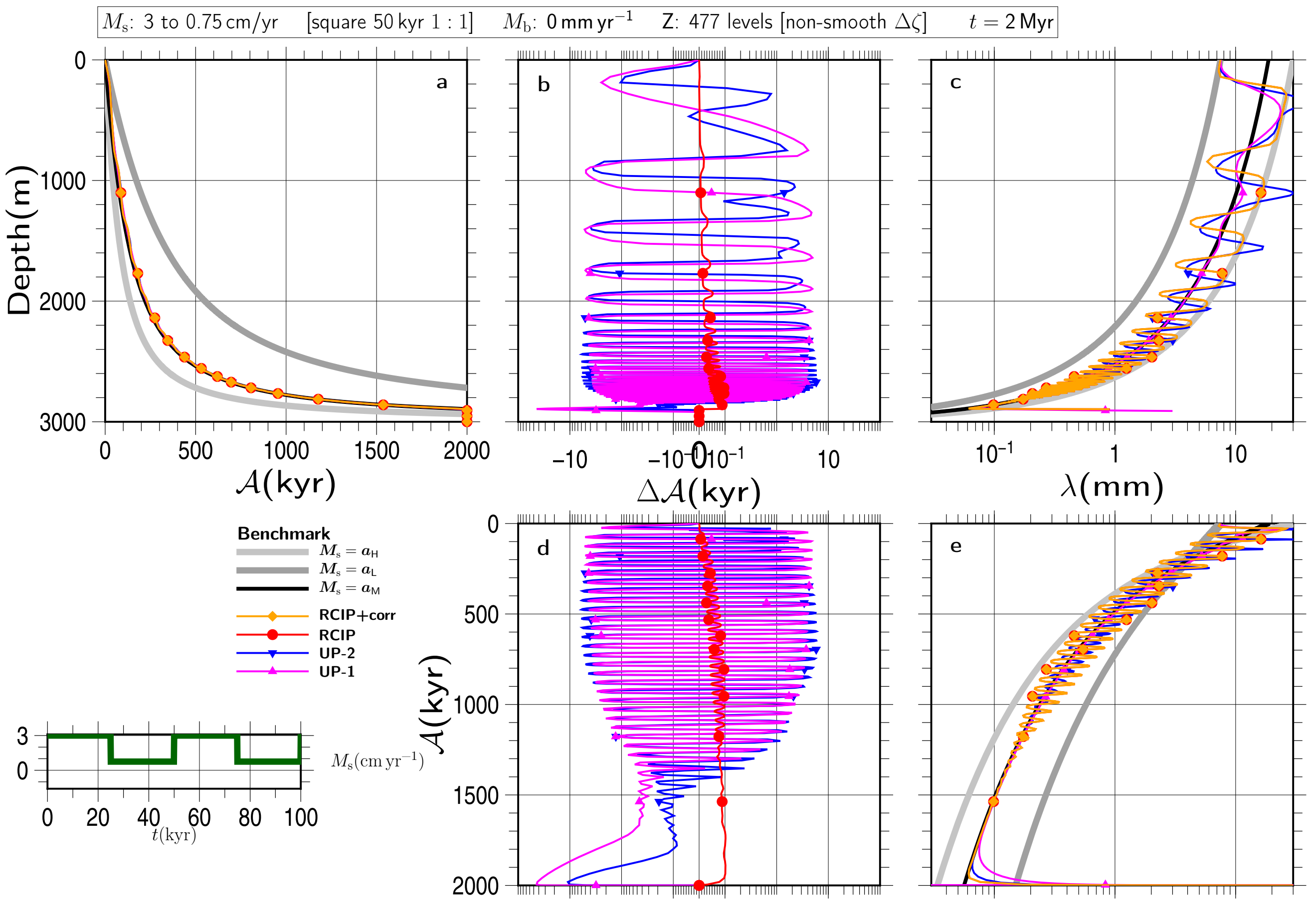

Figure S137

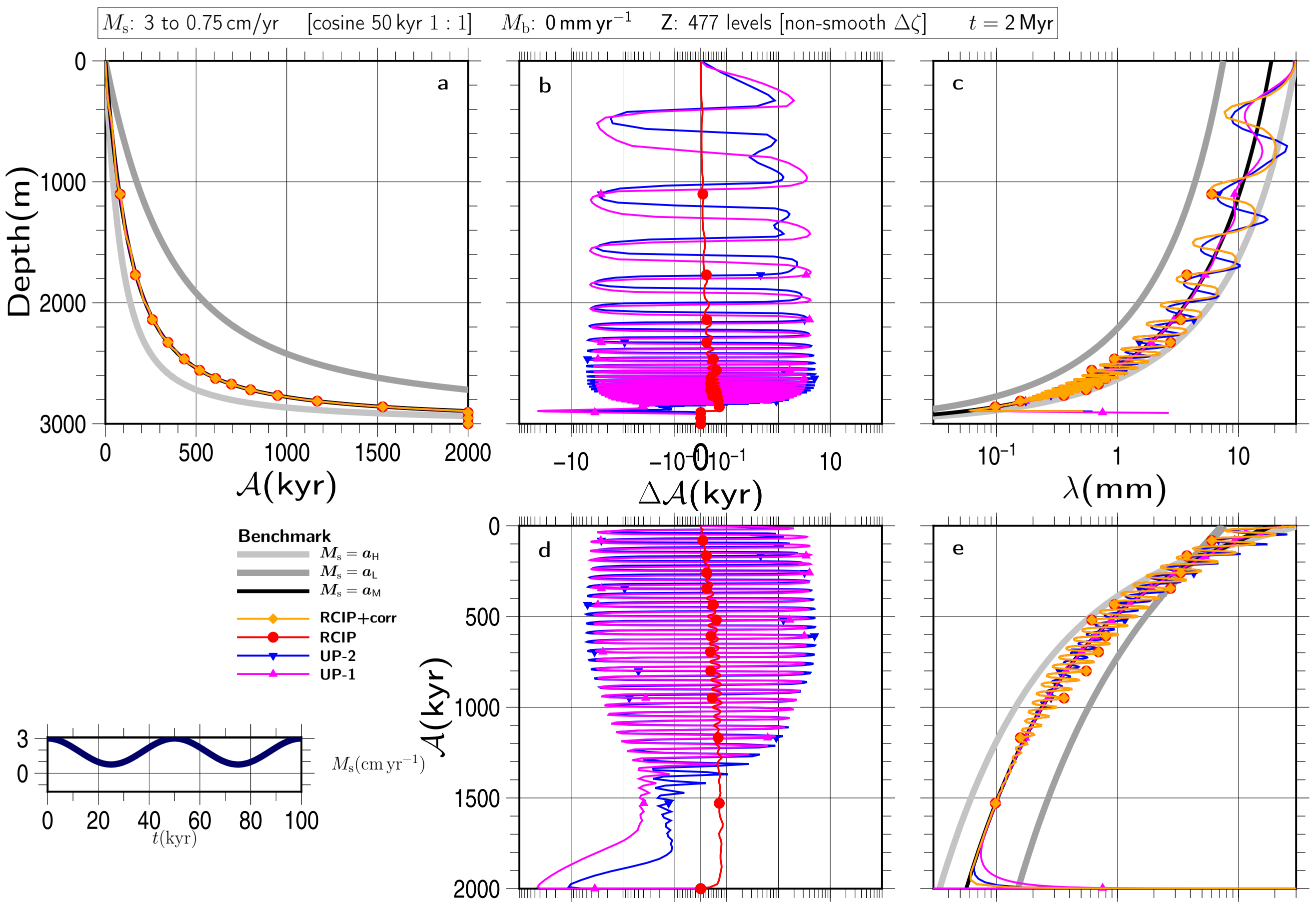

Figure S138

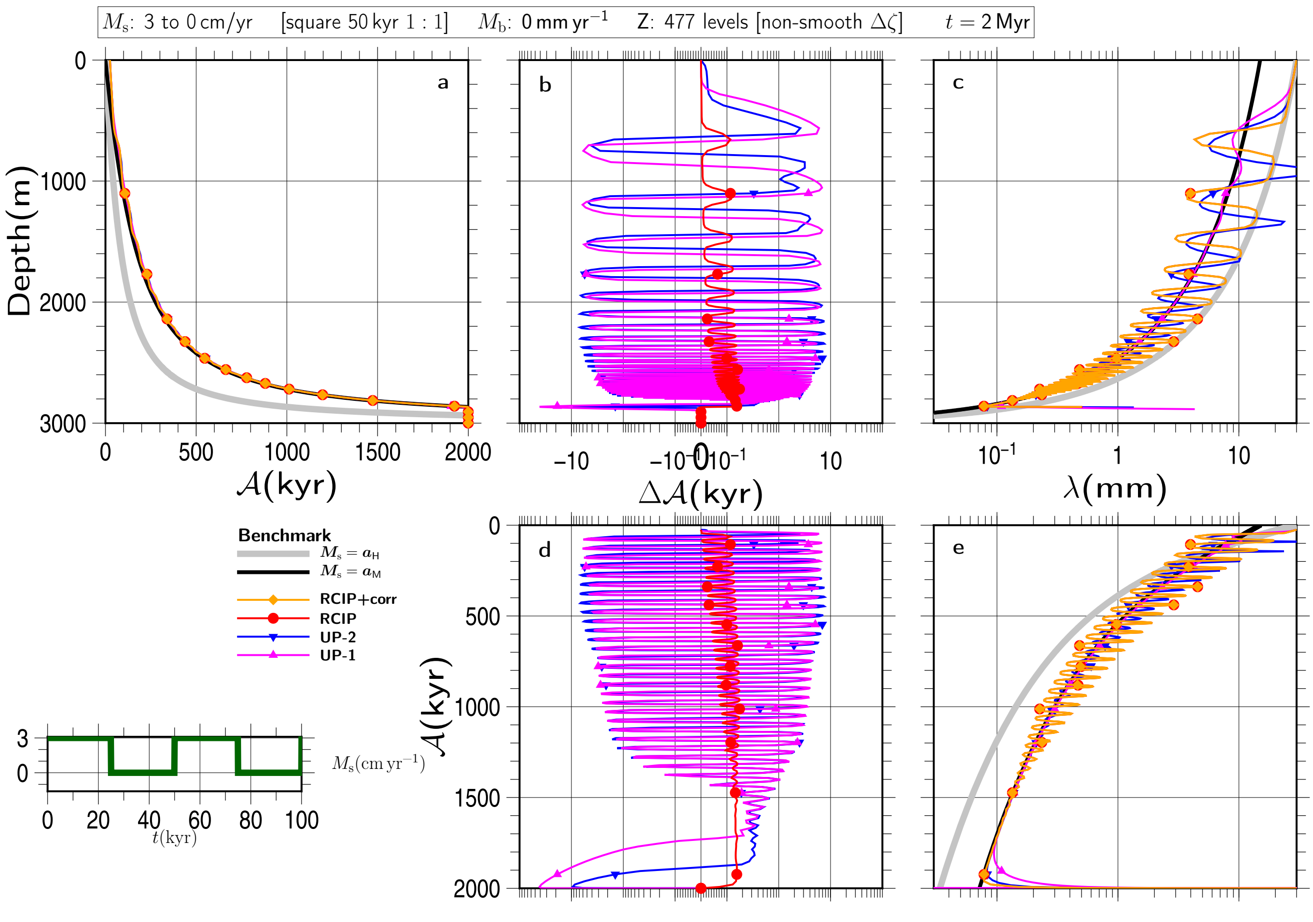

Figure S139

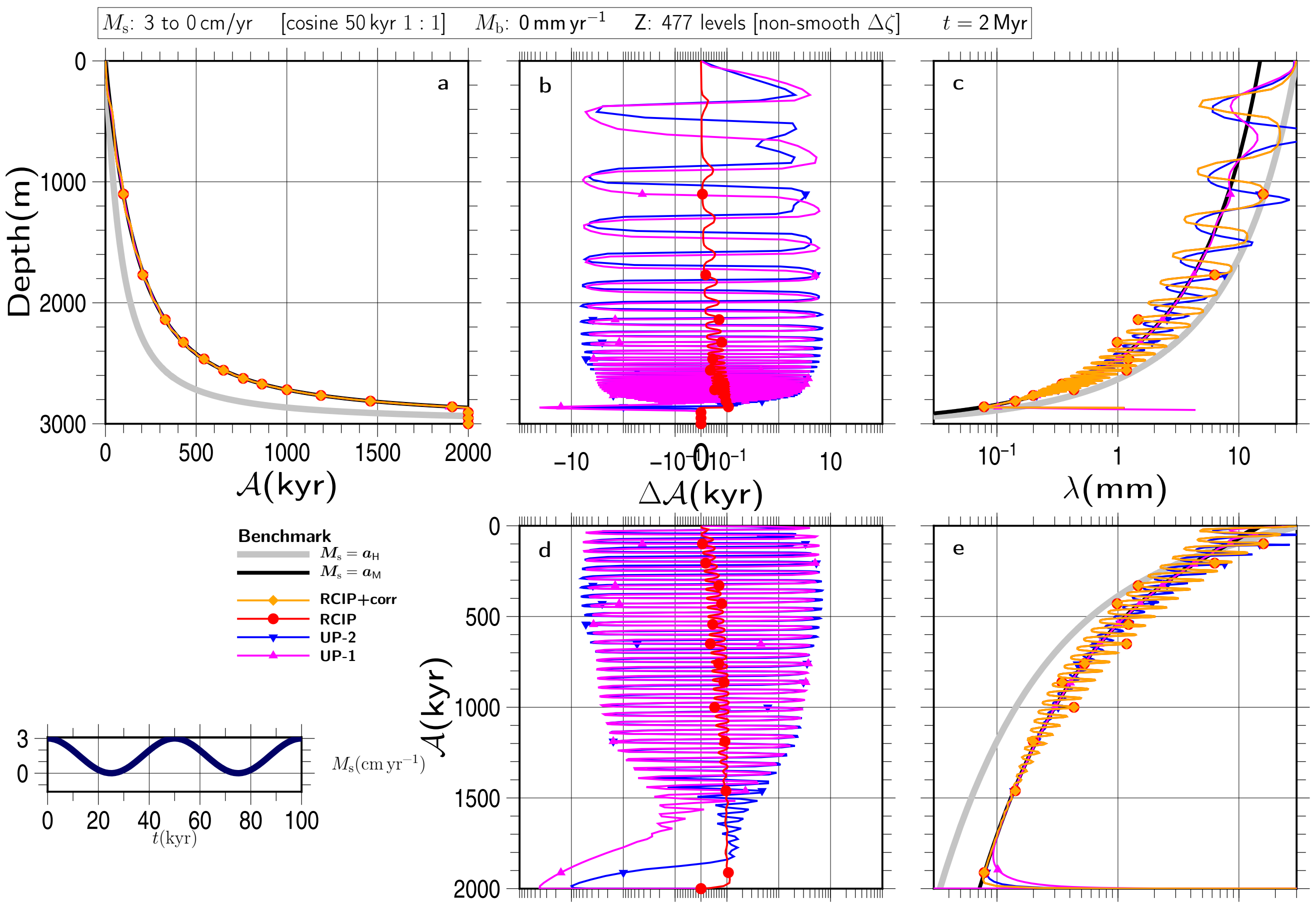

Figure S140

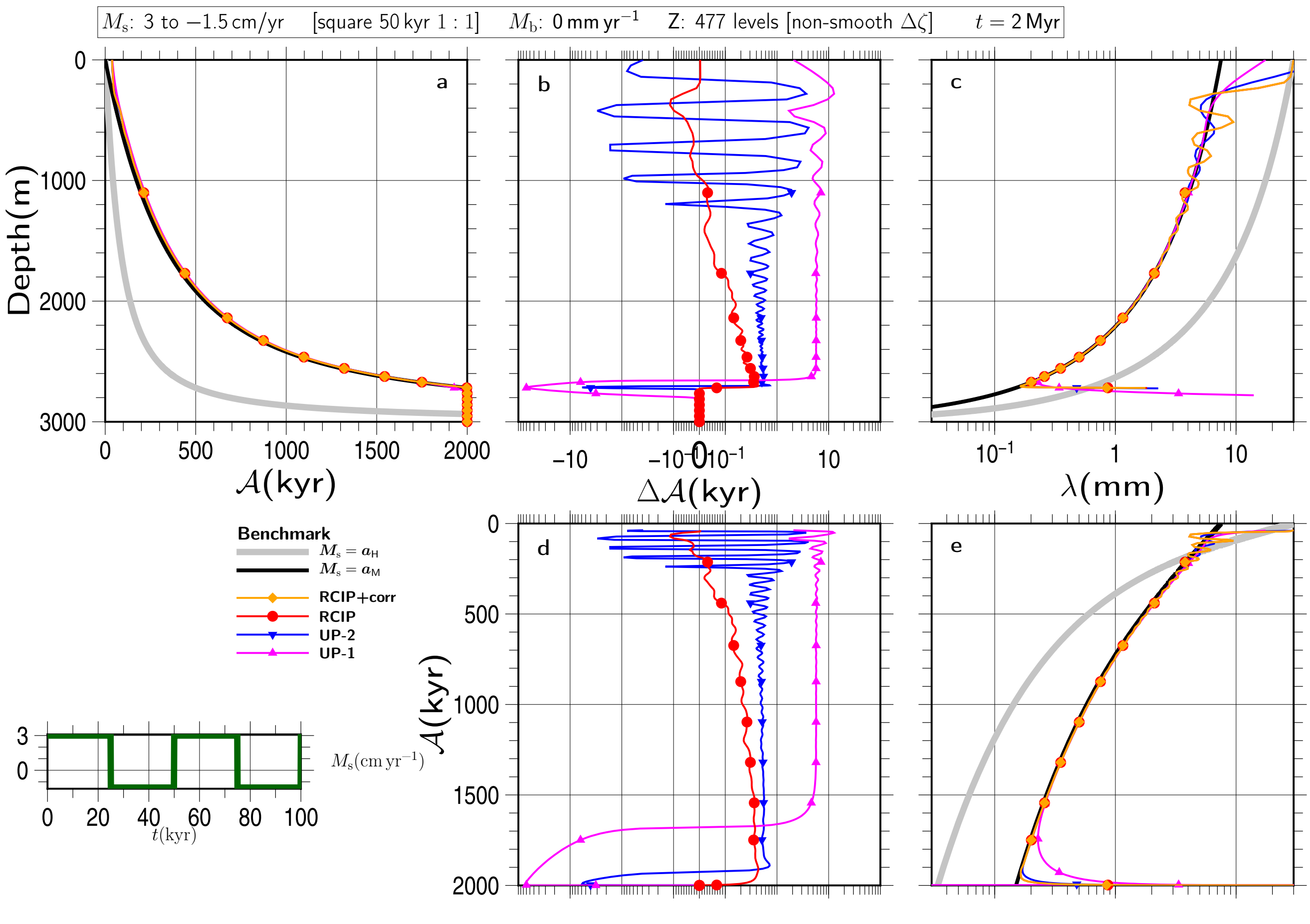

Figure S141

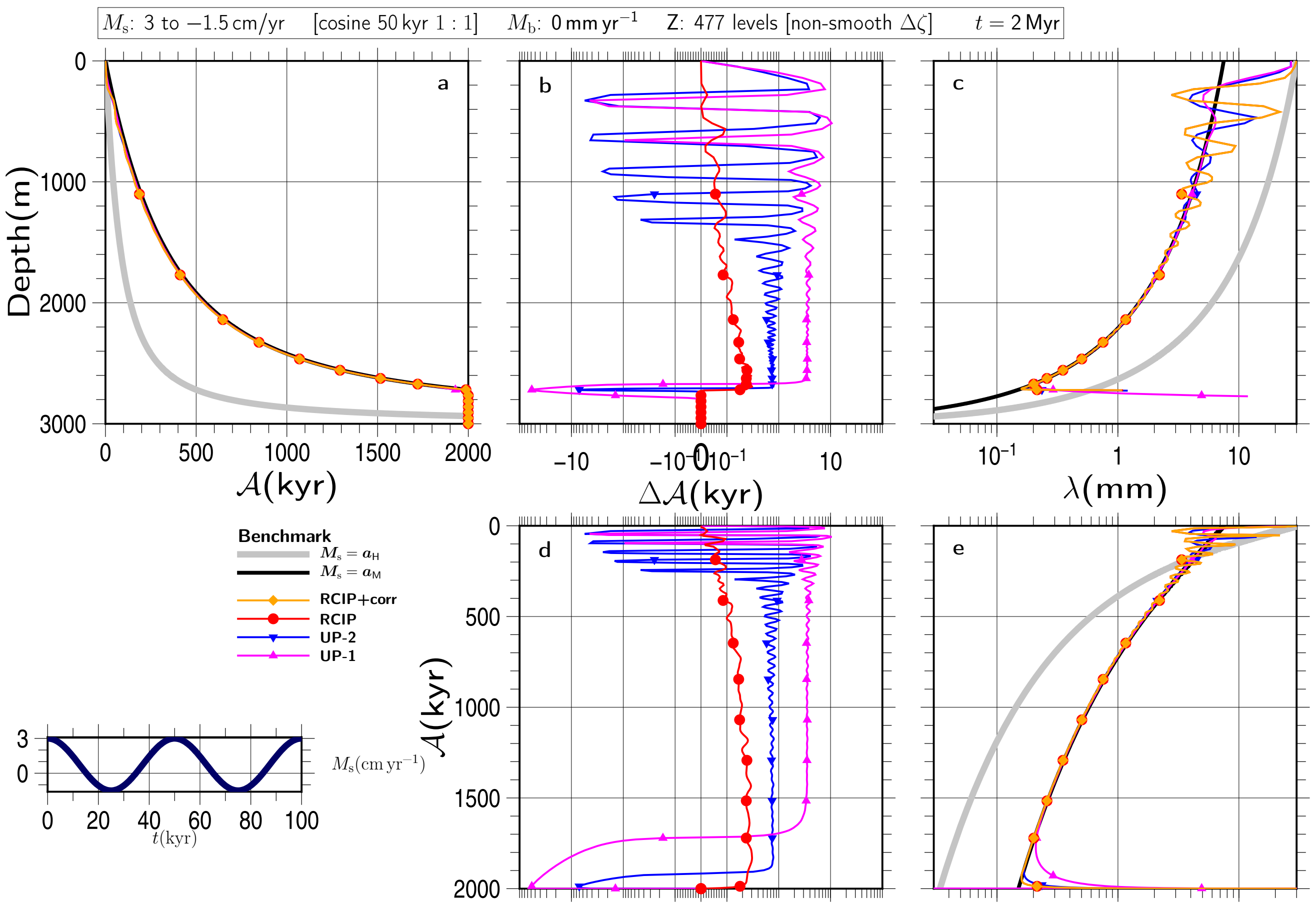

Figure S142

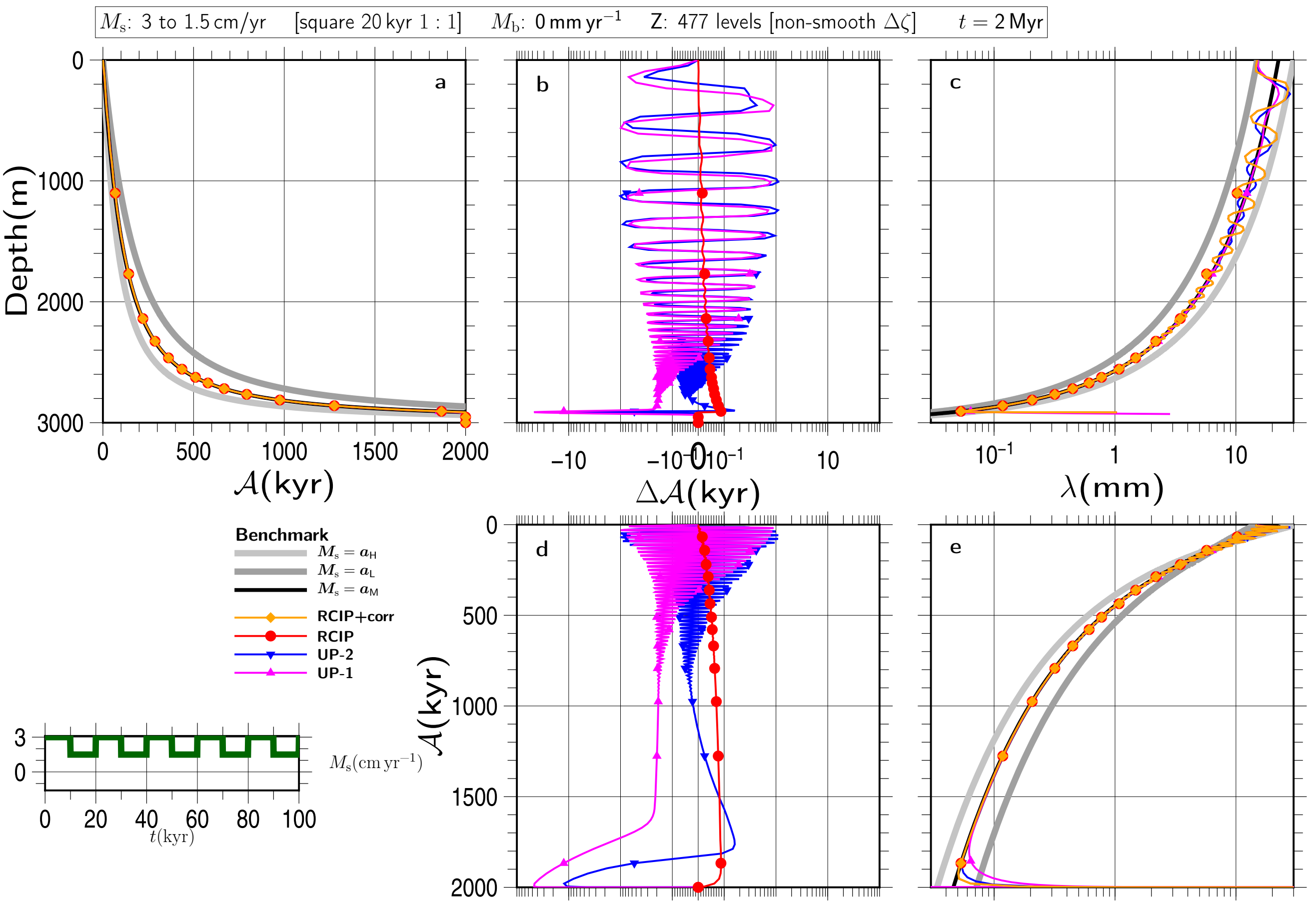

Figure S143

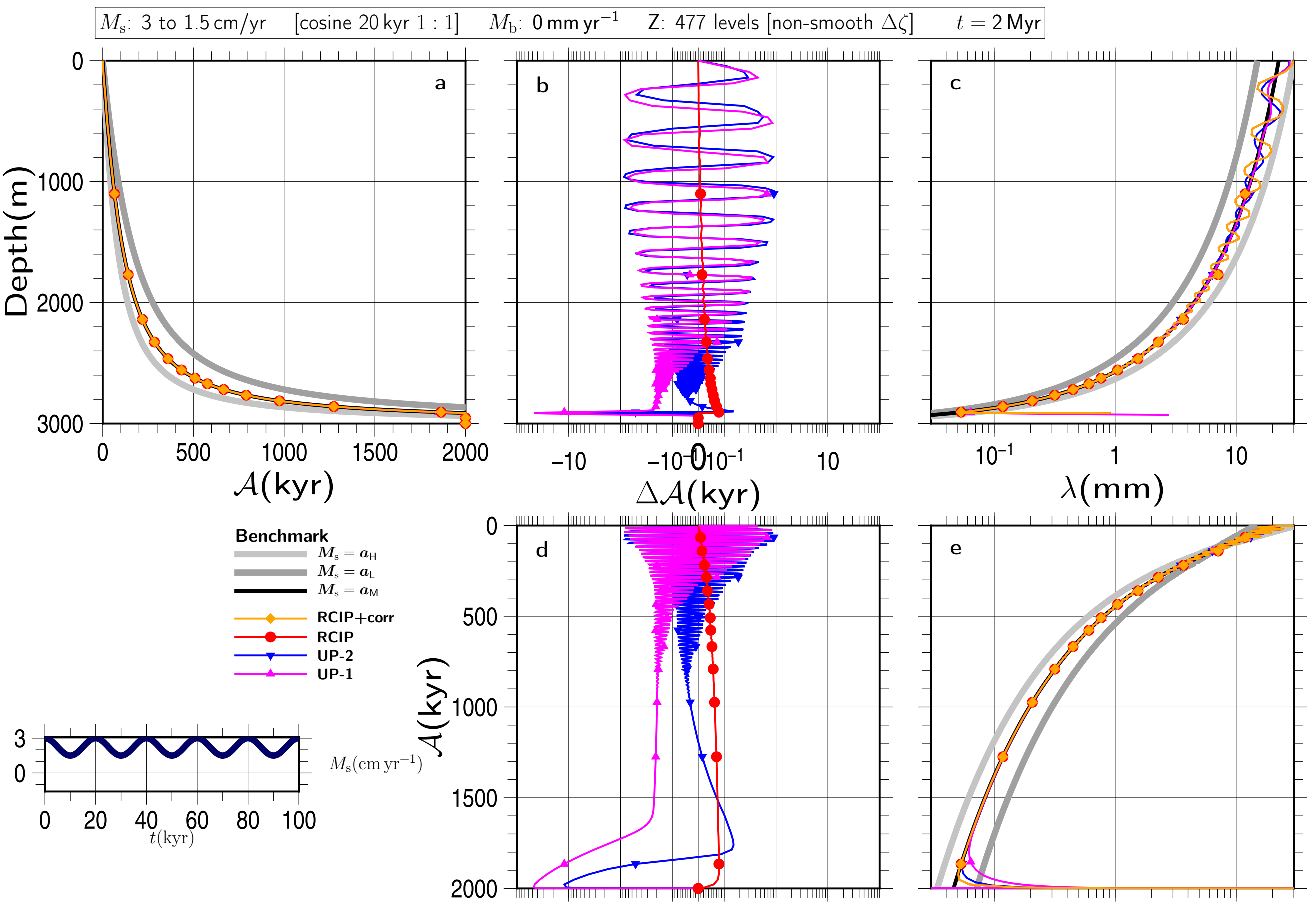

Figure S144

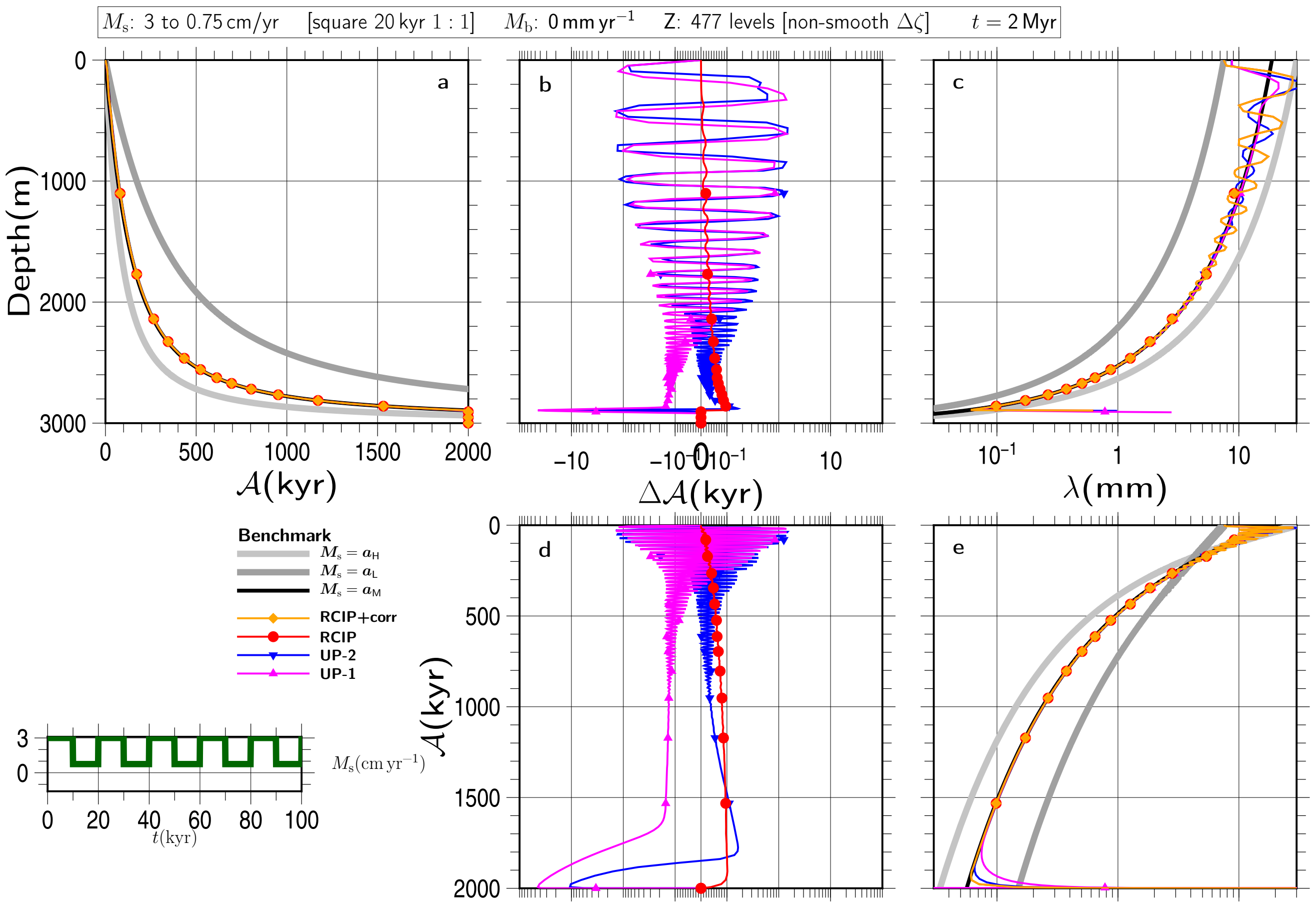

Figure S145

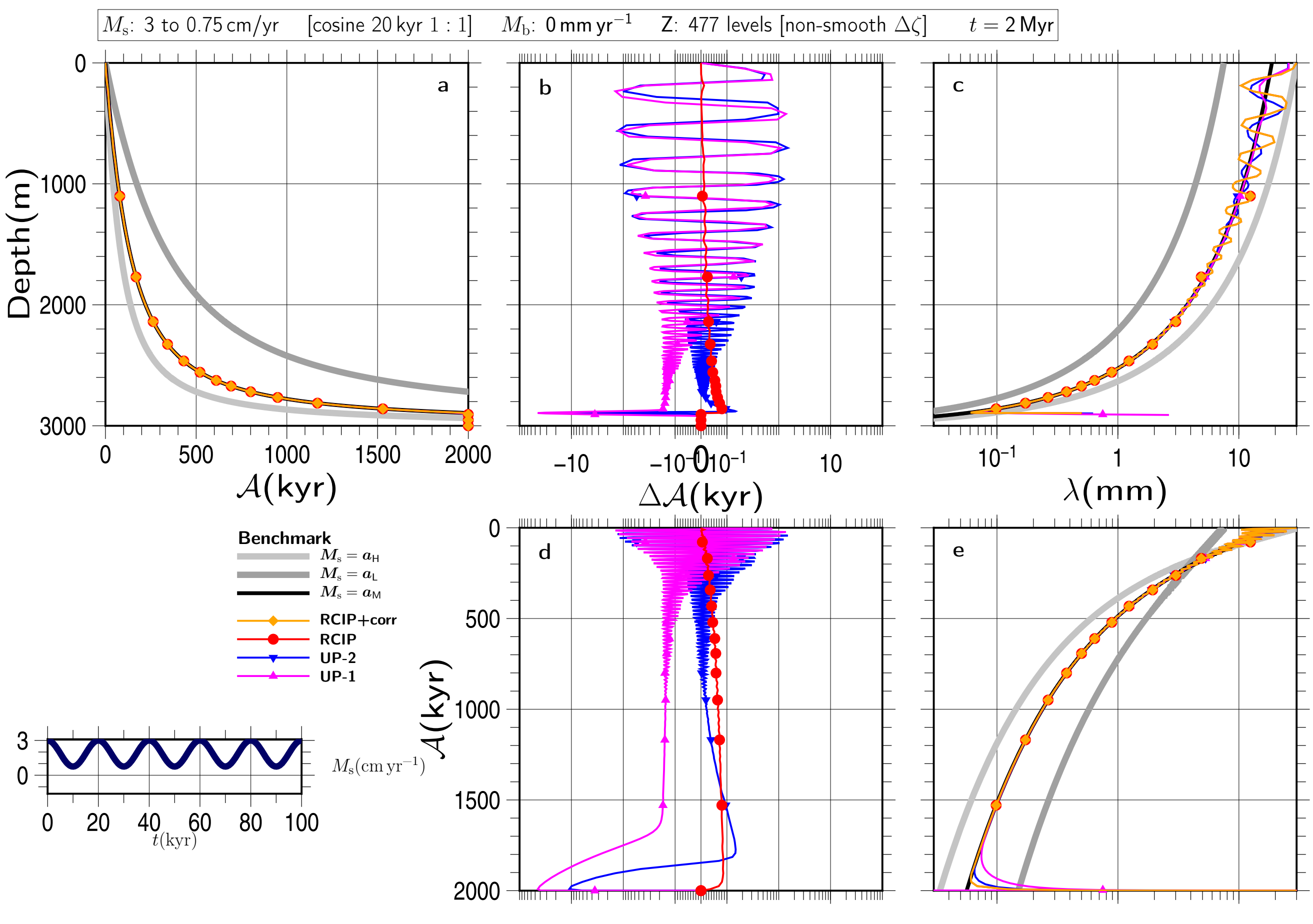

Figure S146

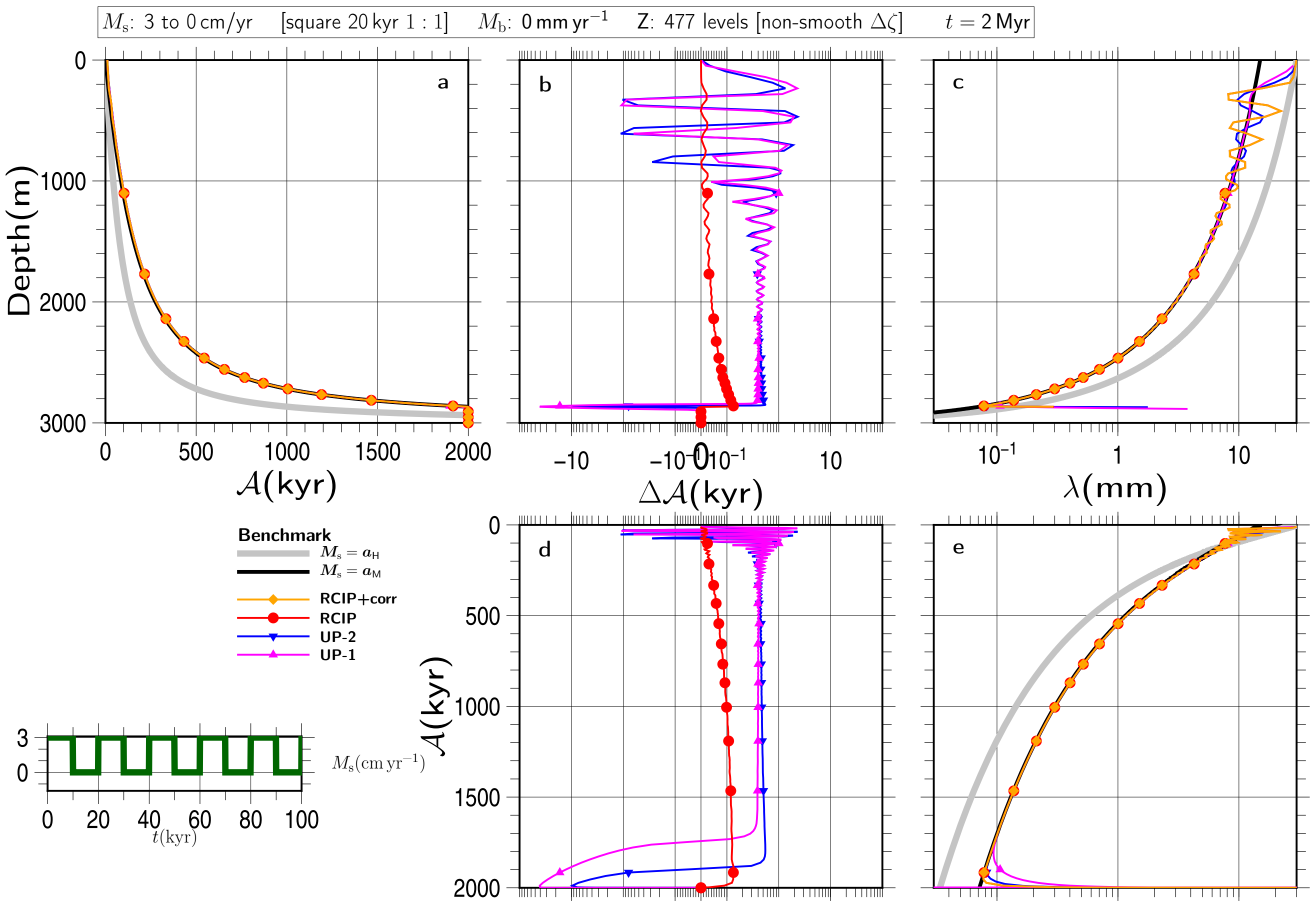

Figure S147

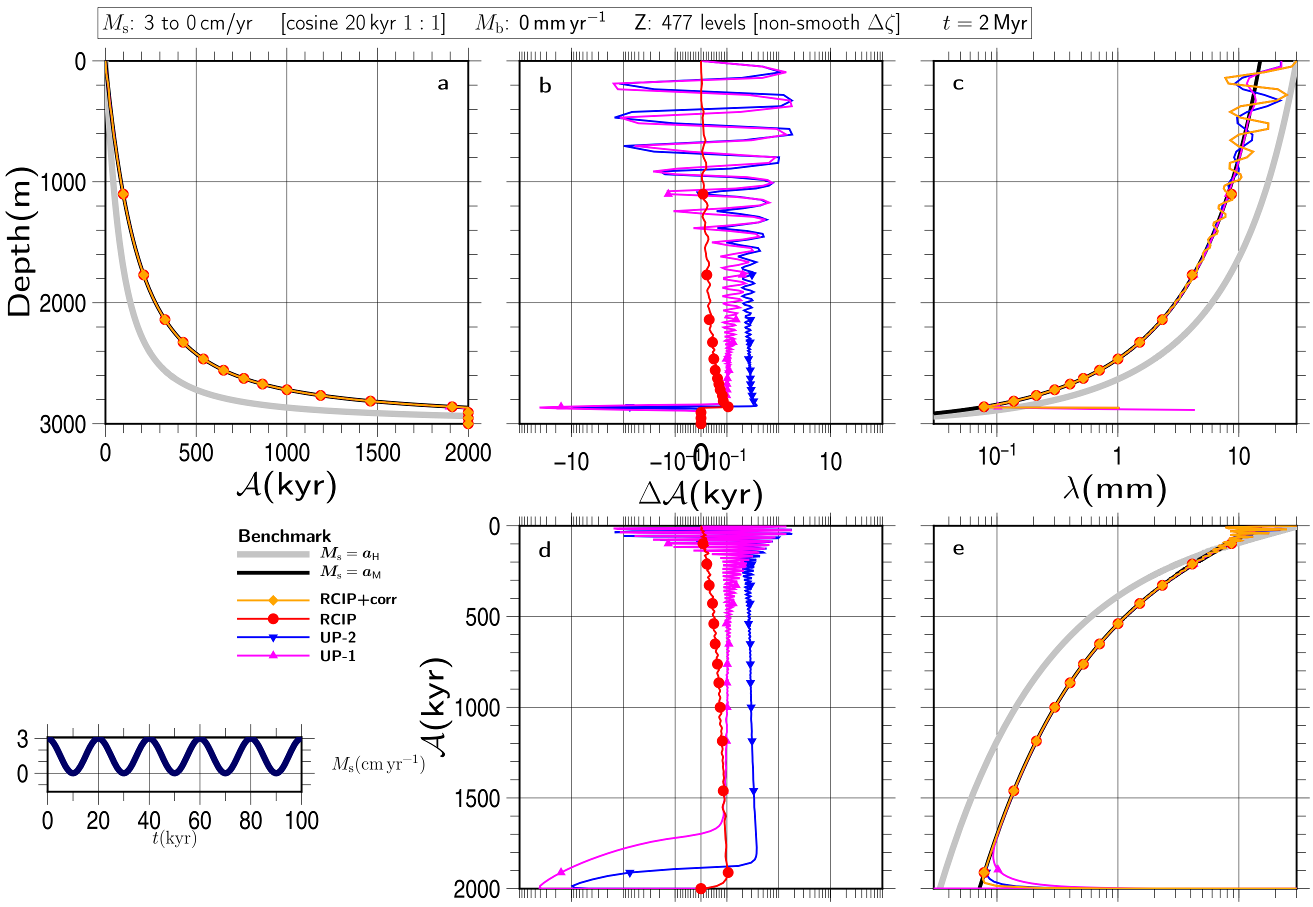

Figure S148

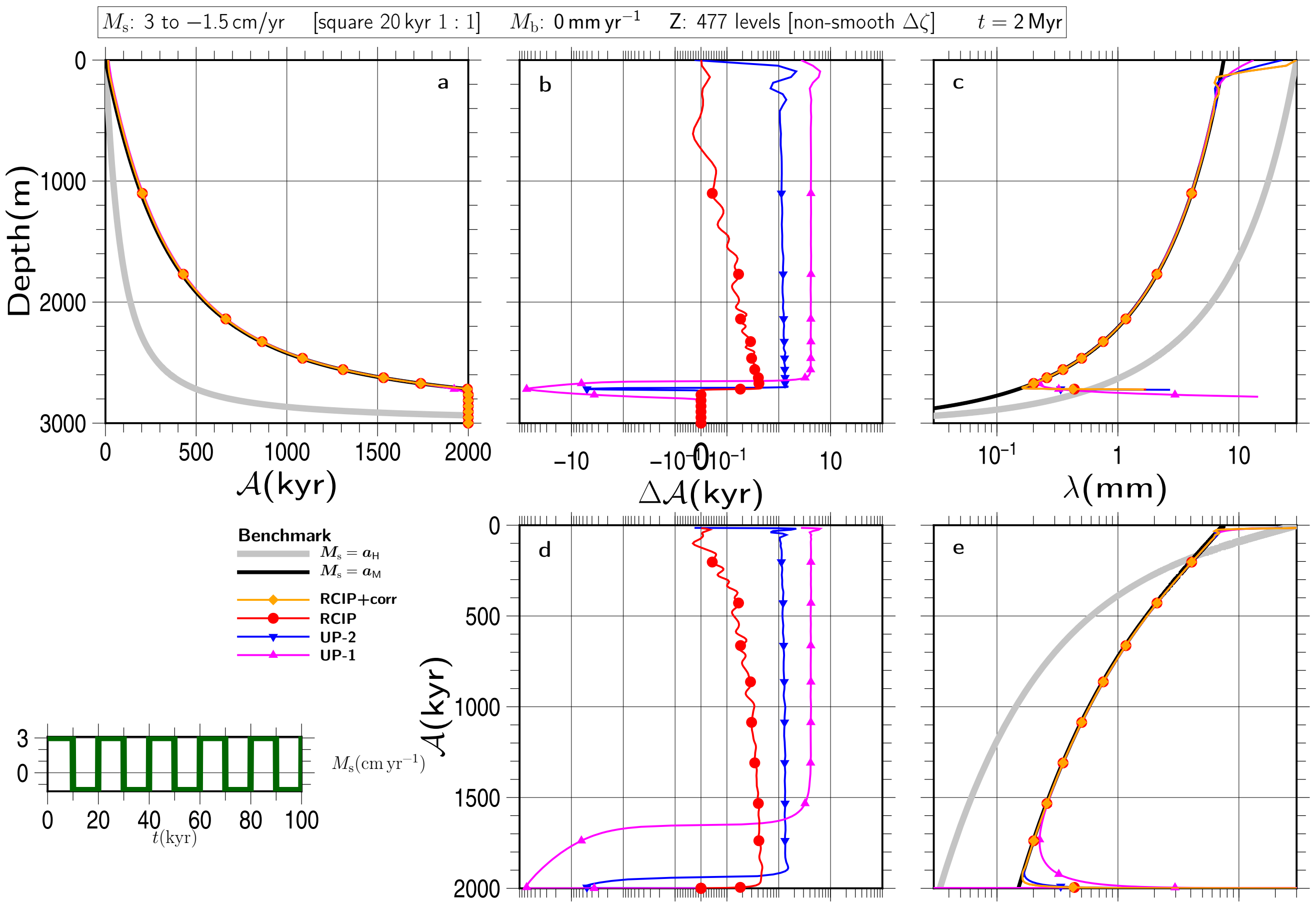

Figure S149

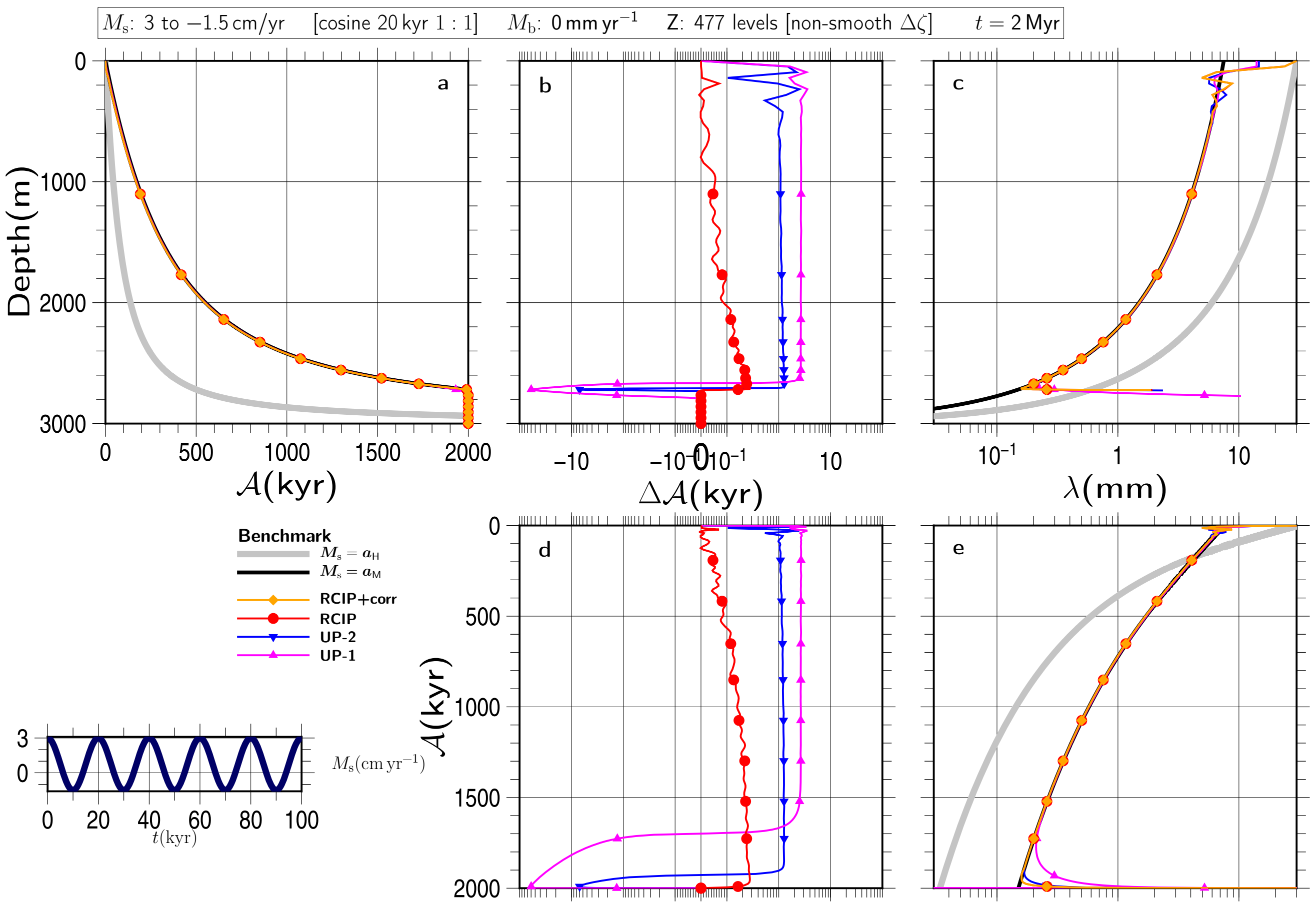

Figure S150

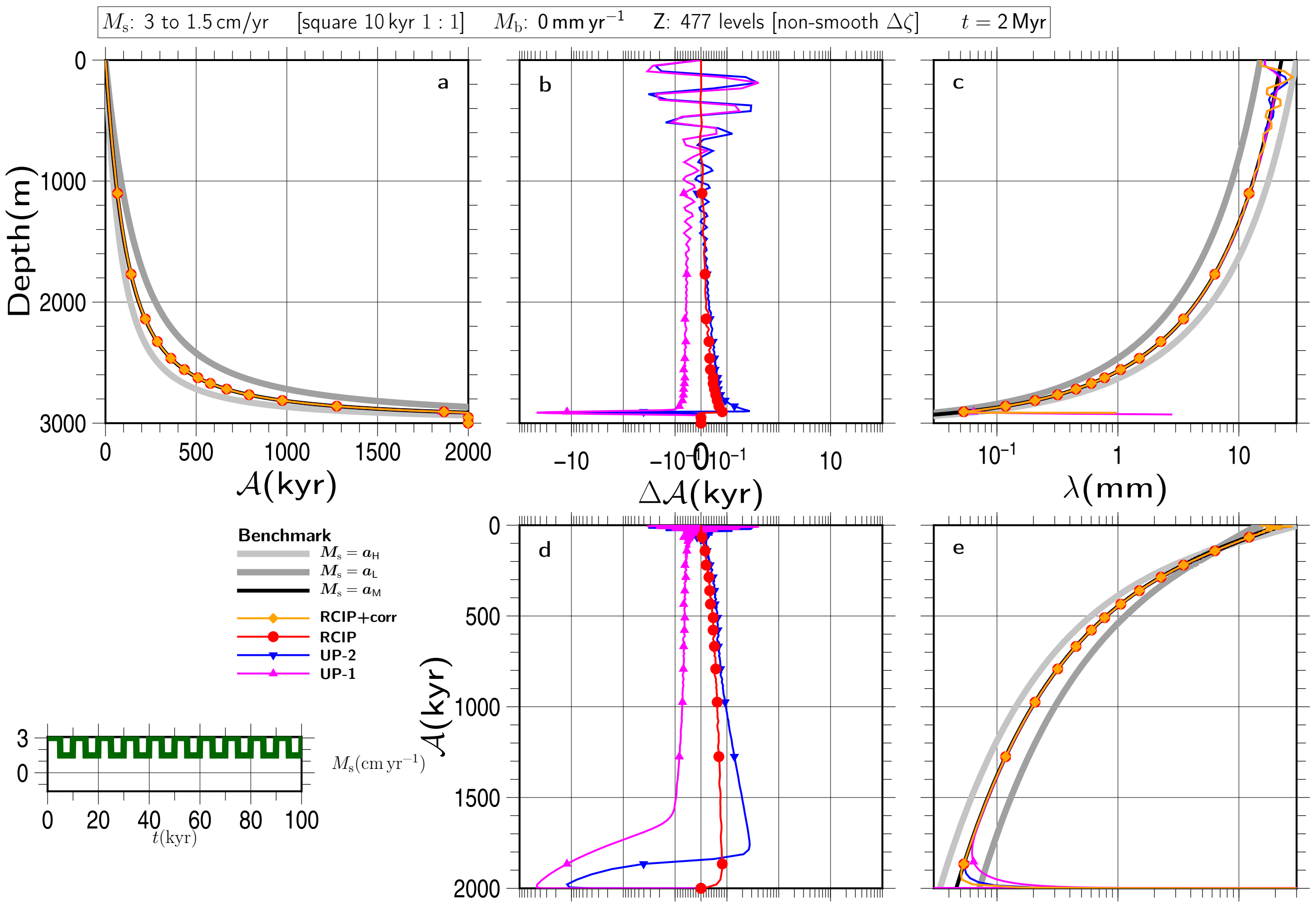

Figure S151

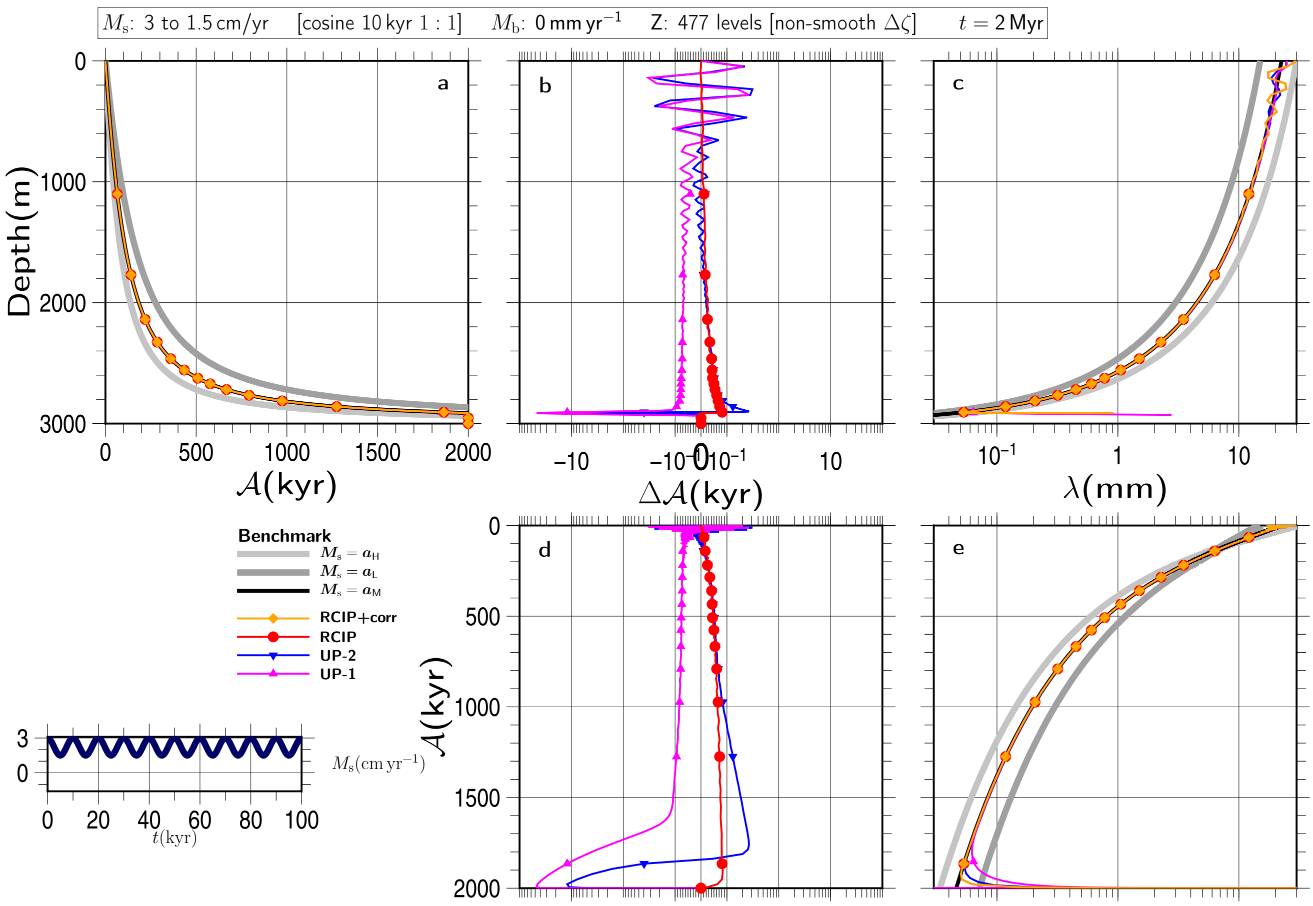

Figure S152

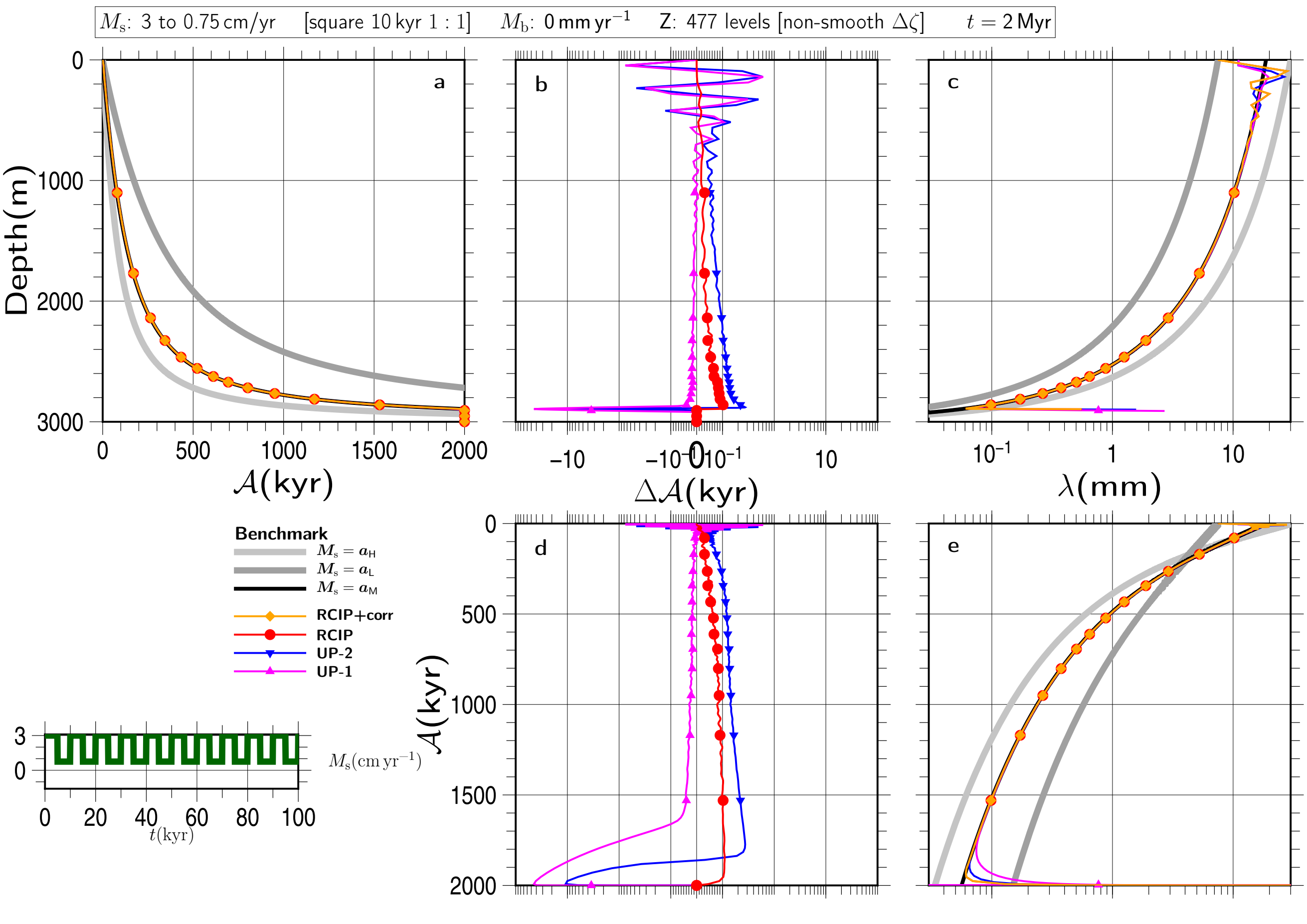

Figure S153

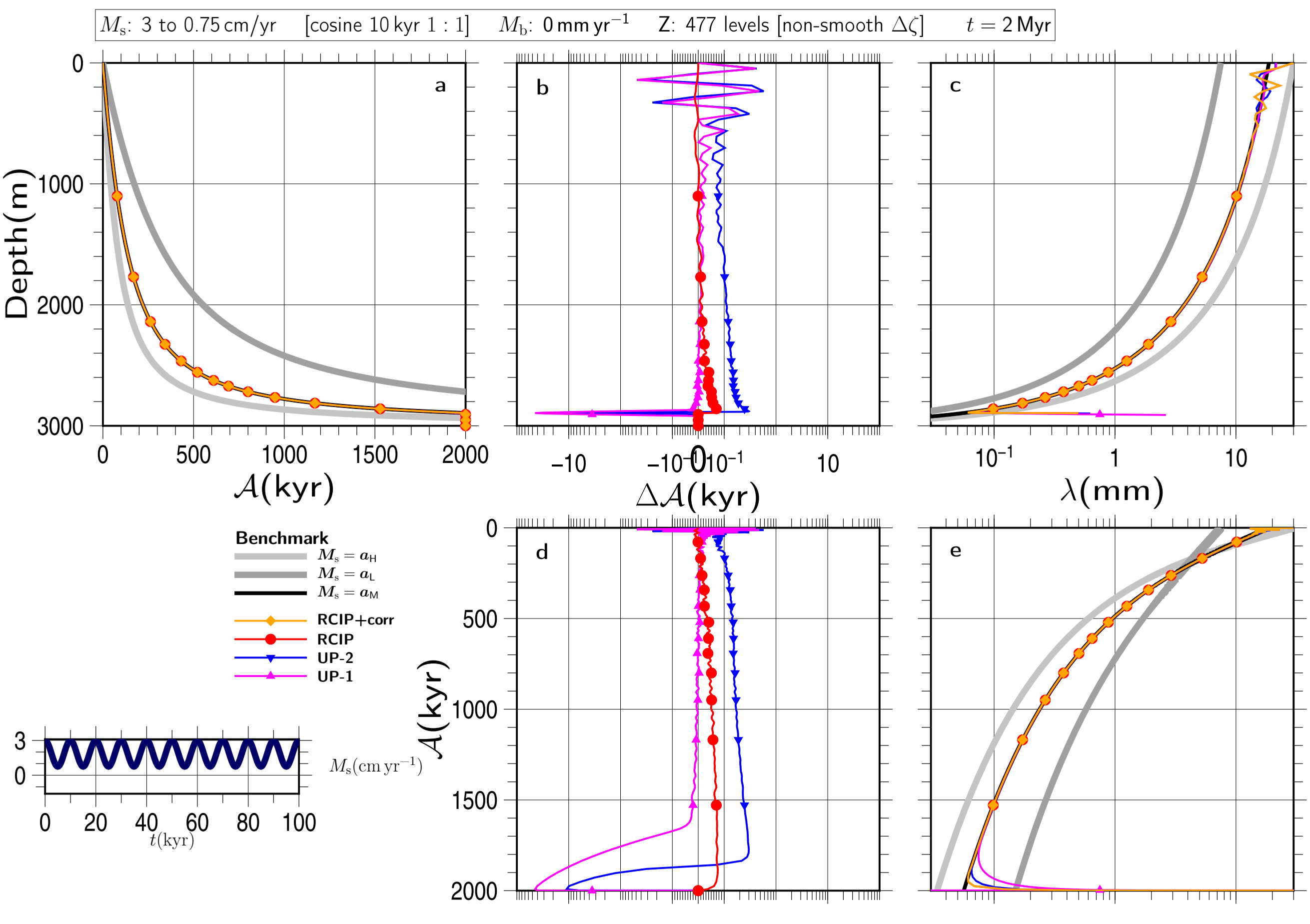

Figure S154

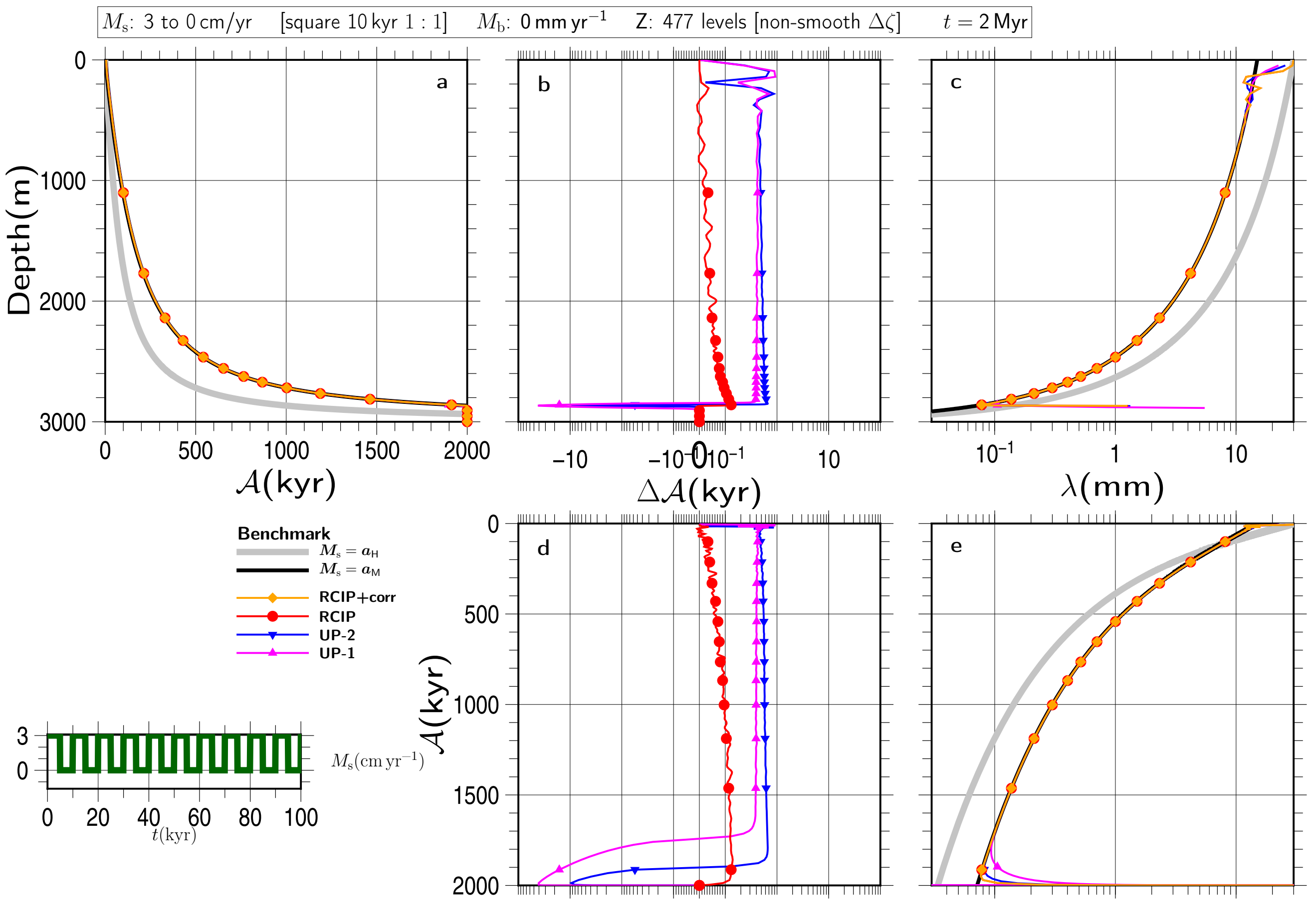

Figure S155

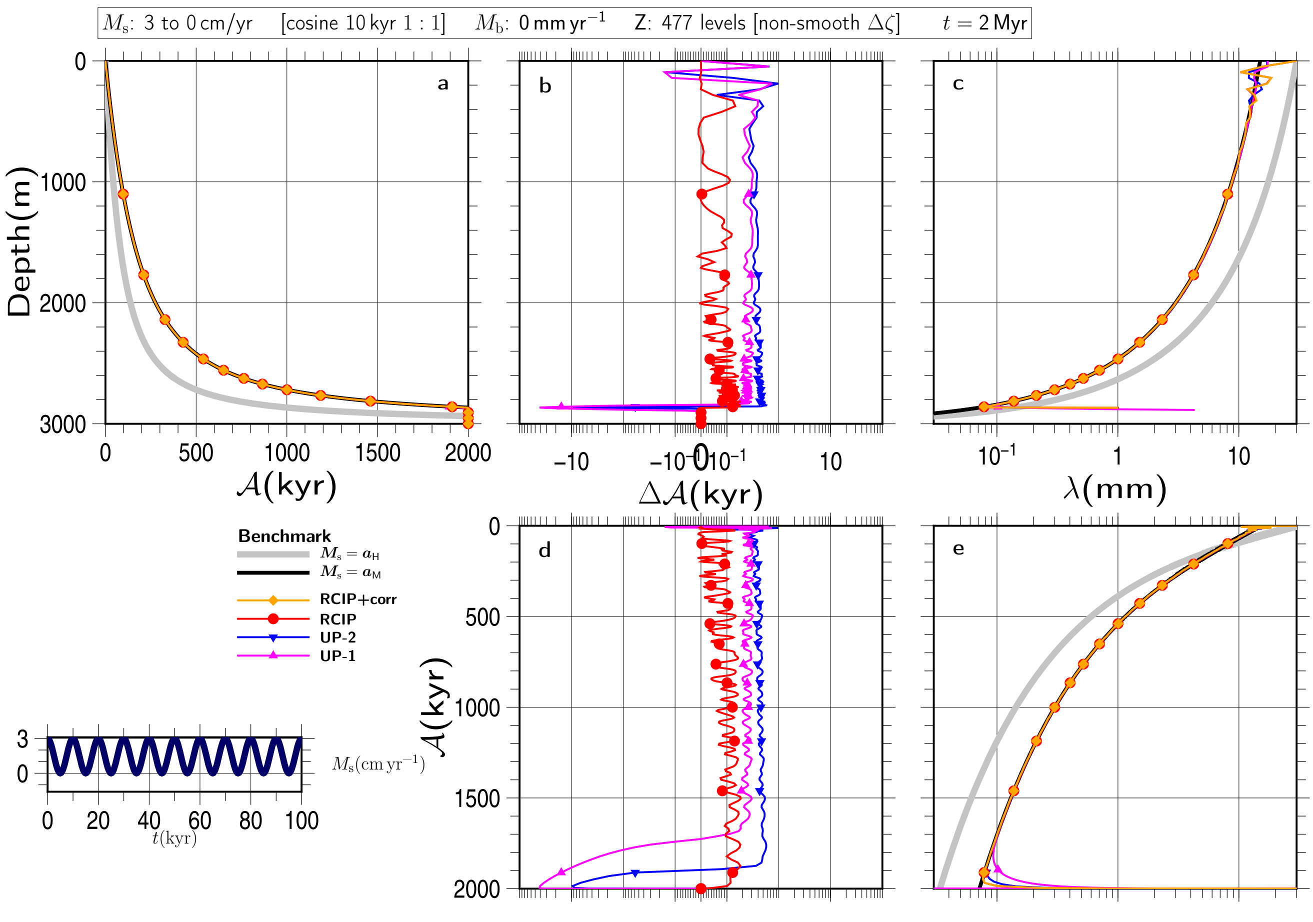

Figure S156

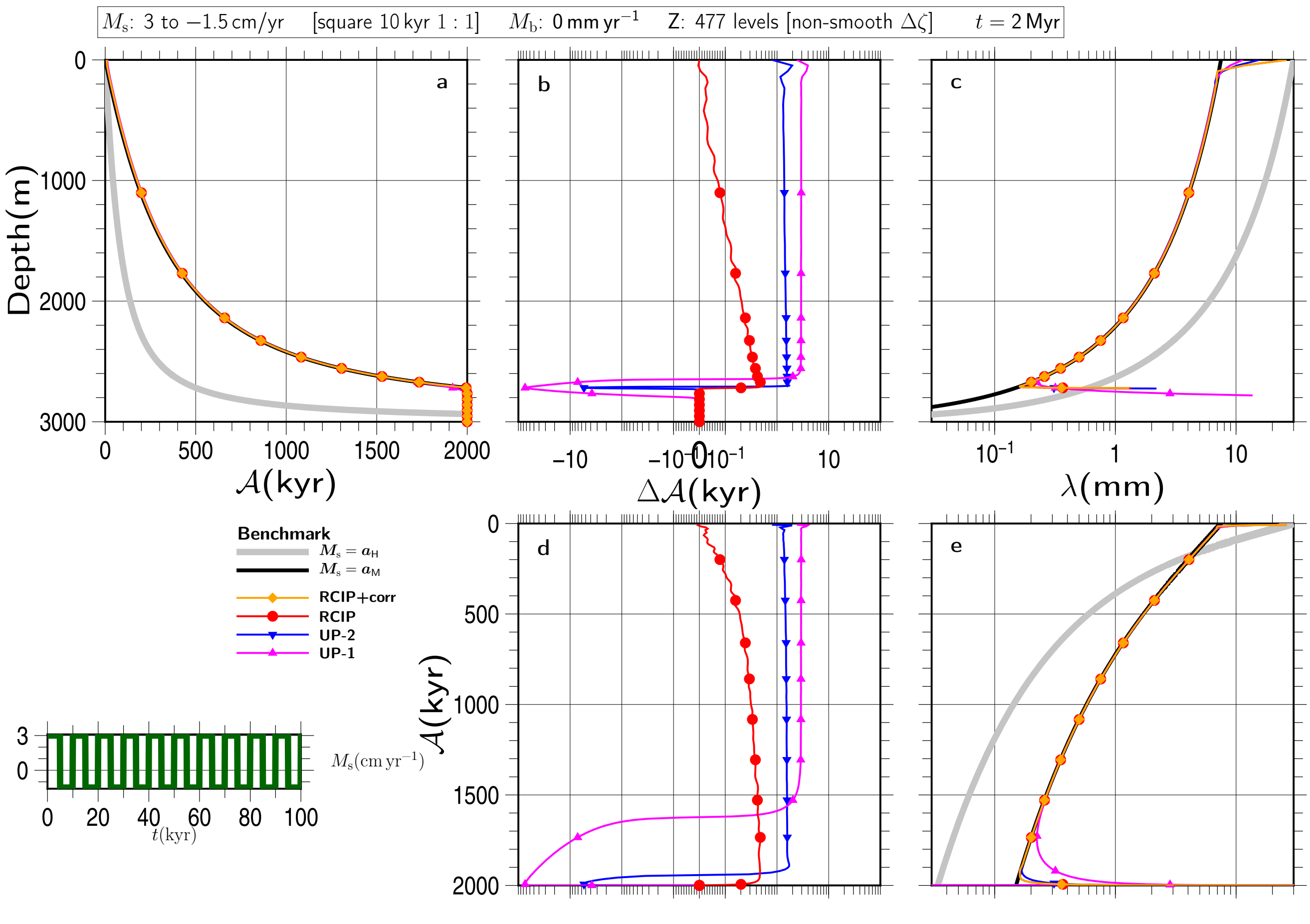

Figure S157

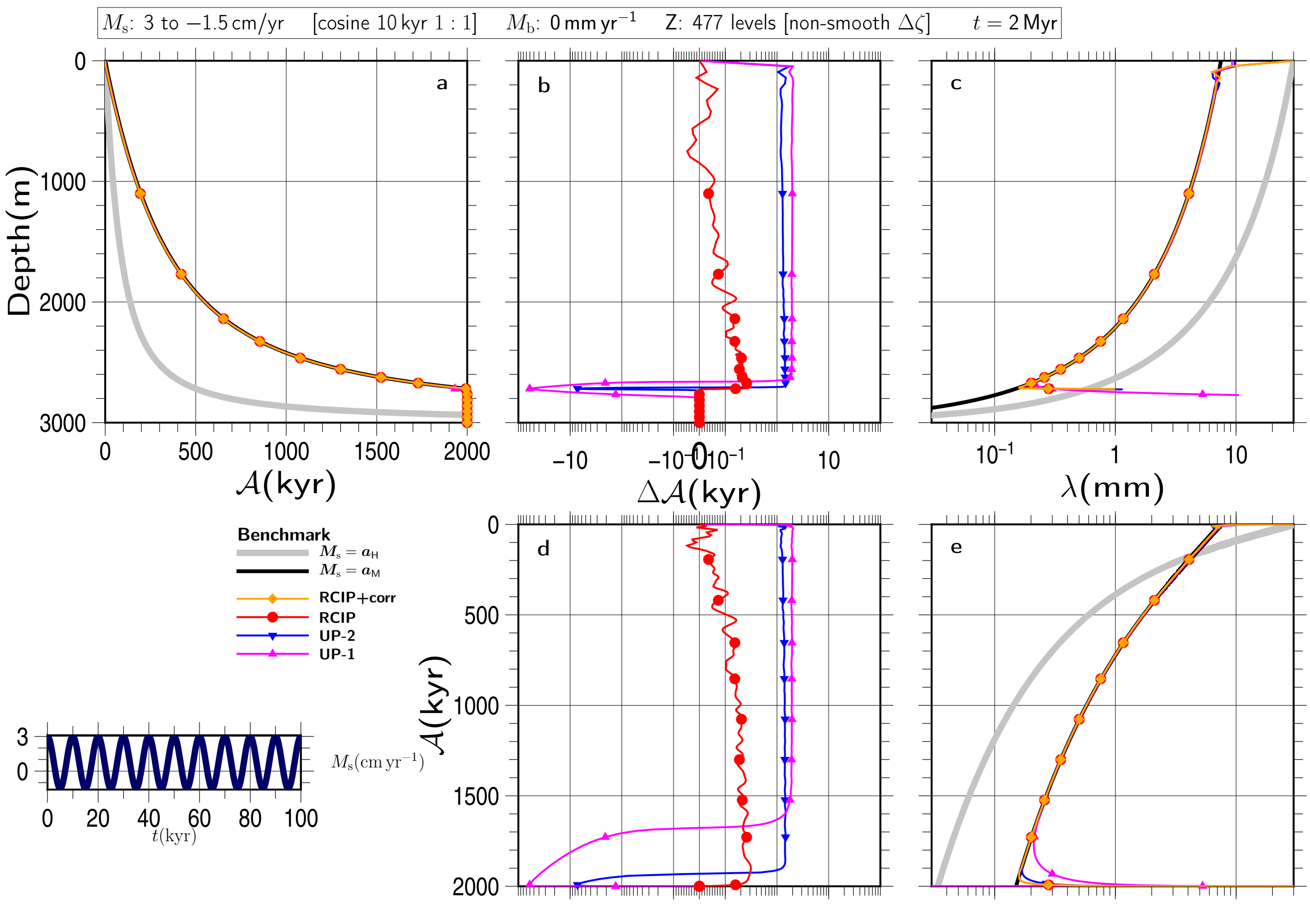

Figure S158

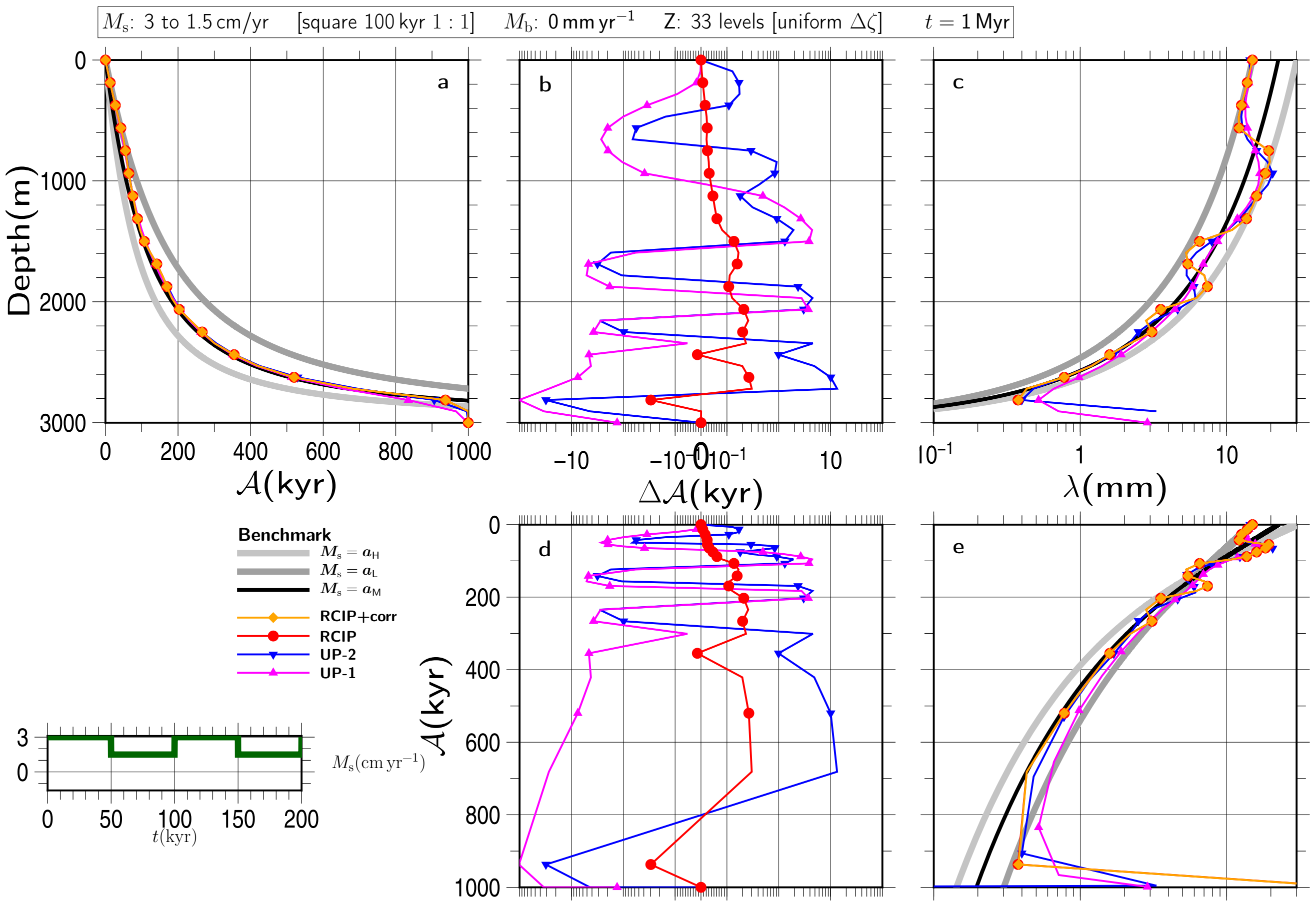

Figure S159

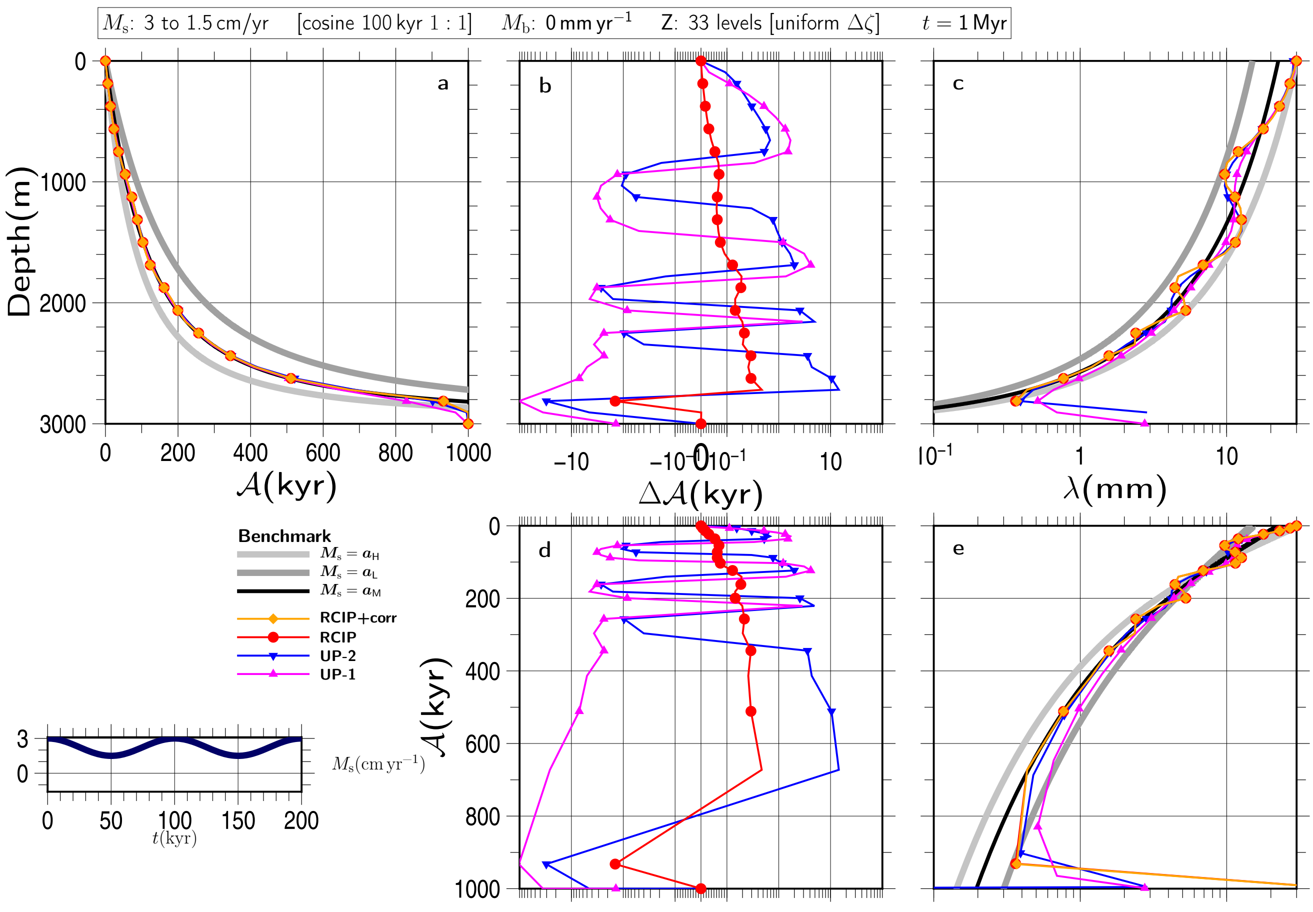

Figure S160

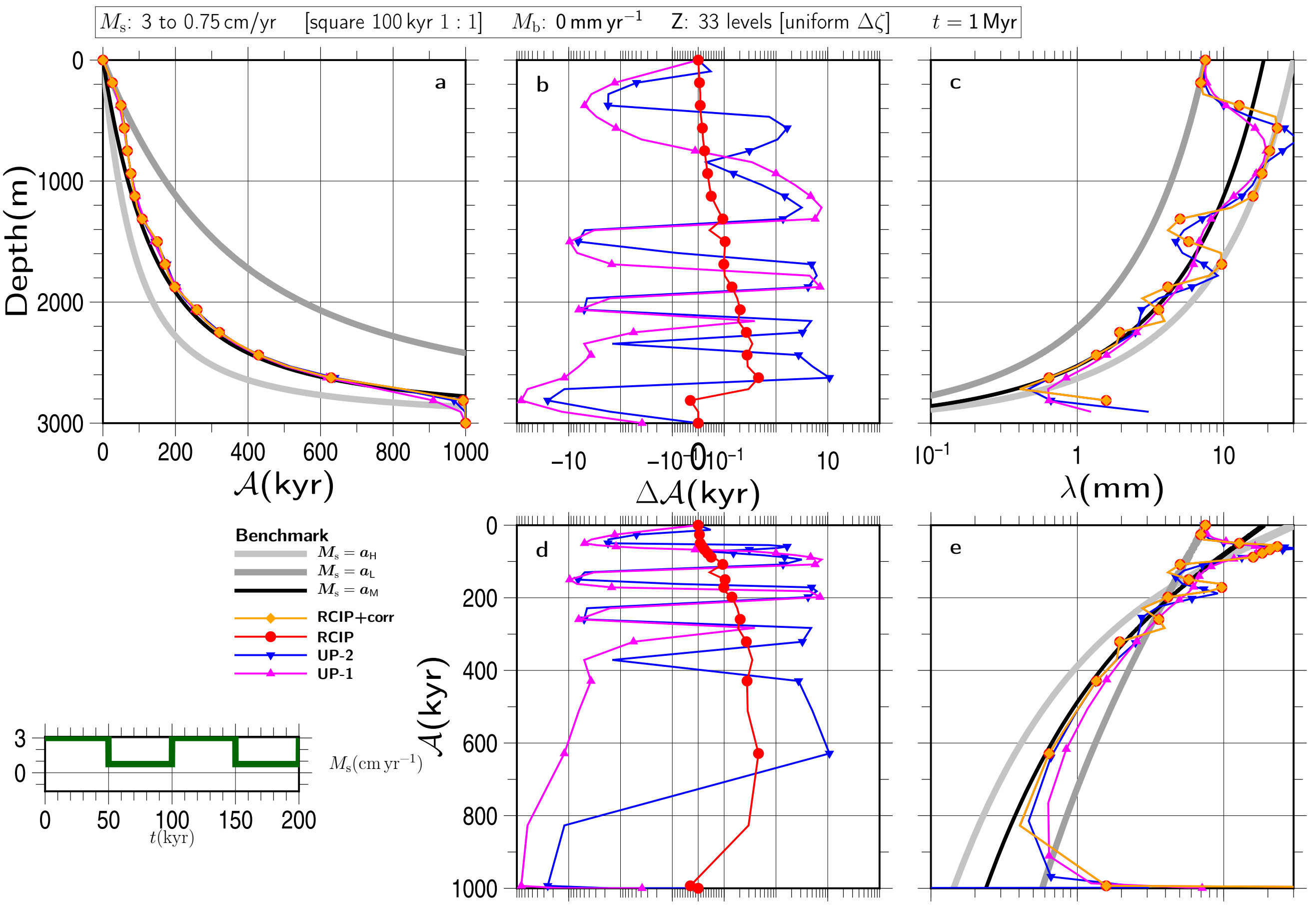

Figure S161

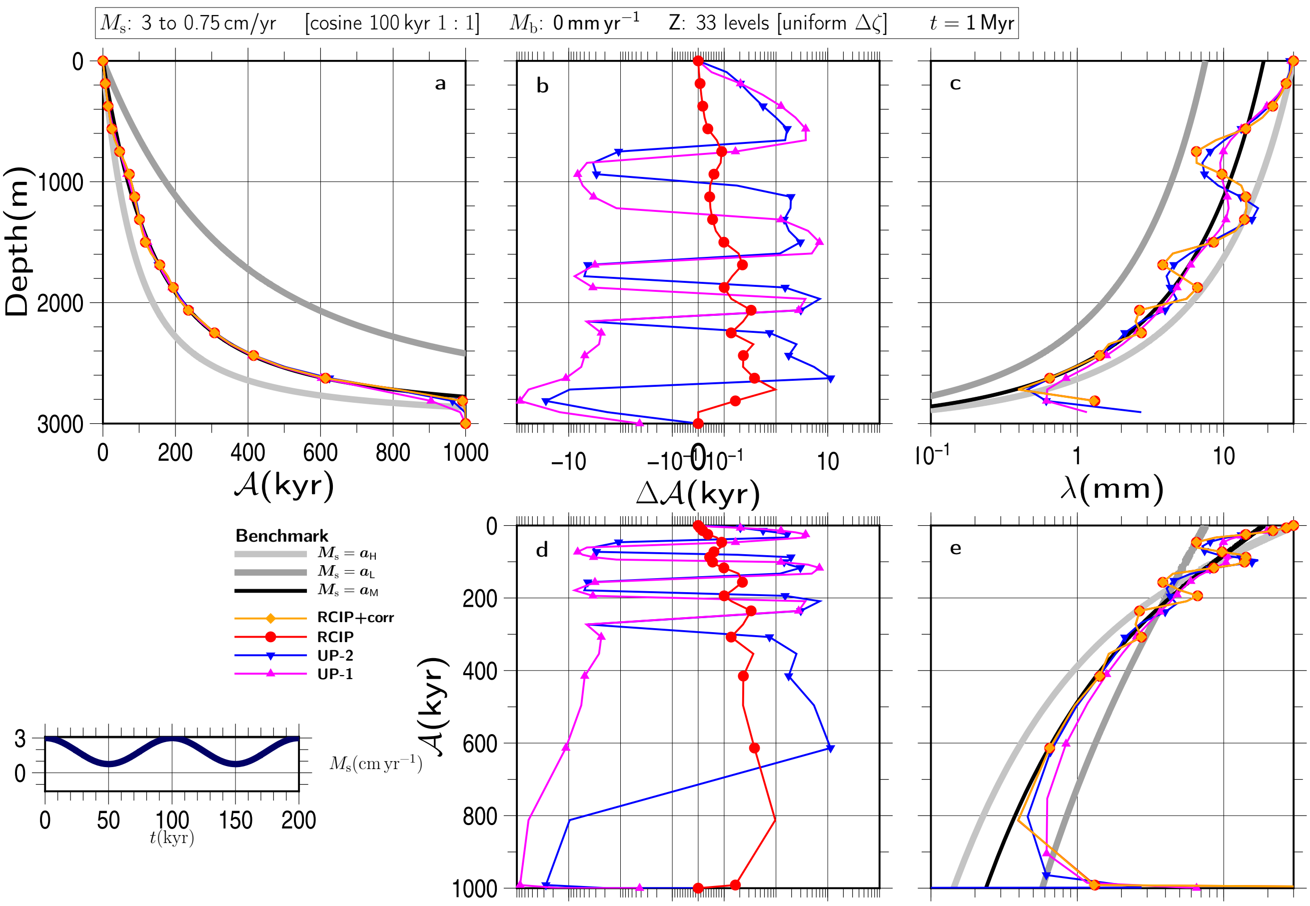

Figure S162

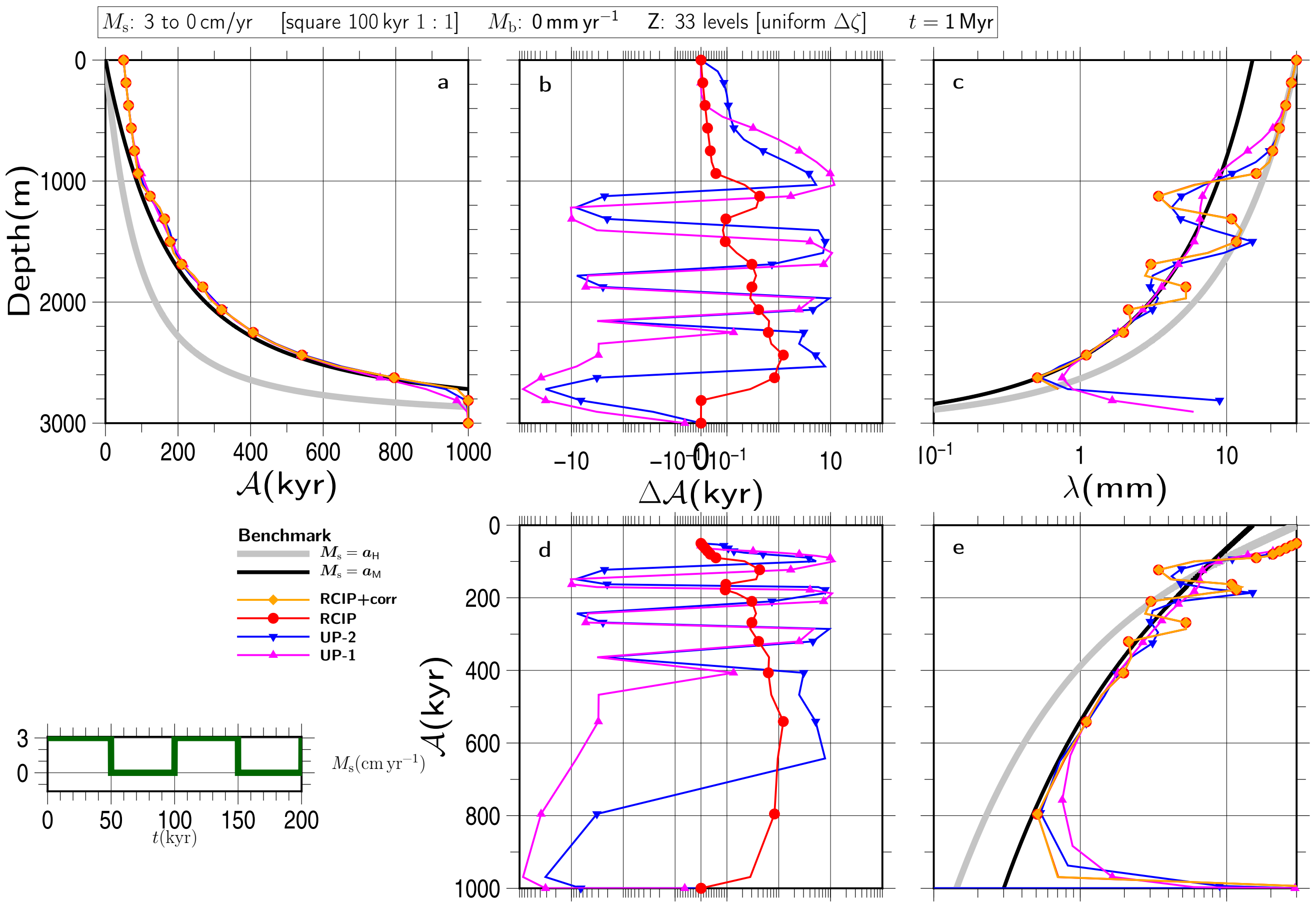

Figure S163

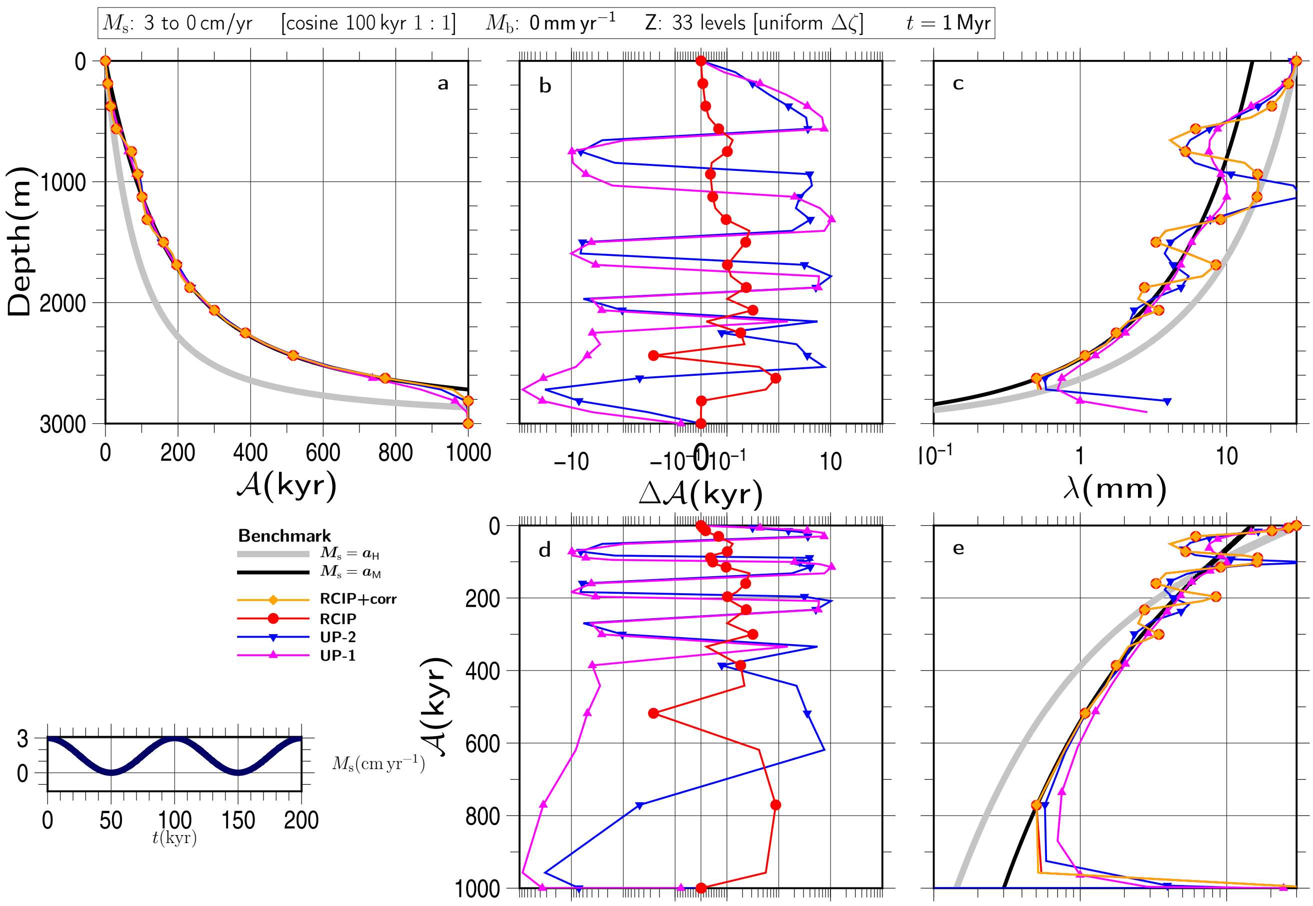

Figure S164

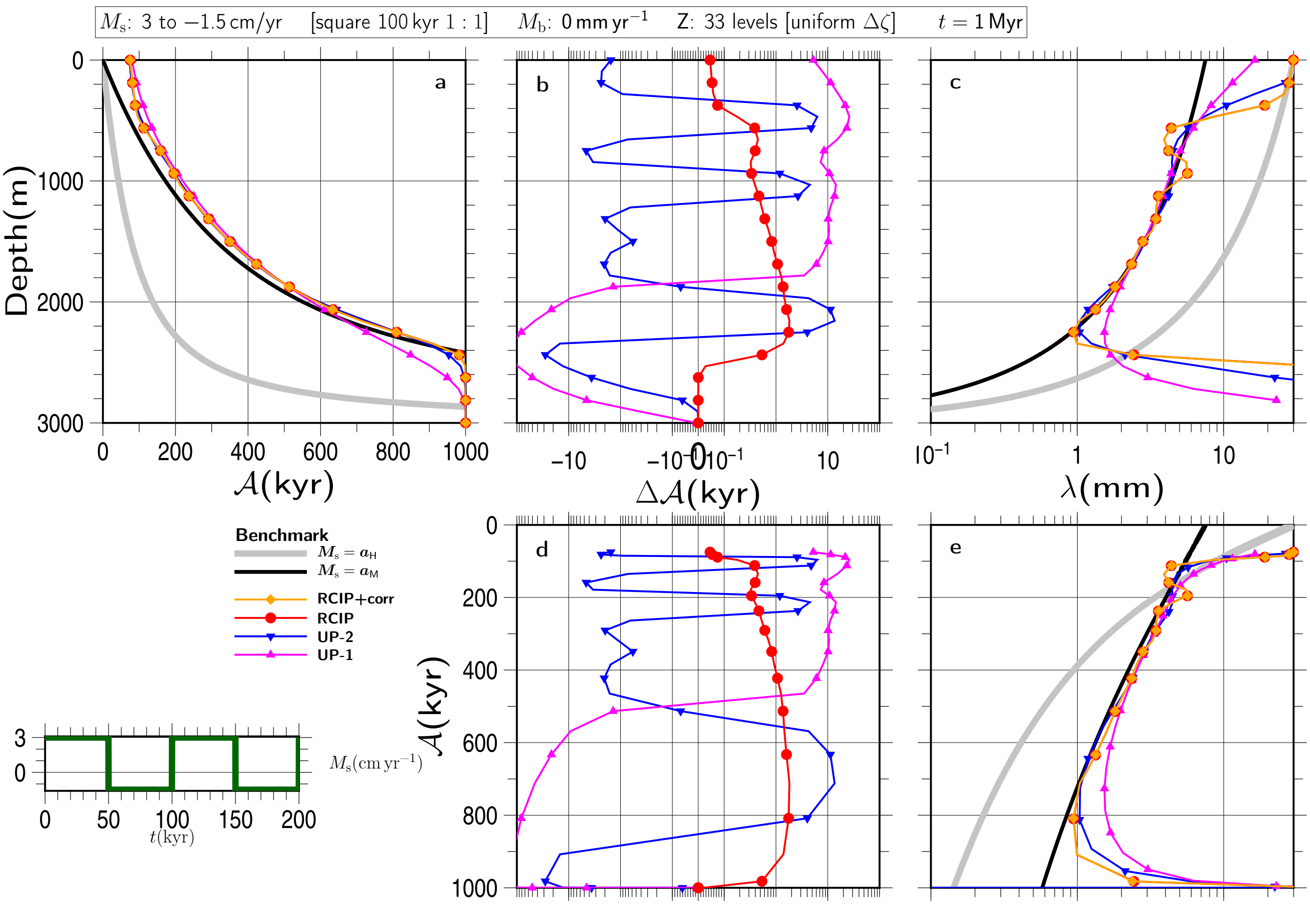

Figure S165

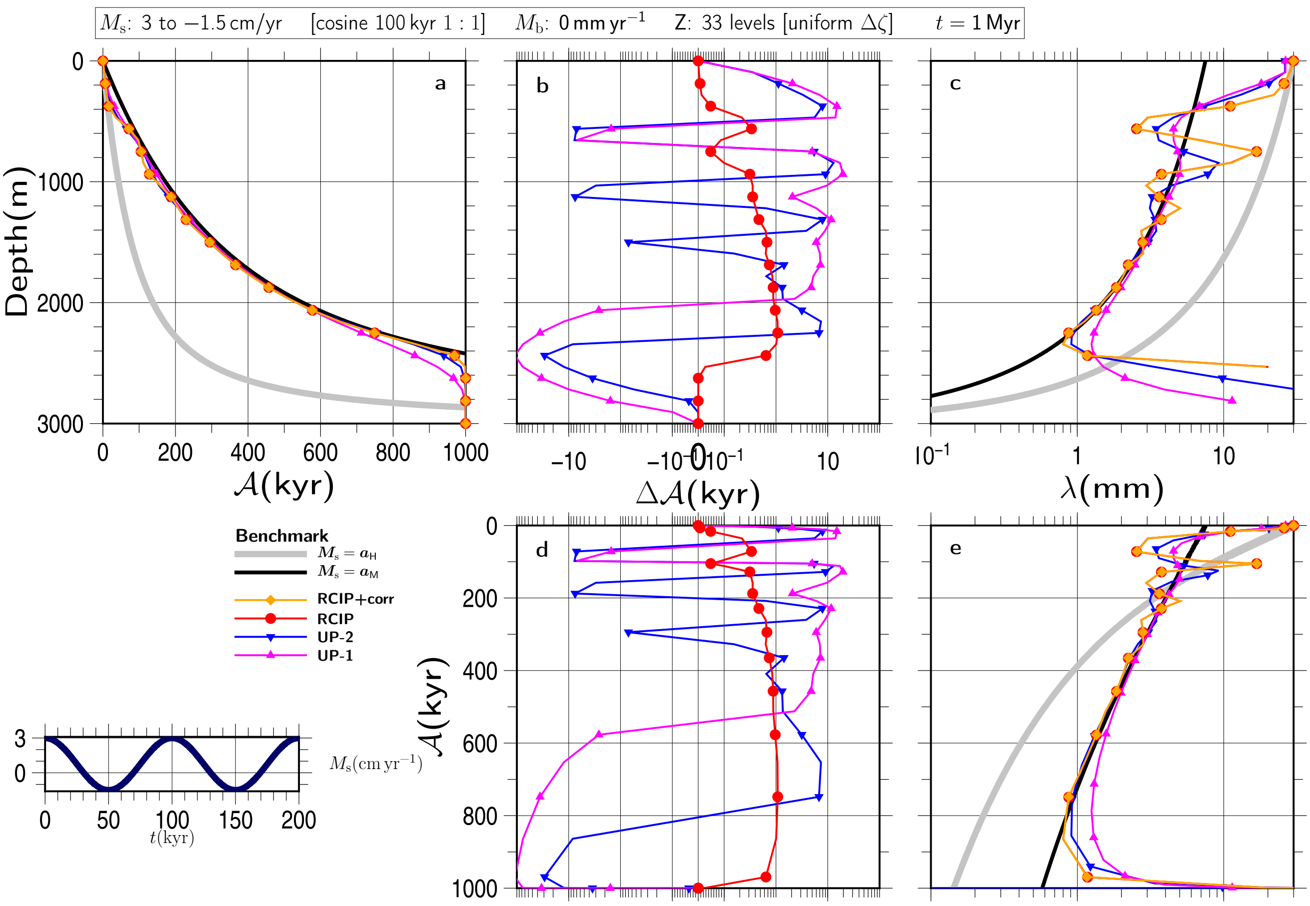

Figure S166